

ONCOTHERMIA JOURNAL

➤ A publication of Oncotherm® ISSN 2191-6438

Volume 30 - April 2021

- 9 **Pastore C.:** Salvage therapy of a patient with metastatic uterine leiomyosarcoma combining chemotherapy and hyperthermia
- 15 **Pastore C.:** Peritoneal carcinomatosis of gastric origin treated with a combination of Capecitabine and oncological hyperthermia: a case report
- 20 **Fiorentini G. et al.:** Updates of the application of regional hyperthermia in the treatment of esophageal, colorectal, and pancreatic cancers
- 37 **Van Gool S. W. et al.:** Addition of Multimodal Immunotherapy to Combination Treatment Strategies for Children with DIPG: A Single Institution Experience
- 54 **Van Gool S. W. et al.:** Randomized Controlled Immunotherapy Clinical Trials for GBM Challenged
- 83 **Mühlberg K.:** Impedance matching and its consequences for modulated electro-hyperthermia
- 104 **Mühlberg K.:** Power transmission of EHY-2000 – A Hypothesis
- 117 **Brockmann W.-P., Arnhold J., Denck M.:** Die Albumin-Carrier-Therapie – Anwendung in der onkologischen Praxis
- 121 **Brockmann W.-P.:** Wird die Bedeutung des Serum-Albumins bei Malignom-Patienten mit Aszites, Ödemen und Pleuraergüssen unter- oder überschätzt? – MTX-HSA als Hilfe bei der Therapie
- 125 **Brockmann W.-P.:** Das PET-CT im onkologischen Alltag – Eine wertvolle Hilfe zur Prognoseverbesserung
- 132 **Roussakow S.:** Modulated electro-hyperthermia in the combined treatment of metastatic colorectal cancer a retrospective cohort study with meta-comparison

Imprint

Executive Editor

Prof. Dr. András Szász

Head of the Department of Biotechnics, St. Istvan University, Godollo, Hungary
Chief Scientific Officer (CSO)

Oncotherm GmbH
Belgische Allee 9
53842 Troisdorf
Germany
☎ +49 2241 31992 0
☎ +36 23 555 510
✉ Szasz@oncotherm.de

Managing Editor

Ilka Schulz

Oncotherm GmbH
Belgische Allee 9
53842 Troisdorf
Germany
☎ +49 2241 31992 12
✉ schulz@oncotherm.de

Editorial Board

Prof. Dr. Alexander Herzog

Chief-physician, Fachklinik Dr. Herzog, Germany

Prof. Dr. Clifford L. K. Pang

Managing Director of Clifford Group, P.R. China

Dr. Friedrich Douwes

Director Klinik St. Georg, Bad Aibling, Germany
President of the German Oncological Society DGO

Prof. Dr. Gabriella Hegyi

Department of Complementary Medicine, Medical School, University of Pecs, Hungary

Assoc. Professor Dr. Olivér Szász

CEO of Oncotherm Group, Germany and Hungary

Dr. habil Marcell A. Szász

Cancer Center, Semmelweis University, Budapest, Hungary

Prof. Dr. Giammaria Fiorentini

Oncology Unit, San Giuseppe General Hospital, Italy

Dr. Gurdev Parmar

Director of Integrated Health Clinic, Canada

Prof. Dr. Chi Kwan-Hwa

President, Taiwan Society Hyperthermic Oncology

Dr. Samuel Yu- Shan Wang

Molecular Medicine and Biochemical Engineering
National Chiao Tung University, Hsinchu, Taiwan

Balázs Tóth

Managing Partner, RWU Consulting

Editorial

Dear Reader, dear Fellow Researchers, dear Colleagues,

Our Oncothermia Journal reached a milestone. You have 30 volumes of this informative publication. We had a long way to go since 2010 when the first volume was published. More and more Oncothermia experts and potential users are interested in the information transmitted by the Journal. This activity is one of the resources for physicians to exchange their experience and study how others use modulated electro-hyperthermia therapies.

There are important topics covered in the articles in this volume. Dr. Brockmann discusses some critical aspects of complex therapies, including PET diagnosis, that seems important to plan the treatment of Oncothermia. PET informs us about metabolic activity and conductivity-based tumor selection.

Dr. Pastore's case reports show very advanced metastatic cases successfully treated with complex Oncothermia treatments, likely giving clues for other doctors to manage the severe stages of cancer.

Dr. Roussakow talked about a retrospective meta-comparison of metastatic colorectal cancer showing excellent results of Oncothermia in this common and severe type of cancer.

Immunotherapy is one of the emerging areas of oncology. We are pleased to see how busy work connects Oncothermia with the promising new method. Prof. van Gool's articles introduce us to the complexity of this therapy and show a remarkable immune activation with Newcastle viruses.

One of the specialties of this volume is a technical discussion. Two articles by Dr. Mühlberg show the importance of a precise tuning method and advice on correcting it. The generalization of her results shows some universal aspects of the topic. An essential part of this technical discussion is the sources of unwanted energy losses, which must be

minimized when the patient is treated with Oncothermia.

I hope this volume also provides relevant and up-to-date information for your daily practice. I would like to direct your attention to the importance of reading the Oncotherm Newsletter as well. This monthly summary provides you with information on the most recent articles published on international domains and brings you news about events and actualities related to hyperthermia in oncology. Reading this news well completes the clinical information included in our Oncothermia Journal.

This volume is bilingual. Some crucial aspects of the clinical application of Oncothermia are published in German, favoring our German-speaking readers. This is a trial to see how the bilingual topic reaches our Oncothermia users and how readers accept this type of edition. I would be happy to hear your opinion on this. Your help and attention would be greatly appreciated.

Enjoy this 30th volume of the Oncothermia Journal.



Prof. Andras Szasz

Editor of the Oncothermia Journal

Professor, Chair, Biotechnics Department of St. Istvan University
Chief Scientific Officer of Oncotherm Group

Liebe Leserinnen und Leser, liebe Kolleginnen und Kollegen aus Forschung und Praxis,

unser Oncothermia Journal hat mit 30 veröffentlichten Bänden einen Meilenstein erreicht und wir haben seit der Publikation des ersten Bandes im Jahr 2010 einen weiten Weg zurückgelegt. Immer mehr Oncothermie-Experten und potenzielle Anwender interessieren sich für die Informationen, die das Journal beinhaltet. Darüber hinaus wird Ärzten so die Möglichkeit geboten, ihre Erkenntnisse auszutauschen und zu erfahren, wie andere Elektrohperthermietherapie anwenden.

In den in diesem Band vorliegenden Arbeiten werden wichtige Themen behandelt. Dr. Brockmann diskutiert einige kritische Aspekte komplexer Therapien, einschließlich der PET-Diagnose, die für die Planung der Behandlung mit Oncothermie wichtig erscheint. PET liefert Informationen zur metabolischen Aktivität und leitfähigkeitsbasierten Tumorselektion.

Dr. Pastores Fallberichte zeigen sehr fortgeschrittene metastatische Fälle, die erfolgreich mit komplexen Oncothermie-Behandlungen therapiert wurden und wahrscheinlich Anhaltspunkte in Bezug auf die Behandlung von schweren Krebserkrankungen für andere Ärzte liefern.

Dr. Roussakow sprach über einen retrospektiven Metavergleich von metastasiertem Darmkrebs, der hervorragende Ergebnisse durch den Einsatz von Oncothermie bei dieser häufigen und schweren Krebsart zeigt.

Die Immuntherapie ist eines der neu entstehenden Gebiete der Onkologie. Wir sind erfreut zu sehen, wie die vielversprechende neue Methode durch viel Arbeit mit Oncothermie verbunden wird. Die Artikel von Prof. van Gool führen uns in die Komplexität dieser Therapie ein und zeigen eine bemerkenswerte Immunaktivierung mit Newcastle-Viren.

Eine technische Diskussion stellt eine der Besonderheiten dieses Bandes dar. Die zwei Artikel von Dr. Mühlberg zeigen die Bedeutung einer präzisen Abstimmungsmethode sowie Hinweise zu deren

Korrektur. Die Verallgemeinerung ihrer Ergebnisse dokumentiert einige universelle Aspekte des Themas. Ein wesentlicher Bestandteil dieser technischen Diskussion sind die Ursprünge unerwünschter Energieverluste. Diese müssen minimiert werden, wenn der Patient mit Oncothermie behandelt wird.

Ich hoffe, dieser Band bietet Ihnen relevante und aktuelle Informationen für Ihre tägliche Praxis. An dieser Stelle möchte ich zudem auf die Bedeutung des Oncotherm-Newsletters hinweisen. Dieser bietet Ihnen jeden Monat einen Überblick über die neuesten Artikel, die auf internationalen Domains veröffentlicht wurden, informiert Sie über Ereignisse und Tatsachen im Zusammenhang mit Hyperthermie in der Onkologie und ergänzt die klinischen Informationen aus unserem Oncothermia Journal.

Dieser zweisprachige Band enthält einige wichtige Aspekte der klinischen Anwendung von Oncothermie in deutscher Sprache und kommt somit unseren deutschsprachigen Lesern zugute. Wir möchten so herausfinden, ob die zwei-sprachigen Inhalte von unseren Oncothermie-Anwendern angenommen werden und inwiefern unseren Lesern diese Art von Ausgabe zusagt. Ich würde mich freuen, Ihre Meinung dazu zu hören und Ihre Hilfe dankend annehmen.

Erfreuen Sie sich am 30. Band des Oncothermia Journals.



Prof. Andras Szasz

Herausgeber des Oncothermia Journals
Lehrstuhl für Biotechnik, St. Istvan Universität
Chief Scientific Officer der Oncotherm Gruppe

Rules of Submission

As the editorial team we are committed to a firm and coherent editorial line and the highest possible printing standards. But it is mainly you, the author, who makes sure that the *Oncothermia Journal* is an interesting and diversified magazine. We want to thank every one of you who supports us in exchanging professional views and experiences. To help you and to make it easier for both of us, we prepared the following rules and guidelines for abstract submission.

Als redaktionelles Team vertreten wir eine stringente Linie und versuchen, unserer Publikation den höchstmöglichen Standard zu verleihen. Es sind aber hauptsächlich Sie als Autor, der dafür Sorge trägt, dass das *Oncothermia Journal* zu einem interessanten und abwechslungsreichen Magazin wird. Wir möchten allen danken, die uns im Austausch professioneller Betrachtungen und Erfahrungen unterstützen. Um beiden Seiten die Arbeit zu erleichtern, haben wir die folgenden Richtlinien für die Texterstellung entworfen.

1. Aims and Scope

The *Oncothermia Journal* is an official journal of the Oncotherm Group, devoted to supporting those who would like to publish their results for general use. Additionally, it provides a collection of different publications and results. The *Oncothermia Journal* is open towards new and different contents, but it should particularly contain complete study-papers, case-reports, reviews, hypotheses, opinions and all the informative materials which could be helpful for the international *Oncothermia* community. Advertisement connected to the topic is also welcome.

- Clinical studies: regional or local or multilocal *Oncothermia* or electro cancer therapy (ECT) treatments, case-reports, practical considerations in complex therapies, clinical trials, physiological effects, *Oncothermia* in combination with other modalities and treatment optimization
- Biological studies: mechanisms of *Oncothermia*, thermal- or non-temperature dependent effects, response to electric fields, bioelectromagnetic applications for tumors, *Oncothermia* treatment combination with other modalities, effects on normal and malignant cells and tissues, immunological effects, physiological effects, etc.
- Techniques of *Oncothermia*: technical development, new technical solutions, proposals
- Hypotheses, suggestions and opinions to improve *Oncothermia* and electro-cancer-therapy methods, intending the development of the treatments.

Further information about the journal, including links to the online sample copies and content pages can be found on the website of the journal: www.oncothermia-journal.com

Umfang und Ziele

Das *Oncothermia Journal* ist das offizielle Magazin der Oncotherm Gruppe und soll diejenigen unterstützen, die ihre Ergebnisse der Allgemeinheit zur Verfügung stellen möchten. Das *Oncothermia Journal* ist neuen Inhalten gegenüber offen, sollte aber vor allem Studienarbeiten, Fallstudien, Hypothesen, Meinungen und alle weiteren informativen Materialien, die für die internationale *Oncothermie*-Gemeinschaft hilfreich sein könnten, enthalten. Werbung mit Bezug zum Thema ist ebenfalls willkommen.

- Klinische Studien: regionale, lokale oder multilokale *Oncothermie* oder Electro Cancer Therapy (ECT) Behandlungen, Fallstudien, praktische Erfahrungen in komplexen Behandlungen, klinische Versuche, physiologische Effekte, *Oncothermie* in Kombination mit anderen Modalitäten und Behandlungsoptimierungen
- Biologische Studien: Mechanismen der *Oncothermie*, thermale oder temperaturunabhängige Effekte, Ansprechen auf ein elektrisches Feld, bioelektromagnetische Anwendungen bei Tumoren, Kombination von *Oncothermie* und anderen Modalitäten, Effekte auf normale und maligne Zellen und Gewebe, immunologische Effekte, physiologische Effekte etc.
- *Oncothermie*-Techniken: technische Entwicklungen, neue technische Lösungen
- Hypothesen und Meinungen, wie die *Oncothermie*- und ECT-Methoden verbessert werden können, um die Behandlung zu unterstützen

Weitere Informationen zum Journal sowie Links zu Online-Beispielen und Inhaltsbeschreibung sind auf der Website zu finden: www.oncothermia-journal.com

2. Submission of Manuscripts

All submissions should be made online via email: info@oncotherm.org

Manuskripte einreichen

Manuskripte können online eingereicht werden: info@oncotherm.org

3. Preparation of Manuscripts

Manuscripts must be written in English, but other languages can be accepted for special reasons, if an English abstract is provided. Texts should be submitted in a format compatible with Microsoft Word for Windows (PC). Charts and tables are considered textual and should also be submitted in a format compatible with Word. All figures (illustrations, diagrams, photographs) should be provided in JPG format.

Manuscripts may be any length, but must include:

- Title Page: title of the paper, authors and their affiliations, 1-5 key words, at least one corresponding author should be listed, email address and full contact information must be provided.
- Abstracts: Abstracts should include the purpose, materials, methods, results and conclusions.
- Text: unlimited volume
- Tables and Figures: Tables and figures should be referred to in the text (numbered figures and tables). Each table and/or figure must have a legend that explains its purpose without a reference to the text. Figure files will ideally be submitted as a jpg-file (300dpi for photos).
- References: Oncothermia Journal uses the Vancouver (Author-Number) system to indicate references in the text, tables and legends, e.g. [1], [1-3]. The full references should be listed numerically in order of appearance and presented following the text of the manuscript.

Manuskripte vorbereiten

Manuskripte müssen in englischer Sprache vorliegen. Andere Sprachen können in Ausnahmefällen akzeptiert werden, wenn ein englisches Abstract vorliegt.

Texte sollten in einem mit Microsoft Word für Windows (PC) kompatiblen Format eingereicht werden. Tabellen sollten in einem Word-kompatiblen Format eingefügt werden. Alle Graphiken (Illustrationen, Diagramme, Photographien) sollten im jpg Format vorliegen.

Manuskripte können jede Länge haben, müssen aber die folgenden Punkte erfüllen:

- Titelseite: Titel der Arbeit, Autor, Klinikzugehörigkeit, 1-5 Schlüsselworte, mindestens ein Autor muss genannt werden, E-Mail-Adresse und Kontaktdetails des Autors
- Abstracts: Abstracts müssen Zielsetzung, Material und Methoden, Ergebnisse und Fazit enthalten.
- Text: beliebige Länge
- Abbildungen und Tabellen: Abbildungen und Tabellen sollten im Text erläutert werden (nummeriert). Jede Abbildung / Tabelle muss eine erklärende Bildunterschrift haben. Bilder sollten als jpg eingereicht werden (300 dpi).
- Zitate: Das Oncothermia Journal verwendet die Vancouver Methode (Autornummer), um Zitate auszuweisen, z.B. [1], [1-3]. Die Bibliografie erfolgt numerisch in Reihenfolge der Erwähnung im Text.

4. Copyright

It is a condition of publication that authors assign copyright or license the publication rights in their articles, including abstracts, to the publisher. The transmitted rights are not exclusive, the author(s) can use the submitted material without limitations, but the Oncothermia Journal also has the right to use it.

Copyright

Es ist eine Publikationsvoraussetzung, dass die Autoren die Erlaubnis zur Publikation ihres eingereichten Artikels und des dazugehörigen Abstracts unterschreiben. Die überschriebenen Rechte sind nicht exklusiv, der Autor kann das eingereichte Material ohne Limitation nutzen.

5. Electronic Proofs

When the proofs are ready, the corresponding authors will receive an e-mail notification. Hard copies of proofs will not be mailed. To avoid delays in the publication, corrections to proofs must be returned within 48 hours, by electronic transmittal or fax.

Elektronische Korrekturfahne

Wenn die Korrekturfahnen fertig gestellt sind, werden die Autoren per E-Mail informiert. Gedruckte Kopien werden nicht per Post versandt. Um Verzögerungen in der Produktion zu verhindern, müssen die korrigierten Texte innerhalb von 48 Stunden per E-Mail oder Fax zurückgesandt werden.

6. Offprints and Reprints

Author(s) will have the opportunity to download the materials in electronic form and use it for their own purposes. Offprints or reprints of the Oncothermia Journal are not available.

Sonderdrucke und Nachdrucke

Die Autoren haben die Möglichkeit, das Material in elektronischer Form herunterzuladen, Sonderdrucke und Nachdrucke des Oncothermia Journals sind nicht erhältlich.

7. Advertisement

The Oncothermia Journal accepts advertising in any language but prefers advertisements in English or at least partially in English. The advertising must have a connection to the topics in the Oncothermia Journal and must be legally correct, having checked that all information is true.

Werbung

Das Oncothermia Journal akzeptiert Werbeanzeigen in allen Sprachen, bevorzugt, aber die zumindest teilweise Gestaltung in englischer Sprache. Die Werbung muss eine Beziehung zu den Themen des Oncothermia Journals haben und der Wahrheit entsprechende Inhalte aufweisen.

8. Legal responsibility

Authors of any publications in the Oncothermia Journal are fully responsible for the material which is published. The Oncothermia Journal has no responsibility for legal conflicts due to any publications. The editorial board has the right to reject any publication if its validity has not been verified enough or the board is not convinced by the authors.

Haftung

Die Autoren aller im Oncothermia Journal veröffentlichten Artikel sind in vollem Umfang für ihre Texte verantwortlich. Das Oncothermia Journal übernimmt keinerlei Haftung für die Artikel der Autoren. Die Redaktion hat das Recht Artikel abzulehnen.

9. Reviewing

The Oncothermia Journal has a special peer-reviewing process, represented by the editorial board members and specialists, to whom they are connected. To avoid personal conflicts the opinion of the reviewer will not be released and her/his name will be handled confidentially. Papers which are not connected to the topics of the journal could be rejected without reviewing.

Bewertung

Die Texte für das Oncothermia Journal werden durch die Redaktion kontrolliert. Um Konflikte zu vermeiden, werden die Namen des jeweiligen Korrektors nicht öffentlich genannt. Artikel, die nicht zu den Themen des Journals passen, können abgelehnt werden.

Contents

Pastore C. Salvage therapy of a patient with metastatic uterine leiomyosarcoma combining chemotherapy and hyperthermia.....	9
Pastore C. Peritoneal carcinomatosis of gastric origin treated with a combination of Capecitabine and oncological hyperthermia: a case report	15
Fiorentini G. et al. Updates of the application of regional hyperthermia in the treatment of esophageal, colorectal, and pancreatic cancers	20
Van Gool S. W. et al. Addition of Multimodal Immunotherapy to Combination Treatment Strategies for Children with DIPG: A Single Institution Experience	37
Van Gool S. W. et al. Randomized Controlled Immunotherapy Clinical Trials for GBM Challenged	54
Mühlberg K. Impedance matching and its consequences for modulated electro-hyperthermia	83
Mühlberg K. Power transmission of EHY-2000 – A Hypothesis	104
Brockmann W.-P., Arnhold J., Denck M. Die Albumin-Carrier-Therapie – Anwendung in der onkologischen Praxis.....	117
Brockmann W.-P. Wird die Bedeutung des Serum-Albumins bei Malignom-Patienten mit Aszites, Ödemen und Pleuraergüssen unter- oder überschätzt? – MTX-HSA als Hilfe bei der Therapie	121
Brockmann W.-P. Das PET-CT im onkologischen Alltag – Eine wertvolle Hilfe zur Prognoseverbesserung	125
Roussakow S. Modulated electro-hyperthermia in the combined treatment of metastatic colorectal cancer a retrospective cohort study with meta-comparison.....	132

Initial publication

Salvage therapy of a patient with metastatic uterine leiomyosarcoma combining chemotherapy and hyperthermia

Carlo Pastore¹

¹Department of Oncology and Clinical Hyperthermia, Villa Salaria Clinic,
Rome, Italy

Citation: Pastore C. (2021): Salvage therapy of a patient with metastatic uterine leiomyosarcoma combining chemotherapy and hyperthermia, initial publication: Oncothermia Journal 30: 9 – 14, http://www.oncotherm.com/sites/oncotherm/files/2021-04/Pastore_Salvage.pdf

Abstract

Uterine leiomyosarcomas in the metastatic phase are unfortunately still burdened with a short period of survival. In this paper, I present the case of Mrs. KP, 48 years old, which came to my observation with the widespread pre-treated disease. A personalized combination of chemotherapy and hyperthermia has made it possible to prolong survival and improve quality of life.

Introduction

Uterine leiomyosarcomas mainly affect young adult women. The disease has considerable biological aggressiveness and frequently tends to metastasize in the lung and bone [1]. However, it is difficult to obtain even a partial disease response after the second therapeutic line. Herewith I report a case of uterine leiomyosarcoma treated with chemo-thermotherapy after the fourth therapeutic line. The case shows a considerable partial remission in combination with a marked improvement in the quality of life and prolonged the expected survival time. The response period was eight months.

Case report

KP had a histological diagnosis, after bilateral hysterectomy, of high-grade uterine leiomyosarcoma. After adjuvant chemotherapy and a year's follow-up with no evidence of residual disease, a single lung lesion was revealed, which underwent surgical resection. Subsequently, the appearance of a vertebral lesion and new lung lesions led to the consideration of multimetastatic disease with the need for periodic systemic pharmacological treatment. After the fourth systemic antineoplastic treatment scheme she came to my observation to set up further personalized treatment. The clinical condition was skeletal and pulmonary metastases with obvious respiratory symptoms. The massive pulmonary metastasis with severe impairment of respiratory capacity was documented by CT and spirometry tests. The patient had been on oxygen support. I worked out a protocol for the fifth therapeutic salvage line. The patient received a combination of biweekly bevacizumab [2][3] with 3 mg/kg dose, together with a daily dose of 100 mg temozolomide [2][4][5] from the first to fifth day of the week. The chemoprotocol was combined with impedance coupled deep capacitive radio frequency hyperthermia (EHY2000, Germany) in alternating days of sessions duration of 55 minutes on the chest [6][7][8][9][10]. After three months, a CT test showed partial response (figure 1, 2, 3) with a reduction of the various disease-related complaints, considerable loss of symptoms, mainly the dyspnoea improved.

The applied complex treatment was well tolerated without noteworthy side effects and continued with disease response for eight months.

Discussion

A neoplastic form in the metastatic phase is certainly drastically could suppress survival. Leiomyosarcomas do not differ. Getting a disease response in a patient who has already received four treatment lines is a rare, great achievement. Generally, the most promising treatment lines are the first two, and most frequently, the neoplastic cells become resistant to the third line of the treatment. The combination of original and personalized medications showed synergy in this case with the treatment of deep capacitive radio frequency hyperthermia. This single success cannot define anything conclusive but can be a notable, interesting inspiration for further study.

Key words: uterine leiomyosarcoma, chemotherapy, oncological hyperthermia, rescue therapy

References

- [1] Seagle BL, Sobecki-Rausch J, Strohl AE, Shilpi A, Grace A, Shahabi S. Prognosis and treatment of uterine leiomyosarcoma: National Cancer Database study. *Gynecol oncol*, 2017, Apr;145(1): 61-70
- [2] Takano M, Kikuchi Y, Susumu N, Kudoh K, Kita T, Kouta H, Goto T, Furuya K Complete remission of recurrent and refractory uterine epithelioid leiomyosarcoma using weekly administration of bevacizumab and temozolomide. *Eur J Obstet Gynecol Reprod Biol*. 2011 Aug;157(2):236-8
- [3] Wright JD, Powell MA, Rader JS, Mutch DG, Gibb RK. Bevacizumab therapy in patients with recurrent uterine neoplasms. *Anticancer Res* 2007 Sep-Oct;27(5B):3525-8.
- [4] Khusnutdinov RR, Boichuk SV. Mechanisms of Sensitivity of Soft Tissue Sarcoma Cells to Temozolomide. *Bull Exp Biol Med* 2017 Jun;163(2):260-262
- [5] Garcia del Muro X, Lopez-Pousa A, Martin J, Buesa JM, Martinez-Trufero J, Casado A, Poveda A, Cruz J, Bover I, Maurel J; Spanish Group for Research on Sarcomas. A phase II trial of temozolomide as a 6-week, continuous, oral schedule in patients with advanced soft tissue sarcoma: a study by the Spanish Group for Research on Sarcomas. *Cancer* 2005 Oct 15;104(8):1706-12
- [6] Falk MH, Issels RD. Hyperthermia in oncology. *Int J Hyperthermia*. 2001 Jan-Feb;17(1):1-18. Review.
- [7] Franchi F, Grassi P, Ferro D, Pigliucci G, De Chicchis M, Castigliani G, Pastore C, Seminara P. Antiangiogenic metronomic chemotherapy and hyperthermia in the palliation of advanced cancer. *Eur J Cancer Care (Engl)*. 2007 May;16(3):258-62
- [8] Lindner LH, Angele M, Dürr HR, Rauch J, Bruns C. [Systemic therapy and hyperthermia for locally advanced soft tissue sarcoma]. [Article in German]. *Chirurg* 2014 May;85(5):398-403
- [9] Issels RD. High-risk soft tissue sarcoma: clinical trial and hyperthermia combined chemotherapy. *Int J Hyperthermia* 2006 May;22(3):235-9
- [10] Shirafuji A, Shinagawa A, Kurokawa T, Yoshida Y. Locally-advanced unresected uterine leiomyosarcoma with triple-modality treatment combining radiotherapy, chemotherapy and hyperthermia: A case report. *Oncol Lett* 2014 Aug;8(2):637-641.

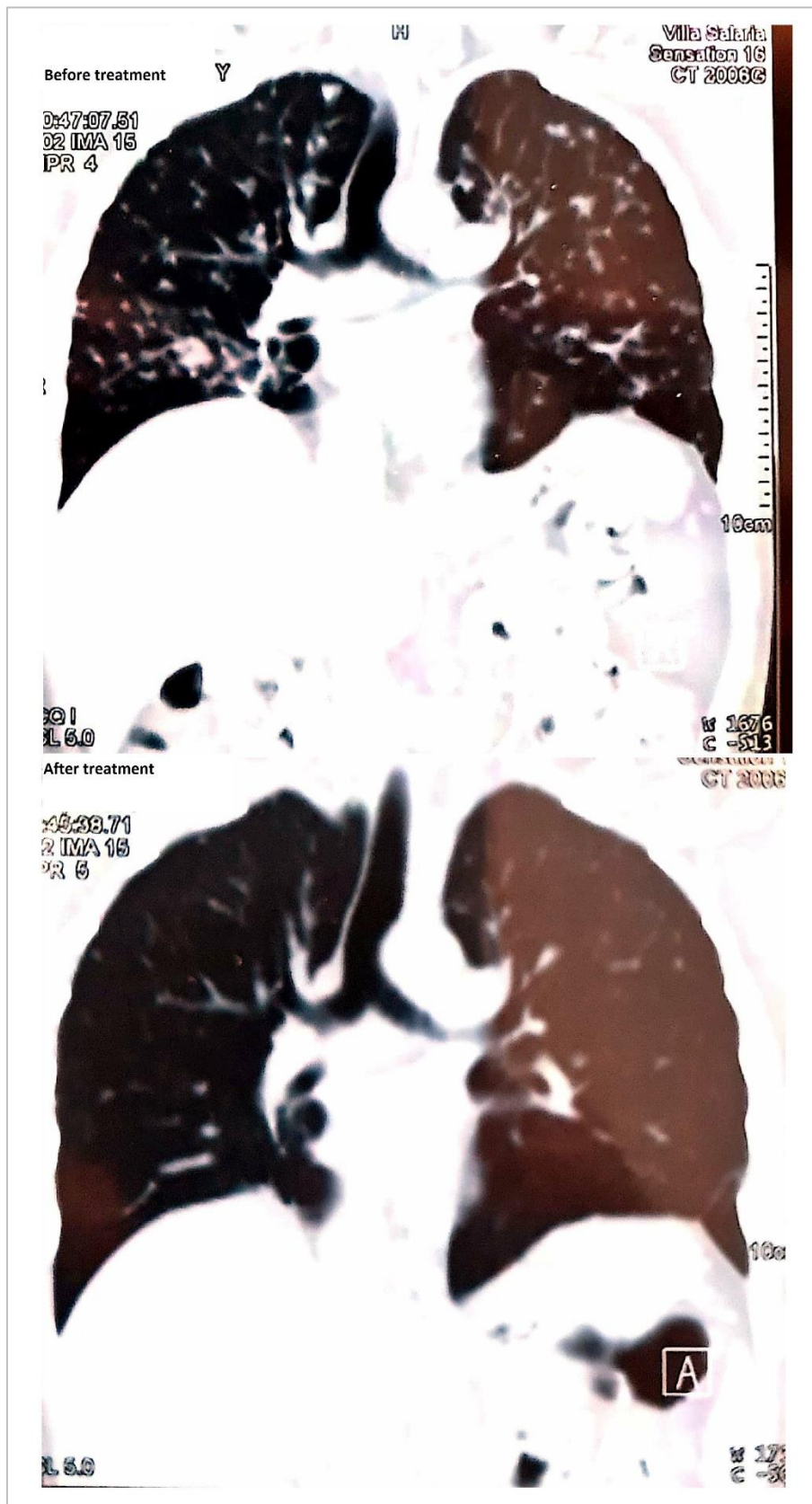


Figure 1

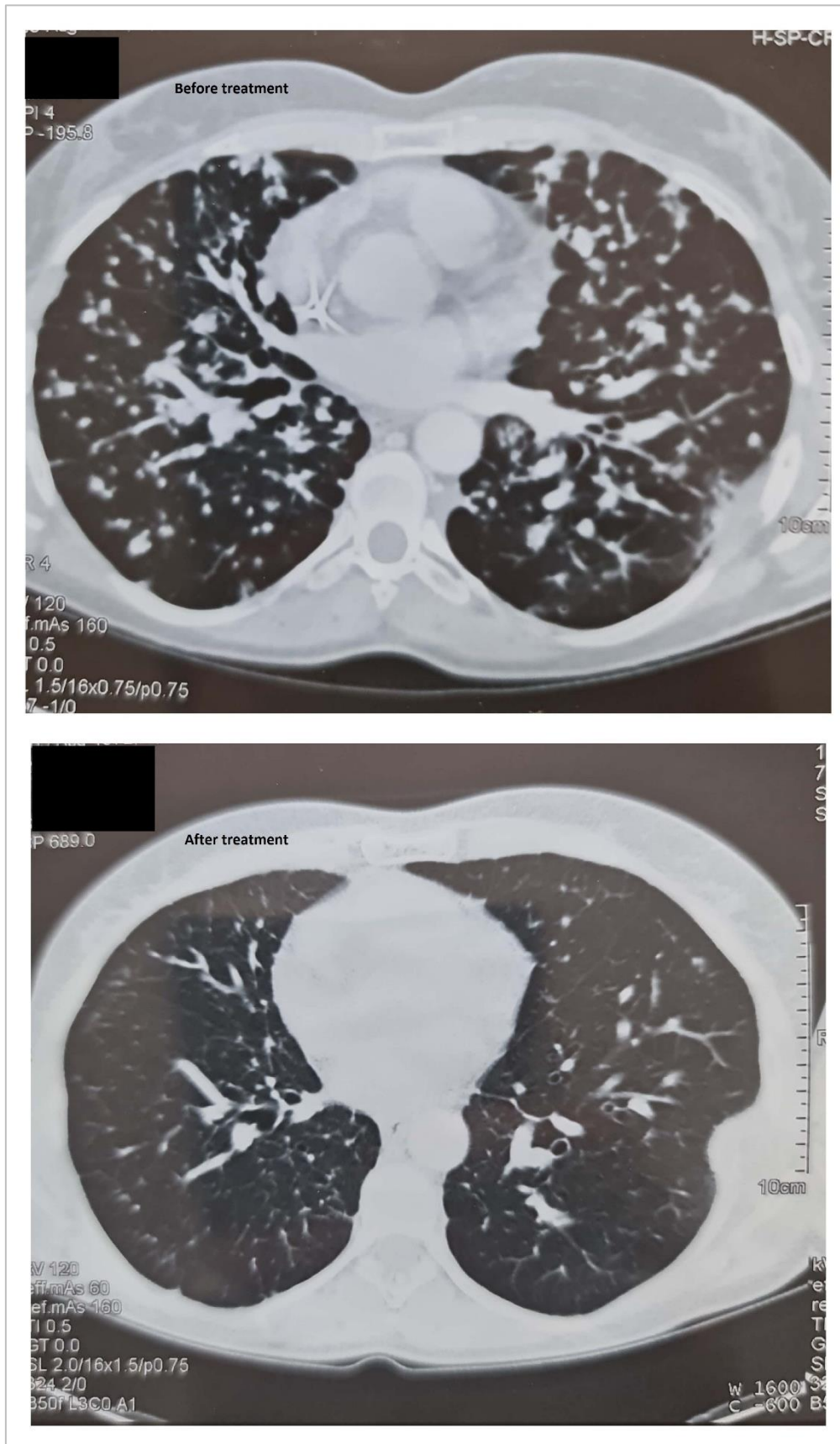
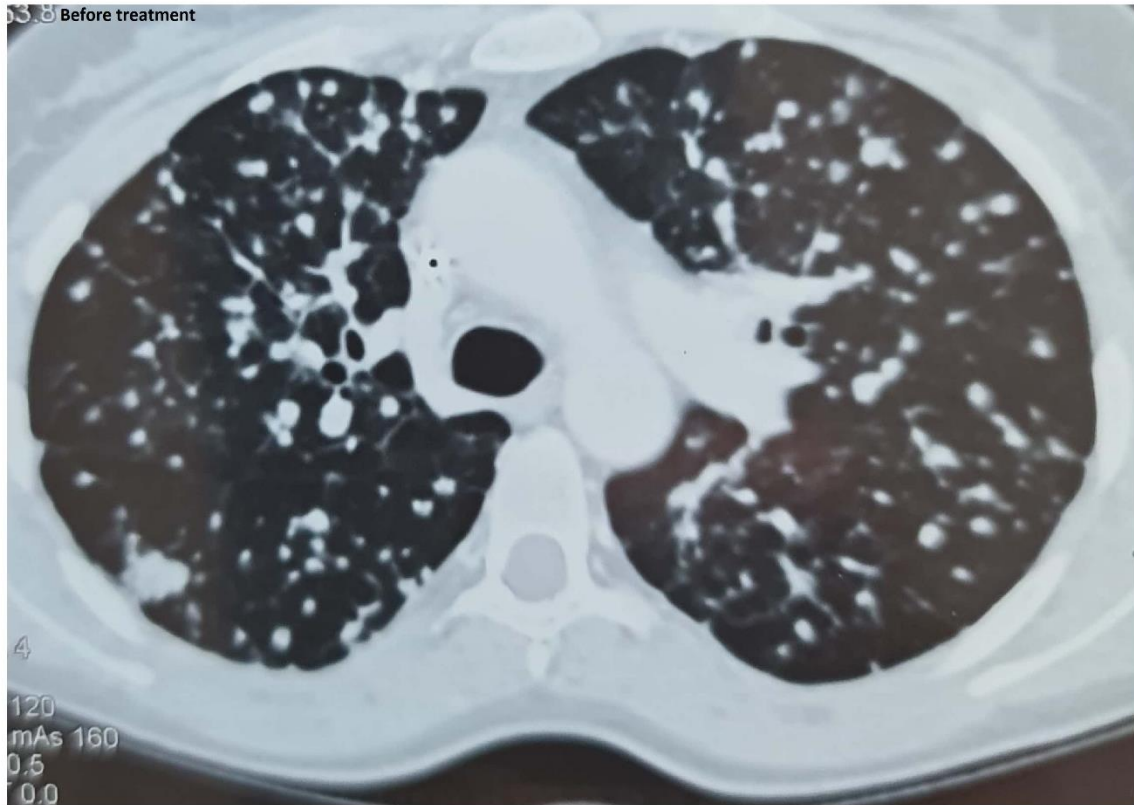


Figure 2

53.8 Before treatment



After treatment

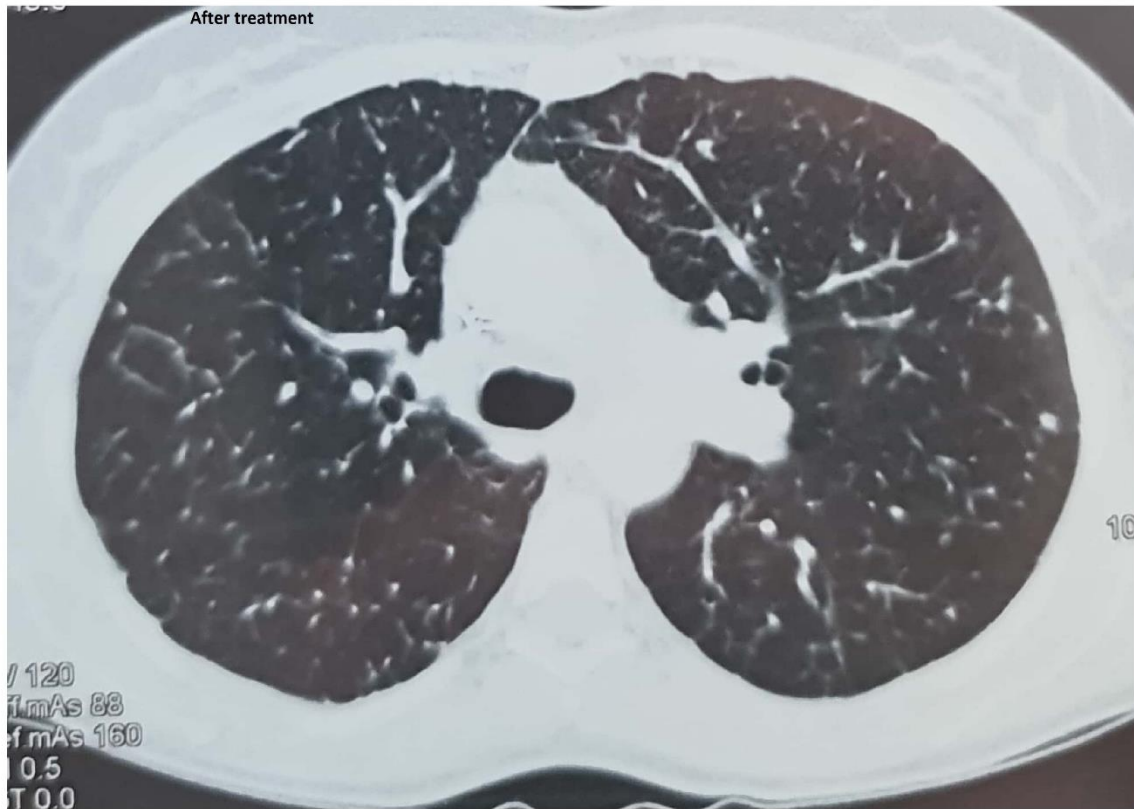


Figure 3

Initial publication

Peritoneal carcinomatosis of gastric origin treated with a combination of Capecitabine and oncological hyperthermia: a case report

Carlo Pastore¹

¹Operative Unit of Oncology and Oncological Hyperthermia, Villa Salaria Clinic,
Rome, Italy

Citation: Pastore C. (2021): Peritoneal carcinomatosis of gastric origin treated with a combination of Capecitabine and oncological hyperthermia: a case report, initial publication: *Oncothermia Journal* 30: 15 – 19,
http://www.oncotherm.com/sites/oncotherm/files/2021-04/Pastore_Peritoneal.pdf

Abstract

My objective in this article is to present and discuss a clinical case of peritoneal carcinomatosis originated from gastric cancer. The case was treated with complex therapy, combined whole-body and local hyperthermia treatments with chemotherapy. The applied multimodal approach achieved complete remission of the disease with a good quality of life.

Introduction

Recurrences and metastases in gastric cancer most frequently involve peritoneal carcinomatosis and are regularly detected only in the advanced gastric cancer stage [1]. These cases are often considered incurable. A clinical study shows that the mean survival is only 6.5 months [2], or even much less (2.2 months, [3]). A meta-analysis also shows the poor therapeutic outcome [4]. The patients with this disease have an extremely poor prognosis. The conventional palliative treatments' effect could provide some improvement when the disease is diagnosed in early stages [5]. These results are significantly worse than cases of other metastases. The peritoneal-plasma barrier [6] is probably one of the factors of poor clinical success. The relatively early detection could be obtained by pathologic investigation of tissue specimens, which may detect microscopic peritoneal carcinomatosis, which is usually not detectable in surgical interventions. The texture analysis could be a useful tool also for early diagnosis [7], and the therapy could be optimized with neoadjuvant treatments, including the hyperthermic intraperitoneal chemotherapy (HIPEC) [8]. It is also shown that in the cases of microscopic carcinomatosis, HIPEC has curative benefit after surgery, too [9]. The German database shows that the combination of cytoreductive surgery and HIPEC improves survival more than HIPEC alone [10]. The concomitant application, using intraoperative HIPEC with cisplatin is also feasible and safe [11].

The high cellular heterogeneity of the intraperitoneal carcinomatosis complicates the disease [12], and probably this is why surgery and HIPEC are relatively effective treatments.

My goal is to present a case showing a non-HIPEC oncological hyperthermia solution with success. The patient had advanced peritoneal carcinomatosis of gastric cancer.

Case presentation

72 years old male patient was diagnosed with stomach cancer by gastroscopy in 2009 May. The patient performed a partial gastric resection not followed by adjuvant chemotherapy as the removed locoregional lymph nodes were disease-free, and there was no evidence of spreading disease in other body regions. In November 2009, he began malaise, progressive weight loss, loss of appetite, abdominal pain until he came to emergency surgery for intestinal obstruction. The surgeon detected extensive peritoneal carcinomatosis, and although he had made a necessary temporal restore, he made a poor prognosis and predicted a very short survival. The patient came to my attention for supportive and palliative care. The therapy set at that moment was a combination of Capecitabine (1000 mg/m² bid per os), deep radiofrequency oncological hyperthermia (Oncotherm EHY-3010 ML device) twice a week for one hour without rest and three hours whole-body infrared hyperthermia (Heckel HT 3000 device) for five consecutive days for a month. The disease went into complete remission. The patient gained his weight by eight kg, had good and has continued appetite, with significantly improved quality of life. A CT scan documented the remission with contrast. The therapy continued for eighteen months with persistent remission. After eighteen months, a resurgence of the disease occurred, which proved intractable and led to death after three months.

Discussion

The prognosis of peritoneal carcinomatosis of gastric origin is extremely poor in such advanced cases as the patient reported above. My strategy differed from the usual hyperthermia applications. My hyperthermic idea was a combination of local, cellularly selective modulated electro-hyperthermia (mEHT) [13] and the whole body homogeneous heating [14] treatments. Deep radiofrequency capacitive hyperthermia is employed in combination with other methods (chemotherapy and radiotherapy) for years now and has proven to be a

valuable complementary therapy. The mEHT had proven as a local treatment in many clinical studies of various cancers [15], [16], and its locality enhanced by immunogenic effects [17]. Case reports proved its particular applicability [18], [19], and a Phase II study was performed to show how mEHT is effective in peritoneal carcinomatosis with malignant ascites [20]. The whole body hyperthermia with its physiological effect to increase the blood flow and through this, the drug delivery to the tumor is also well proven [21]. In contrast, the most common chemotherapies in HIPEC are Mitomycin C, Cisplatin, Doxorubicin, Paclitaxel, and 5-FU [22]. I had chosen Capecitabine in my hyperthermia protocol, as used by others too [23]. Capecitabine has a proven effect on gastric cancer, and it is very indicated for this clinical situation for the favorable tolerability profile [24] [25] [26].

The temperature rises from 40 to 43°C during the hyperthermic treatments in the irradiated tissue and the selected malignant cells. This temperature triggers apoptosis in diseased cells. There is an enhancement for any radiotherapy treatment. Locoregional vasodilatation favors the penetration of the drug where needed [27] [28] [29] [30] and also there has been a strengthening of local immunity, induced by the heat-mediated release of cytokines [31]. Vasodilation is even more crucial in poorly vascularized body districts than the peritoneum. Whole-body mild hyperthermia also enhances immune system activity, primarily through dendritic cell activation, and promotes drugs' penetration into tissues [32] [33].

Conclusion

The case report presented describes an unusual and very favorable clinical history. I had remarkable success with this protocol without using invasive surgical or laparoscopic HIPEC application. This case report may suggest a new approach to peritoneal disseminated cancer pathology and indeed may be the starting point to investigate further the effectiveness of this complex therapy protocol in other tumors with peritoneal dissemination.

Key words: gastric cancer, peritoneal carcinosis, hyperthermia, Capecitabine

References

- [1] Thomassen I , van Gestel YR , van Ramshorst B , et al. Peritoneal carcinomatosis of gastric origin: a population-based study on incidence, survival and risk factors. *Int J Cancer* 2014;134:622–8
- [2] Sadeghi B , Arvieux C , Glehen O , Beaujard AC , Rivoire M , Baulieux J , et al. Peri- toneal carcinomatosis from non-gynecologic malignancies: results of the EVOCAPE 1 multicentric prospective study. *Cancer* 2000;88:358–63
- [3] Chu DZ , Lang NP , Thompson C , Osteen PK , Westbrook KC . Peritoneal carcinomatosis in non-gynecologic malignancy. A prospective study of prognostic factors. *Cancer* 1989;63:364–7.
- [4] Lu Y, Jin Z, Zheng S, et.al. (2020) Hyperthermic intraperitoneal chemotherapy combined with systemic chemotherapy for gastric cancer peritoneal carcinomatosis, A protocol for systematic review and meta-analysis of randomized controlled trials, *Medicine*, 99:27, 1-5
- [5] Yarema R, Ohorchak M, Hyrya P, et.al. (2020) Gastric cancer with peritoneal metastases: Efficiency of standard treatment methods, *World Journal of Gastrointestinal Oncology*, 12(5): 569-581
- [6] Macrì A, Morabito F. (2019) The use of intraperitoneal chemotherapy for gastric malignancies. *Expert Rev Anticancer Ther*;19:879–888
- [7] Wang Z, Chen J-q, Liu J-l, et.al. (2019) Issues on peritoneal metastasis of gastric cancer: an update, *World Journal of Surgical Oncology*, 17:215, 1-8
- [8] Leiting JL, Grotz TE. (2018) Optimizing outcomes for patients with gastric cancer peritoneal carcinomatosis, *World J Gastrointest Oncol*, 10(10): 282-289
- [9] Pasqual EM, Bertozzi S, Londero AP, et.al. (2018) Microscopic peritoneal carcinomatosis in gastric cancer: Prevalence, prognosis and predictive factors, *Oncology Letters*, 15: 710-716
- [10] Rau B, Brandi A, Piso P, Pelz j, et.al. (2020) Peritoneal metastasis in gastric cancer? Results from the German database, *Gastric Cancer*, 23:11-22
- [11] Fan - 2021 -Phase II trial of prophylacticHYPEC - locally advanced gastric cancer after curative surgery.pdf
- [12] Ruiping Wang, Minghao Dang, Kazuto Harada, Guangchun Han, Fang Wang, Melissa Pool Pizzi, Meina Zhao, Ghia Tatlonghari, Shaojun Zhang, Dapeng Hao, Yang Lu, Shuangtao Zhao, Brian D. Badgwell, Mariela Blum Murphy, Namita Shanbhag, Jeannelyn S. Estrella, Sinchita Roy-Chowdhuri, Ahmed Adel Fouad Abdelhakeem, Yuanxin Wang, Guang Peng, Samir Hanash, George A. Calin, Xingzhi Song, Yanshuo Chu, Jianhua Zhang, Mingyao Li, Ken Chen, Alexander J. Lazar, Andrew Futreal, Shumei Song, Jaffer A. Ajani, Linghua Wang. (2021) Single-cell dissection of intratumoral heterogeneity and lineage diversity in metastatic gastric adenocarcinoma. *Nature Medicine*.; DOI: 10.1038/s41591-020-1125-8
- [13] Hegyi G, Szigeti GP, Szasz A. (2013) Hyperthermia versus oncothermia: Cellular effects in complementary cancer therapy. *Evid Based Complement Alternat Med* 2013:672873, <http://www.hindawi.com/journals/ecam/2013/672873/>
- [14] Mallory M, Gogineni E, Jones GC, Greer L, Simone CB 2nd (August 2015). "Therapeutic hyperthermia: The old, the new, and the upcoming". *Crit Rev Oncol Hematol*. 97 (15): 30018–4
- [15] Szasz AM, Minnaar CA, Szentmartoni Gy, et al. (2019) Review of the clinical evidences of modulated electro-hyperthermia (mEHT) method: an update for the practicing oncologist, *Frontiers in Oncology*, Vol. 9, Article 1012, pp. 1-8., <https://www.frontiersin.org/articles/10.3389/fonc.2019.01012/full>
- [16] Parmar G, Rurak E, Elderfield M, et.al. (2020) 8-year observational study on naturopathic treatment with modulated electro-hyperthermia (mEHT): A single-centre experience, in book *Challenges and solutions of oncological hyperthermia*, ed. Szasz A., Ch. 13, pp.227-266, Cambridge Scholars, <https://www.cambridgescholars.com/challenges-and-solutions-of-oncological-hyperthermia>
- [17] Szasz O. (2020) Local treatment with systemic effect: Abscopal outcome, in book *Challenges and solutions of oncological hyperthermia*, ed. Szasz A., Ch. 11, pp.192-205, Cambridge Scholars, <https://www.cambridgescholars.com/challenges-and-solutions-of-oncological-hyperthermia>
- [18] Iyikesici MS. (2020) Survival outcomes of metabolically supported chemotherapy combined with Ketogenic diet, hyperthermia, and hyperbaric oxygen therapy in advanced gastric cancer, *Nigerian Journal of Clinical Practice*, 23:734-40, <https://www.ncbi.nlm.nih.gov/pubmed/32367884>
- [19] Jeung TS, Ma SY, Yu J, et al. (2013) Cases that respond to oncothermia monotherapy, *Conf. Papers in Medicine*, Vol. 2013, Article ID 392480, Hindawi, <https://www.hindawi.com/journals/cpis/2013/392480/>
- [20] Pang CLK, Zhang X, Wang Z, et.al. (2017) Local modulated electro-hyperthermia in combination with traditional Chinese medicine vs. intraperitoneal chemoinfusion for the treatment of peritoneal carcinomatosis with malignant ascites: A phase II randomized trial, *Molecular and Clinical Oncology*, 6:723-732, <https://pubmed.ncbi.nlm.nih.gov/28529748/>

- [21] Lassche G, Crezee J, Van Herpen CML (2019) Whole-body hyperthermia in combination with systemic therapy in advanced solid malignancies; *Crit Rev Oncol Hematol.* 139:67-74., doi: 10.1016/j.critrevonc.2019.04.023
- [22] Parray A, Gupta V, Chaudhari VA, et.al. (2020) Role of intraperitoneal chemotherapy in gastric cancer, *Surgery in Practice and Science*, 4, 10025, doi: 10.1016/j.sipas.2020.100025
- [23] Brenkman HJF, Paeva M, van Hillegersberg R, et.al. (2019) Prophylactic hyperthermic intraperitoneal chemotherapy (HIPEC) for gastric cancer – A systematic review, *J Clinical Medicine*, 8, 1685, doi: 10.3390/jcm8101685
- [24] Rosati G, Ferrara D, Manzione L (2009) New perspectives in the treatment of advanced or metastatic gastric cancer. *World J Gastroenterol.* Jun 14;15(22):2689-92
- [25] Pieters A, Laurent S, Dero I, Van Damme N, Peeters M. (2008) The role of oral fluoropyrimidines in the treatment of advanced gastric cancer. *Acta Gastroenterol Belg.* Oct-Dec;71(4):361-6. Review
- [26] Benson AB. (2008) Advanced gastric cancer: an update and future directions. *Gastrointest Cancer Res.* Jul;2(4 Suppl):S47-53
- [27] Beuth J. (2010) Evidence-based complementary oncology: innovative approaches to optimise standard therapy strategies. *Anticancer Res.* May;30(5):1767-71
- [28] Minakuchi H, Hirayama R, Sawai S, Kawachi Y, Tominaga S, Nihei Z, Mishima Y. (1990) Clinical trials of long-term RF local hyperthermia for advanced gastric cancer. *Jpn J Surg.* 1990 Mar ;20 (2):238-9
- [29] Dubois JB, (1992) [Hyperthermia in the treatment of cancers] *J Chir (Paris).* Apr;129(4):227-31. Review. French.
- [30] Franchi F, Grassi P, Ferro D, Pigliucci G, De Chicchis M, Castigliani G, Pastore C, Seminara P. (2007) Antiangiogenic metronomic chemotherapy and hyperthermia in the palliation of advanced cancer. *Eur J Cancer Care (Engl).* May;16(3):258-62
- [31] Ostapenko VV, Tanaka H, Miyano M, Nishide T, Ueda H, Nishide I, Tanaka Y, Mune M, Yukawa S. (2005) Immune-related effects of local hyperthermia in patients with primary liver cancer. *Hepatogastroenterology.* Sep-Oct;52(65):1502-6
- [32] Ostberg JR, Repasky EA (2000) Use of mild, whole body hyperthermia in cancer therapy. *Immunol Invest* May;29(2):139-42
- [33] Park K (2013) Improved tumor targeting by mild hyperthermia *J Control Release* Apr 28;167(2):220. doi: 10.1016/j.jconrel.2013.03.002

Initial publication

Updates of the application of regional hyperthermia in the treatment of esophageal, colorectal, and pancreatic cancers

Giammaria Fiorentini^{1,2}, Donatella Sarti¹, Girolamo Ranieri³, Cosmo Damiano Gadaleta⁴, Caterina Fiorentini⁵, Tommaso Carfagno⁶, Carlo Milandri⁷, Andrea Mambrini⁸, Stefano Guadagni⁹

¹Department of Onco-Hematology, Azienda Ospedaliera "Ospedali Riuniti Marche Nord"
Pesaro, Italy

²Oncology Service and Unit of Hyperthermia, Private Clinic Ravenna33,
Ravenna, Italy

³Interventional and Integrated Medical Oncology, National Cancer Research Centre,
IRCCS Istituto Tumori "Giovanni Paolo II",
Bari, Italy,

⁴Integrated Section Translational Medical Oncology, Interventional Radiology Unit,
National Cancer Institute of Bari,
Bari, Italy

⁵Department of Medical Biothechnologies, Division of Cardiology, University of Siena,
Siena, Italy

⁶Department of Radiotherapy, University Hospital of Siena,
Siena, Italy

⁷Medical Oncology Unit, San Donato Hospital
Arezzo, Italy

⁸Oncology Department, Apuane Hospital,
Massa-Carrara, Italy

⁹Applied Clinical Sciences and Biotechnology, Section of General Surgery, University of L'Aquila,
L'Aquila, Italy

Citation: Fiorentini G. et al. (2021): Updates of the application of regional hyperthermia in the treatment of esophageal, colorectal, and pancreatic cancers, initial publication: *Oncothermia Journal* 30: 20 – 36,
http://www.oncotherm.com/sites/oncotherm/files/2021-04/Fiorentini_Updates.pdf

Abstract

The therapeutic value of regional hyperthermia (RHT) in oncological treatments has been known for years. Several studies report RHT efficacy for tumor response and survival. RHT can also be used in combination with chemotherapy (CHT), radiotherapy (RT), chemoradiotherapy (CRT), and immunotherapy, enhancing their benefit, also in the treatment of gastrointestinal tumors as esophageal, colorectal, and pancreatic cancer. However, RHT has not yet become a common therapy in regular clinical practice due to the difficulty in measuring the temperature increase inside the tissues, the long duration of treatment, the need to have dedicated nurses and doctors, adequate equipment and facilities.

Modulated electro-hyperthermia (mEHT) is a recent RHT method that targets malignant cell membranes and the extracellular matrix, allowing deep tumor sensitization, notwithstanding the adipose tissue's thickness and overcoming the issue of homogenous heating.

Several studies confirm the advantage of RHT and mEHT association to CRT, CHT, and RT as neoadjuvant and palliative setting in esophageal, colorectal, and pancreatic cancer. This article summarizes the available data of RHT for these tumors.

Key words: regional hyperthermia, modulated electro-hyperthermia, colorectal cancer, esophageal cancer, pancreatic cancer

Introduction

Regional hyperthermia (RHT) efficacy in remission of malignant tumors has been known for decades. RHT increases the tissue/body temperature with an external radiofrequency (RF) electromagnetic field. The modern technologies of local/locoregional heating offer safe therapies in clinical practice. The mild temperatures of RHT (39.5–43°C) show beneficial effects accompanied with increased safety by optimizing the treatment for minimal hot spot occurrence [1], [2]. Temperature rise >43°C, indeed, has potential risks, such as damage of surrounding normal tissues and enhancement of blood flow that can potentially increase malignant cells dissemination and distant metastases [3].

Nowadays, an increasing number of clinical studies show RHT efficacy in the treatment of different types of cancers. However, the number of clinics using the RHT method in their practice is suboptimal [1].

The primary biological rationale of heat utilization is enhancing radiation efficacy, increasing the delivery and permeability of various chemotherapeutic medications, and supporting the immunotherapy effects. Heat triggers tumor perfusion and oxygenation changes, inhibiting DNA repair mechanisms and stimulating the immune system [1], [2]. In association with RHT, local radiotherapy increases tumor immunogenicity and systemically acts through immune-mediated abscopal effects [3]. Modulated electro-hyperthermia (mEHT) is a recent RHT method that targets malignant cell membranes and the extracellular matrix, allowing deep tumor sensitization, notwithstanding the adipose tissue's thickness. The complementary application of regional hyperthermia and mEHT with chemo-(CHT) or radiotherapy (RT) is reported to be successful in several types of tumors, including esophageal, pancreatic, and colorectal cancers [3], [4], [5].

The analysis of elder evidence-based clinical data of the five-year survivals concluded [6], that the 5-year survivals have been changing only a little from 1950 to 1995, and these changes depend more on the better diagnosis than on the therapy. The contribution of curative and adjuvant cytotoxic chemotherapy to 5-year survival in adults (counting 22 different localizations) was estimated to be 2.3% in Australia and 2.1% in the USA [7] in 2004 over 20 years. It is a minor contribution to the observed 5 years survival rate, which is over 50% in the same time period.

The progress, of course, was debated: “We are losing the war against cancer” [8], which was immediately corrected in a broader view, [9], taking into account the successes in pediatric cancer and in the quality of life of the patients during the curative and palliative treatments. This picture was a little diluted: “Perhaps not lost, but

certainly not won.” [10]. This was also supported ten years later [11]. The emotional aggravation induces very hurting opinions as the double Nobel-laureate L. Pauling formulated it, “Everyone should know that the ‘war on cancer’ is largely a fraud” [12]. This is naturally hurting but completely false opinion, which was induced by this excellent researcher’s heated emotional background. The emotions are not surprising even nowadays because cancer is the number one disease in many countries, touching not only the suffering patients but also their families, friends colleagues, and motivating despair in society.

Filtering out the extreme opinions, the statistical data [13] supported the shadowed picture even 20 years ago: the mortality data from 1975-2000 are fairly constant, while the incidence (morbidity) slightly grows in the same time-interval. (Interestingly, the incidence has a definite peak in the first half of the 1990s in the group of males, but the mortality does not follow it.) Unfortunately, neither the incidence-rate nor the mortality rate correlated with the five-year survival [6] for the same localization. It showed the imperfectness that cancers with high incidence- and high mortality-rate growths, like lung, liver, brain, and pancreas, had low gain in their 5-year survival in that time. This is the essence of the negative answer to the question [6]: “Are increasing 5-year survival rates evidence of success against cancer?” Today the situation had improved dramatically. We have a significant improvement in mortality data, significantly elongated survival time characterizes the nowadays development, however, in the area of gastrointestinal cancer, especially in pancreatic localization, we see less development of successes of conventional therapies than for other localizations in the human body.

Our objective is to show the possible addition to the conventional therapies by complementary application of hyperthermia. We review the updated clinical applications of RHT complementary with RT and/or CHT in the therapies of esophageal, colorectal, and pancreatic cancers. We include into this review a new emerging hyperthermia method: the modulated electro-hyperthermia (mEHT), which has promising data in gastrointestinal treatments [14], [15] in neoadjuvant treatment [16], [17], or complementary to adequate CHT, treatment of the frequent colorectal metastases in liver [18]. The feasibility of mEHT in the therapies of pancreatic cancer is especially promising [19], [20], [21].

Types of hyperthermia

There are different hyperthermia types: superficial hyperthermia, deep/regional hyperthermia, whole-body hyperthermia, interstitial hyperthermia, intraperitoneal laparoscopic hyperthermia, of hyperthermia in the body cavities or lumens. [22].

Whole-body hyperthermia increases the entire body’s temperature up to a maximum of 41.8°C, using thermal conduction or radiant infrared techniques. Interstitial hyperthermia places heating electromagnetic devices (needles or catheters) directly inside the tumor. This therapy’s main advantage is that the heating occurs directly inside the tumor, enabling it to reach higher local tumor temperatures and lower normal surrounding tissue temperatures. Similarly, hyperthermia can be achieved by inserting heating devices into natural body cavities and lumens with tumors [22]. Deep/regional hyperthermia can increase the temperature of a portion of the body (at the tumor site) up to the depth of >5 cm with electromagnetic fields, minimizing the heating of the surrounding tissue [22].

Superficial hyperthermia heats tissues <5cm in depth from the body’s surface, using electromagnetic fields. As in all types of hyperthermia, the blood flow variability within the treated region also contributes to the temperature variation within the tumor region [22].

Regional Hyperthermia

Different methods are used for regional hyperthermia, such as using infrared-A (IR-A) radiation, microwave radiation by antenna-array, capacitive, and modulated electro-hyperthermia techniques.

The water filter IR-A radiation method uses a light source (halogen lamp at 24 V/150W) and a water-filter which is built in as a closed cuvette and absorbs the energy, avoiding painful sensations and burns of the skins [23]. Both IR-A radiation microwave radiation and capacitive systems are used for superficial hyperthermia to tumors

infiltrating up to 4 cm into the tissue, such as melanoma [24]. Two electrodes are positioned on opposite sides of the body, and the heat is produced by the electric current flowing between them. The electrodes are placed in direct contact with the body surface through a water bolus.

There are several types of commercially available radiative superficial systems, including flexible microwave applicators. They all create heating at frequencies of 434 to 915 MHz and are positioned directly in contact with the treated surface [24]. Both methods allow to homogeneous target heating and limiting hot spots. However, radiative heating yields more favorable temperature distributions than capacitive heating, especially within heterogeneous tissues [24].

Modulated electro-hyperthermia

Tumor blood flow increase is rather limited upon heating; hence, the heat dissipation is slower than that in normal tissues. This is why tumor temperature rises higher than that in normal tissue during hyperthermia [3]. However, a tumor's homogenous heating to a specified temperature is rather challenging due to the heterogeneous distribution of vasculature inside malignant tissue. The tumor blood flow varies widely among different tumor types and inside the same tumor, especially in the presence of necrotic areas within the tumor [3].

A new method has been recently developed to improve the results and reduce thermal therapy's adverse effects: the modulated electro-hyperthermia (mEHT) [25]. This method targets malignant cell membranes and the extracellular matrix. This allows sensitizing deep tumors, notwithstanding the adipose tissue's thickness, and to heating the malignant cells [9] selectively. mEHT uses impedance coupled capacitive arrangement with 13.56 MHz (EHY-2000+, OncoTherm Ltd., Germany) and has comparable benefits to other types of hyperthermia for a variety of tumors: hepatocellular carcinoma, rectal, cervical, brain, lung, and pancreatic cancers, improving local disease control and in some cases, the survival [25], [26], [27], [28], [29]. This type of hyperthermia increases malignant cells' temperature to 41.5°C for >90% of treatment duration [26].

Literature search

The literature search was performed in this narrative review in the databases PubMed-MEDLINE, Embase, Cochrane, and ClinicalTrials.gov. with the search terms: hyperthermia, pancreatic, gastrointestinal, esophageal, colon, rectal, colorectal, anal cancer. 934 articles were retrieved. The further selection included only full-text articles in the English language, reporting results from the observational or experimental trial about tumor response, survival or progression-free survival or toxicity, among these were published in the time interval between 2000 and 2020. We selected 38 articles and divided these according to tumor type, and finally, only 25 original articles were included in tables. The other papers were used for the introduction and conclusions sections.

Esophageal Cancer

The prognosis of esophageal cancer remains poor, and the overall survival (OS) after potentially curative surgery is 5–20% [30], [31]. Several studies on neo-adjuvant chemotherapy (NCHT) alone fail to prove the benefit of this pre-operative treatment. However, promising results have been achieved with the combination of heat and chemotherapy in this setting [31], [32], [33], [34].

NCHT or chemoradiotherapy (CRT) combined with RHT have positive results concerning survival and tumor response of esophageal cancer patients (table 1).

Table 1) Esophageal cancer

Author	Year	Treatment	Hyperthermia protocol	No. of Pts. (n)	Survival	Tumor Response	RHT related toxicity
Sheng [34]	2017	CRT with cisplatin-based regimens+RHT	Radiofrequency capacitive heating device, with microwave spiral strip applicators, HRL-001, within 30 min from RT, or 2h after CHT	50	3-year OS=42.5% PFS= 34.9%	ND	Pain (G1-2) =38.0%
Nishimura [29]	2015	CRT with cisplatin/5-fluorouracil, oral fluoropyrimidine and irinotecan+RHT	8-MHz radiofrequency, capacitive heating system (Thermotron RF-8), at 400-1400 W (median 1200 W) for 50 min once or twice a week	11	1 year OS=72.7% 2 years OS=54.5% 5 years OS=9.1%	CR=27% SD=45%	ND
Nakajima [32]	2015	CRT with docetaxel + RHT	ND	24	3 years OS=56.3% 5 years OS=50.0%	DCR=41.7% CR=17.6%	toxicity G2 occurred in six patients
Hulshof [33]	2009	Neoadjuvant CRT with carboplatin and paclitaxel+ RHT	home-made AMC (academical medical center), phased array of four 70MHz antennas, at a power of 800 W for 1.5 hour	28	1 year OS=79% 2 years OS=57% 3 years OS= 54%	CR=19% PR=31% SD=23%	pain (sternal or shoulder) or general discomfort in seven patients and in two patients
Albregts [31]	2009	Neoadjuvant CHT with cisplatin and etoposide+HRT	home-made AMC (academical medical center), phased array of four 70MHz antennas, at a power range of 800-1000 W	26	1 year OS=86% 2 years OS=76%	CR=9%	Discomfort in 1 patient and 'sock-like' sensory neuropathy (G2) in 1 patient

RT = radiotherapy, RHT = hyperthermia, OS = overall survival, SR = survival rate, Clinical benefit = complete response + partial response + stable disease, CHT = chemotherapy, DFS = Disease free survival, CRT = chemoradiotherapy, LRF5 = local relapse-free survival, n.s. = not significant, ND = not reported

Neoadjuvant CRT with docetaxel associated with RHT results in a response rate of 41.7% with a CR of 17.6% after surgery. This treatment has low toxicity, and 3- and 5-year survival rates are 56.3% and 50.0%, respectively [34].

A phase II study with chemotherapy (carboplatin and paclitaxel) and radiotherapy in association with RHT as neoadjuvant treatment results are in good locoregional control and overall survival for esophageal cancer patients that have all R0 resection. Tumor response is complete response (CR), partial response (PR), and stable disease (SD) in 19%, 31%, and 23% of patients, respectively. The survival rates at 1, 2, and 3 years are 79%, 57%, and 54%, respectively. Quality of life is improved for these patients, and the toxicity is low [33]. Similar results in survival are reported by another phase I/II study, showing 1- and 2-year survival rates of 69 and 62%, respectively [31].

Intensity-modulated radiotherapy (IMRT) in association with hyperthermia results in a 3-year progression-free survival (PFS) rate and overall survival (OS) rate was 34.9% and 42.5%, respectively, with low toxicity and excellent local control of esophageal cancer with supraclavicular lymph node metastasis [34].

The results of a meta-analysis comparing the CRT+RHT and RT groups show that RHT increased significantly the 1-, 2-, 3- and 5-year OS of esophageal cancer patients; decreased both recurrence, distant metastases, and gastrointestinal reaction rates [30]. This evidence of CRT+RHT benefits in esophageal cancer neoadjuvant therapy is very promising. However, further randomized clinical trials with a more significant number of patients are required to confirm these data.

Colorectal cancer

Colorectal cancer (CRC) is the third most common cause of cancer death in both men and women in the United States [35]. In the past decades, neoadjuvant radiotherapy alone or in association with chemotherapy followed by surgery has become standard treatment for advanced rectal cancer [36]. CHT is used to enhance RT effects of radiotherapy. RHT is another method to amplify radiotherapy, overcoming the low oxygen concentrations that are present in large size tumors and hamper the effect of radiotherapy. RHT, indeed, increases the tumor blood flow and hence promotes the RT with the tissue oxygenation [37].

Neoadjuvant CRT + RHT results in greater 5-year long-term local control (98% vs 87%, $p=0.09$) and OS (88% versus 76%, $p=0.08$) than CRT alone in locally advanced non-metastatic rectal cancer [38]. Similar results are reported in other studies on neoadjuvant CRT + RHT in locally advanced non-metastatic rectal cancer, resulting in 5-year OS ranging 60-87.3% (table 2), distant metastases-free survival (DMFS) and local control (LC) of 79.9% and 95.8% respectively [39], [40], [41].

In particular, a study compares OS of CRT alone or combined with RHT and reports that the complementary therapy shows longer OS than CRT alone (5 years OS=76% versus 88% $p < 0.08$) [38]. This improvement in survival is also observed when the neoadjuvant CRT and RHT is performed for anal cancer treatment with 5 years OS (95.8 vs. 74.5%, $P=0.045$), disease-free survival (DFS=89.1 vs. 70.4%, $P=0.027$), and the local relapse-free survival (LRFS =97.7 vs. 78.7%, $P=0.006$) is more favorable than CRT alone [42].

As concerning the tumor response, the disease control rates (DCR) of CRT combined to RHT range is 28.5%-94.8% in rectal cancer patients (table 2) [43], [44], [45], [46], [47]. The association of RHT to CRT in neoadjuvant treatment of rectal cancer does not increase the toxicity of CRT, and the hyperthermia-related adverse events were mainly of mild-moderate intensity and are reported by 26-34% of patients [43], [44], [45], [46], [47].

mEHT in association with CHT is used in a study for the treatment of metastatic colon cancer patients with good tumor response rates and survival; indeed, the DCR is 95% at 90 days and 89.5% at 3 months, and PFS is 12.1 months (range 3.5–32.6 months) [48]. Another study applies mEHT in association with CRT to treat rectal cancer patients, reporting minimal, moderate, near-complete, and complete regression of primary tumor of 15.0%, 51.7%, 18.3%, and 15.0%, respectively [49]. In both studies, the mEHT is well tolerated, with mostly mild hyperthermia toxicity [48], [49].

Table 2) Colorectal and anal cancer

Author	Year	Type of tumor	Treatment	Hyperthermia protocol	No. Pts. (n)	Survival	Tumor Response	RHT related toxicity
Ranieri [49]	2020	Metastatic colon cancer	CHT with Beva+FOLFOX4+mEHT	mEHT with 13.56 MHz (EHY-2000) twice a week (8 times)	40	PFS=12.1 months (range 3.5–32.6 months).	90 days: PR=30% SD=65% PD=5% DCR=95% 3 months: CR=5.3%, PR=26.3%, SD=55%, PD=10%, DCR=89.5%	mild positional pain in four patients, Erythema in the target area in 3 patients, power-related pain occurred in two cases
You [48]	2020	Rectal cancer	Neoadjuvant CRT with 5-fluorouracil or oral capecitabine+ mEHT	mEHT with 13.56 MHz (EHY-2000) twice a week (8 times)	60	ND	minimal, moderate, near total, and total regression of primary tumor was 15.0%, 51.7%, 18.3% and 15.0% respectively.	26.7% developed thermal toxicity, which was mostly G1 (93.8%)
Zwirner [39]	2018	Locally advanced rectal cancer	Neoadjuvant CRT with 5-fluorouracil +RHT	Deep regional hyperthermia once or twice a week	86	5-years OS =87.3% DFS =79.9 LRFS =95.8%	ND	ND
Gani [38]	2016	Rectal cancer	Neoadjuvant 43 CRT with 5-fluorouracil vs 60 CRT with 5-fluorouracil +RHT	RHT with Sigma Eye or Sigma-60 applicator (BSD 2000/3D) once or twice a week	103	5-years OS= 76% vs 88% p < 0.08 DFS= 73% vs 78% LRFS =77% vs 75%	ND	ND

Author	Year	Type of tumor	Treatment	Hyperthermia protocol	No. Pts. (n)	Survival	Tumor Response	RHT related toxicity
Shoji [43]	2015	Rectal cancer	Neoadjuvant CRT with Capecitabine+RHT 33 were resected 16 non-resected	RHT with 8 MHz RF capacitive heating device (Thermotron RF-8) after RT for 50 minutes (5 weeks)	49	ND	DCR=28.5%	One grade 3 patient had perianal dermatitis, 29.7% suffered pain, and 2.1% had subcutaneous induration
Kato [44]	2014	Rectal cancer	Neoadjuvant CRT+RHT	RHT with Thermotron RF-8, Once a week (2-5 times)	48	ND	CR=29.2%	No hematological toxicity
Schroede [45]	2012	Locally advanced rectal cancer	Neoadjuvant 61 CRT with 5-Fluorouracil+RHT vs 45 CRT with 5-Fluorouracil	RHT with BSD-2000 Once or twice a week (1-9 times)	106	ND	pCR rate 16.4% vs 6.7%	34% hyperthermia discontinuation, due to pain or hot-spot phenomena, urinary tract infections, hypertension, tachycardia or severe skin toxicity
Kang [47]	2011	Locally advanced rectal cancer	Neoadjuvant CRT with 5-FU, leucovorin and mitomycin C+RHT	RHT with 8-MHz radiofrequency capacitive heating device (Cancermia GHT-RF8) twice a week during RT	214	5 years OS=73.9% DFS=75.1% LRFS=93.9% DMFS=79.8%	DCR=50.9%	ND

Author	Year	Type of tumor	Treatment	Hyperthermia protocol	No. Pts. (n)	Survival	Tumor Response	RHT related toxicity
Maluta [40]	2010	Locally advanced rectal cancer	Neoadjuvant CRT+RHT	RHT with BSD-2000 Once a week (1-5 times)	76	5-years OS=86,5% DFS=74,5% LRFS=73,2%	CR=23,6% DCR=94,8%	G0-2 general or local discomfort in 15%, no G3, G4 Subcutaneous burns in 5.2%
Rau [41]	2000	primary rectal cancer (PRC)	Neoadjuvant CRT with 5-fluorouracil and leucovorin +RHT	RHT with BSD-2000 Once a week (1-5 times)	37	5-year OS=60%	DCR=59%	none
		recurrent rectal cancer (RRC)			18		DCR=28%	
Ott [42]	2019	Squamous anal cancer	CRT with 5-fluorouracil and mitomycin C vs CRT with 5-fluorouracil and mitomycin C + RHT	RHT with the BSD 2000-3D- and BSD 2000-3D-MR-Hyperthermia System once or twice weekly (5-10 times)	112	5 years OS= 95.8 vs. 74.5%, P = 0.045 DFS=89.1 vs. 70.4%, P = 0.027 LRFS =97.7 vs. 78.7%, P = 0.006	ND	Comparable toxicity for Grades 3–4 early side effects: skin reaction, diarrhea, stomatitis, and nausea/emesis, with the only exception of a higher hematotoxicity rate for the CRT+RHT group (66 vs. 43%, P= 0.032).

RT = radiotherapy, RHT = hyperthermia, OS = overall survival, SR = survival rate, Clinical benefit = complete response + partial response + stable disease, CHT = chemotherapy, DFS = Disease free survival, CRT = chemoradiotherapy, LRFS = local relapse-free survival, ND = not specified

Neoadjuvant CRT in association with RHT and mEHT does not increase toxicity and allows to achieve encouraging results in terms of tumor response and survival in the rectal, colon, and anal cancer patients. Further randomized studies are required to confirm these data.

Pancreatic cancer

Pancreatic cancer has a poor prognosis with a 5-year OS < 10%. This may be because pancreatic cancer is quite resistant to RT and CHT because of its hypoxic microenvironment that diminishes sensitivity to these therapies [50]. Most used CHT schedules include gemcitabine-based regimes, nab-paclitaxel, and for fit patients, the FOLFIRINOX (leucovorin, fluorouracil, irinotecan, and oxaliplatin) [51], [52]. These drugs, however, have high toxicity and often low efficacy. For this reason, the association of RHT to conventional CHT and RHT has also been introduced for pancreatic cancer treatment, enhancing the drug delivery and diffusion inside the tumor, improving blood flow, reducing hypoxia, and inhibiting DNA repair, hence enhancing tumor apoptosis.

Three studies compared the survival of locally advanced pancreatic cancer after treatment with the combination of CRT and RHT versus CRT alone. Their results show that the addition of RHT increased significantly the survival: OS=8.8 vs. 4.9 months ($p = 0.02$), OS= 15 vs 11 months ($p = 0.025$), 1 year OS=80% vs 57% ($p=0.021$) and PFS=18.6 vs. 9.6 months ($p = 0.01$) (table 3) [53], [54], [55].

The association of CHT to RHT also results in encouraging survival: median OS of 12.9 -17.7 months, 1 year OS=41%, and 2 years OS=15% [56], [57], [58]. As concerning the tumor response of locally advanced pancreatic carcinoma, the association of CHT to RHT resulted in DCR of 50-61%, [58]. The treatment is well tolerated with a toxicity of G2 pain and a skin rash, and 5% grade III-IV toxicity [54], [58].

A significant increase in survival is also observed when CRT is associated with mEHT than CRT alone, as reported by Fiorentini et al. (OS= 18.0 vs. 10.9 months, $p<0.001$) [26]. The other two studies report similar survivals on mEHT to treat locally advanced pancreatic carcinoma, OS of 8.9-15.8 months and PFS of 3.9-12.9 months [59], [60]. mEHT also shows high tumor response in locally advanced pancreatic carcinoma with DCR of 71-96% and safety without grade III-IV toxicity [26], [59]. These better tumor response and survival results of CHT and/or RT in association with mEHT are also observed in geriatric (>65 years) patients with pancreatic cancer. Indeed, a greater DCR, OS, and PFS are reported for the mEHT group and no-mEHT group in this population (table 3) [61].

Table 3) Locally advanced pancreatic cancer

Author	Year	Treatment	Hyperthermia protocol	No. of Pts. (n)	Survival	Tumor Response	RHT related toxicity
Sarti [61]	2020	mEHT+RT or CHT with gemcitabine regimen vs RT or CHT	mEHT with 13.56 MHz (EHY-2000) twice a week (8 times)	32	OS= 18 months (range 10.3-28.6) versus 10.97 months (range 4.00-22.16) PFS=12 months (range 3-28.6) versus 4.53 months (range 1.33-17.57) (p=0.003)	DCR= 85% vs 26% (p=0.0018).	3% of G1-G2 skin pain and burns
Fiorentini [26]	2019	mEHT+RT or CHT with gemcitabine regimen vs RT or CHT	mEHT with 13.56 MHz (EHY-2000) twice a week (8 times)	106	OS= 18.0 months vs 10.9 months (p<0.001)	3 months DCR= 92% vs 66%	no grade III-IV toxicity
Iyikesici [60]	2019	CHT with gemcitabine or FOLFIRINOX regimen +mEHT	mEHT with 13.56 MHz (EHY-3010) at 110-130W power for 60 minutes	25	OS=15.8 months (95% CI, 10.5-21.1) PFS=12.9 months (95% CI, 11.2-14.6)	3 months DCR=96%	None
Ono [56]	2019	CHT with FOLFIRINOX, Gemcitabin plus nab-Pacritaxel or S-1 +RHT	RHT with Thermotron RF-8, for 50 minutes after CHT once a week (5 times)	28	1 year OS=41% 2 years OS=15%	3 months DCR=57% 6 months DCR=45% 12 months DCR=12% 18 months DCR=6%	ND

Author	Year	Treatment	Hyperthermia protocol	No. of Pts. (n)	Survival	Tumor Response	RHT related toxicity
Maebayashi [53]	2017	CRT with 5-fluorouracil or gemcitabine + RHT vs CRT	RHT with Thermotron RF-8, for 50 minutes at 800-1200W power once or twice a week (5 times)	13	1 year OS=80% vs 57% (p=0.021)		Lower hematological and gastrointestinal toxicity than CRT alone
Tschoep-Lechner [57]	2013	CHT with gemcitabine and cisplatin +RHT	RHT with BSD-2000 day 2 and 4, 1 hour twice a week for 4 months	27	PFS = 5.9 months OS 12.9 months	DCR=50%	no grade III-IV toxicity
Maluta [55]	2011	CRT with gemcitabine based regimens+RHT vs CRT	RHT with BSD-2000 Once a week (1-5 times)	68	Median OS= 15 vs 11 months (p = 0.025)		
Volovat [59]	2014	CHT (GEMOX) +mEHT	mEHT with EHY-2000 device at 70-150 W on day 1, 3, 5 of every CHT cycle	26	Median PFS= 3.9 months. Median OS= 8.9 months.	DCR=71%	no grade III-IV toxicity
Ishikawa [58]	2012	CHT with gemcitabine+RHT	RHT with Thermotron RF-8 at 1100 to 1500 W power for 40 minutes once a week	18	Median OS=17.7 months	ORR=11.1% DCR= 61.1%	G2 pain and a skin rash
Ohguri [54]	2008	CRT with gemcitabine+RHT vs CRT	RHT with Thermotron RF-8 at 900W power, once a week 1-3 hours after RT and during CHT	29	Median OS=8.8 vs. 4.9 months, P = 0.02, Median PFS=18.6 vs. 9.6 months, P = 0.01	ND	5% grade III-IV toxicity

RT = radiotherapy, RHT = hyperthermia, OS = overall survival, SR = survival rate, Clinical benefit = complete response + partial response + stable disease, CHT = chemotherapy, DFS = Disease free survival, CRT = chemoradiotherapy, LRF5 = local relapse-free survival, DCR = disease control rate, mEHT = modulated electro-hyperthermia, ORR = overall response rate

These data suggest that RHT increases CRT and CHT benefit both in median OS and DCR in locally advanced or metastatic pancreatic cancer with low toxicity. Further studies to investigate CRT and RHT in locally advanced pancreatic cancer include the HEATPAC trial, a phase II randomized trial [62].

Summary

In association with radiotherapy and/or chemotherapy, regional hyperthermia may increase median OS, PFS, and tumor response of patients with esophageal, colon, rectal, anal, and locally advanced or metastatic pancreatic cancer. The mEHT is a relatively new regional hyperthermia method that targets tumor cell membranes and extra matrix tissue to increase cancer tissue temperature and sensitize it to cancer therapies. This method has relatively few published studies. However, the results are interesting and comparable to those of other RHT, amplifying both chemotherapy and radiotherapy's benefits in all the considered tumors and it is well tolerated.

Conclusion

The data presented in this narrative review are from retrospective and prospective studies and suggests that regional hyperthermia in association with radiotherapy and/or chemotherapy may increase median OS, PFS, and tumor response of patients with esophageal, colon, rectal, anal, and locally advanced or metastatic pancreatic cancer. mEHT is a relatively new method of regional hyperthermia that targets tumor cell membranes and extra matrix tissue to increase the temperature inside cancer tissue and sensitize it to cancer therapies. This method has few published studies in gastrointestinal cancers. However, the results are comparable to those of other RHT, amplifying both chemotherapy and radiotherapy's benefits in all the considered tumors and is well tolerated [63].

The studies presented have a heterogeneity as concerning the RHT protocols, for this reason, it is difficult to compare the results of different studies. Standardized RHT protocols and more randomized clinical trials are needed for each tumor type to address this issue.

References

- [1] Peeken JC, Vaupel P, Combs SE. Integrating Hyperthermia into Modern Radiation Oncology: What Evidence Is Necessary? *Front Oncol.* 2017;7:132. [doi:10.3389/fonc.2017.00132]
- [2] Sauer R, Creeze H, Hulshof M, Issels R, Ott O; Interdisciplinary Working Group for Clinical Hyperthermia (Atzelsberg Circle) of the German Cancer Society and the German Society of Radiooncology. Concerning the final report "Hyperthermia: a systematic review" of the Ludwig Boltzmann Institute for Health Technology Assessment, Vienna, March 2010. *Strahlenther Onkol.* 2012;188(3):209-13. [doi: 10.1007/s00066-012-0072-9]
- [3] Datta NR, Ordóñez SG, Gaipal US, Paulides MM, Crezee H, Gellermann J, et al. Local hyperthermia combined with radiotherapy and/or chemotherapy: recent advances and promises for the future. *Cancer Treat Rev.* 2015;41:742-53. [doi: 10.1016/j.ctrv.2015.05.009]
- [4] Lee SY, Fiorentini G, Szasz AM, Szigeti G, Szasz A, Minnaar CA. Quo Vadis Oncological Hyperthermia (2020)? *Front Oncol.* 2020;10:1690. [doi: 10.3389/fonc.2020.01690]
- [5] Song CW. Effect of local hyperthermia on blood flow and microenvironment: a review. *Cancer Res.* 1984;44(10):4721s-4730s. [PMID: 6467226]
- [6] Welch HG, Schwartz LM, Woloshin S (2000) Are increasing 5-year survival rates evidence of success against cancer? *JAMA* 283(22):2975-2978
- [7] Morgan G, Ward R, Barton M (2004) The contribution of cytotoxic chemotherapy to 5-year survival in adult malignancies. *Clin Oncol (R Coll Radiol)* 16(8):549-560
- [8] Bailair JC, Smith EM (1986) Progress against cancer? *The New England Journal of Medicine* 314(19):1226-1232
- [9] Holleb AI (1986) Progress against cancer? A broader view. *CA Cancer Journal for Clinicians* 36:243-244
- [10] Schoenbach VJ (1999) Descriptive studies and surveillance-solutions. www.epidemiolog.net/evolving/DescriptiveStudiesSolns.pdf Cited 12 September 2007
- [11] Bailair JC, Gornik HL (1997) Cancer undefeated. *The New England Journal of Medicine* 336(22):1569-1574
- [12] Pauling L (1989) Quoted by Moss RW: *The Cancer Syndrome*. Equinox Press, New York
- [13] Arnold K (2003) Statistics offer insights into progress against cancer. *Journal of the National Cancer Institute* 95(17):1266-1267
- [14] Parmar G, Rurak E, Elderfield M, et.al. (2020) 8-year observational study on naturopathic treatment with modulated electro-hyperthermia (mEHT): A single-centre experience, in book *Challenges and solutions of oncological hyperthermia*, ed. Szasz A., Ch. 13, pp.227-266, Cambridge Scholars, <https://www.cambridgescholars.com/challenges-and-solutions-of-oncological-hyperthermia>
- [15] Garay T, Kiss E, Szentmartoni Gy, et.al. (2020) Gastrointestinal cancer series treated with modulated electro-hyperthermia (mEHT) – A single centre experience, in book *Challenges and solutions of oncological hyperthermia*, ed. Szasz A., Ch. 8, pp.159-162, Cambridge Scholars, <https://www.cambridgescholars.com/challenges-and-solutions-of-oncological-hyperthermia>
- [16] Kim S, Lee JH, Cha J, You SH. (2021) Beneficial effects of modulated electro-hyperthermia during neoadjuvant treatment for locally advanced rectal cancer, *Int J Hyperthermia*, 38:1, 144-151, DOI: 10.1080/02656736.2021.1877837, <https://pubmed.ncbi.nlm.nih.gov/33557636/>
- [17] Kim J-H, Kim M-Y, Kim H-Y. (2019): Potential Application of Neoadjuvant Chemotherapy Plus Modulated Electrohyperthermia (mEHT, trade name: Oncothermia) Among Patients with Advanced Cancer: Retrospective Clinical Analysis of Single Hospital Experiences, *Oncothermia Journal* 27: 62-75, www.oncotherm.com/sites/oncotherm/files/2019-10/Potential_Application_of_Neoadjuvant.pdf
- [18] Hager ED, Dziambor H, Höhmann D, et al. (1999) Deep hyperthermia with radiofrequencies in patients with liver metastases from colorectal cancer. *Anticancer Res* 19(4C):3403-3408, <http://www.ncbi.nlm.nih.gov/pubmed/10629627>
- [19] Douwes FR. (2006) Thermochemotherapy of the advanced pancreas carcinoma. *Biologische Medizin* 35:126-130, https://www.researchgate.net/publication/287861898_Thermochemotherapy_of_the_advanced_pancreas_carcinoma
- [20] Douwes F. (2018): Therapy of advanced, therapy resistant pancreas cancer, with local hyperthermia in combination with chemotherapy; *Oncothermia Journal* 24:91-108, https://oncotherm.com/sites/oncotherm/files/2018-10/Therapy_of_advanced.pdf
- [21] Dani A, Varkonyi A, Magyar T, Szasz A (2008) Clinical study for advanced pancreas cancer treated by oncothermia. *Forum Hyperthermie* 1:13-20, <http://www.pyatthealth.com/wp-content/uploads/2015/03/Hyperthermia-Pancreatic-Cancer.pdf>

- [22] Turner PF, Schaefermeyer T. Technical Aspects of Hyperthermia. In: Issels RD, Wilmanns W. (eds) Application of Hyperthermia in the Treatment of Cancer. Recent Results in Cancer Research. Springer, Berlin, Heidelberg. 1988;107. [https://doi.org/10.1007/978-3-642-83260-4_10]
- [23] Kelleher DK, Thews O, Rzeznik J, Scherz A, Salomon Y, Vaupel P. Water-filtered infrared-A radiation: a novel technique for localized hyperthermia in combination with bacteriochlorophyll-based photodynamic therapy. *Int J Hyperthermia*. 1999;15(6):467-74. [doi: 10.1080/026567399285468]
- [24] Kok HP, Crezee J. A comparison of the heating characteristics of capacitive and radiative superficial hyperthermia. *Int J Hyperthermia*. 2017;33(4):378-386. [doi: 10.1080/02656736.2016.1268726]
- [25] Szasz AM, Minnaar CA, Szentmártoni G, Szigeti GP, Dank M. Review of the Clinical Evidences of Modulated Electro-Hyperthermia (mEHT) Method: An Update for the Practicing Oncologist. *Front Oncol*. 2019;9:1012. [doi: 10.3389/fonc.2019.01012]
- [26] Fiorentini G, Sarti D, Casadei V, Milandri C, Dentico P, Mambrini A, Nani R, Fiorentini C, Guadagni S. Modulated Electro-Hyperthermia as Palliative Treatment for Pancreatic Cancer: A Retrospective Observational Study on 106 Patients. *Integr Cancer Ther*. 2019;18:1534735419878505. [doi: 10.1177/1534735419878505].
- [27] Forika G, Balogh A, Vancsik T, Zalathnai A, Petovari G, Benyo Z, Krenacs T. Modulated Electro-Hyperthermia Resolves Radioresistance of Panc1 Pancreas Adenocarcinoma and Promotes DNA Damage and Apoptosis In Vitro. *Int J Mol Sci*. 2020; 21(14):5100 [<https://doi.org/10.3390/ijms21145100>]
- [28] Vancsik T, Forika G, Balogh A, Kiss E, Krenacs T. Modulated electro-hyperthermia induced p53 driven apoptosis and cell cycle arrest additively support doxorubicin chemotherapy of colorectal cancer in vitro. *Cancer Med*. 2019;8(9):4292-4303. doi: 10.1002/cam4.2330. Epub 2019 Jun 10. [PMID: 31183995; PMCID: PMC6675742]
- [29] Nishimura S, Saeki H, Nakanoko T, Kasagi Y, Tsuda Y, Zaitzu Y, Ando K, Nakashima Y, Imamura YU, Ohgaki K, Oki E, Ohga S, Nakamura K, Morita M, Maehara Y. Hyperthermia combined with chemotherapy for patients with residual or recurrent oesophageal cancer after definitive chemoradiotherapy. *Anticancer Res*. 2015;35(4):2299-303. [PMID: 25862892]
- [30] Hu Y, Li Z, Mi DH, Cao N, Zu SW, Wen ZZ, Yu XL, Qu Y. Chemoradiation combined with regional hyperthermia for advanced oesophageal cancer: a systematic review and meta-analysis. *J Clin Pharm Ther*. 2017;42(2):155-164. [doi:10.1111/jcpt.12498]
- [31] Albregts M, Hulshof MC, Zum Vörde Sive Vörding PJ, van Lanschot JJ, Richel DJ, Crezee H, Fockens P, van Dijk JD, González González D. A feasibility study in oesophageal carcinoma using deep loco-regional hyperthermia combined with concurrent chemotherapy followed by surgery. *Int J Hyperthermia*.
- [32] Nakajima M, Kato H, Sakai M, Sano A, Miyazaki T, Sohda M, Inose T, Tanaka N, Suzuki S, Masuda N, Fukuchi M, Kuwano H. Planned Esophagectomy after Neoadjuvant Hyperthermo-Chemoradiotherapy using Weekly Low-Dose Docetaxel and Hyperthermia for Advanced Esophageal Carcinomas. *Hepatogastroenterology*. 2015;62(140):887-91 [PMID: 26902022]
- [33] Hulshof MC, Van Haaren PM, Van Lanschot JJ, Richel DJ, Fockens P, Oldenburg S, Geijssen ED, Van Berge Henegouwen MI, Crezee J. Preoperative chemoradiation combined with regional hyperthermia for patients with resectable esophageal cancer. *Int J Hyperthermia*. 2009;25(1):79-85 [doi: 10.1080/02656730802464078]
- [34] Sheng L, Ji Y, Wu Q, Du X. Regional hyperthermia combined with radiotherapy for esophageal squamous cell carcinoma with supraclavicular lymph node metastasis. *Oncotarget*. 2017;8(3):5339-5348. [doi:10.18632/oncotarget.14148]
- [35] Siegel RL, Miller KD, Goding Sauer A, Fedewa SA, Butterly LF, Anderson JC, Cercek A, Smith RA, Jemal A. Colorectal cancer statistics, 2020. *CA Cancer J Clin*. 2020;70(3):145-164. [doi: 10.3322/caac.21601]
- [36] De Haas-Kock DFM, Buijsen J, Pijls-Johannesma M, Lutgens L, Lammering G, Mastrigt GAV, et al. Concomitant hyperthermia and radiation therapy for treating locally advanced rectal cancer. *Cochrane Database Syst Rev* 2009;3:CD006269. [doi: 10.1002/14651858.CD006269.pub2]
- [37] Elming PB, Sørensen BS, Oei AL, Franken NAP, Crezee J, Overgaard J, Horsman MR. Hyperthermia: The Optimal Treatment to Overcome Radiation Resistant Hypoxia. *Cancers (Basel)*. 2019;11(1):60. [doi:10.3390/cancers11010060]
- [38] Gani C, Schroeder C, Heinrich V, Spillner P, Lamprecht U, Berger B, Zips D. Long-term local control and survival after preoperative radiochemotherapy in combination with deep regional hyperthermia in locally advanced rectal cancer. *Int J Hyperthermia*. 2016;32(2):187-92. doi: 10.3109/02656736.2015.1117661. Epub 2016 Jan 11. PMID: 26754458

- [39] Zwirner K, Bonomo P, Lamprecht U, Zips D, Gani C. External validation of a rectal cancer outcome prediction model with a cohort of patients treated with preoperative radiochemotherapy and deep regional hyperthermia. *Int J Hyperthermia*. 2018;34(4):455-460. [doi: 10.1080/02656736.2017.1338364]
- [40] Maluta S, Romano M, Dall'oglio S, Genna M, Oliani C, Pioli F, Gabbani M, Marciai N, Palazzi M. Regional hyperthermia added to intensified preoperative chemo-radiation in locally advanced adenocarcinoma of middle and lower rectum. *Int J Hyperthermia*. 2010;26(2):108-17. [doi: 10.3109/02656730903333958]
- [41] Rau B, Wust P, Tilly W, Gellermann J, Harder C, Riess H, Budach V, Felix R, Schlag PM. Preoperative radiochemotherapy in locally advanced or recurrent rectal cancer: regional radiofrequency hyperthermia correlates with clinical parameters. *Int J Radiat Oncol Biol Phys*. 2000;48(2):381-91. [doi: 10.1016/s0360-3016(00)00650-7]
- [42] Ott OJ, Schmidt M, Semrau S, Strnad V, Matzel KE, Schneider I, Raptis D, Uter W, Grützmann R, Fietkau R. Chemoradiotherapy with and without deep regional hyperthermia for squamous cell carcinoma of the anus. *Strahlenther Onkol*. 2019;195(7):607-614. [doi: 10.1007/s00066-018-1396-x]
- [43] Shoji H, Motegi M, Osawa K, Okonogi N, Okazaki A, Andou Y, Asao T, Kuwano H, Takahashi T, Ogoshi K. A novel strategy of radiofrequency hyperthermia (neothermia) in combination with preoperative chemoradiotherapy for the treatment of advanced rectal cancer: a pilot study. *Cancer Med*. 2015;4(6):834-43. [doi: 10.1002/cam4.431]
- [44] Kato T, Fujii T, Ide M, Takada T, Sutoh T, Morita H, Yajima R, Yamaguchi S, Tsutsumi S, Asao T, Oyama T, Kuwano H. Effect of long interval between hyperthermochemoradiation therapy and surgery for rectal cancer on apoptosis, proliferation and tumor response. *Anticancer Res*. 2014;34(6):3141-6. [PMID: 24922685]
- [45] Schroeder C, Gani C, Lamprecht U, von Weyhern CH, Weinmann M, Bamberg M, Berger B. Pathological complete response and sphincter-sparing surgery after neoadjuvant radiochemotherapy with regional hyperthermia for locally advanced rectal cancer compared with radiochemotherapy alone. *Int J Hyperthermia*. 2012;28(8):707-14. [doi: 10.3109/02656736.2012.722263]
- [46] Tsutsumi S, Tabe Y, Fujii T, Yamaguchi S, Suto T, Yajima R, Morita H, Kato T, Shioya M, Saito J, Asao T, Nakano T, Kuwano H. Tumor response and negative distal resection margins of rectal cancer after hyperthermochemoradiation therapy. *Anticancer Res*. 2011;31(11):3963-7. [PMID: 22110227]
- [47] Kang MK, Kim MS, Kim JH. Clinical outcomes of mild hyperthermia for locally advanced rectal cancer treated with preoperative radiochemotherapy. *Int J Hyperthermia*. 2011;27(5):482-90. [doi: 10.3109/02656736.2011.563769]
- [48] You SH, Kim S. Feasibility of modulated electro-hyperthermia in preoperative treatment for locally advanced rectal cancer: Early phase 2 clinical results. *Neoplasma*. 2020;67(3):677-683. [doi: 10.4149/neo_2020_190623N538]
- [49] Ranieri G, Laface C, Laforgia M, De Summa S, Porcelli M, Macina F, Ammendola M, Molinari P, Lauletta G, Di Palo A, Rubini G, Ferrari C, Gadaleta CD. Bevacizumab Plus FOLFOX-4 Combined With Deep Electro-Hyperthermia as First-line Therapy in Metastatic Colon Cancer: A Pilot Study. *Front Oncol*. 2020;10:590707. [doi: 10.3389/fonc.2020.590707]
- [50] van der Horst A, Versteijne E, Besselink MGH, Daams JG, Bulle EB, Bijlsma MF, Wilmink JW, van Delden OM, van Hooft JE, Franken NAP, van Laarhoven HWM, Crezee J, van Tienhoven G. The clinical benefit of hyperthermia in pancreatic cancer: a systematic review. *Int J Hyperthermia*. 2018;34:969-979. [doi: 10.1080/02656736.2017.1401126.]
- [51] Liu X, Yang X, Zhou G, Chen Y, Li C, Wang X. Gemcitabine based regional intra-arterial infusion chemotherapy in patients with advanced pancreatic adenocarcinoma. *Medicine (Baltimore)*. 2016;95:e3098. [doi: 10.1097/MD.0000000000003098]
- [52] Suker M, Beumer BR, Sadot E, Marthey L, Faris JE, Mellon EA, El-Rayes BF, Wang-Gillam A, Lacy J, Hosein PJ, Moorcraft SY, Conroy T, Hohla F, Allen P, Taieb J, Hong TS, Shridhar R, Chau I, van Eijck CH, Koerkamp BG. A patient-level meta analysis of FOLFIRINOX for locally advanced pancreatic cancer. *Lancet Oncol*. 2016;17:801-810. [doi: 10.1016/S1470-2045(16)00172-8]
- [53] Maebayashi T, Ishibashi N, Aizawa T, Sakaguchi M, Sato T, Kawamori J, Tanaka Y. Treatment outcomes of concurrent hyperthermia and chemoradiotherapy for pancreatic cancer: Insights into the significance of hyperthermia treatment. *Oncol Lett*. 2017;13(6):4959-4964. [doi: 10.3892/ol.2017.6066]
- [54] Ohguri T, Imada H, Yahara K, Morioka T, Nakano K, Korogi Y. Concurrent chemoradiotherapy with gemcitabine plus regional hyperthermia for locally advanced pancreatic carcinoma: initial experience. *Radiat Med*. 2008;26:587-596. [DOI 10.1007/s11604-008-0279-y]

- [55] Maluta S, Schaffer M, Pioli F, Dall'oglio S, Pasetto S, Schaffer PM, Weber B, Giri MG. Regional hyperthermia combined with chemoradiotherapy in primary or recurrent locally advanced pancreatic cancer: an open-label comparative cohort trial. *Strahlenther Onkol*. 2011;187(10):619-25. [doi: 10.1007/s00066-011-2226-6]
- [56] Ono E, Yano M, Ohshiro T, Shishida M, Sumitani D, Yuzou ,Okamoto Y, Och M. Effectiveness of hyperthermia in clinical stage IV pancreatic cancer. *Oncothermia Journal*. 2019;27:88-93 [https://oncotherm.com/sites/oncotherm/files/2019-10/Effectiveness_of_hyperthermia.pdf]
- [57] Tschöep-Lechner KE, Milani V, Berger F, Dieterle N, Abdel-Rahman S, Salat C, Issels RD. Gemcitabine and cisplatin combined with regional hyperthermia as second-line treatment in patients with gemcitabine-refractory advanced pancreatic cancer. *Int J Hyperthermia*. 2013;29(1):8-16. [doi: 10.3109/02656736.2012.740764]
- [58] Ishikawa T, Kokura S, Sakamoto N, Ando T, Imamoto E, Hattori T, Oyamada H, Yoshinami N, Sakamoto M, Kitagawa K, Okumura Y, Yoshida N, Kamada K, Katada K, Uchiyama K, Handa O, Takagi T, Yasuda H, Sakagami J, Konishi H, Yagi N, Naito Y, Yoshikawa T. Phase II trial of combined regional hyperthermia and gemcitabine for locally advanced or metastatic pancreatic cancer. *Int J Hyperthermia*. 2012;28(7):597-604. [doi: 10.3109/02656736.2012.695428]
- [59] Volovat C, Volovat SR, Scripcaru V, Miron L. Second-line chemotherapy with gemcitabine and oxaliplatin in combination with loco-regional hyperthermia (EHY-2000) in patients with refractory metastatic pancreatic cancer—preliminary results of a prospective trial. *Rom Rep Phys*. 2014;66:166-174 [http://rrp.infim.ro/2014_66_1/A18.pdf]
- [60] Iyikesici MS. Long-Term Survival Outcomes of Metabolically Supported Chemotherapy with Gemcitabine-Based or FOLFIRINOX Regimen Combined with Ketogenic Diet, Hyperthermia, and Hyperbaric Oxygen Therapy in Metastatic Pancreatic Cancer. *Complement Med Res*. 2020;27(1):31-39. [doi: 10.1159/000502135]
- [61] Sarti D, Milandri C, Fiorentini C, Mambrini A, Fiorentini G. Modulated electro-hyperthermia for the treatment of elderly pancreatic cancer patients. *Arguments of Geriatric Oncology*. 2020;5(1):1 – 7. [https://www.edisciences.org/scheda-d027]
- [62] Datta NP, Pestalozzi B, Clavien PA, Members of the HEATPAC Trial Group. “HEATPAC”—a phase II randomized study of concurrent thermochemoradiotherapy versus chemoradiotherapy alone in locally advanced pancreatic cancer. *Radiat Oncol*. 2017;12:183. [DOI 10.1186/s13014-017-0923-8]
- [63] Minnaar CA, Szasz AM, Arrojo E, Lee S-Y, Fiorentini G, Borbenyi E, Pang CLK, Dank M. Summary and update of the method modulated electrohyperthermia, *Oncothermia Journal Special Edition*. 2020;2:49-130. [https://oncotherm.com/sites/oncotherm/files/2020-09/specialedition02.pdf]

Addition of Multimodal Immunotherapy to Combination Treatment Strategies for Children with DIPG: A Single Institution Experience

**Stefaan W. Van Gool¹, Jennifer Makalowski¹, Erin R. Bonner^{2,3}, Oliver Feyen⁴,
Matthias P. Domogalla¹, Lothar Prix⁵, Volker Schirrmacher¹, Javad Nazarian⁶ and
Wilfried Stuecker¹**

¹Immun-Onkologisches Zentrum Köln
Köln, Germany

²Center for Genetic Medicine, Children's National Health System,
Washington, D.C., USA

³Institute for Biomedical Sciences,
The George Washington University School of Medicine and health Sciences,
Washington, D.C., USA

⁴Zyagnum,
Pfungstadt, Germany

⁵Biofocus,
Recklinghausen, Germany

⁶DIPG Research Institute, Universitäts-Kinderspital Zürich,
Zürich, Switzerland

Citation: Van Gool S. W. et al. (2020): Addition of Multimodal Immunotherapy to Combination Treatment Strategies for Children with DIPG: A Single Institution Experience, *Oncothermia Journal* 30: 37 – 53,
http://www.oncotherm.com/sites/oncotherm/files/2021-04/VanGool_Addition.pdf
Reprinted from: <https://www.mdpi.com/2305-6320/7/5/29>



Article

Addition of Multimodal Immunotherapy to Combination Treatment Strategies for Children with DIPG: A Single Institution Experience

Stefaan W. Van Gool ^{1,*} , Jennifer Makalowski ¹, Erin R. Bonner ^{2,3}, Oliver Feyen ⁴, Matthias P. Domogalla ¹, Lothar Prix ⁵, Volker Schirmacher ¹ , Javad Nazarian ⁶ and Wilfried Stuecker ¹

¹ Immun-Onkologisches Zentrum Köln, Hohenstaufenring 30-32, 50674 Köln, Germany; makalowski@iozk.de (J.M.); domogalla@iozk.de (M.P.D.); v.schirmacher@web.de (V.S.); stuecker@iozk.de (W.S.)

² Center for Genetic Medicine, Children's National Health System, Washington, DC 20010, USA; ebonner@childrensnational.org

³ Institute for Biomedical Sciences, The George Washington University School of Medicine and Health Sciences, Washington, DC 20052, USA

⁴ Zyagnum, Reißstrasse 1, 64319 Pfungstadt, Germany; oliver.feyen@zyagnum.com

⁵ Biofocus, Berghäuser Strasse 295, 45659 Recklinghausen, Germany; l.prix@ladr.de

⁶ DIPG Research Institute, Universitäts-Kinderspital Zürich; Steinwiesstrasse 75, CH-8032 Zürich, Switzerland; javad.nazarian@kispi.uzh.ch

* Correspondence: vangoolstefaan@gmail.com; Tel.: +49-221-420-39925

Received: 20 March 2020; Accepted: 13 May 2020; Published: 19 May 2020



Abstract: **Background:** The prognosis of children with diffuse intrinsic pontine glioma (DIPG) remains dismal despite radio- and chemotherapy or molecular-targeted therapy. Immunotherapy is a powerful and promising approach for improving the overall survival (OS) of children with DIPG. **Methods:** A retrospective analysis for feasibility, immune responsiveness, and OS was performed on 41 children treated in compassionate use with multimodal therapy consisting of Newcastle disease virus, hyperthermia, and autologous dendritic cell vaccines as part of an individualized combinatorial treatment approach for DIPG patients. **Results:** Patients were treated at diagnosis ($n = 28$) or at the time of progression ($n = 13$). In the case of 16 patients, histone H3K27M mutation was confirmed by analysis of biopsy ($n = 9$) or liquid biopsy ($n = 9$) specimens. PDL1 mRNA expression was detected in circulating tumor cells of ten patients at diagnosis. Multimodal immunotherapy was feasible as scheduled, until progression, in all patients without major toxicity. When immunotherapy was part of primary treatment, median PFS and OS were 8.4 m and 14.4 m from the time of diagnosis, respectively, with a 2-year OS of 10.7%. When immunotherapy was given at the time of progression, median PFS and OS were 6.5 m and 9.1 m, respectively. A longer OS was associated with a Th1 shift and rise in PanTum Detect test scores. **Conclusions:** Multimodal immunotherapy is feasible without major toxicity, and warrants further investigation as part of a combinatorial treatment approach for children diagnosed with DIPG.

Keywords: DIPG; multimodal immunotherapy; DC vaccination; Newcastle disease virus; hyperthermia; PanTum Detect test; Th1 shift

1. Introduction

Diffuse intrinsic pontine glioma (DIPG) is a rare brainstem tumor that typically occurs in children. The overall incidence rate of all primary brain tumors ranges between 3–6 per 100,000 children and

adolescents between 0 and 19 years of age [1,2]. About 10–15% of these tumors are located in the brain stem [2,3] and 75–80% of pediatric brainstem tumors are DIPG [3], making its incidence less than one per 100,000 children each year. DIPG is diagnosed by assessment of clinical symptoms derived from the pyramidal tract, the cerebellum, and the cranial nerves, together with the typical imaging on MRI, which manifests as a T1-weighted hypointensity, T2-weighted hyperintensity involving >50% of the pons, with occasional ring contrast enhancement [4]. Most, but not all, of these lesions are driven by histone mutations [5], classifying them as diffuse midline gliomas (DMG), according to the current WHO brain tumor classification [6]. About 85% of DIPGs harbor histone mutations [7].

There is no known cure for DIPG [7] and the 2-year overall survival (OS) remains below 10%. Insufficient data in the literature preclude analysis of the 5-year OS of this disease [8]. The poor prognosis of DIPG is in contrast to the more favorable prognosis of pediatric glioblastoma multiforme (GBM), which results in a 5-year OS of about 20% in cases involving favorable clinical risk factors (e.g., age, location, extent of resection) [9]. In contrast, DIPG is inoperable, and radiotherapy is generally accepted as the standard-of-care treatment, reducing temporarily acute symptoms [10–13]. Changing radiotherapy modalities, or the addition of (neo)adjuvant chemotherapy or other drugs, has not changed the OS over the past 30 years [14]. Re-irradiation is possible [15]. A breakthrough came when biopsy was developed as a safe and feasible procedure [16,17]. Knowledge on the molecular biology of the tumor has resulted in the development of molecular-driven treatment strategies [18,19]. The worldwide networks for biology data and the DIPG registry for clinical and radiological data together form the basis for future development in the field [20,21]. Apart from radiotherapy as a single treatment modality or clinical trials combining radiotherapy with classic chemotherapy [22], innovative treatment modalities have emerged such as local treatments via convection-enhanced delivery [23–25].

Immunotherapy and biologic treatments for DIPG are emerging fields of research. A Clinicaltrials.gov search (September 2019) for “DIPG/Immunotherapy” yielded six trials studying the role of vaccines including two trials with dendritic cell (DC) vaccines (NCT03396575, phase 1, recruiting; NCT02840123, phase 1, active, not recruiting), two trials focused on immunomodulation with Indoximod (NCT04049669, phase 2, not yet recruiting; NCT02502708, phase 1, recruiting), one trial with tumor-initiating-cells (NCT01400672, phase 1, suspended), and one with the H3.3K27M peptide vaccine (NCT02960230, phase 1, active, not recruiting). One trial was registered using the oncolytic virus Adenovirus DNX-2401 (NCT03178032, phase 1, recruiting). Each of these studies included a limited number of patients, and focused on feasibility, toxicity, or preliminary efficacy. Treatments typically included radiotherapy. Data from these trials would give important, but limited, information on the research question.

In addition, individualized combination treatment strategies outside of clinical trials are a well-known phenomenon, not only in the scientific community but also in patient communities. Particularly for DIPG, treatment approaches outside of clinical trials are common [26]. It is of utmost importance for both the scientific and patient community that the results from these individualized treatment approaches are analyzed and reported. We therefore aimed to present the data of a retrospective analysis of 41 children with DIPG consecutively treated with multimodal immunotherapy in compassionate use at the Immun-Onkologisches Zentrum Köln (IOZK), between October 2011 and February 2018.

2. Materials and Methods

The database consisting of all patients who had contact with the IOZK was fixed at 15 July 2018. A search for DIPG as the primary diagnosis yielded 142 records of patients from at least 33 countries (data not available for 16 patients). Forty-one of these patients (29%) were actively treated with immunotherapy at the IOZK as an individualized treatment approach in compassionate use (“individueller Heilversuch”) between October 2011 and February 2018. Thirty-six patients (88%) began treatment between 2016–2017. The last OS analysis was performed at the end of September 2019.

All patients started immunotherapy with a blood investigation focused on the functional status of the immune system. The immunotherapy consisted of vaccination cycles and/or immunogenic cell death (ICD) therapy. Full vaccination cycles consisted of five consecutive days of treatment with intravenous injection of Newcastle disease virus (NDV) in combination with local modulated electrohyperthermia (mEHT) via the Oncothermia EHY-2000 device (Oncotherm GmbH, Troisdorf, Germany) for 40 min at an intensity of 40 W. During mEHT, 0.9% NaCl infusion was administered. On the eighth day, a sixth session of NDV/mEHT was administered. Autologous mature DCs were loaded with NDV/mEHT-induced serum-derived antigenic extracellular microvesicles and apoptotic bodies. DCs were injected intradermally in the upper third of the arm. This personalized vaccine, approved as an advanced therapy medicinal product since May 2015 and registered as IO-VAC[®], was prepared as described [27]. The therapy consisted of two consecutive vaccination cycles with an interval of three weeks between each cycle. ICD therapy consisted of three days of NDV/mEHT. ICD therapy was incorporated at days 8, 9, and 10 in conjunction with 5/28 days oral TMZ. Following the maintenance chemotherapy, vaccination cycles were started following a similar schedule as described for adults with GBM [27]. ICD therapy was also given as maintenance immunotherapy after two full vaccination cycles for all patients who reached that stage.

Plasma circulating tumor DNA (ctDNA) analysis was used to screen for H3.3K27M mutation in 21 patients, as described previously [28,29]. Briefly, cell free DNA was isolated from 1 mL of plasma, and digital droplet PCR (ddPCR) was performed as per [29] to detect, and quantify the abundance of the *H3F3A* wildtype and K27M mutant alleles.

Patients were monitored during treatment at three levels. Routine cell numbers and immune functional tests were determined in the clinical laboratory (www.synlab.com). The percentage of IL-4 and IFN- γ expression within CD4⁺ T cells was determined using FACS. Circulating tumor cells (CTC) were isolated and the mRNA expression level of PDL1 was analyzed by Biofocus (www.biofocus.de). The PanTum Detect tests were performed at IOZK using the Epitope Detection In Monocyte (EDIM) technology as described [30–33].

3. Results

3.1. Patient Characteristics

Forty-one children (n = 10 male, 31 female) from 16 countries were effectively treated with multimodal immunotherapy at the IOZK, following an in-depth explanation of the treatment strategy and written informed consent from the patient or patient's guardian. Our retrospective analysis focused on this group of patients. An additional 101 children with DIPG were registered in the database, but did not follow treatment for various reasons. The treated children were subdivided into three groups: Group 1, children receiving immunotherapy before radio- and chemotherapy (n = 6); Group 2, children receiving immunotherapy in conjunction with the first line of treatment provided by the local oncology center (n = 22 total; radiotherapy only = 13, radiotherapy and chemotherapy = 9); and Group 3, children treated with immunotherapy upon disease progression following the first line of standard treatment, which consisted of radiotherapy for all patients, and a combination of radio/chemotherapy in the case of nine patients (n = 13 total). The median age at diagnosis for all children was five years, with a range from two to 19 years (Figure 1A). The age range did not differ between the three patient groups (Kruskal–Wallis test). The median Lansky Playing Scores (LPS) of the three patients groups were 80, 90, and 60, respectively, indicating no significant difference between the groups (Kruskal–Wallis test), although the minimum LPS were 70, 60, and 20, respectively (Figure 1B).

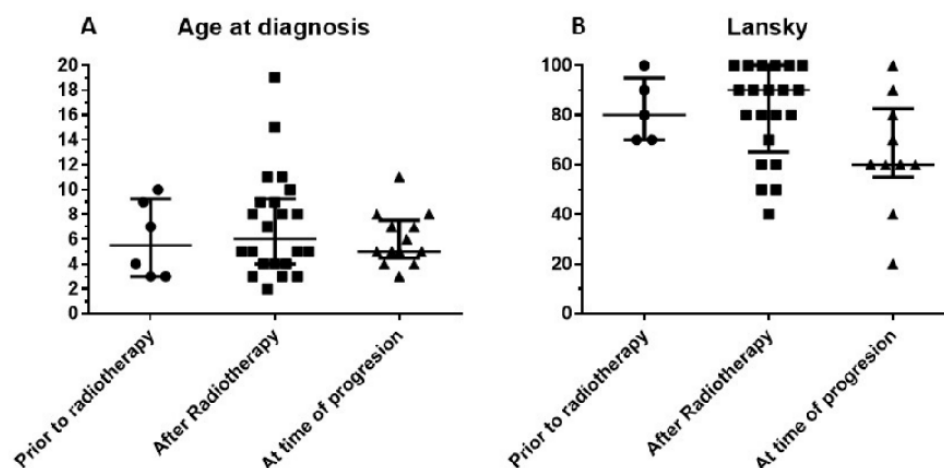


Figure 1. Characteristics of retrospective cohort consisting of 41 children with diffuse intrinsic pontine glioma (DIPG). Patients included in this retrospective cohort were stratified into three groups based on the treatment modalities they received in addition to immunotherapy. Patients in Group 1 received immunotherapy prior to radiation therapy, while patients in Group 2 received radiation therapy before beginning immunotherapy as their first line of treatment. Patients in Group 3 received immunotherapy at the time of progressive disease, following their first line of treatment. (A) Age distribution (median and interquartile range). (B) Lansky score at admission for immunotherapy (median and interquartile range).

All children received the diagnosis of DIPG based on MRI diagnostics in the local treating oncology center and were counseled accordingly. A retrospective central radiology review was not organized. Data on the length of symptoms prior to diagnosis were not systematically captured. Histone mutations were molecularly confirmed by tissue biopsy in nine patients (19.5%) ($n = 1/6$ patients from Group 1, 5/22 from Group 2, and 3/13 from Group 3). ddPCR analysis of plasma ctDNA indicated that 9/21 patients tested were positive for H3.3K27M mutation [34,35]. Plasma ctDNA mutation detection was in accordance with histone mutation status confirmed by tissue biopsy in 2/3 patients. Hence, molecular support for the DIPG diagnosis was present in 16/41 patients ($n = 1/6$ patients from Group 1, 12/22 from Group 2, and 3/13 from Group 3).

An immune diagnostic procedure was performed on patients prior to the start of immunotherapy (Figure 2). Three different categories of tests were performed. (1) The number and functions of T cells, B cells, and NK cells were compared to the reference values of the laboratory. The relatively high proportion of patients falling below the lower reference limit reflects their first line of treatment with chemotherapy (administered to three patients in Group 1) and/or radiotherapy (administered to all patients in Group 2). The three children who did not receive chemotherapy or radiotherapy from Group 1 had also at least one variable below the reference limit for cytokine production. These children did not receive steroids. Patients from Group 3 were no more affected than patients from Groups 1 or 2. (2) A PanTum Detect test was performed in all children at diagnosis. The PanTum Detect test is a novel screening test based on two general markers in cancer, Apo10 and TKTL1, which can be detected with intracellular staining and FACS analysis in CD14+CD16+ gated circulating monocytes using EDIM technology [30–33]. The Apo10 protein epitope marks tumor cells with abnormal apoptosis and proliferation. The transketolase-like protein 1 (TKTL1) represents the enzymatic basis for anaerobic glucose metabolism even in the presence of oxygen, which is concomitant with a more malignant phenotype due to invasive growth/metastasis and resistance to radical and apoptosis-inducing therapies. Interestingly, at least one PanTum Detect test score was in the pathologic range in all patients. Only four patients, all belonging to Group 2, had a borderline Apo10 value with a normal value for TKTL1. (3) Although plasma for ctDNA analysis was not systematically sampled at diagnosis, circulating tumor cell (CTC) detection was performed in almost all children. The latter test isolates CTCs derived from brain tumors as these cells are larger than circulating blood cells, remain on top of a filter, and harbor

oncogenic mRNA expression profiles (e.g., elevated expression of telomerase, ERBB2, C-kit, and EGFR, relative to the expression of housekeeping genes). CTCs were detected in 2/5 patients from Group 1, 17/20 patients from Group 2, and 5/8 patients from Group 3. Increased PDL1 mRNA expression in CTCs was detected in one, seven, and two patients from Groups 1 to 3, respectively. In five patients with positive CTC detection, PDL1 mRNA expression was not elevated compared to the housekeeping genes. In 3/9 patients tested, no CTCs were detected in the blood. In one biopsied patient from Group 3, no CTC data were available. Together, the immune function variables, the PanTum Detect test variables, and the evidence of PDL1 mRNA expression in CTCs all indirectly provide information on the tumor microenvironment including the interaction between the tumor and the host's immune system. The results of these tests can inform and refine personalized immunotherapy.

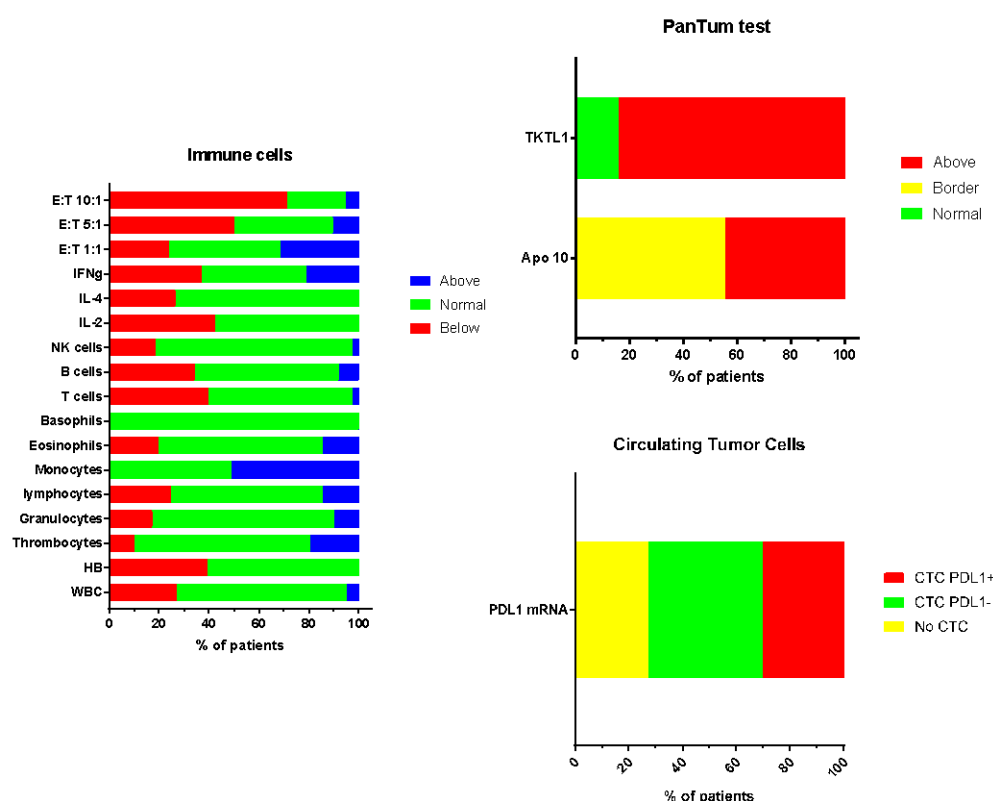


Figure 2. (A) Proportion of patients deviating from the normal reference values: White blood cell count, hemoglobin, thrombocyte count; relative values for white blood cell subpopulations as percentage (granulocytes, lymphocytes, monocytes, eosinophils, basophils); absolute values for lymphocyte subpopulations (T cells, B cells, NK cells); percentage cytokine producing CD4+ T cells (IL-2; IL-4, IFN-g) and cytotoxic NK cell function at three effector target ratios (E:T 1:1, 5:1, 10:1). (B) Proportion of patients showing levels (normal, border, above the reference values) of Apo10 and TKTL1 within the CD14+CD16+ monocytes. (C) Proportion of patients without (no CTC) or with CTCs, and with negative (CTC PDL1-) or positive (CTC PDL1+) PDL1 mRNA expression.

3.2. Treatment Data

Before the start of immunotherapy, three patients in Group 1 received chemotherapy prior to radiotherapy, according to the Polish standard of care. One of these patients received a complex cocktail of different repurposing and complementary drugs (Agomelatine, minocycline, valproic acid, curcumin, Boswellia, scorpion venom extract, CBD), and another patient received photodynamic treatment (PDT, www.webermedical.com). This latter child and one additional patient were further treated with PDT during immunotherapy. Patients in Group 2 were all treated with radiotherapy prior to immunotherapy. Nine patients also received chemotherapy, five of whom continued Temozolomide

(TMZ) maintenance chemotherapy together with immunogenic cell death (ICD) treatment until the first progression, after which full dendritic cell (DC) vaccination cycles were initiated. One patient was treated respectively with CED treatment, oral panobinostat, gallium maltonate, and Bevacizumab as part of the first line of treatment prior to immunotherapy. During immunotherapy, one patient was also treated with CED, PDT, and gallium maltonate, respectively. As a result, 14/22 patients from Group 2 received multimodal immunotherapy following radiotherapy without any concomitant treatment modality. Two of the 13 children in Group 3 combined multimodal immunotherapy with gallium maltonate treatment. The use of complementary drugs or diet was not systematically reviewed.

The technical details of the multimodal immunotherapy are shown in Figure 3. ICD treatment consisted of the combination of intravenous NDV administration together with mEHT. Each DC vaccination cycle consisted of six NDV/mEHT treatments combined with intradermal injection of autologous mature DCs loaded with NDV/mEHT-induced serum-derived antigenic extracellular microvesicles and apoptotic bodies from the patient's tumor. There was no significant difference in the numbers of DCs, vaccinations, hyperthermia sessions, or NDV administrations between the three groups of patients (Kruskal–Wallis test).

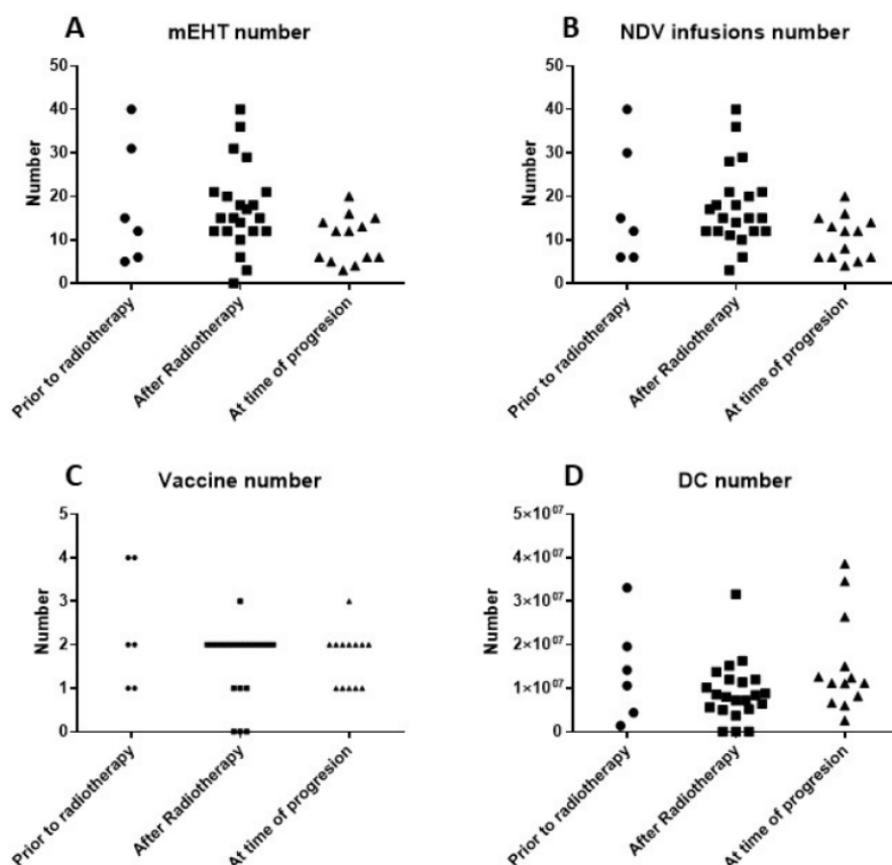


Figure 3. (A) Number of sessions of modulated electrohyperthermia (mEHT); (B) number of injections of Newcastle disease virus (NDV); (C) number of dendritic cell (DC) vaccines; and (D) number of DCs injected for the three patient groups.

3.3. Clinical Evolution

All treatments were administered in an ambulatory setting. Twenty-four children received a central venous access device placed prior to the start of immunotherapy, while 15 children received the immunotherapy without central venous access. Two children received a central venous access during immunotherapy. One child with fast progressive DIPG and LPS of 40 received a central venous access device, aimed at providing general support including a short hospitalization. This patient discontinued

immunotherapy after one week. Treatment-induced side effects were not systematically screened using questionnaires. At each patient contact, clinical signs were discussed. Most symptomatology was attributed to the DIPG itself and/or other antitumoral treatments given. Nevertheless, low grade complaints of fever ($n = 1$), dizziness ($n = 2$), neuralgia ($n = 1$), and headache ($n = 1$), all likely related to immunotherapy, and ascites in the context of a ventriculo-peritoneal drainage ($n = 1$) were registered in the database.

MRI was performed at the local oncology center. Progressive disease can be difficult to discern in the context of DIPG, and, reference radiology was not systematically performed in all patients, further complicating the identification of disease progression. Moreover, the contribution of immunotherapy made the interpretation of MRI findings more difficult. IOZK provided all information when requested for the assessments at the local hospitals. For the analysis in this retrospective study, PFS was defined as the moment when a new treatment strategy was implemented by the local oncology center. Data were available for 22 patients from the 28 first-line DIPG patients belonging to Group 1 (immunotherapy before radiotherapy) and Group 2 (immunotherapy after radiotherapy). The median PFS was 8.4 m (Figure 4A). The six-month PFS was 90.9% (CI95%: +6.7, −22.6). We recognized that our patient group was highly biased with children still being able to travel, and with parents putting maximal effort and resources for treatment. A similar profile, however, was present in the 13 children from Group 3 who came for immunotherapy at the time of progressive disease. In these children, we calculated PFS as the time between diagnosis and the date of a second event, hence first-line treatment without immunotherapy. For these 13 children, the median PFS was 6.5 m, and the 6-month PFS was 53.8% (CI95%: +22.1, −29.0), which was significantly (Log-rank test: $p = 0.013$) less than that of the patients who received immunotherapy as part of their first-line treatment.

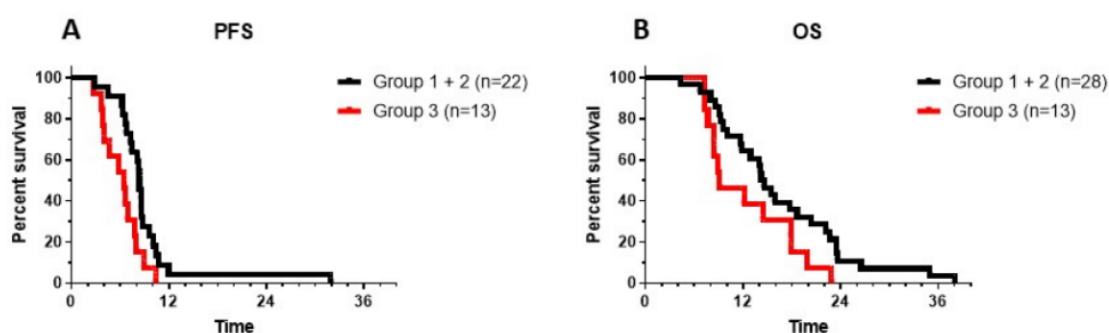


Figure 4. Progression-free survival (PFS) (A) and overall survival (OS) (B) are shown for patients from Groups 1 and 2 (black line: patients receiving immunotherapy as the first line of treatment either before (Group 1) or after (Group 2) radiotherapy) and from Group 3 (red line: patients receiving immunotherapy at the time of progressive disease, following the first line of treatment). Log-rank test for PFS showed a p value of 0.014. Log-rank test for OS showed a p value of 0.057.

It is generally accepted that OS is the ultimate outcome to be considered in patients with DIPG. A similar approach was therefore performed to assess the OS of patients from each group. Data from all children were available, and all had an event. The median OS of the Groups 1 and 2 patients combined was 14.4 m, with a 1-year OS of 64.3% (CI95%: +14.6, −20.5), and a 2-year OS of 10.7% (CI95%: +14.3, −8.0) (Figure 4B). The longest OS of patients in Groups 1 and 2 was 38 m (Figure 4B). There was no significant difference between Group 1 (median OS: 16.9 m; 2-year OS: 16.6%, CI95%: +35, −15.9) and Group 2 (median OS: 14.4 m; 2-year OS: 9%, CI95%: +16, −7.5). The OS for the patients in Group 3, calculated from the time of initial diagnosis, was 9.1 m, with the longest OS of 22.9 m. There was a trend toward a longer OS when patients were treated with immunotherapy as part of first-line treatment ($p = 0.057$).

Two patients from Group 3 with progressive disease were treated prior to 2015. One patient from Group 1 began treatment in September 2015. One patient from Group 2 began treatment in

February 2018. All other patients were treated between 2016–2017. Thus, the general policy for rescue treatments was quite homogeneous. A total of 8/28 patients from Groups 1 and 2 received re-irradiation upon progression. One of these eight patients received CED therapy in London, and subsequently received intra-arterial chemotherapy in Monterrey (idoimexico.com). One other patient proceeded with antineoplaston treatment followed by intra-arterial chemotherapy in Monterrey. We are not aware whether chemotherapy rescue protocols were initiated. Most patients went to palliative treatments.

3.4. Laboratory Data Monitoring

Data on the evolution of the above described values over time were available for 14 patients with longer follow up (one patient from Group 1, 11 patients from Group 2, and two patients from Group 3). Data on the PanTum Detect test scores were available for two further patients from Group 2 (23794 and 23887). Ten patients from Groups 1 and 2 had an OS that was longer than the median OS, while four patients had an OS that was shorter than the median OS. Data on the shift in Th1/Th2 balance are shown in Figure 5A. Although mostly within the normal reference range, 5/9 patients with an OS longer than the median shifted toward Th1 upon immunotherapy, and 4/9 toward Th2. The three patients with a shorter OS all shifted toward Th2 upon immunotherapy. One patient (22837) first shifted to Th1, but then clearly to Th2. The median OS of the patients that shifted to Th1 was 23.5 months, whereas the median OS of the patients that shifted to Th2 was 17.7 m (not significant). The two patients from Group 3 shifted toward Th1 immediately following their two vaccination cycles.

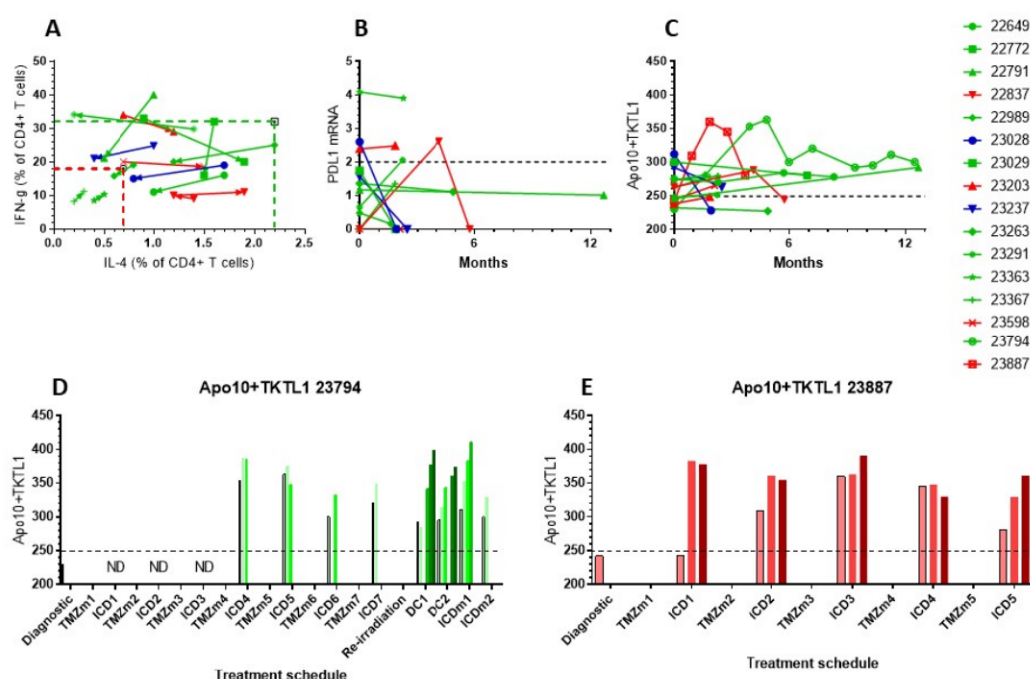


Figure 5. Evolution of immune variables in blood was followed in 14 patients. Patients treated with immunotherapy as part of their primary treatment with an OS longer than the median OS are shown in green, and patients with an OS shorter than the median OS are shown in red. Marked in blue are two patients treated with immunotherapy at the time of progressive disease following the first line of treatment. (A) Percentage IL-4 and IFN-g producing CD4+ T cells measured at different time points. The arrow indicates the evolution. (B) Longitudinal PDL1 mRNA expression in CTCs over the course of 12 months. The reference cut-off was 2 (dashed line). (C) The evolution of the sum of Apo10 and TKTL1 over 12 months. The maximum cut-off was 249 (dashed line). (D,E) Individual data of Apo10 + TKTL1 scores in patients 23794 and 23887. Each treatment block is indicated. During each immunotherapeutic intervention, Apo10 + TKTL1 scores were measured before the start of, and at each consecutive day during treatment.

Available mRNA values for PDL1 in CTCs (Figure 5B) did not change significantly over time as compared to the immunodiagnostic test. Values for the sum of Apo10 and TKTL1 scores were also followed over months in this subset of patients (Figure 5C). The values reflect the content of tumor-derived Apo10 and TKTL1 within CD14+CD16+ monocytes in peripheral blood. The levels of these values are influenced by the volume of tumor cell damage as well as tumor cell death in response to treatment. The two patients treated at the time of relapse had a reduction in Apo10 and TKTL1 scores over time. Additionally, two patients from Groups 1 and 2 with shorter than median OS had decreasing values, while patients from Groups 1 and 2 who showed longer than median OS had mostly stable or increasing values, reflecting persistent uptake of Apo10 and TKTL1 from dying tumor cells. The more detailed curves of patients 23794 and 23387 showed an initial increase followed by a stable and decreasing curve, respectively (Figure 5C). Of note, these two children were treated according to the German standard of care with radiochemotherapy and up to 12 maintenance TMZ cycles, to which ICD treatments were added, similar to the schedule published previously for adults with GBM [27]. At the immune diagnostic blood sampling, both patients had a low content of Apo10 and TKTL1 in the CD14+CD16+ monocytes, though both were treated only with radiochemotherapy. Both patients showed an increase in their PanTum Detect test scores and a subsequent decrease, potentially reflecting the effect of transient radiochemotherapy and maintenance chemotherapy plus ICD therapy. Patient 23794 received seven TMZ cycles with ICD treatment, experienced disease progression, and was then re-irradiated and received two DC vaccination cycles and further maintenance ICD treatments. Patient 23387 received five TMZ maintenance cycles with ICD treatment, experienced disease progression, and finished immunotherapy, but then received re-irradiation and anti-GD2 antibody.

Focusing on the evolution of the PanTum Detect test results as a marker of response to ICD treatment [36], we began daily PanTum Detect test measurements during treatment. Data from two patients (23794 and 23387) were available. Figure 5D,E show the daily evolution of the available PanTum Detect test results during immunotherapy at different treatment episodes. The retrospectively sampled dataset was incomplete, however, one can appreciate the marked increase in the PanTum Detect test results in Patient 23387 upon the first 3-day ICD treatment (Figure 5E). The ICD treatment did not induce a further increase in the PanTum Detect test scores on a day-by-day basis when the starting value of the treatment block was increased, but the increase in the PanTum Detect test scores became clear again when the starting value of the treatment block was lowered. In Patient 23794, at the time of DC vaccinations and the 5-day ICD treatment, an apparent day-by-day increase was again observed upon injection with NDV and treatment with mEHT (Figure 5D). Together, the data suggest that the values of the PanTum Detect test scores evolve over time, and that this evolution is likely to be influenced by both the response to the standard antitumor treatment (transient increase and decrease over months) and the response to ICD treatment (rapid increase day-by-day).

4. Discussion

In this study, we summarized the data obtained from a retrospective analysis of a cohort of children diagnosed with DIPG who received multimodal immunotherapy as a primary treatment, or at the time of progressive disease, at the IOZK mainly between 2016–2017. These children were treated using an individualized approach. As such, the data should be taken with great caution, and no firm conclusions can be drawn. The authors, however, do believe that the reporting of such data is of high value to the field of DIPG research, and also holds value for the community of patients and their families. It is critical to provide comprehensive data gathered from retrospective analyses, in order to aid in (1) the counseling and guidance of future patients on the basis of the analyzed data, and (2) the development of new innovative clinical trials.

Immunotherapy and molecular biology-based treatments are emerging in the field of DIPG. H3K27M is recognized as a tumor-specific antigen [37,38], and vaccination strategies using the long-peptide are under consideration. Immune responses have been generated using autologous DCs loaded with lysate from DIPG cell lines [39]. Moreover, DC vaccination technology has

been shown to be feasible and safe. The tumor microenvironment remains a major obstacle in immunotherapy approaches [40], and oncolytic virus therapy can play a major role in modulating the tumor microenvironment [41,42]. NDV was shown *in vitro* to reduce the viability of DIPG cell lines (Carolien Koks, unpublished data). Infiltration of tumor-reacting T cells within a DIPG microenvironment was demonstrated in animal models upon treatment with the Delta-24-RGD oncolytic virus [43,44]. A concern in the field of oncolytic virus therapy is the antiviral immunity of the patient. However, anti-viral immunity in an animal model using NDV as the oncolytic virus has been shown to potentiate its immunotherapeutic efficacy [45]. mEHT is a method to treat cancer by inducing heat stress, which selectively targets tumor cells due to their altered metabolic dependencies relative to healthy cells, resulting in different conductivity of electromagnetic waves [46]. mEHT is known to induce immunogenic cell death [47–50], and has been previously utilized in the treatment of brain tumors [51]. Overall, there are sufficient data as well as experience at the IOZK to support multimodal immunotherapy for these children as an individualized treatment approach.

While the patient group is small, the collation of retrospective data from 36 patients with DIPG over a period of two years in one institution remains remarkable. The drive for this retrospective study was mainly the interest both among clinicians and parents of children with DIPG, as evidenced by social media. The authors realize that this is a highly biased patient group at multiple levels including the medical condition and the attitude of the parents. However, when considering the age distribution and LPS distribution of this cohort, the patient group reflects the typical DIPG patient profile. The LPS was very low in some patients from Group 3, presenting with progressive disease. Whereas all patients had typical clinical symptoms and MRI findings to substantiate the diagnosis of DIPG, the diagnosis was further supported in 16/41 patients (39%) by molecular analysis via tissue or plasma liquid biopsy, facilitating the identification of diagnostic histone H3K27M mutations in a subset of patients. Nonetheless, MR imaging was the key factor in DIPG diagnosis. The available data did not allow an appropriate matching analysis between tissue biopsy and liquid biopsy.

All patients were counseled and treated for DIPG by the oncologic center. Thirteen children from Group 2 were treated with radiotherapy as the first line treatment alone, while in total, three children from Group 1 (Polish protocol, though meant to be followed by radiotherapy) and nine children from Group 2 were treated with radiotherapy and chemotherapy. This distribution also reflects the current reality for DIPG treatment practices [26]: 52% of our patients with first diagnosis were treated by the oncologic center with radiotherapy alone.

A surprisingly high proportion of patients exhibited immune variables below the reference values at the time of presentation for multimodal immunotherapy. Both the disease itself and the treatments given have a clear effect on immune potency. Even the three children who were not treated with steroids or other prior treatments (radio- or chemotherapy) had levels below the reference limit for at least one functional immune variable (cytokine production, NK killing function). This is a notable finding, as the DIPG tumor microenvironment has been recently characterized as neither highly immunosuppressive nor inflammatory [40]. Furthermore, approximately half of the patients with newly diagnosed DIPG were treated with only radiotherapy prior to blood sampling. However, radiotherapy given only locally can still have a systemic effect on the immune system [52]. The addition of Temozolomide during and after radiotherapy further affects immune function. Nevertheless, a strategy to combine maintenance Temozolomide with immunogenic cell death treatment and subsequent DC vaccination after maintenance chemotherapy has already been published for adults with GBM [27]. Together, the data point to a weakened immune status of the patient at the time of DIPG diagnosis, which is worsened by any further medical intervention.

Another remarkable finding is the presence of CTCs in the blood at the time of the immunodiagnostic blood sampling prior to immunotherapy. This test, provided by LADR Biofocus, detects CTCs based on filtration techniques for the enrichment of cancer cells from the blood [53–55]. Molecular detection is subsequently performed by quantitative real-time PCR to measure the mRNA expression of Telomerase, ERBB2, C-kit, and EGFR in comparison to GADPH mRNA expression.

These general markers for brain tumors are used for tumor cell detection, as specific H3K27M mRNA markers are not currently available. CTCs were detected in 73% of patients, a detection rate higher than the detection rate for brain tumors (60%) mentioned by the company. Although there is emerging knowledge on CTCs in patients with GBM [56,57], no specific literature is available for DIPG. Nevertheless, this finding might lead to more systematic detection in these patients, as the presence of CTCs in peripheral blood may reflect changing tumor biology and treatment resistance. Importantly, 42% of CTC-positive samples showed elevated mRNA expression for PDL1 relative to the housekeeping gene mRNA. PDL1 positivity in these CTCs might contribute to immune resistance, similar to the mechanism published for PDL1-expressing GBM-derived extracellular vesicles [58]. Correlations between the expression of PDL1 mRNA in CTCs and data on the tumor–host interaction derived from pathology investigations on biopsies is not currently available, but warrants further study.

All patients were treated with an individualized treatment approach in compassionate use (“individueller Heilversuch”) with the goal of prolonging individual survival and maintaining quality of life. The OS is the most important read-out of any clinical approach for DIPG patients, but remains very poor. All previous attempts to date to improve OS have failed [10–12]. The survival prediction model published in 2015 can be considered as actual [13]. In this model, the age, duration of symptoms, and use of chemotherapy are linked to improved OS, whereas ring contrast enhancement on MRI at diagnosis is an unfavorable predictor of OS [13]. In the presented retrospective series, we did not have all the data available to calculate the individual DIPG risk score for each patient. However, only one child from Group 2 was younger than three years of age at diagnosis, and 14/22 (64%) patients did not receive chemotherapy; these two important factors influenced the DIPG risk score for most patients with “+7” in the absence of “−4”. Accordingly, one can estimate that most patients belong to the intermediate and high risk groups. Although the patient cohort in this study remains biased in many respects, and no definite conclusions can be drawn from this retrospective analysis, the observed 14.4 month median OS for Group 2 exceeded the published median OS of 9.7 months for intermediate risk patients and seven months for high risk patients, respectively, in the published survival prediction model [13]. All patients from Group 3 were older than three years, and only four patients (31%) did not receive chemotherapy. The median OS of 9.1 months from diagnosis in this group reflects the published data [13]. These patients represent an equally biased patient group as those from Groups 1 and 2. Therefore, one can conclude that the introduction of immunotherapy as a first line treatment may provide potential benefit, compared to the introduction of immunotherapy at the time of progressive disease. This finding is further supported by the data showing that the estimated PFS shifted by about two months upon introduction of immunotherapy as first line treatment. Immunotherapy at an early stage of disease is generally accepted to be more effective than at a later stage of disease [59]. As most patients did not undergo a tumor biopsy, and hence no tumor DNA was available to determine mutation status or other molecular biology characteristics, we could not further compare the OS data in this study with data published on patient groups defined by the molecular biology of the tumor [60].

We were able to measure cytokine production during treatment in several patients. For all monitoring data, patients from Groups 1 and 2 were divided into (a) those living longer or shorter than the median OS, and (b) patients treated at relapse. The authors realize that this is a rough descriptive analysis. A total of 67% of patients with longer OS had an immune response shift toward Th1, while all patients with shorter OS shifted toward Th2. A Th1 shift linked to a better OS upon immunotherapy has also been observed in patients with GBM treated with immunotherapy [27]. In GBM, the profile of the myeloid cells and microglia within the tumor microenvironment contributes to the Th1/Th2 balance, and hence the Th2 shift upon treatment might reflect a more immunosuppressive tumor microenvironment [61]. Similarly, the Th1/Th2 balance has been linked to PDL1/PD2 axis activity [62]. However, the tumor–host mechanisms observed in GBM cannot be transferred to the DIPG tumor microenvironment [40]. Furthermore, the peripheral blood immune status does not necessarily reflect the intra-tumor status. We were not able to detect links between oncologic, immune, or treatment characteristics predicting the shift direction.

During the years in which the 41 children in this cohort were treated, we developed the PanTum Detect tests using the EDIM platform as a potential marker of response to treatment [36]. These tests were originally developed for cancer screening purposes [30–33], but showed value in the temporal monitoring of patient responses [63,64]. Data in GBM patients suggested that high PanTum Detect test scores could reflect responsive patients with better survival [27]. A similar observation was present in this cohort of patients. The kinetics of these markers showed a transient response to the different treatment modalities and allowed a day-by-day assessment of the effect of ICD treatment. Both NDV [41,42] and mEHT [47–50] have been shown to induce ICD. The *in vivo* assessment of ICD is difficult, as biomarkers in blood are strongly diluted and are not fully representative of the biological processes occurring within the tumor. Most *in vivo* assessment of ICD relies on the abscopal effect that can be studied in pre-clinical *in vivo* models. Intracellular staining of tumor-related markers such as Apo10 and TKTL1 can be considered as a methodology using the circulating CD14+CD16+ myeloid cells in the blood, which may provide information on the tumor. Any kind of tumor cell damage causing leakage of Apo10 and TKTL1 could be picked up by myeloid cells. Thus, the interpretation of the PanTum Detect test scores is complex and influenced by many factors. However, the repetitive day-by-day increase upon ICD treatment might suggest a causal relationship between ICD treatment and increased biomarker levels.

5. Conclusions

We report our experiences with multimodal immunotherapy in a large cohort of children with DIPG treated within a short time frame. This retrospective analysis has uncovered several interesting observations that may allow further optimization of multimodal immunotherapy for DIPG as part of primary treatment, focusing on Th1/Th2 shifting, the mode of NDV application, and the intensity of mEHT. The evolution of PanTum Detect test scores may emerge as a tool for assessing treatment response on a daily basis. This retrospective analysis consisted of a biased group of patients, and all associated limitations should be considered. Further preclinical mechanistic data should be generated to support the treatment concept. Nevertheless, the observed median OS of 14.4 months, 1-year survival of 65%, and 2-year survival of 10% for children belonging to intermediate or high-risk profiles remain remarkable. The data suggest that multimodal immunotherapy may be useful when integrated with the first line of treatment. A phase I/II clinical trial incorporating multimodal immunotherapy after the standard radiotherapy, and measuring the variables described here, is the most appropriate design at the current stage. This report aims to provide information to the scientific community for appropriate counseling of patients, and ultimately for consideration of the inclusion of multimodal immunotherapy in innovative clinical trials.

Author Contributions: Conceptualization, S.W.V.G. and W.S.; Formal Analysis, S.W.V.G.; Methodology, S.W.V.G., J.M., E.R.B., O.F., M.P.D., L.P., J.N., and W.S.; Data curation, S.W.V.G.; Writing—original draft preparation, S.W.V.G.; Writing—review & editing, J.M., E.R.B., O.F., M.P.D., L.P., V.S., J.N., and W.S.; Supervision, S.W.V.G. All authors have read and agreed to the published version of the manuscript.

Funding: This research received no external funding.

Acknowledgments: The authors thank the clinical team, the team from the immune-diagnostic laboratory, and the team from the GMP laboratory at the IOZK for their excellent work making this complex treatment possible for children with DIPG. The authors thank Sara Werr for her practical and emotional support for the patients coming from the USA. The authors thank all patients and their parents and families for their confidence in our attempt to provide help.

Conflicts of Interest: The authors declare no conflicts of interest.

References

1. Johnson, K.J.; Cullen, J.; Barnholtz-Sloan, J.S.; Ostrom, Q.T.; Langer, C.E.; Turner, M.C.; McKean-Cowdin, R.; Fisher, J.L.; Lupo, P.J.; Partap, S.; et al. Childhood brain tumor epidemiology: A brain tumor epidemiology consortium review. *Cancer Epidemiol. Biomark. Prev.* **2014**, *23*, 2716–2736. [\[CrossRef\]](#) [\[PubMed\]](#)
2. Ostrom, Q.T.; Gittleman, H.; Liao, P.; Vecchione-Koval, T.; Wolinsky, Y.; Kruchko, C.; Barnholtz-Sloan, J.S. CBTRUS Statistical Report: Primary brain and other central nervous system tumors diagnosed in the United States in 2010–2014. *Neuro Oncol.* **2017**, *19*, v1–v88. [\[CrossRef\]](#) [\[PubMed\]](#)
3. Warren, K.E. Diffuse intrinsic pontine glioma: Poised for progress. *Front. Oncol.* **2012**, *2*, 205. [\[CrossRef\]](#) [\[PubMed\]](#)
4. Van Zanten, S.E.V.; Jansen, M.H.; Aliaga, E.S.; van Vuurden, D.G.; Vandertop, W.P.; Kaspers, G.J. A twenty-year review of diagnosing and treating children with diffuse intrinsic pontine glioma in The Netherlands. *Expert Rev. Anticancer. Ther.* **2015**, *15*, 157–164. [\[CrossRef\]](#)
5. Khuong-Quang, D.A.; Buczkowicz, P.; Rakopoulos, P.; Liu, X.Y.; Fontebasso, A.M.; Bouffet, E.; Bartels, U.; Albrecht, S.; Schwartzentruber, J.; Letourneau, L.; et al. K27M mutation in histone H3.3 defines clinically and biologically distinct subgroups of pediatric diffuse intrinsic pontine gliomas. *Acta Neuropathol.* **2012**, *124*, 439–447. [\[CrossRef\]](#) [\[PubMed\]](#)
6. Louis, D.N.; Perry, A.; Reifenberger, G.; von Deimling, A.; Figarella-Branger, D.; Cavenee, W.K.; Ohgaki, H.; Wiestler, O.D.; Kleihues, P.; Ellison, D.W. The 2016 World Health Organization Classification of Tumors of the Central Nervous System: A summary. *Acta Neuropathol.* **2016**, *131*, 803–820. [\[CrossRef\]](#)
7. Karremann, M.; Gielen, G.H.; Hoffmann, M.; Wiese, M.; Colditz, N.; Warmuth-Metz, M.; Bison, B.; Claviez, A.; van Vuurden, D.G.; von Bueren, A.O.; et al. Diffuse high-grade gliomas with H3 K27M mutations carry a dismal prognosis independent of tumor location. *Neuro Oncol.* **2018**, *20*, 123–131. [\[CrossRef\]](#)
8. Hassan, H.; Pinches, A.; Picton, S.V.; Phillips, R.S. Survival rates and prognostic predictors of high grade brain stem gliomas in childhood: A systematic review and meta-analysis. *J. Neurooncol.* **2017**, *135*, 13–20. [\[CrossRef\]](#)
9. Lam, S.; Lin, Y.; Zinn, P.; Su, J.; Pan, I.W. Patient and treatment factors associated with survival among pediatric glioblastoma patients: A Surveillance, Epidemiology, and End Results study. *J. Clin. Neurosci.* **2018**, *47*, 285–293. [\[CrossRef\]](#)
10. Hargrave, D.; Bartels, U.; Bouffet, E. Diffuse brainstem glioma in children: Critical review of clinical trials. *Lancet Oncol.* **2006**, *7*, 241–248. [\[CrossRef\]](#)
11. Jansen, M.H.; van Vuurden, D.G.; Vandertop, W.P.; Kaspers, G.J. Diffuse intrinsic pontine gliomas: A systematic update on clinical trials and biology. *Cancer Treat. Rev.* **2012**, *38*, 27–35. [\[CrossRef\]](#) [\[PubMed\]](#)
12. Bredlau, A.L.; Korones, D.N. Diffuse intrinsic pontine gliomas: Treatments and controversies. *Adv. Cancer Res.* **2014**, *121*, 235–259. [\[CrossRef\]](#) [\[PubMed\]](#)
13. Jansen, M.H.; van Zanten, S.E.V.; Aliaga, E.S.; Heymans, M.W.; Warmuth-Metz, M.; Hargrave, D.; van der Hoeven, E.J.; Gidding, C.E.; de Bont, E.S.; Eshghi, O.S.; et al. Survival prediction model of children with diffuse intrinsic pontine glioma based on clinical and radiological criteria. *Neuro Oncol.* **2015**, *17*, 160–166. [\[CrossRef\]](#) [\[PubMed\]](#)
14. Rechberger, J.S.; Lu, V.M.; Zhang, L.; Power, E.A.; Daniels, D.J. Clinical trials for diffuse intrinsic pontine glioma: The current state of affairs. *Childs Nerv. Syst.* **2019**, *36*, 39–46. [\[CrossRef\]](#) [\[PubMed\]](#)
15. Janssens, G.O.; Gandola, L.; Bolle, S.; Mandeville, H.; Ramos-Albiac, M.; van Beek, K.; Benghiat, H.; Hoeben, B.; Madrid, A.M.L.; Kortmann, R.D.; et al. Survival benefit for patients with diffuse intrinsic pontine glioma (DIPG) undergoing re-irradiation at first progression: A matched-cohort analysis on behalf of the SIOP-E-HGG/DIPG working group. *Eur. J. Cancer* **2017**, *73*, 38–47. [\[CrossRef\]](#)
16. Roujeau, T.; Machado, G.; Garnett, M.R.; Miquel, C.; Puget, S.; Geoerger, B.; Grill, J.; Boddaert, N.; Di, R.F.; Zerah, M.; et al. Stereotactic biopsy of diffuse pontine lesions in children. *J. Neurosurg.* **2007**, *107*, 1–4. [\[CrossRef\]](#)
17. Puget, S.; Beccaria, K.; Blauwblomme, T.; Roujeau, T.; James, S.; Grill, J.; Zerah, M.; Varlet, P.; Sainte-Rose, C. Biopsy in a series of 130 pediatric diffuse intrinsic Pontine gliomas. *Childs Nerv. Syst.* **2015**, *31*, 1773–1780. [\[CrossRef\]](#)

18. Cohen, K.J.; Jabado, N.; Grill, J. Diffuse intrinsic pontine gliomas-current management and new biologic insights. Is there a glimmer of hope? *Neuro Oncol.* **2017**, *19*, 1025–1034. [[CrossRef](#)]
19. Pfaff, E.; Damaty, A.E.; Balasubramanian, G.P.; Blattner-Johnson, M.; Worst, B.C.; Stark, S.; Witt, H.; Pajtler, K.W.; van Tilburg, C.M.; Witt, R.; et al. Brainstem biopsy in pediatric diffuse intrinsic pontine glioma in the era of precision medicine: The INFORM study experience. *Eur. J. Cancer* **2019**, *114*, 27–35. [[CrossRef](#)]
20. Van Zanten, S.E.V.; Baugh, J.; Chaney, B.; De Jongh, D.; Sanchez Aliaga, E.; Barkhof, F.; Noltes, J.; De Wolf, R.; Van Dijk, J.; Cannarozzo, A.; et al. Development of the SIOPE DIPG network, registry and imaging repository: A collaborative effort to optimize research into a rare and lethal disease. *J. Neurooncol.* **2017**, *132*, 255–266. [[CrossRef](#)]
21. Van Zanten, S.E.M.V.; Lane, A.; Heymans, M.W.; Baugh, J.; Chaney, B.; Hoffman, L.M.; Doughman, R.; Jansen, M.H.A.; Sanchez, E.; Vandertop, W.P.; et al. External validation of the diffuse intrinsic pontine glioma survival prediction model: A collaborative report from the International DIPG Registry and the SIOPE DIPG Registry. *J. Neurooncol.* **2017**, *134*, 231–240. [[CrossRef](#)] [[PubMed](#)]
22. Wolff, J.E.; Driever, P.H.; Erdlenbruch, B.; Kortmann, R.D.; Rutkowski, S.; Pietsch, T.; Parker, C.; Metz, M.W.; Gnekow, A.; Kramm, C.M. Intensive chemotherapy improves survival in pediatric high-grade glioma after gross total resection: Results of the HIT-GBM-C protocol. *Cancer* **2010**, *116*, 705–712. [[CrossRef](#)] [[PubMed](#)]
23. Anderson, R.C.; Kennedy, B.; Yanes, C.L.; Garvin, J.; Needle, M.; Canoll, P.; Feldstein, N.A.; Bruce, J.N. Convection-enhanced delivery of topotecan into diffuse intrinsic brainstem tumors in children. *J. Neurosurg. Pediatr.* **2013**, *11*, 289–295. [[CrossRef](#)] [[PubMed](#)]
24. Singleton, W.G.B.; Bienemann, A.S.; Woolley, M.; Johnson, D.; Lewis, O.; Wyatt, M.J.; Damment, S.J.P.; Boulter, L.J.; Killick-Cole, C.L.; Asby, D.J.; et al. The distribution, clearance, and brainstem toxicity of panobinostat administered by convection-enhanced delivery. *J. Neurosurg. Pediatr.* **2018**, *22*, 288–296. [[CrossRef](#)] [[PubMed](#)]
25. Souweidane, M.M.; Kramer, K.; Pandit-Taskar, N.; Zhou, Z.; Haque, S.; Zanzonico, P.; Carrasquillo, J.A.; Lyashchenko, S.K.; Thakur, S.B.; Donzelli, M.; et al. Convection-enhanced delivery for diffuse intrinsic pontine glioma: A single-centre, dose-escalation, phase 1 trial. *Lancet Oncol.* **2018**, *19*, 1040–1050. [[CrossRef](#)]
26. El-Khouly, F.E.; van Zanten, S.E.M.V.; Lopez, V.S.-M.; Hendrikse, N.H.; Kaspers, G.J.L.; Loizos, G.; Sumerauer, D.; Nysom, K.; Pruunsild, K.; Pentikainen, V.; et al. Diagnostics and treatment of diffuse intrinsic pontine glioma: Where do we stand? *J. Neurooncol.* **2019**, *145*, 177–184. [[CrossRef](#)] [[PubMed](#)]
27. Van Gool, S.W.; Makalowski, J.; Feyen, O.; Prix, L.; Schirmacher, V.; Stuecker, W. The induction of immunogenic cell death (ICD) during maintenance chemotherapy and subsequent multimodal immunotherapy for glioblastoma (GBM). *Austin Oncol. Case Rep.* **2018**, *3*, 1010.
28. Panditharatna, E.; Kilburn, L.B.; Aboian, M.S.; Kambhampati, M.; Gordish-Dressman, H.; Magge, S.N.; Gupta, N.; Myseros, J.S.; Hwang, E.I.; Kline, C.; et al. Clinically Relevant and Minimally Invasive Tumor Surveillance of Pediatric Diffuse Midline Gliomas Using Patient-Derived Liquid Biopsy. *Clin. Cancer Res.* **2018**, *24*, 5850–5859. [[CrossRef](#)]
29. Bonner, E.R.; Saoud, K.; Lee, S.; Panditharatna, E.; Kambhampati, M.; Mueller, S.; Nazarian, J. Detection and Monitoring of Tumor Associated Circulating DNA in Patient Biofluids. *J. Vis. Exp.* **2019**. [[CrossRef](#)]
30. Feyen, O.; Coy, J.F.; Prasad, V.; Schierl, R.; Saenger, J.; Baum, R.P. EDIM-TKTL1 blood test: A noninvasive method to detect upregulated glucose metabolism in patients with malignancies. *Future Oncol.* **2012**, *8*, 1349–1359. [[CrossRef](#)]
31. Grimm, M.; Schmitt, S.; Teriete, P.; Biegner, T.; Stenzl, A.; Hennenlotter, J.; Muhs, H.J.; Munz, A.; Nadtsch, T.; König, K.; et al. A biomarker based detection and characterization of carcinomas exploiting two fundamental biophysical mechanisms in mammalian cells. *BMC Cancer* **2013**, *13*, 569. [[CrossRef](#)] [[PubMed](#)]
32. Grimm, M.; Feyen, O.; Coy, J.F.; Hofmann, H.; Teriete, P.; Reinert, S. Analysis of circulating CD14+/CD16+ monocyte-derived macrophages (MDMs) in the peripheral blood of patients with oral squamous cell carcinoma. *Oral Surg. Oral Med. Oral Pathol. Oral Radiol.* **2016**, *121*, 301–306. [[CrossRef](#)] [[PubMed](#)]
33. Coy, J.F. EDIM-TKTL1/Apo10 Blood Test: An Innate Immune System Based Liquid Biopsy for the Early Detection, Characterization and Targeted Treatment of Cancer. *Int. J. Mol. Sci.* **2017**, *18*, 878. [[CrossRef](#)] [[PubMed](#)]
34. Nikbakht, H.; Panditharatna, E.; Mikael, L.G.; Li, R.; Gayden, T.; Osmond, M.; Ho, C.Y.; Kambhampati, M.; Hwang, E.I.; Faury, D.; et al. Spatial and temporal homogeneity of driver mutations in diffuse intrinsic pontine glioma. *Nat. Commun.* **2016**, *7*, 11185. [[CrossRef](#)] [[PubMed](#)]

35. Bonner, E.R.; Bornhorst, M.; Packer, R.J.; Nazarian, J. Liquid biopsy for pediatric central nervous system tumors. *NPJ Precis. Oncol.* **2018**, *2*, 29. [[CrossRef](#)] [[PubMed](#)]
36. Van Gool, S.W.; Feyen, O.; Makalowski, J.; Neinhuis, A.; Schirmacher, V.; Stuecker, W. How to monitor immunogenic cell death in patients with glioblastoma. *Neuro Oncol.* **2018**, *20*, vi7–vi8. [[CrossRef](#)]
37. Chheda, Z.S.; Kohanbash, G.; Okada, K.; Jahan, N.; Sidney, J.; Pecoraro, M.; Yang, X.; Carrera, D.A.; Downey, K.M.; Shrivastav, S.; et al. Novel and shared neoantigen derived from histone 3 variant H3.3K27M mutation for glioma T cell therapy. *J. Exp. Med.* **2017**, *215*, 141–157. [[CrossRef](#)]
38. Ochs, K.; Ott, M.; Bunse, T.; Sahm, F.; Bunse, L.; Deumelandt, K.; Sonner, J.K.; Keil, M.; von Deimling, A.; Wick, W.; et al. K27M-mutant histone-3 as a novel target for glioma immunotherapy. *Oncoimmunology* **2017**, *6*, e1328340. [[CrossRef](#)]
39. Benitez-Ribas, D.; Cabezón, R.; Florez-Grau, G.; Molero, M.C.; Puerta, P.; Guillen, A.; Paco, S.; Carcaboso, A.M.; Lopez, V.S.-M.; Cruz, O.; et al. Immune Response Generated With the Administration of Autologous Dendritic Cells Pulsed With an Allogenic Tumoral Cell-Lines Lysate in Patients With Newly Diagnosed Diffuse Intrinsic Pontine Glioma. *Front. Oncol.* **2018**, *8*, 127. [[CrossRef](#)]
40. Lieberman, N.A.P.; DeGolier, K.; Kovar, H.M.; Davis, A.; Hoglund, V.; Stevens, J.; Winter, C.; Deutsch, G.; Furlan, S.N.; Vitanza, N.A.; et al. Characterization of the immune microenvironment of diffuse intrinsic pontine glioma: Implications for development of immunotherapy. *Neuro Oncol.* **2019**, *21*, 83–94. [[CrossRef](#)]
41. Koks, C.A.E.; Garg, A.D.; Ehrhardt, M.; Riva, M.; De Vleeschouwer, S.; Agostinis, P.; Graf, N.; Van Gool, S.W. Newcastle disease virotherapy induces long-term survival and tumor-specific immune memory in orthotopic glioma through the induction of immunogenic cell death. *Int. J. Cancer* **2014**, *136*, e313–e325. [[CrossRef](#)] [[PubMed](#)]
42. Qu, Y.; Zhan, Y.; Yang, S.; Ren, S.; Qiu, X.; Rehamn, Z.U.; Tan, L.; Sun, Y.; Meng, C.; Song, C.; et al. Newcastle disease virus infection triggers HMGB1 release to promote the inflammatory response. *Virology* **2018**, *525*, 19–31. [[CrossRef](#)]
43. Martinez-Velez, N.; Marigil, M.; Garcia-Moure, M.; Gonzalez-Huarriz, M.; Aristu, J.J.; Ramos-Garcia, L.I.; Tejada, S.; Diez-Valle, R.; Patino-Garcia, A.; Becher, O.J.; et al. Delta-24-RGD combined with radiotherapy exerts a potent antitumor effect in diffuse intrinsic pontine glioma and pediatric high grade glioma models. *Acta Neuropathol. Commun.* **2019**, *7*, 64. [[CrossRef](#)] [[PubMed](#)]
44. Martinez-Velez, N.; Garcia-Moure, M.; Marigil, M.; Gonzalez-Huarriz, M.; Puigdelloses, M.; Perez-Larraya, J.G.; Zalacain, M.; Marrodan, L.; Varela-Guruzeaga, M.; Laspidea, V.; et al. The oncolytic virus Delta-24-RGD elicits an antitumor effect in pediatric glioma and DIPG mouse models. *Nat. Commun.* **2019**, *10*, 2235. [[CrossRef](#)] [[PubMed](#)]
45. Ricca, J.M.; Oseledchyk, A.; Walther, T.; Liu, C.; Mangarin, L.; Merghoub, T.; Wolchok, J.D.; Zamarin, D. Pre-existing Immunity to Oncolytic Virus Potentiates Its Immunotherapeutic Efficacy. *Mol. Ther.* **2018**, *26*, 1008–1019. [[CrossRef](#)] [[PubMed](#)]
46. Szasz, O. Bioelectromagnetic paradigm of cancer treatment—Modulated electro-hyperthermia (mEHT). *Open J. Biophys.* **2019**, *9*, 98–109. [[CrossRef](#)]
47. Vandenberk, L.; Belmans, J.; Van Woensel, M.; Riva, M.; Van Gool, S.W. Exploiting the Immunogenic Potential of Cancer Cells for Improved Dendritic Cell Vaccines. *Front. Immunol.* **2015**, *6*, 663. [[CrossRef](#)]
48. Schirmacher, V.; Lorenzen, D.; Van Gool, S.W.; Stuecker, W. A new strategy of cancer immunotherapy combining hyperthermia/oncolytic virus pretreatment with specific autologous anti-tumor vaccination—A Review. *Austin Oncol. Case Rep.* **2017**, *2*, 1006.
49. Vancsik, T.; Kovago, C.; Kiss, E.; Papp, E.; Forika, G.; Benyo, Z.; Meggyeshazi, N.; Krenacs, T. Modulated electro-hyperthermia induced loco-regional and systemic tumor destruction in colorectal cancer allografts. *J. Cancer* **2018**, *9*, 41–53. [[CrossRef](#)]
50. Minnaar, C.A.; Kotzen, J.A.; Ayeni, O.A.; Naidoo, T.; Tunmer, M.; Sharma, V.; Vangu, M.D.; Baeyens, A. The effect of modulated electro-hyperthermia on local disease control in HIV-positive and -negative cervical cancer women in South Africa: Early results from a phase III randomised controlled trial. *PLoS ONE* **2019**, *14*, e0217894. [[CrossRef](#)]
51. Fiorentini, G.; Sarti, D.; Milandri, C.; Dentico, P.; Mambriani, A.; Fiorentini, C.; Mattioli, G.; Casadei, V.; Guadagni, S. Modulated Electrohyperthermia in Integrative Cancer Treatment for Relapsed Malignant Glioblastoma and Astrocytoma: Retrospective Multicenter Controlled Study. *Integr. Cancer Ther.* **2018**, *18*, 1534735418812691. [[CrossRef](#)] [[PubMed](#)]

52. Belka, C.; Ottinger, H.; Kreuzfelder, E.; Weinmann, M.; Lindemann, M.; Lepple-Wienhues, A.; Budach, W.; Grosse-Wilde, H.; Bamberg, M. Impact of localized radiotherapy on blood immune cells counts and function in humans. *Radiother. Oncol.* **1999**, *50*, 199–204. [\[CrossRef\]](#)
53. Truchaud, C.; Caldani, C.; Bisconte, J.C.; Bergogne-Berezin, E.; Buisson, Y. Filtration cytometry: Parallel real-time analysis for bacteria, cells, and particles. *Clin. Chem.* **1992**, *38*, 1650–1951.
54. Vona, G.; Sabile, A.; Louha, M.; Sitruk, V.; Romana, S.; Schutze, K.; Capron, F.; Franco, D.; Pazzagli, M.; Vekemans, M.; et al. Isolation by size of epithelial tumor cells: A new method for the immunomorphological and molecular characterization of circulating tumor cells. *Am. J. Pathol.* **2000**, *156*, 57–63. [\[CrossRef\]](#)
55. Bockmann, B.; Grill, H.J.; Giesing, M. Molecular characterization of minimal residual cancer cells in patients with solid tumors. *Biomol. Eng.* **2001**, *17*, 95–111. [\[CrossRef\]](#)
56. Chistiakov, D.A.; Chekhonin, V.P. Circulating tumor cells and their advances to promote cancer metastasis and relapse, with focus on glioblastoma multiforme. *Exp. Mol. Pathol.* **2018**, *105*, 166–174. [\[CrossRef\]](#)
57. Van Schaijik, B.; Wickremesekera, A.C.; Mantamadiotis, T.; Kaye, A.H.; Tan, S.T.; Stylli, S.S.; Itinteang, T. Circulating tumor stem cells and glioblastoma: A review. *J. Clin. Neurosci.* **2019**, *61*, 5–9. [\[CrossRef\]](#)
58. Ricklefs, F.L.; Alayo, Q.; Krenzlin, H.; Mahmoud, A.B.; Speranza, M.C.; Nakashima, H.; Hayes, J.L.; Lee, K.; Balaj, L.; Passaro, C.; et al. Immune evasion mediated by PD-L1 on glioblastoma-derived extracellular vesicles. *Sci. Adv.* **2018**, *4*, eaar2766. [\[CrossRef\]](#)
59. Shore, N.D. Advances in the understanding of cancer immunotherapy. *BJU Int.* **2015**, *116*, 321–329. [\[CrossRef\]](#)
60. Castel, D.; Philippe, C.; Calmon, R.; Dret, L.L.; Truffaux, N.; Boddaert, N.; Pages, M.; Taylor, K.R.; Saulnier, P.; Lacroix, L.; et al. Histone H3F3A and HIST1H3B K27M mutations define two subgroups of diffuse intrinsic pontine gliomas with different prognosis and phenotypes. *Acta Neuropathol.* **2015**, *130*, 815–827. [\[CrossRef\]](#)
61. Tivnan, A.; Heilinger, T.; Lavelle, E.C.; Prehn, J.H. Advances in immunotherapy for the treatment of glioblastoma. *J. Neurooncol.* **2017**, *131*, 1–9. [\[CrossRef\]](#) [\[PubMed\]](#)
62. Takashima, Y.; Kawaguchi, A.; Kanayama, T.; Hayano, A.; Yamanaka, R. Correlation between lower balance of Th2 helper T-cells and expression of PD-L1/PD-1 axis genes enables prognostic prediction in patients with glioblastoma. *Oncotarget* **2018**, *9*, 19065–19078. [\[CrossRef\]](#) [\[PubMed\]](#)
63. Grimm, M.; Kraut, W.; Hoefert, S.; Krimmel, M.; Biegner, T.; Teriete, P.; Cetindis, M.; Polligkeit, J.; Kluba, S.; Munz, A.; et al. Evaluation of a biomarker based blood test for monitoring surgical resection of oral squamous cell carcinomas. *Clin. Oral Investig.* **2016**, *20*, 329–338. [\[CrossRef\]](#) [\[PubMed\]](#)
64. Grimm, M.; Hoefert, S.; Krimmel, M.; Biegner, T.; Feyen, O.; Teriete, P.; Reinert, S. Monitoring carcinogenesis in a case of oral squamous cell carcinoma using a panel of new metabolic blood biomarkers as liquid biopsies. *Oral Maxillofac. Surg.* **2016**, *20*, 295–302. [\[CrossRef\]](#) [\[PubMed\]](#)



© 2020 by the authors. Licensee MDPI, Basel, Switzerland. This article is an open access article distributed under the terms and conditions of the Creative Commons Attribution (CC BY) license (<http://creativecommons.org/licenses/by/4.0/>).

Randomized Controlled Immunotherapy Clinical Trials for GBM Challenged



Stefaan W. Van Gool¹, Jennifer Makalowski¹, Simon Fiore¹, Tobias Sprenger¹, Lothar Prix², Volker Schirrmacher¹ and Wilfried Stuecker¹

¹Immun-Onkologisches Zentrum Köln
Köln, Germany
²Biofocus
Recklinghausen, Germany

Citation: Van Gool S. W. et al. (2020): Randomized Controlled Immunotherapy Clinical Trials for GBM Challenged, *Oncothermia Journal* 30: 54 – 82,
http://www.oncotherm.com/sites/oncotherm/files/2021-04/VanGool_Randomized.pdf
Reprinted from: <https://www.mdpi.com/2072-6694/13/1/32>

Review

Randomized Controlled Immunotherapy Clinical Trials for GBM Challenged

Stefaan W. Van Gool ^{1,*} , Jennifer Makalowski ¹, Simon Fiore ¹, Tobias Sprenger ¹, Lothar Prix ², Volker Schirmacher ¹  and Wilfried Stuecker ¹

¹ Immun-Onkologisches Zentrum Köln, Hohenstaufenring 30-32, 50674 Köln, Germany; makalowski@iozk.de (J.M.); fiore@iozk.de (S.F.); tobias@sprenger-praxis.de (T.S.); v.schirmacher@web.de (V.S.); stuecker@iozk.de (W.S.)

² Biofocus, Berghäuser Strasse 295, 45659 Recklinghausen, Germany; l.prix@ladr.de

* Correspondence: vangool@iozk.de; Tel.: +49-221-420-39925

Simple Summary: Although multiple meta-analyses on active specific immunotherapy treatment for glioblastoma multiforme (GBM) have demonstrated a significant prolongation of overall survival, no single research group has succeeded in demonstrating the efficacy of this type of treatment in a prospective, double-blind, placebo-controlled, randomized clinical trial. In this paper, we explain how the complexity of the tumor biology and tumor–host interactions make proper stratification of a control group impossible. The individualized characteristics of advanced therapy medicinal products for immunotherapy contribute to heterogeneity within an experimental group. The dynamics of each tumor and in each patient aggravate comparative stable patient groups. Finally, combinations of immunotherapy strategies should be integrated with first-line treatment. We illustrate the complexity of a combined first-line treatment with individualized multimodal immunotherapy in a group of 70 adults with GBM and demonstrate that the integration of immunogenic cell death treatment within maintenance chemotherapy followed by dendritic cell vaccines and maintenance immunotherapy might provide a step towards improving the overall survival rate of GBM patients.



Citation: Van Gool, S.W.; Makalowski, J.; Fiore, S.; Sprenger, T.; Prix, L.; Schirmacher, V.; Stuecker, W. Randomized Controlled Immunotherapy Clinical Trials for GBM Challenged. *Cancers* **2021**, *13*, 32. <https://dx.doi.org/10.3390/cancers13010032>

Received: 28 October 2020

Accepted: 21 December 2020

Published: 24 December 2020

Publisher's Note: MDPI stays neutral with regard to jurisdictional claims in published maps and institutional affiliations.



Copyright: © 2020 by the authors. Licensee MDPI, Basel, Switzerland. This article is an open access article distributed under the terms and conditions of the Creative Commons Attribution (CC BY) license (<https://creativecommons.org/licenses/by/4.0/>).

Abstract: Immunotherapies represent a promising strategy for glioblastoma multiforme (GBM) treatment. Different immunotherapies include the use of checkpoint inhibitors, adoptive cell therapies such as chimeric antigen receptor (CAR) T cells, and vaccines such as dendritic cell vaccines. Antibodies have also been used as toxin or radioactive particle delivery vehicles to eliminate target cells in the treatment of GBM. Oncolytic viral therapy and other immunogenic cell death-inducing treatments bridge the antitumor strategy with immunization and installation of immune control over the disease. These strategies should be included in the standard treatment protocol for GBM. Some immunotherapies are individualized in terms of the medicinal product, the immune target, and the immune tumor–host contact. Current individualized immunotherapy strategies focus on combinations of approaches. Standardization appears to be impossible in the face of complex controlled trial designs. To define appropriate control groups, stratification according to the Recursive Partitioning Analysis classification, MGMT promotor methylation, epigenetic GBM sub-typing, tumor microenvironment, systemic immune functioning before and after radiochemotherapy, and the need for/type of symptom-relieving drugs is required. Moreover, maintenance of a fixed treatment protocol for a dynamic, deadly cancer disease in a permanently changing tumor–host immune context might be inappropriate. This complexity is illustrated using our own data on individualized multimodal immunotherapies for GBM. Individualized medicines, including multimodal immunotherapies, are a rational and optimal yet also flexible approach to induce long-term tumor control. However, innovative methods are needed to assess the efficacy of complex individualized treatments and implement them more quickly into the general health system.

Keywords: GBM; newcastle disease virus; modulated electrohyperthermia; dendritic cell vaccination; clinical trial; individualized multimodal immunotherapy

1. Introduction

Cancer is the second leading cause of death, accounting for about 1 in 6 human deaths. Worldwide, in 2018, about 9.6 million deaths were due to cancer [1]. Between 2013 and 2017, the cancer death rate (mortality rate) in the US was 158/100,000 individuals per year. The rate of new cases (incidence) in a similar period was 442/100,000 individuals per year [2]. Intensive preclinical and clinical research is being performed to find solutions. In some domains, like pediatric hemato-oncology, major progress has been realized towards a cure through systematic randomized controlled clinical trials (RCTs). In each trial, a new experimental arm is assessed versus the best current treatment as the control arm [3,4], in combination with careful monitoring of (long-term) side effects [5].

Despite being an orphan disease, brain tumors are the leading cause of cancer death in males aged 20 to 39 years and the fourth most common cause of cancer death in females in the same age range [6]. Glioblastoma Multiforme (GBM) is the most frequently diagnosed malignant brain cancer in adults and has the worst prognosis [7,8]. The cause of GBM formation is not known. Ageing that progressively suppresses normal immune surveillance has been mentioned to contribute to GBM cell initiation and/or outgrowth [9]. Irradiation is certainly a cause for GBM formation, and the prognosis of a second malignant GBM is extremely poor [10]. Long-term exposure to higher doses of non-ionising irradiation has been associated with the formation of GBM [11]. Finally, viral infections like CMV (variants) have been mentioned as being potential triggers for GBM formation [12]. The classic pillars of treatment for GBM nowadays are neurosurgery, radiochemotherapy, and maintenance chemotherapy [13,14]. In recent years, the standard of care has not changed. Intensive research in different domains has been performed to improve the prognosis of GBM patients, including research in tumor-treating fields, anti-angiogenic treatments, targeted therapies, oncolytic virus therapy, and immunotherapies. The latter term covers different approaches, like restorative immunotherapy, modulating immunotherapy, passive immunotherapy, adoptive immunotherapy, and active-specific immunotherapy with vaccines [15]. For the development and production of mostly personalized cell-based therapies, Good Manufacturing Practice (GMP) facilities are required.

On the occasion of a regulatory audit in July 2019, in connection with the installation of a new GMP facility at the Immune Oncologic Centre in Köln (IOZK, www.iozk.de) and the running GMP-compatible production of IO-Vac® Dendritic cell (DC) vaccines, a discussion was raised with respect to RCTs within the spectrum of delivered individualized multimodal immunotherapy (IMI) activities. The background of this question is a subject of current global debate regarding the future use of controlled RCTs to obtain evidence of the efficacy of immunotherapies. This was exemplified by the symposium organized in Brussels on 22 April 2020, entitled “are randomized trials obsolete?” [16]. On 27 May 2015, the IOZK received a certificate of GMP manufacturing compliance (DE_NW_04_GMP_2015_0030) and approval to produce specific autologous anti-tumor DC vaccines for intradermal injection (DE_NW_04_MIA_2015_0033). Since then, multimodal immunotherapy has been implemented in several domains of cancer. Both certificates were renewed on 20 May 2020 (i.e., DE-NW-04-GMP-2020-0054 and DE-NW-04-MIA-2020-0017).

The IOZK is a translational immune-oncology center specializing in the fast translation of emerging novel insights derived from multiple domains of immunotherapy into clinical applications for use on a compassionate basis (“Individueller Heilversuch”) for patients with cancer. The key medicinal product is IO-Vac®, which is an approved Advanced Therapy Medicinal Product (ATMP). The IO-Vac® vaccine consists of autologous mature DCs loaded with autologous tumor antigens and matured with danger signals including the Newcastle Disease Virus (NDV). Over the years, the IOZK has established its value for the treatment of cancer patients. Several case reports and retrospective analyses of patient groups have been published [17–20]. For the current retrospective analysis, the database was fixed at 28 June 2020, including all records registered from 1 June 2015 to 31 May 2020. Over this 5-year time period, 1456 medical records were initiated at the IOZK. The patients came from 69 countries (with 46% from Germany). From this group

of patients, 1098 patients agreed to go through an immune-oncologic evaluation and immunodiagnostic blood sampling in order to study the cell numbers and functioning of their immune compartment, the tumor–host immune interactions, their general health status, and their infection status. Ultimately, 651 were able to, and individually consented to, starting multimodal immunotherapy, after being extensively informed about all aspects of the treatment. These patients belonged to all categories of cancer disease. The three most frequent cancer disease categories were neuro-oncology (42%), digestive oncology (18%), and breast cancer (11%). The domain of neuro-oncology represents almost half of all patients effectively treated at the IOZK. This group of patients is still a very heterogeneous group, including multiple types of brain cancer disease, and including patients at different stages of disease. From the 276 patients, 171 patients (62%) were recorded as having GBM.

Based on this large number of patients and the presence of extensive preclinical, translational, and clinical expertise in immunotherapy for GBM, the discussion about the challenges in setting up RCTs for immunotherapy herein will be focused on IMI for GBM, in particular to demonstrate why RCTs to prove the efficacy of this type of treatment are lacking, despite several meta-analyses pointing to a significant shift in overall survival (OS) rates due to the use of active specific immunotherapy with DC vaccines [21–25]. We aim to discuss this complex problem by reviewing the literature (Sections 2–7). Afterwards, we illustrate elements from this narrative review with our own data obtained by a retrospective analysis of our patient records (Sections 8–10).

2. Current Anti-Cancer Treatment Strategies for GBM

GBM is one of the leading causes of death due to cancer in humans and is a major burden for the community [26,27]. Earlier, in the period of poor imaging possibilities, neurosurgery was the only treatment for GBM, and this was mostly performed to make pathological diagnoses and to temporarily relieve symptoms. Only during the last century other treatment modalities became available, of which radiotherapy was the first approach. Radiotherapy became part of the standard care for GBM in the 1940s. The authors could not find any RCTs from that period. Evidence of the efficacy of radiotherapy was certainly created by the demonstration of a dose–response relationship [28]. An RCT, including radiotherapy, chemotherapy, or best available care for anaplastic astrocytoma, was realized around the same period, clearly demonstrating the effect of radiotherapy on OS [29]. Radiotherapy was shown to improve the median OS of GBM patients by some months, and 60 Gy appeared to be the most efficacious and safe dose [30]. More recently, chemotherapeutic agents and combination treatments have been implemented. The addition of temozolomide (TMZ) during radiotherapy, followed by TMZ maintenance chemotherapy (TMZm), further improved the median OS (again, by some months). Proof of evidence was generated through a prospective RCT. In this trial, patients were stratified by World Health Organization (WHO) performance status, type of surgery, and institution [13]. Later on, the data were presented according to an adapted Recursive Partitioning Analysis (RPA) classification, which included age, WHO performance status, extent of surgery, and mental status as variables, resulting in Class III, Class IV, and Class V patients [14].

The MGMT promotor methylation status of the tumor was rapidly recognized as a key factor in the efficacy of TMZ [31]. Retrospective analyses of available MGMT promotor methylation data in relation to the survival data in the RCT have shed new light on such data [14]. The progression-free survival (PFS) benefit attained through the addition of TMZ to surgery and radiotherapy lost its significance in MGMT promotor unmethylated patients, and the gain in median OS was only 0.8 months (i.e., 24 to 25 days), albeit still being significant. Although the results of the original prospective RCT were published 15 years ago, this so-called Stupp regimen is still the standard of care world-wide for both MGMT promotor-methylated and unmethylated patients. Due to its major effect, even in multivariate analyses, the MGMT promotor methylation status has become part of the in/exclusion criteria for RCTs or is used in the stratification of the randomization. Step by step, more insight into the transcriptomic and genomic dimensions were found, and

GBM molecular stratification appeared, pointing to EGFR, NF1, and PDGFRA/IDH1 as playing roles in triggering intracellular pathways but also in influencing the response to anti-GBM treatments, formation of the tumor microenvironment, and tumor spread [32]. A further molecular biological analysis including epigenetic profiling unraveled at least six sub-types of GBM, all having different disease characteristics and prognoses [33].

Radiotherapy and chemotherapy treatment modalities are directed against the cancer itself, but cause acute and long-term side effects to the body. These treatments might, however, also have important effects on the immune system. It is already well-known that neurosurgical removal of the tumor transiently “relieves” the systemic immune system from tumor-induced immunosuppression [34], which returns upon disease progression [35]. Both radiotherapy and TMZ have effects on inflammation and the systemic immune compartment but may also influence the tumor microenvironment [36–40].

The improvement in therapeutic approaches has been paralleled by improvements in imaging technologies. Furthermore, knowledge of the molecular biology domain has increased rapidly, thereby introducing new approaches to the development of targeted treatments with less toxicity. A whole series of targeted therapies have been investigated for GBM, as single drugs in relapsed patients or as add-ons to the Stupp regimen [41–46]. Fast molecular biological diagnostic procedures and initiation of adapted drug combinations have opened the door to so-called personalized medicine. For the first time, a particular tumor entity is no longer treated according to pre-designed treatments or study protocols but may become adapted to the individual tumor biology profile of each individual patient. Along the same line, targeted therapies can be implemented to treat any type of cancer, regardless of where in the body it started or the type of tissue from which it developed, pointing to the term “tumor-agnostic treatment” [47].

3. Challenges for RCTs

RCTs, originally conceived as a study concept by Sir Austin Bradford Hill (who also developed the criteria for determining a causal association) and applied for the first time in 1948 [48], aim to control for selection bias and allocation bias by balancing patient groups based on known and unknown prognostic factors. Blinding further reduces experimenter and subject biases. The study methodology allows the efficacy of an intervention under investigation to be demonstrated with the greatest amount of evidence in a defined patient population compared to a control population without this particular intervention. RCTs are the gold standard for proving the efficacy of an intervention. Nevertheless, over the years, research has neglected the additional value of observational studies, demonstrating the effectiveness of interventions [49–54].

Evolution towards the personalization of medicine is challenging for classic RCTs, especially when related to GBM [55]. Stratification is a requirement to avoid differences between patients treated in an experimental arm versus patients treated in a control arm. The need for larger patient groups has resulted in longer recruitment periods and more expensive clinical trials. The rapid introduction of new drugs has forced clinical researchers to form innovative statistical designs for clinical trials, such as Continual Reassessment Method designs, Sequential Multiple Assignment Randomized Trial designs, and Multi-Arm Multi-Stage clinical designs [56].

At present, most (if not all) single-drug-targeted therapy trials for GBM have failed [57], and a new challenge has emerged. Indeed, GBM is a mixture of different tumor cell clones, including glioma cancer stem cells, and there are dynamic changes in emerging and disappearing clones during the course of the disease and in relation to the treatment(s) given [58,59]. Keeping a patient under a fixed treatment protocol over time, eventually in clinical trials, to treat a dynamically and rapidly changing deadly tumor might no longer be considered appropriate in light of advances in modern medicine. Much more effort should be put into studies on liquid biopsies in patients with GBM [60]. These tests should be performed repeatedly during treatment in order to monitor changes in tumor biology during treatment, as has been shown for other cancer diseases [61].

Inflammatory reactions occurring in the context of immunotherapy might necessitate medical intervention, such as the use of steroids or Bevacizumab, for a short period of time. Due to the deadly nature of the disease, changes over time should be taken into account when treating the patient using a study protocol. Such changes during the protocol might induce drop-out of the trial, which is—from a medical perspective—an emotional burden for the patient. Otherwise, changes in treatment have to be taken as data within the protocol, which creates statistical conflicts with the control group of patients, who must then be treated differently.

One of the particular statistical challenges in demonstrating the efficacy of an active specific immunotherapy is the need to assess the increase of percentage long-term OS, rather than the shift of PFS [62], the latter being the usual primary read-out for testing new drugs in late stage phase II RCTs. A phenomenon of GBM pseudo-progression due to immunotherapy makes the read-out of PFS virtually impossible. Similar to the change in using the MacDonald's criteria [63] to the RANO criteria [64] to define progression at a time when TMZ was implemented in routine clinical treatment, iRANO criteria have been developed to assess the progression of GBM disease in the context of immunotherapy [65,66]. The increase in the percentage of long-term OS due to DC vaccines as a primary read-out necessitates the use of a much higher number of patients in a RCT, as compared with examining a shift in the median PFS, to yield results showing a significant difference with high enough power. Still, long-term OS is the only relevant read-out from immunotherapy trials.

4. Immunotherapy for GBM

Immunotherapy was called a “break-through for cancer” by Science in 2013. In 2011 and 2018, Nobel Prizes for Medicine were devoted to researchers who discovered important insights into the use of immunotherapy for cancer. At present, immunotherapy is definitively an important pillar in anticancer treatment in general, including GBM. Immunotherapy is a very broad term, comprising several technologies. Immunomodulation with checkpoint inhibitors is considered to belong to the domain of tumor-agnostic treatments [47]. Immunotherapies generally do not point to the molecular biological characteristics inside tumor cells, but, rather, to the surface of tumor cells, including a heterogeneous number of known and unknown tumor antigens [67] and immune costimulatory and inhibitory molecules on the surface [68–70], as well as the production of cytokines and chemokines that influence the immune system and the inflammatory response [71]. Terms like “cold” versus “hot” tumors, describing differences in lymphocyte infiltration in the tumor microenvironment, have become highly relevant [72]. The tumor mutational burden might be related to the presence of more or less tumor antigens on the surface [73,74]. Some genetic abnormalities, such as the p53 mutation, affect the extent of the expression of MHC molecules on the tumor cell surface [75]. An immunogram is created using the tumor foreignness, general immune status, immune cell infiltration, absence/presence of checkpoints, absence/presence of soluble inhibitors, absence/presence of inhibitory tumor metabolism, and sensitivity of the tumor to immune effectors [76]. The recognition that almost half of GBM tumors consist of cells belonging to the myeloid compartment (e.g., M1/M2 macrophages, tumor-associated macrophages, myeloid-derived suppressor cells, microglia) makes the understanding of the response to treatment and the ultimate outcome of patients more difficult [77,78]. Overall, the tumor microenvironment can be categorized into three functional sub-types that play significant roles in the outcomes of patients [79]. Interestingly, Hallaert et al. [80] also observed that the connection of GBM to the sub-ventricular zone appears to be a novel, independent risk factor leading to a worse prognosis. An association between sub-ventricular zone contact and markers related to the epithelial–mesenchymal transition was discovered [81]. Moreover, there is a definite influence of the tumor and the response to treatment on the systemic immune and inflammatory compartments [34]. Finally, steroids, radiotherapy, and chemotherapy all influence antitumor immune responses [39]; this, again, differs from patient to patient. A

strong correlation was found between OS and the systemic immune profile after neurosurgical resection and after radiochemotherapy when the extent of resection and timing of immunotherapy were taken into account [40].

5. Risk Factors and Levels of Personalized Medicine

All in all, in addition to the clinical risk profile, the intracellular molecular biology, and the epigenetic profiling of tumor cells, the anatomic location of the tumor, tumor–host interactions in the tumor microenvironment, the systemic immune system, the combination treatment design and the reaction of the body, and dynamic changes in the tumor should be taken into account and used as mandatory stratification tools in the design of RCTs with experimental versus control groups (Table 1). Some of these have been included in novel molecular RPA classification (GBM-molRPA) systems [82].

Table 1. Risk factors for stratification in randomization or for in/exclusion criteria.

1. Recursive Partitioning Analysis (RPA) clinical classification
<ul style="list-style-type: none"> • Grading • Extent of resection • Age • Karnofsky performance index • Mental status • Dose of radiotherapy
2. Molecular biology of tumor
<ul style="list-style-type: none"> • Tumor mutational burden • Epigenetic sub-typing • Molecular machinery of tumor cell clones • Metabolic features of tumor
3. Load of glioma cancer stem cells in connection to periventricular zones of the brain
4. Tumor–host immune reaction
<ul style="list-style-type: none"> • Tumor antigen expression • Check point expression • Inflammatory response, M1/M2 balance, Tumor-associated macrophages, myeloid-derived suppressor cells, microglia reactivity • T-cell infiltration • Vascularization and oxidative stress
5. Systemic immune compartment
<ul style="list-style-type: none"> • Cell numbers under standard of care treatment • Th1/Th2 balance • Presence of Treg • Presence of MDSC • Level of natural killer cell reactivity
6. Systemic treatments outside standard of care
<ul style="list-style-type: none"> • Steroids • Anti-angiogenic drugs • Complementary medicines

Immunotherapy covers many treatment modalities. Some of these treatment modalities, such as cytokines, are not personalized to each patient. Other drugs, like antibodies, are themselves not personalized, but are directed against personalized targets on the tumor cell surface. For adoptive cell therapies with chimeric antigen receptor (CAR) T-cells or T cell receptor-transduced T-cells, both the ATMP itself and the target are personalized [83–85]. In the domain of active specific immunotherapy with vaccines, the vaccine itself can be an individual product at the level of the antigen carrier (like autologous DCs) and/or at the

level of the antigen, such as tumor-derived antigens and, especially, highly individualized tumor-specific epitopes [86–88]. Extensive individualization of the treatment drug and target makes the design of a homogeneous experimental arm versus control arm very challenging. By introducing immunotherapy into a first-line treatment combination, new dimensions of personalization for the treatment of GBM have become clear (Table 2).

Table 2. Levels of personalized medicine for Glioblastoma Multiforme (GBM).

1. Molecular biology of tumor
• Tumor mutational burden
• Epigenetic sub-typing
• Molecular machinery of tumor cell clones
• Metabolic features of the tumor
2. Tumor–host immune reaction
• Tumor antigen expression
• Check point expression
• Inflammatory response, M1/M2 balance, TAM, MDSC, microglia reactivity
• T-cell infiltration
• Vascularization and oxidative stress
• Load of glioma cancer stem cells in connection to periventricular zones of the brain
3. Immune reactivity against the tumor
• Th1/Th2 balance
• Presence of Treg
• Presence of MDSC
• Level of NK cell reactivity
4. Reaction of the immune system upon other treatments
• Sensitivity to radiotherapy
• Sensitivity to chemotherapy
• Use of steroids
• Use of anti-angiogenic drugs
5. Response to treatment
6. Immunotherapy components
• Tumor antigens
• Patient-derived cell products

Overwhelming evidence of the efficacy of DC vaccination for GBM has been presented in preclinical models [89–101], as well as in phase I and early phase II non-controlled clinical trials [88,102–164]. The observation of long-term OS in patients after DC vaccination, noting that the intervention abruptly changes the 100% lethality of disease, has generated strong evidence of its efficacy. Several meta-analyses have demonstrated a significant improvement in long-term OS when GBM patients were treated with DC vaccines as compared with patients given a control treatment [21–25]. Of note, the latter meta-analysis also demonstrated a lack of additional toxicity due to immunotherapy in comparison with the standard of care. This means that the set-up of new phase I or phase IIa clinical trials is no longer innovative.

As has already been pointed out for the changes in molecular sub-clones over time during treatment, evidence that tumor–host immune interactions can also change over time has been obtained. Examples are the downregulation of specific target antigens [165] or the upregulation of PDL1 on tumor cells, allowing them to escape from immune attack during immunotherapy [19]. Dynamic changes in the expression of tumor-associated antigens and immunosuppressive factors in the tumor microenvironment during treatment have also been described [164].

6. Current Landscape

On 12 October 2020, we performed a search of [Clinicaltrials.gov](https://clinicaltrials.gov) using the terms “dendritic cell”, “interventional studies” “glioblastoma”, and “interventional phase 2 phase 3 phase 4”. Twenty-nine studies were available, with 12 of them reporting to be recruiting (Table 3). Seven of these studies were RCTs, with six having OS in the read-out analysis. Only one study (NCT04277221) was a phase 3 study. NCT03395587, NCT04115761, and NCT01567202 integrated DC vaccination into the primary standard of care for IDH1 wt GBM. Similarly, NCT03548571 integrated DC vaccination into the primary standard of care, but only for MGMT promotor non-methylated patients. The RCTs NCT02465268 and NCT03688178 integrated DC vaccination into the standard of care, but did not mention the requirement of IDH1 wild-type status.

Hence, at the moment of writing, seven RCTs are recruiting and studying DC vaccination for patients with initial diagnosis of GBM. None of these studies mentioned further stratification. The median number of patients used for randomization was 106, ranging from 24 to 136. Nevertheless, based on the analysis above, stratification at multiple levels (as summarized in Table 1) should be used in order to design a proper control group. Such stratification affects the number of patients recruited, and this number seems, in all running trials, to be too small to yield a significant difference with sufficient power in the efficacy of DC vaccination to increase the percentage of patients with long-term OS versus an appropriate control group.

Table 3. ClinicalTrials.gov Search Results on 12/10/2020 for “dendritic cell”, “interventional studies” “glioblastoma”, and “interventional phase 2 phase 3 phase 4”.

Label	Phase	Number of Patients	Randomized	Status	Primary Outcome	Estimated Study Completion
NCT00576537	2	50	No	Completed	Safety/Toxicity	10/2011
NCT02649582	1 + 2	20	No	Recruiting	OS, Safety/Toxicity Feasibility	12/2020
NCT00846456	1 + 2	20	No	Completed	Toxicity, Immune response	02/2013
NCT00323115	2	11	No	Completed	Immune response, Toxicity, PFS	07/2013
NCT02366728	2	100	RCT	Active, not recruiting	OS, DC migration	08/2020
NCT01204684	2	60	RCT	Active, not recruiting	PFS, OS	01/2021
NCT03927222	2	48	No	Recruiting	OS, DC migration	12/2023
NCT01006044	2	26	No	Completed	PFS, Toxicity	08/2014
NCT03395587	2	136	RCT	Recruiting	OS, PFS	06/2023
NCT04523688	2	28	No	Not recruiting	PFS	12/2025
NCT03548571	2 + 3	60	RCT	Recruiting	PFS, OS	05/2023
NCT04115761	2	24	RCT	Recruiting	PSF	06/2022
NCT03014804	2	0	RCT	Withdrawn		
NCT03879512	1 + 2	25	No	Recruiting	OS, PFS	01/2022
NCT02772094	2	50	No	Unknown	OS, Toxicity	12/2016
NCT01567202	2	100	RCT	Recruiting	Response, PFS, OS	02/2020
NCT01213407	2	87	RCT	Completed	PFS, OS	11/2015
NCT01291420	1 + 2	10	No	Unknown	Immune response	Unknown
NCT02465268	2	120	RCT	Recruiting	OS, Immune response, PFS	06/2024
NCT04277221	3	118	RCT	Recruiting	OS, PFS	12/2022
NCT00323115	2	11	No	Completed	T-cell response	07/2013
NCT03400917	2	55	No	Completed	OS	02/2023
NCT02546102	3	414	RCT	Suspended	OS	12/2021
NCT01280552	2	124	RCT	Completed	OS	12/2015
NCT00045968	3	348	RCT	Unknown	PFS	11/2016
NCT03688178	2	112	RCT	Recruiting	OS, Varlimumab safety, Treg level	03/2025
NCT01759810	2 + 3	60	No	Enrolling by invitation	OS	12/2020
NCT02754362	2		No	Withdrawn	Immune response	06/2019
NCT04388033	1 + 2	10	No	Recruiting	Safety, PFS	12/2023

DC: dendritic cell; OS: overall survival; PFS: progression free survival; RCT: randomized controlled trial.

7. Non-Scientific Challenges

In the design of larger RCTs with a control arm, clinical researchers have run into new problems. GBM is a deadly disease. The first interest of the patient is the prolongation of a good-quality life. As DC vaccination has already been shown to significantly prolong long-term OS with a good quality of life, it eventually became unethical to prevent patients in the control arm from being given this innovative fourth anti-GBM immunotherapy modality. Therefore, some RCTs published with PFS as the primary endpoint used a cross-over protocol from the control group to the DC vaccination group, either structurally within the trial design (EudraCT 2009-018228-14) [151] or after reaching the primary end-point (NCT00045968) [160]. By doing so, the OS assessment was, in fact, no longer controlled. In the former study, stratification of RPA classification was used. In the latter study, stratification for MGMT methylation was used.

It is notable that the three largest RCTs initiated to date have faced huge logistic/financial problems, as follows: (1) The EudraCT 2009-018228-14 trial aimed to include 146 study objects but was abruptly closed by the sponsor after the inclusion of 135 patients. The reasons for this were kept confidential. Nevertheless, the scientific data were made available, were extremely well-documented, and were partially transferred onto the platform of the EU Project Computational Horizons in Cancer (www.chic-vph.eu). Data on 132 patients were finally brought into a new study, named the Glioma Translat Study, and published [166,167]; (2) NCT00045968 was designed to include 348 study objects with PFS as the primary read-out and OS as the secondary read-out. Eighty sites in four countries were used for recruitment. The study screened 1268 patients and ended up with 331 randomizations into the main study [160]. Patient recruitment was initiated in 2007 but was paused from 2009 to 2011 for economic reasons. The final patient was enrolled in November 2015. This resulted in a recruitment period of nine years, an effective inclusion period of six years, and a mean of four patients per recruiting site at an effective rate of less than one patient per year per site. Five years later, at the time of writing, the final results regarding the randomized data collected on these patients and the answer to the primary question (PFS) have not yet been published; (3) NCT02546102 suspended further patient randomization due to financial reasons [168]. It is not clear how many patients had already been recruited into the trial.

Finally, patients have started searching on blogs and in social media communities for solutions to surviving GBM. An impressive list of complementary medicines and diets is available and freely accessible to patients. Some of these complementary medicines surely influence the course of the disease or the reactivity of the host [169–173]. It seems impossible to control for this when setting up and running RCTs at present.

8. Individualized Multimodal Immunotherapy for GBM

Two conclusions have become clear: (1) Individualized treatment at multiple levels, with strategies that follow the dynamic changes in both the tumor and host (e.g., immunity, inflammation) during treatment, is needed for the treatment of GBM; and (2) IMI is becoming part of the first-line treatment for GBM, integrated into the standard of care. The potential inherent immunization component of standard anti-GBM strategies (e.g., neurosurgery, radiotherapy, and chemotherapy) and the proven induction of immunogenic cell death (ICD) through the use of innovative anti-cancer treatments (e.g., modulated electrohyperthermia, oncolytic virus therapy) [174,175] should be exploited and strengthened with active immunization strategies and further optimized with immunomodulatory strategies in the context of optimized complementary medicine. Only broad and long-term immune control over GBM is able to induce long-term OS. The rationale of such a strategy has been published [176]. In Sections 8–10, we aim to illustrate several elements discussed in the former narrative review with observational data obtained by a retrospective analysis of our own patient records. Over the years, we have developed a multistep treatment approach, in which ICD is induced by the combination of bolus injections with NDV and modulated electrohyperthermia (mEHT) integrated as an add-in treatment during

the alkylating mode of tumor cell killing induced by TMZ chemotherapy, followed by IO-Vac[®] DC vaccination, in order to actively induce an antitumor immune response in combination with individually adapted immunomodulatory strategies. Finally, ICD treatment is maintained with immunomodulation [19].

Of the 171 recorded patients with GBM in the IOZK database, 90 patients (53%) received IMI in combination with first-line treatment for compassionate use (“individueller Heilversuch”). For the current retrospective analysis, we excluded all patients below 18 and above 75 years of age, patients with a proven pre-history of low-grade glioma and/or proven IDH1 mutation, patients with proven histone mutations, and patients with radiotherapy-induced GBM as a second malignancy, leaving 70 patients for analysis.

The final patient group consisted of 70 patients (33 females, 37 males). The median age of the patients was 50 years (range 18–69 years). The median Karnofsky performance index score was 90 (range 50–100). Clinical patient characteristics are shown in Figure 1. The patients presented for immune diagnostic blood sampling at IOZK at a median of three months after operation (range 0.5–23 months); hence, most sampling was done after radiochemotherapy. General blood counts and immune cell counts and functioning, as analyzed in the routine clinical laboratory, are shown in Figure 2A. A large proportion of patients were lymphopenic at that time—caused by the radiochemotherapy—a finding compatible with published data [39].

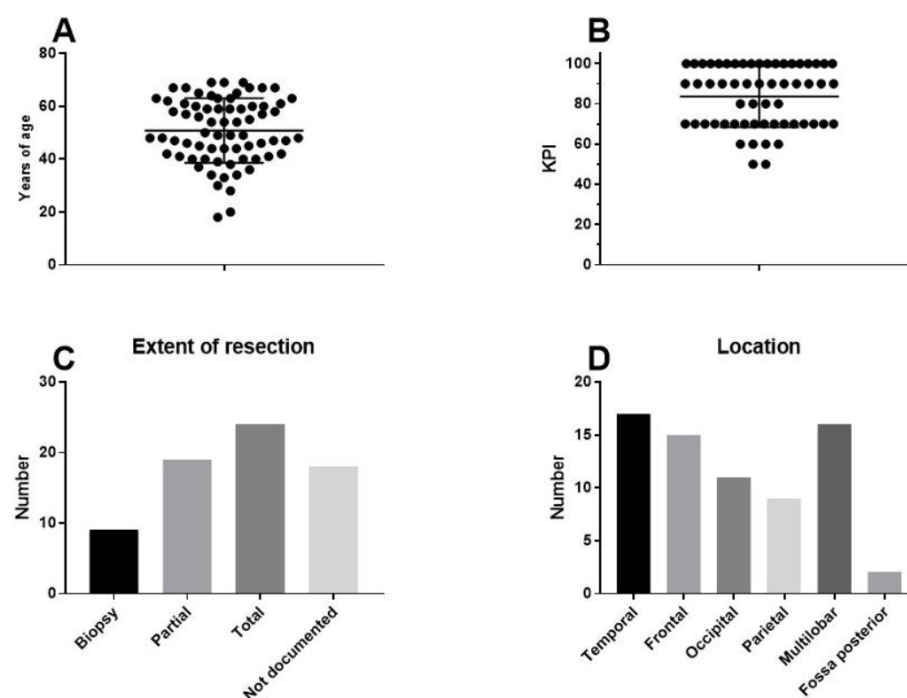


Figure 1. Clinical characteristics of the patients. Seventy adults with primary GBM receiving first-line standard of care in combination with individualized multimodal immunotherapy were included in this retrospective analysis: (A) age distribution; (B) distribution of Karnofsky performance index scores; (C) reported resection (number of patients); and (D) reported location (number of patients).

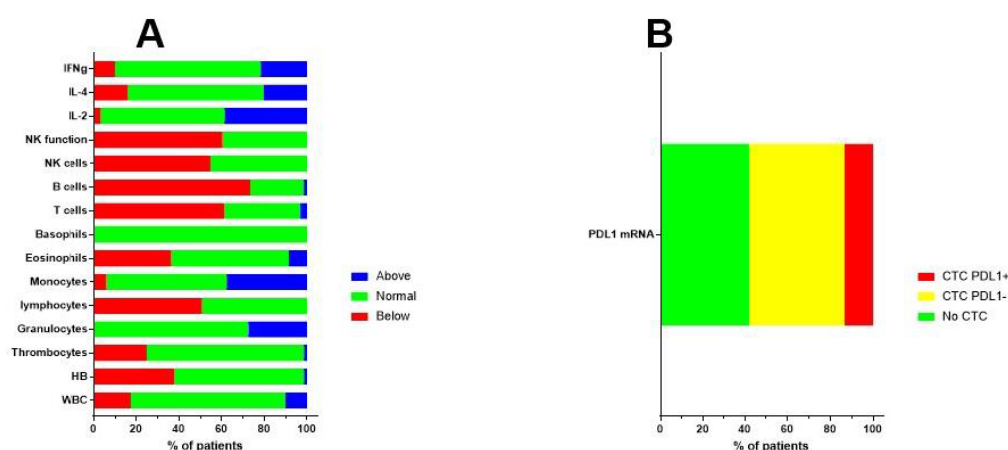


Figure 2. Immune variables before the start of immunotherapy. (A) Before the start of individualized multimodal immunotherapy, blood was drawn and sent to the routine clinical lab for analysis. Different immune variables are shown. The percentages of patients with values above (blue), within (normal, green), or below (red) the normal range are shown. (B) Blood was also sent to Biofocus in order to detect circulating tumor cells based on mRNA expression of GBM-related oncogenes. When cells were detected, the RNA expression for PDL1 was subsequently analyzed and cells were defined as negative (yellow) or positive (red) for the expression of mRNA for PDL1.

The MGMT promotor methylation status of the resected tumor was documented in 52 cases, from which 32 patients were categorized as unmethylated. In 67 patients, the presence of circulating tumor cells (CTCs) was investigated at the time of immune diagnostic blood sampling. Blood samples were sent to Biofocus (<https://www.biofocus.de/>) for analysis. In 28 patients, no CTCs were detected. CTCs were detected in 39 patients, based on the presence of large cells with mRNA expression for specific oncogenes (EGFR, ERBB2, C-kit, and Telomerase) above a cut-off in comparison with house-keeping mRNA expression. In nine patients, mRNA expression for PDL1 was above the cut-off value of 2 (Figure 2B). In 11 patients, increased mRNA expression for MGMT was observed, of which seven patients were histologically classified as being MGMT promotor unmethylated, while three patients were classified as being methylated (one patient had an unknown histology result). For 16 patients who had CTC without increased mRNA for MGMT, six samples matched with a histologic classification as MGMT promotor methylated, while nine samples mismatched with the histologic classification and were classified as MGMT promotor unmethylated. It should be noted that the categories for both histology-based MGMT promotor methylation and the mRNA expression of MGMT in CTCs were derived from continuous variables linked with methylated versus unmethylated status. Moreover, GBM might depict heterogeneity for MGMT promotor methylation, such that histology sampling errors cannot be excluded. Finally, the presence of CTCs was investigated at a median of three months after operation, thereby potentially illustrating clonal evolution during the first period of radiochemotherapy.

To further illustrate the biological evolutions that occurred during treatment, we looked at the evolution of mRNA expressions in CTCs for the oncogenes EGFR, ERBB2, C-kit, and Telomerase, as well as the mRNA for MGMT and PDL1 over time. For this, available data on mRNA expression in CTCs were sampled and put on a time line for each patient starting from neurosurgery. As mentioned earlier, the patients started immunotherapy at different time points and were treated individually. This is reflected by the use of an individual monitoring schedule for each patient. Figure 3A shows the evolution of the EGFR mRNA expression over time for individual patients. Changes in mRNA expression were only observed in three patients. On the contrary, as shown in Figure 3B, mRNA expression for ERBB2, C-kit, Telomerase, MGMT, and PDL1, in comparison to mRNA expression for the house-keeping gene NADPH, clearly changed over time and was often visible around the appearance of relapse. As an example, the mRNA expression for PDL1

in the CTCs of patients 22,731 and 23,346 was low at the start of immunotherapy treatment. These values, however, increased during treatment and were ultimately accompanied by relapse. Patient 23,346 was treated with pembrolizumab. Patient 24,005 also had a very high level of mRNA expression for PDL1 when the CTCs became positive for the first time. This patient also received four doses of pembrolizumab, after which the CTCs became negative for the PDL1 marker. These descriptive data indirectly demonstrate the possible relative changes in sub-clones during the disease process, which might contribute to the occurrence of relapse and which might be monitored for timely intervention. GBM is thus a dynamic tumoral process. The descriptive analysis illustrates the heterogeneity within these 70 patients at the levels of clinical risk factors, immune variables in the peripheral blood, and molecular tumor biology data, as well as the dynamic processes occurring in the molecular biology of the tumor.

The patients received IMI within the first-line treatment. Table 4 shows the details of the IMI treatment. A median of two (range 0–5) IO-Vac[®] DC vaccines, 25 (range 0–77) NDV administrations, and 30 (range 0–77) sessions of modulated electrohyperthermia were given to each patient. One IO-Vac[®] DC vaccine consisted of a median of 12.2×10^6 autologous mature IO-Vac[®] DCs loaded with autologous tumor proteins derived from tumor lysate (when available and appropriate to the GMP requirements) or obtained as ICD-therapy-induced, serum-derived, antigenic, extracellular microvesicles, and apoptotic bodies.

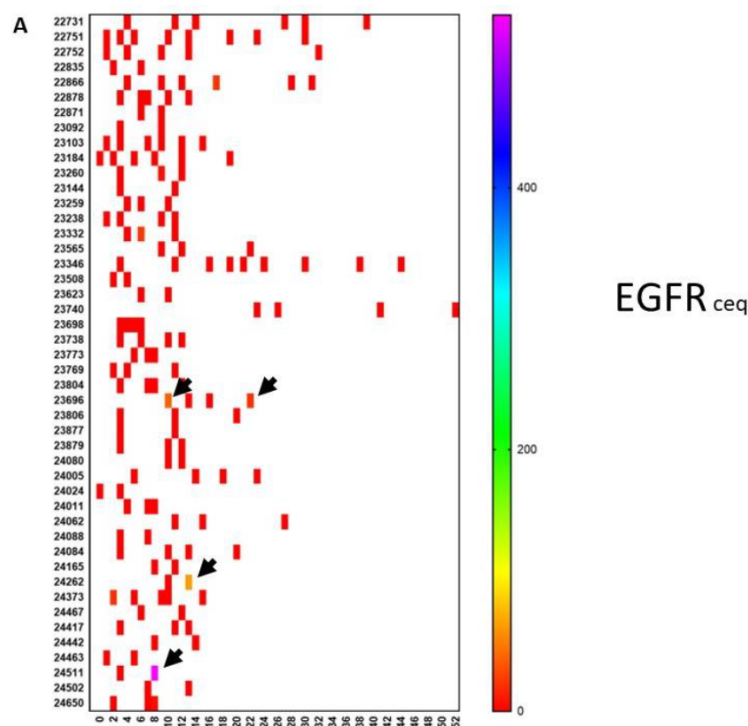


Figure 3. Cont.

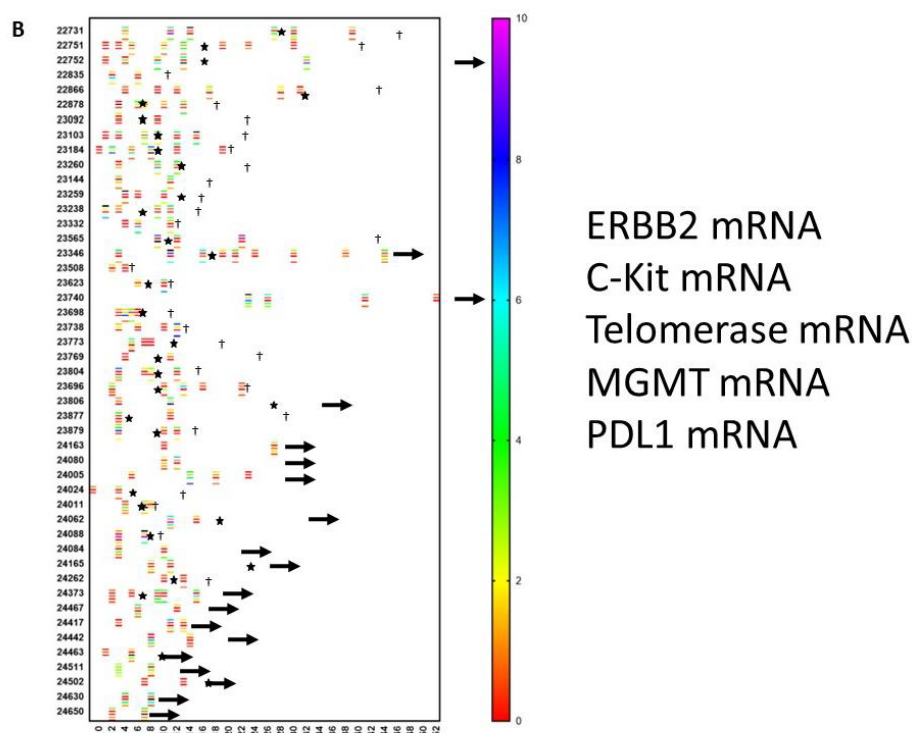


Figure 3. Evolution of oncogene expression in circulating tumor cells. Circulating tumor cells were measured repetitively in 46 patients. Each patient is referenced with a number on the y-axis. Time in months is indicated on the x-axis. The scale of the color of each test is shown on the right-hand side. (A) The level of mRNA expression for EGFR is expressed as the ceq (cell equivalent). Most of the values are negative (red). However, as indicated by the arrows, some patients showed an upregulation of EGFR during the disease course. (B) This shows a similar data set-up as in panel A. For each patient, data on mRNA expression are relative to the house-keeping gene GADPH and are shown in a particular color, for which the scale is shown on the right-hand side. For each patient, up to five lines are shown at different moments during the disease course. From top to bottom, values for ERBB2, c-Kit, telomerase, MGMT, and PDL1 are shown for each patient. Stars indicate new events. A † indicates when the patient died. An arrow to the right indicates the time at which the patient was censored in the analysis.

Table 4. Treatment details.

	Vaccine	Local Hyperthermia	NDV	DC Total	DC/Vaccine
N	69	70	69	70	112
Minimum	0	0	0	0	2,400,000
25%P	1	13	17	6,950,000	8,075,000
Median	2	25	30	20,115,000	12,200,000
75%	2	42	42	34,200,000	19,145,000

NDV: Newcastle Disease Virus.

9. A Case of Complete Remission and Specific T-Cell Response

In our retrospective analysis of these 70 patients, one particular innovative finding emerged. As the tumor-specific antigens were not known when using tumor lysate or serum-derived, extracellular vesicles and apoptotic bodies, the immune monitoring in our clinical setting was not a major focus. Nevertheless, proof of principle of ICD therapy in combination with TMZ maintenance chemotherapy followed by vaccination with IO-Vac[®] DC vaccines loaded with ICD therapy-induced, serum-derived, antigenic, extracellular

microvesicles, and apoptotic bodies [19] for the induction of a tumor-neo-epitope-specific immune response was demonstrated in one patient. This 18-year-old patient had an incomplete resection of a left frontal lobe IDH1 wild-type and MGMT unmethylated GBM. The tumor mutational burden was low (0.5 variants/megabase), and there was no evidence for microsatellite instability or germline variants. She was treated with radiochemotherapy and, subsequently, five cycles of TMZ chemotherapy (Figure 4). At presentation, her Karnofsky performance index was 90. She was lymphopenic with 279/uL CD3+ T-cells, 78/uL CD19+ B-cells, and 56/uL CD16+CD56+ NK cells. Her NK cell functioning was below the reference value. She had Th2/Th17 skewing. Her CTCs showed upregulated expression (3.44) of mRNA for MGMT, which was compatible with the known unmethylated MGMT promoter status. The expression of mRNA for PDL1 was 1.13 (cut-off for positivity = 2). She continued treatment for another seven TMZ chemotherapy cycles combined with 5-day ICD treatments, which were given during each TMZ cycle at days 8 to 12. Afterwards, she received two IO-Vac[®] DC vaccinations loaded with ICD treatment-induced, serum-derived, antigenic, extracellular microvesicles, and apoptotic bodies. Later on, she received two IO-Vac[®] DC vaccines loaded with tumor-specific peptides based on the individualized tumor-specific neo-antigen detection tests performed at CeGaT (www.CeGaT.de). At the time of writing, she receives monthly maintenance ICD treatments and is still in complete remission. Interestingly, we were able to monitor the tumor antigen-specific T-cell responses as, in this case, the neo-antigens were known. A first sample was available after the fifth TMZ cycle, prior to the addition of multimodal immunotherapy. A second sample was available at the time of blood sampling to prepare the second IO-Vac[®] DC vaccine (Figure 4). From the data, it is clear that surgery, radiochemotherapy, and five cycles of TMZ did not induce a tumor-specific T-cell response. However, the addition of seven ICD treatments to the last seven TMZ treatments and the first IO-Vac[®] DC vaccine loaded with ICD-treatment-induced, serum-derived, antigenic, extracellular microvesicles, and apoptotic bodies generated a clear tumor antigen-specific CD4+ and CD8+ T-cell response. The impact of this observation might be meaningful. First, it is not mandatory to have fresh frozen tumor material to prepare a tumor lysate as an antigenic source. This avoids the critical challenges of yielding, freezing, transporting, analyzing, and preparing tumor material within a GMP context. Secondly, and even more importantly, if molecular subclones can change over time, their antigenic profiles can change as well. ICD treatment allows the yield of tumor antigens that are expressed within the body at the time of treatment and makes it possible for the vaccine to immunize against the antigens that are actually present, instead of tumor antigens identified at the time of tumor resection prior to radiotherapy and chemotherapy and hence prior to eventual treatment-induced tumor clone changes.

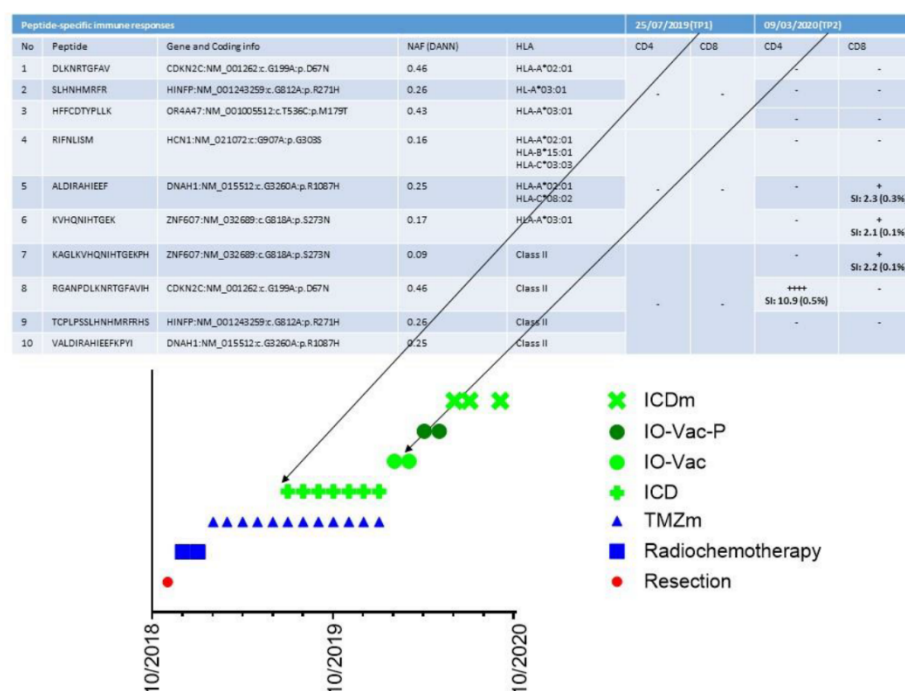


Figure 4. Detection of tumor-specific T-cell clones. The treatment timeline for patient 24442 and its multiple components are shown in the bottom part of the figure. TMZm indicates five days of temozolomide maintenance treatment in cycles (every 28 days). ICD indicates immunogenic cell death (ICD) treatment consisting of the combination of five injections with Newcastle Disease Virus and five sessions of modulated electrohyperthermia. IO-Vac indicates a vaccination cycle including six ICD treatments and an injection of IO-Vac[®] DC vaccine, consisting of autologous mature dendritic cells loaded with ICD-treatment-induced, serum-derived, antigenic, extracellular microvesicles and apoptotic bodies. IO-Vac-P vaccination cycles are equal to IO-Vac vaccination cycles, but the DCs are loaded with tumor-specific neo-peptides. The upper part of the curve shows the specific peptide sequences, the respective gene and coding information, the Novel Allele Frequency (NAF), and the HLA phenotype. TP1 and TP2 indicate the two respective time points at which T-cells were frozen for immune monitoring purposes. SI is the stimulation index, the ratio of polyfunctional activated CD4+ or CD8+ T-cells (positive for at least two activation markers from CD154, IFN- γ , TNF, and/or IL-2) in the peptide-stimulated sample, compared with the unstimulated control. Additionally, the percentage of activated CD4+ or CD8+ T-cells (positive for at least one activation marker of CD154, IFN- γ , TNF, and/or IL2) above the background and after *in vitro* amplification is given. This percentage does not directly reflect the frequencies *in vivo*. SI ≥ 2 : weak response (+); SI ≥ 3 : positive response (++); SI ≥ 5 : strong response (+++); SI ≥ 10 : very strong response (++++). Peptides 1–3, 4–6, and 7–10 were pooled for the analysis of TP1. Peptides 9 and 10 were pooled for the analysis of TP2.

10. Results in Term of OS

As we did not have reference radiology for the independent assessment of new events, given the need to follow the iRANO criteria [65,66] and as OS is certainly the most important outcome in the context of immunotherapy, we focused on the OS of the patients. As described earlier in Section 8, the retrospectively analyzed group of 70 patients was a heterogeneous group of patients. They best reflected adapted RPA class 4 patients, as published by Stupp et al. [14]. This reference was used as a historical control. Data were analyzed using GraphPad Prism version 7.00 for Windows (GraphPad Software, La Jolla, CA, USA, www.graphpad.com). One patient was lost during follow up. The median OS was 20.03 months (Figure 5A) with a 2-year OS of 38.83% (CI95%: +13.04, −13.25) and a 3-year OS of 31.41% (CI95%: +13.35, −12.55). Patients younger than 50 years (21 MGMT

promoter unmethylated, 7 methylated, and 7 unknown) had a median OS of 22.07 months, which was not statistically different from the median OS of 18.07 months observed for patients older than 50 years (11 unmethylated, 13 methylated, and 11 unknown). We found MGMT promotor methylation status to be a significant factor (Figure 5B, log-rank test: $p = 0.0004$): patients ($n = 20$) with patients with MGMT promotor methylation having a median OS of 42.85 months versus 11.77 months for patients with unmethylated MGMT promotor status ($n = 32$).

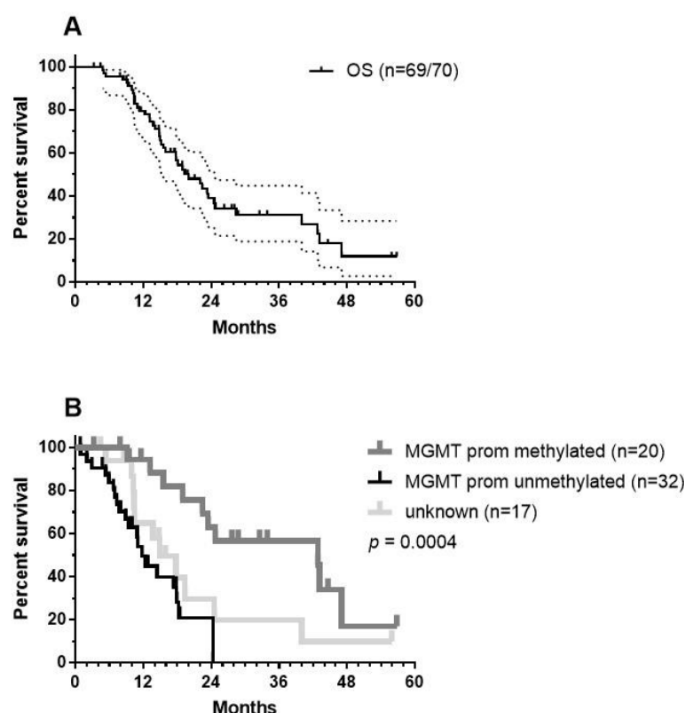


Figure 5. OS data: (A) OS data of the total patient group (CI95% values are shown). One patient out of 70 was lost during the follow up period and (B) the patient group was divided according to MGMT promotor methylation status—methylated (grey), unmethylated (black), data not registered (light grey). The p -values show significance using the Log-rank (Mantel–Cox) test.

For 16 patients, local therapy (neurosurgery, radiochemotherapy) was followed by IMI (Group 1). ICD therapy (the combination of IV bolus injections of NDV together with mEHT [19]) integrated into the TMZm chemotherapy cycles followed by IO-Vac® DC vaccines and maintenance ICD therapy was given to 46 patients (Group 2). Eight patients started with IMI after the last TMZ maintenance chemotherapy cycle (Group 3). The OS data were significantly different for the three treatment groups: 13.08 months for group 1, 22.46 months for group 2, and undefined for group 3 (median follow-up of surviving patients: 28.59 months, range 26.3–55.9 months; Figure 6A). The latter likely points to favorable selection of a small group of patients who experienced no events until after the end of the maintenance chemotherapy and profited from subsequent IMI treatment. The median OS of the patients with unmethylated MGMT promotor status was 11.25 months for group 1 ($n = 7$) and 18.07 months for group 2 ($n = 21$), with a 2-year OS of 0% in group 1 versus 17.18% (CI95%: +31.65, −15.86) in group 2 (Figure 6B, log-rank test: $p = 0.0273$). The median OS of the patients with methylated MGMT promotor status was 42.85 months for group 2 ($n = 15$) with a 2-year OS of 66.66% (CI95%: +19.3, −32.96). There were only three patients in group 1 who had a tumor with MGMT promotor methylation status. Within treatment group 2, the differences in the OS curve due to MGMT promotor methylation status were significant (Figure 6C, Log-rank test: $p = 0.0036$).

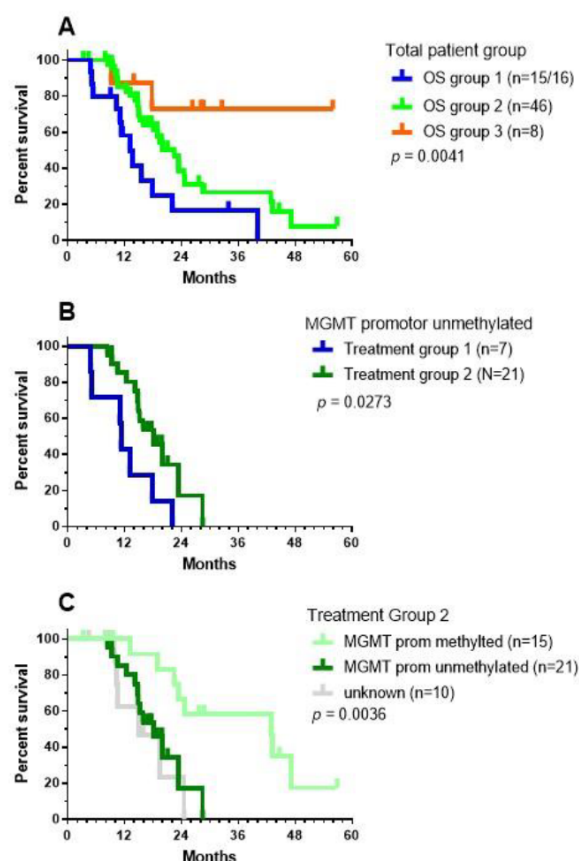


Figure 6. OS data for the treatment groups. As explained in the text, patients were categorized into three different treatment groups: (A) OS data for the three different patient groups; (B) OS data for the patients without MGMT promotor methylation belonging to treatment groups 1 (blue) and 2 (green); and (C) OS data of patients from treatment group 2, divided according to MGMT promotor methylation status. The p -values show the significance calculated using the Log-rank (Mantel–Cox) test.

Considering these data and the data published by Stupp et al. [14], patients with MGMT promotor unmethylated status have no relevant benefit from the addition of TMZ [14] or from treatment with IMI alone. However, the data from treatment group 2 suggest the potential benefit of the integration of ICD treatment within TMZm chemotherapy followed by IO-Vac® DC vaccinations, which was found to increase the median OS by about six months. On the other hand, treatment with IMI after local therapy for patients with MGMT promotor methylated GBM yielded similar median OS data as treatment with TMZm chemotherapy, while the integration of ICD treatment with TMZm chemotherapy followed by IO-Vac® DC vaccinations increased the median OS further—by about 18 months. These data are worth validating in prospective clinical research.

11. Conclusions

In this paper, we reviewed the multiple challenges related to the use of immunotherapy RCTs for GBM (Sections 2–7) and illustrated these challenges in a retrospective analysis of GBM patients treated at IOZK (Sections 8–10). GBM treatment is affected by the complexity of the tumor, the complexity of the immune and inflammatory micro-environment, the complexity of combined treatment approaches, and the complexity of dynamic changes occurring within the tumor, the tumor microenvironment, and the immune system. The set-up of immunotherapy RCTs for GBM is affected by the need for multiple stratifications

to create an appropriate control group. Both stratification and the read-out of OS necessitate the use of a large number of study participants. The costs to run such RCTs are related not only to the Good Clinical Practice (GCP) documentation but also to the production of the ATMP in a GMP environment. As already mentioned, there has been an abundance of smaller phase I and phase II single-arm clinical trials, and several meta-analyses have shown the efficacy and safety of DC vaccination for GBM treatment. The high cost of non-innovative small RCTs with predicted negative outcomes due to a lack of appropriate stratification makes them not appropriate at this time due to limited resources. Models for OS and immunotherapy responses in patients with GBM based on DNA-methylation-driven, gene-based, molecular classifications and multi-omic analyses may be better tools for predicting the efficacy individually for each patient [177]. However, patients suffering today from GBM need better treatments, including the use of first-line immunotherapy to fight their cancers.

The multimodality of immunotherapy, besides the standard of care, presents a further challenge to the classic step-wise research methodology used in clinical research. IOZK aims to contribute to the general knowledge and communicate their gained experiences to the wider scientific community. The ATMP IO-Vac[®] DC vaccine has been used as part of IMI treatment in the framework of “Individueller Heilversuch”. Each patient is treated at all personalized levels necessary. For each individual patient, the best possible solution for their medical needs is worked out. Prospective medical research questions on groups of patients are not generated. Nevertheless, the IOZK aims to repetitively freeze the database at certain time points and sample patient data to carry out scientifically correct retrospective analyses. The current analysis suggests that the addition of ICD treatment with NDV and mEHT during the application of TMZ maintenance chemotherapy, followed by IO-Vac[®] DC vaccinations and maintenance ICD treatment, may be beneficial for both MGMT promotor unmethylated and methylated GBM patients.

A final challenge in the broad implementation of innovative therapies like IMI, given that its effectiveness has been accepted without the use of RCTs, is the expected cost versus the length of additional survival. The production of personalized ATMPs under GMP conditions is expensive. The control over the ATMP quality, and hence over the costs, belongs to the authorities, who are also responsible for health policies in general. This topic points to the need for a cost-effectiveness analysis to compare the costs and outcomes of treatment options. The aim is to ensure the greatest possible health benefits are attained with a given budget. For macroeconomic considerations, cost-effectiveness thresholds (CETs) are usually related to the gross domestic product (GDP) per capita [178]. To the best of our knowledge, no representative data related to the integration of IMI into standard of care treatment of GBM are available. Single studies have appraised the additional cost of targeted therapies per year of survival if combined with chemotherapy. In non-small-cell lung cancer, for example, the additional cost for using atezolizumab in combination with carboplatin/nab-paclitaxel amounts to 333,199 USD per quality-adjusted life year [179]. Understandably, the respective costs are difficult to calculate and depend heavily on the type of cancer, the treatment in question, and the parameters used in the cost-effectiveness study. Accordingly, different methods have been described [180]. What we can say is that overall spending on cancer drugs has been increasing. For example, spending on cancer drugs rose from €7.6 billion in 2005 to €19.1 billion in 2014 in the EU [181]. For some types of cancer, calculations are available. Between 2007 and 2012, the mean amounts of money spent in the first year after diagnosis was \$35,849, \$26,295, \$55,597, and \$63,063 for breast, prostate, lung, and colorectal cancers, respectively [182]. In view of the overall increase in costs, even higher expenditure must be expected today. A more recent study on breast cancer reported the average cost per patient in the year after diagnosis as being between \$60,637 and \$134,682, depending on the cancer stage [183]. Newly approved pharmaceuticals easily cost more than \$100,000 US per year. Costs are driven by various factors that are not proportional to their often modest additional benefits [184,185], exceeding the cost-effectiveness thresholds. In comparison, the addition of modulated

electrohyperthermia to dose-dense temozolomide for the treatment of recurrent GBM has proven to be cost-effective [186]. Taken together, it is methodically difficult to compare the cost-benefit ratio of the integration of IMI into standard of care treatment. Considering the far higher overall costs of targeted therapies, one may expect that the ratio would not be unfavorable.

Author Contributions: Ideation, S.W.V.G., T.S., V.S. and W.S.; literature search, S.W.V.G., J.M. and T.S.; data analysis, S.W.V.G., S.F. and L.P.; Writing—original draft preparation, S.W.V.G.; Writing—review & editing, J.M., S.F., T.S., L.P., V.S. and W.S. All authors have read and agreed to the published version of the manuscript.

Funding: This research received no external funding.

Informed Consent Statement: All patients gave written informed consent for individualized multimodal immunotherapy as compassionate use treatment (“individueller Heilversuch”).

Data Availability Statement: The data presented in Sections 8–10 are available on request from the corresponding author. The data are not publicly available due to privacy reasons.

Acknowledgments: The authors thank the clinical team, the team from the immune-diagnostic laboratory, and the team from the GMP laboratory at the IOZK for their excellent work in making this complex treatment possible for patients with GBM.

Conflicts of Interest: The authors declare no conflict of interest.

References

- Available online: <https://www.who.int/news-room/fact-sheets/detail/cancer> (accessed on 18 December 2020).
- Available online: <https://www.cancer.gov> (accessed on 18 December 2020).
- Creutzig, U.; Zimmermann, M.; Dworzak, M.N.; Ritter, J.; Schellong, G.; Reinhardt, D. Development of a curative treatment within the AML-BFM studies. *Klin. Padiatr.* **2013**, *225* (Suppl. 1), S79–S86. [CrossRef]
- Schrapp, M.; Reiter, A.; Ludwig, W.D.; Harbott, J.; Zimmermann, M.; Hiddemann, W.; Niemeyer, C.; Henze, G.; Feldges, A.; Zintl, F.; et al. Improved outcome in childhood acute lymphoblastic leukemia despite reduced use of anthracyclines and cranial radiotherapy: Results of trial ALL-BFM 90. German-Austrian-Swiss ALL-BFM Study Group. *Blood* **2000**, *95*, 3310–3322.
- Loning, L.; Zimmermann, M.; Reiter, A.; Kaatsch, P.; Henze, G.; Riehm, H.; Schrapp, M. Secondary neoplasms subsequent to Berlin-Frankfurt-Munster therapy of acute lymphoblastic leukemia in childhood: Significantly lower risk without cranial radiotherapy. *Blood* **2000**, *95*, 2770–2775. [CrossRef]
- Siegel, R.L.; Miller, K.D.; Jemal, A. Cancer Statistics, 2020. *Ca Cancer J. Clin.* **2020**, *70*, 7–30. [CrossRef]
- Thakkar, J.P.; Dolecek, T.A.; Horbinski, C.; Ostrom, Q.T.; Lightner, D.D.; Barnholtz-Sloan, J.S.; Villano, J.L. Epidemiologic and molecular prognostic review of glioblastoma. *Cancer Epidemiol. Biomark. Prev.* **2014**, *23*, 1985–1996. [CrossRef] [PubMed]
- Louis, D.N.; Perry, A.; Reifenberger, G.; von Deimling, A.; Figarella-Branger, D.; Cavenee, W.K.; Ohgaki, H.; Wiestler, O.D.; Kleihues, P.; Ellison, D.W. The 2016 World Health Organization Classification of Tumors of the Central Nervous System: A summary. *Acta Neuropathol.* **2016**, *131*, 803–820. [CrossRef]
- Ladomersky, E.; Scholtens, D.M.; Kocherginsky, M.; Hibler, E.A.; Bartom, E.T.; Otto-Meyer, S.; Zhai, L.; Lauing, K.L.; Choi, J.; Sosman, J.A.; et al. The Coincidence between Increasing Age, Immunosuppression, and the Incidence of Patients with Glioblastoma. *Front. Pharm.* **2019**, *10*, 200. [CrossRef] [PubMed]
- Izycka-Swieszewska, E.; Bien, E.; Stefanowicz, J.; Szurowska, E.; Szurowska-Zielinska, E.; Koczkowska, M.; Sigorski, D.; Kloc, W.; Rogowski, W.; Adamkiewicz-Drozynska, E. Malignant Gliomas as Second Neoplasms in Pediatric Cancer Survivors: Neuropathological Study. *Biomed. Res. Int.* **2018**, *2018*, 4596812. [CrossRef] [PubMed]
- Hardell, L.; Carlberg, M.; Hansson Mild, K. Use of mobile phones and cordless phones is associated with increased risk for glioma and acoustic neuroma. *Pathophysiology* **2013**, *20*, 85–110. [CrossRef] [PubMed]
- Soderberg-Nauder, C.; Johnsen, J.I. Cytomegalovirus infection in brain tumors: A potential new target for therapy? *Oncoimmunology* **2012**, *1*, 739–740. [CrossRef]
- Stupp, R.; Mason, W.P.; van den Bent, M.J.; Weller, M.; Fisher, B.; Taphoorn, M.J.; Belanger, K.; Brandes, A.A.; Marosi, C.; Bogdahn, U.; et al. Radiotherapy plus concomitant and adjuvant temozolomide for glioblastoma. *New Eng. J. Med.* **2005**, *352*, 987–996. [CrossRef] [PubMed]
- Stupp, R.; Hegi, M.E.; Mason, W.P.; van den Bent, M.J.; Taphoorn, M.J.; Janzer, R.C.; Ludwin, S.K.; Allgeier, A.; Fisher, B.; Belanger, K.; et al. Effects of radiotherapy with concomitant and adjuvant temozolomide versus radiotherapy alone on survival in glioblastoma in a randomised phase III study: 5-year analysis of the EORTC-NCIC trial. *Lancet Oncol.* **2009**, *10*, 459–466. [CrossRef]
- De Vleeschouwer, S.; Van Gool, S.W.; Van Calenbergh, F. Immunotherapy for malignant gliomas: Emphasis on strategies of active specific immunotherapy using autologous dendritic cells. *Childs Nerv. Syst.* **2005**, *21*, 7–18. [CrossRef] [PubMed]
- Available online: <https://www.iddi.com/news/news-events/symposium-are-randomized-trials-still-needed-in-2020/> (accessed on 18 December 2020).

17. Schirmacher, V.; Bihari, A.S.; Stucker, W.; Sprenger, T. Long-term remission of prostate cancer with extensive bone metastases upon immuno- and virotherapy: A case report. *Oncol. Lett.* **2014**, *8*, 2403–2406. [\[CrossRef\]](#) [\[PubMed\]](#)
18. Schirmacher, V.; Stucker, W.; Lulei, M.; Bihari, A.S.; Sprenger, T. Long-term survival of a breast cancer patient with extensive liver metastases upon immune and virotherapy: A case report. *Immunotherapy* **2015**, *7*, 855–860. [\[CrossRef\]](#)
19. Van Gool, S.W.; Makalowski, J.; Feyen, O.; Prix, L.; Schirmacher, V.; Stuecker, W. The induction of immunogenic cell death (ICD) during maintenance chemotherapy and subsequent multimodal immunotherapy for glioblastoma (GBM). *Austin Oncol. Case Rep.* **2018**, *3*, 1010.
20. Van Gool, S.W.; Makalowski, J.; Bonner, E.R.; Feyen, O.; Domogalla, M.P.; Prix, L.; Schirmacher, V.; Nazarian, J.; Stuecker, W. Addition of Multimodal Immunotherapy to Combination Treatment Strategies for Children with DIPG: A Single Institution Experience. *Medicines* **2020**, *7*, 29. [\[CrossRef\]](#)
21. Cao, J.X.; Zhang, X.Y.; Liu, J.L.; Li, D.; Li, J.L.; Liu, Y.S.; Wang, M.; Xu, B.L.; Wang, H.B.; Wang, Z.X. Clinical efficacy of tumor antigen-pulsed DC treatment for high-grade glioma patients: Evidence from a meta-analysis. *PLoS ONE* **2014**, *9*, e107173. [\[CrossRef\]](#)
22. Wang, X.; Zhao, H.Y.; Zhang, F.C.; Sun, Y.; Xiong, Z.Y.; Jiang, X.B. Dendritic cell-based vaccine for the treatment of malignant glioma: A systematic review. *Cancer Investig.* **2014**, *32*, 451–457. [\[CrossRef\]](#)
23. Eagles, M.E.; Nassiri, F.; Badhiwala, J.H.; Suppiah, S.; Almenawer, S.A.; Zadeh, G.; Aldape, K.D. Dendritic cell vaccines for high-grade gliomas. *Clin. Risk Manag.* **2018**, *14*, 1299–1313. [\[CrossRef\]](#)
24. Vatu, B.I.; Artene, S.A.; Staicu, A.G.; Turcu-Stolica, A.; Folcuti, C.; Dragoi, A.; Cioc, C.; Baloi, S.C.; Tataranu, L.G.; Silosi, C.; et al. Assessment of efficacy of dendritic cell therapy and viral therapy in high grade glioma clinical trials. A meta-analytic review. *J. Immunoass. Immunochem.* **2019**, *40*, 70–80. [\[CrossRef\]](#) [\[PubMed\]](#)
25. Lv, L.; Huang, J.; Xi, H.; Zhou, X. Efficacy and safety of dendritic cell vaccines for patients with glioblastoma: A meta-analysis of randomized controlled trials. *Int. Immunopharmacol.* **2020**, *83*, 106336. [\[CrossRef\]](#) [\[PubMed\]](#)
26. Burnet, N.G.; Jefferies, S.J.; Benson, R.J.; Hunt, D.P.; Treasure, F.P. Years of life lost (YLL) from cancer is an important measure of population burden—and should be considered when allocating research funds. *Br. J. Cancer* **2005**, *92*, 241–245. [\[CrossRef\]](#) [\[PubMed\]](#)
27. Rouse, C.; Gittleman, H.; Ostrom, Q.T.; Kruchko, C.; Barnholtz-Sloan, J.S. Years of potential life lost for brain and CNS tumors relative to other cancers in adults in the United States, 2010. *Neuro Oncol.* **2016**, *18*, 70–77. [\[CrossRef\]](#)
28. Walker, M.D.; Strike, T.A.; Sheline, G.E. An analysis of dose-effect relationship in the radiotherapy of malignant gliomas. *Int. J. Radiat. Oncol. Biol. Phys.* **1979**, *5*, 1725–1731. [\[CrossRef\]](#)
29. Walker, M.D.; Alexander, E., Jr.; Hunt, W.E.; MacCarty, C.S.; Mahaley, M.S., Jr.; Mealey, J., Jr.; Norrell, H.A.; Owens, G.; Ransohoff, J.; Wilson, C.B.; et al. Evaluation of BCNU and/or radiotherapy in the treatment of anaplastic gliomas. A cooperative clinical trial. *J. Neurosurg.* **1978**, *49*, 333–343. [\[CrossRef\]](#)
30. Gzell, C.; Back, M.; Wheeler, H.; Bailey, D.; Foote, M. Radiotherapy in Glioblastoma: The Past, the Present and the Future. *Clin. Oncol. R Coll. Radiol.* **2017**, *29*, 15–25. [\[CrossRef\]](#)
31. Hegi, M.E.; Diserens, A.C.; Gorlia, T.; Hamou, M.F.; de Tribolet, N.; Weller, M.; Kros, J.M.; Hainfellner, J.A.; Mason, W.; Mariani, L.; et al. MGMT gene silencing and benefit from temozolomide in glioblastoma. *New Engl. J. Med.* **2005**, *352*, 997–1003. [\[CrossRef\]](#)
32. Verhaak, R.G.; Hoadley, K.A.; Purdom, E.; Wang, V.; Qi, Y.; Wilkerson, M.D.; Miller, C.R.; Ding, L.; Golub, T.; Mesirov, J.P.; et al. Integrated genomic analysis identifies clinically relevant subtypes of glioblastoma characterized by abnormalities in PDGFRA, IDH1, EGFR, and NF1. *Cancer Cell.* **2010**, *17*, 98–110. [\[CrossRef\]](#)
33. Sturm, D.; Witt, H.; Hovestadt, V.; Khuong-Quang, D.A.; Jones, D.T.; Konermann, C.; Pfaff, E.; Tonjes, M.; Sill, M.; Bender, S.; et al. Hotspot mutations in H3F3A and IDH1 define distinct epigenetic and biological subgroups of glioblastoma. *Cancer Cell.* **2012**, *22*, 425–437. [\[CrossRef\]](#)
34. Dix, A.R.; Brooks, W.H.; Roszman, T.L.; Morford, L.A. Immune defects observed in patients with primary malignant brain tumors. *J. Neuroimmunol.* **1999**, *100*, 216–232. [\[CrossRef\]](#)
35. Grabowski, M.M.; Sankey, E.W.; Ryan, K.J.; Chongsathidkiet, P.; Lorrey, S.J.; Wilkinson, D.S.; Fecci, P.E. Immune suppression in gliomas. *J. Neurooncol.* **2020**. [\[CrossRef\]](#)
36. North, R.J. Gamma-irradiation facilitates the expression of adoptive immunity against established tumors by eliminating suppressor T cells. *Cancer Immunol. Immunother.* **1984**, *16*, 175–181. [\[CrossRef\]](#) [\[PubMed\]](#)
37. Jordan, J.T.; Sun, W.; Hussain, S.F.; DeAngulo, G.; Prabhu, S.S.; Heimberger, A.B. Preferential migration of regulatory T cells mediated by glioma-secreted chemokines can be blocked with chemotherapy. *Cancer Immunol. Immunother.* **2008**, *57*, 123–131. [\[CrossRef\]](#) [\[PubMed\]](#)
38. Fadul, C.E.; Fisher, J.L.; Gui, J.; Hampton, T.H.; Cote, A.L.; Ernstoff, M.S. Immune modulation effects of concomitant temozolomide and radiation therapy on peripheral blood mononuclear cells in patients with glioblastoma multiforme. *Neuro Oncol.* **2011**, *13*, 393–400. [\[CrossRef\]](#)
39. Dutoit, V.; Philippin, G.; Widmer, V.; Marinari, E.; Vuilleumier, A.; Migliorini, D.; Schaller, K.; Dietrich, P.Y. Impact of Radiochemotherapy on Immune Cell Subtypes in High-Grade Glioma Patients. *Front. Oncol.* **2020**, *10*, 89. [\[CrossRef\]](#)
40. Antonopoulos, M.; Van Gool, S.W.; Dionysiou, D.; Graf, N.; Stamatakis, G. Immune phenotype correlates with survival in patients with GBM treated with standard temozolomide-based therapy and immunotherapy. *Anticancer Res.* **2019**, *39*, 2043–2051. [\[CrossRef\]](#)

41. Sathornsumetee, S.; Rich, J.N. Designer therapies for glioblastoma multiforme. *Ann. N. Y. Acad. Sci.* **2008**, *1142*, 108–132. [\[CrossRef\]](#)
42. Chen, R.; Cohen, A.L.; Colman, H. Targeted Therapeutics in Patients with High-Grade Gliomas: Past, Present, and Future. *Curr. Treat. Options Oncol.* **2016**, *17*, 42. [\[CrossRef\]](#)
43. Dos Santos, M.A.; Pignon, J.P.; Blanchard, P.; Lefevre, D.; Levy, A.; Touat, M.; Louvel, G.; Dhermain, F.; Soria, J.C.; Deutsch, E.; et al. Systematic review and meta-analysis of phase I/II targeted therapy combined with radiotherapy in patients with glioblastoma multiforme: Quality of report, toxicity, and survival. *J. Neurooncol.* **2015**, *123*, 307–314. [\[CrossRef\]](#)
44. Su, J.; Cai, M.; Li, W.; Hou, B.; He, H.; Ling, C.; Huang, T.; Liu, H.; Guo, Y. Molecularly Targeted Drugs Plus Radiotherapy and Temozolomide Treatment for Newly Diagnosed Glioblastoma: A Meta-Analysis and Systematic Review. *Oncol. Res.* **2016**, *24*, 117–128. [\[CrossRef\]](#) [\[PubMed\]](#)
45. Cihoric, N.; Tsikkinis, A.; Minniti, G.; Lagerwaard, F.J.; Herrlinger, U.; Mathier, E.; Soldatovic, I.; Jeremic, B.; Ghadjar, P.; Elicin, O.; et al. Current status and perspectives of interventional clinical trials for glioblastoma-analysis of ClinicalTrials.gov. *Radiat. Oncol.* **2017**, *12*, 63. [\[CrossRef\]](#)
46. Sim, H.W.; Morgan, E.R.; Mason, W.P. Contemporary management of high-grade gliomas. *Cns Oncol.* **2018**, *7*, 51–65. [\[CrossRef\]](#) [\[PubMed\]](#)
47. Lavacchi, D.; Roviello, G.; D'Angelo, A. Tumor-Agnostic Treatment for Cancer: When How is Better than Where. *Clin. Drug Investig.* **2020**, *40*, 519–527. [\[CrossRef\]](#) [\[PubMed\]](#)
48. Medical Research Council Streptomycin in Tuberculosis Trials Committee. Streptomycin treatment of pulmonary tuberculosis. *Br. Med. J.* **1948**, *2*, 769–782. [\[CrossRef\]](#)
49. Sorensen, H.T.; Lash, T.L.; Rothman, K.J. Beyond randomized controlled trials: A critical comparison of trials with nonrandomized studies. *Hepatology* **2006**, *44*, 1075–1082. [\[CrossRef\]](#)
50. Shikata, S.; Nakayama, T.; Noguchi, Y.; Taji, Y.; Yamagishi, H. Comparison of effects in randomized controlled trials with observational studies in digestive surgery. *Ann. Surg.* **2006**, *244*, 668–676. [\[CrossRef\]](#)
51. Vincent, J.L. We should abandon randomized controlled trials in the intensive care unit. *Crit. Care Med.* **2010**, *38*, S534–S538. [\[CrossRef\]](#)
52. Jones, D.S.; Podolsky, S.H. The history and fate of the gold standard. *Lancet* **2015**, *385*, 1502–1503. [\[CrossRef\]](#)
53. Trentino, K.; Farmer, S.; Gross, I.; Shander, A.; Isbister, J. Observational studies-should we simply ignore them in assessing transfusion outcomes? *BMC Anesth.* **2016**, *16*, 96. [\[CrossRef\]](#)
54. Sharma, M.; Nazareth, I.; Petersen, I. Observational studies of treatment effectiveness: Worthwhile or worthless? *Clin. Epidemiol.* **2019**, *11*, 35–42. [\[CrossRef\]](#) [\[PubMed\]](#)
55. Aldape, K.; Brindle, K.M.; Chesler, L.; Chopra, R.; Gajjar, A.; Gilbert, M.R.; Gottardo, N.; Gutmann, D.H.; Hargrave, D.; Holland, E.C.; et al. Challenges to curing primary brain tumours. *Nat. Rev. Clin. Oncol.* **2019**. [\[CrossRef\]](#) [\[PubMed\]](#)
56. Halabi, S.; Michiels, S. (Eds.) *Textbook of Clinical trials in Oncology. A Statistical Perspective*; CRC Press: Boca Raton, FL, USA, 2019.
57. Stepanenko, A.A.; Chekhonin, V.P. Recent Advances in Oncolytic Virotherapy and Immunotherapy for Glioblastoma: A Glimmer of Hope in the Search for an Effective Therapy? *Cancers* **2018**, *10*, 492. [\[CrossRef\]](#) [\[PubMed\]](#)
58. Jain, K.K. A Critical Overview of Targeted Therapies for Glioblastoma. *Front. Oncol.* **2018**, *8*, 419. [\[CrossRef\]](#) [\[PubMed\]](#)
59. Suter, R.; Rodriguez-Blanco, J.; Ayad, N.G. Epigenetic pathways and plasticity in brain tumors. *Neurobiol. Dis.* **2020**, 105060. [\[CrossRef\]](#) [\[PubMed\]](#)
60. Muller Bark, J.; Kulasinghe, A.; Chua, B.; Day, B.W.; Punyadeera, C. Circulating biomarkers in patients with glioblastoma. *Br. J. Cancer* **2020**, *122*, 295–305. [\[CrossRef\]](#)
61. Fiegl, H.; Millinger, S.; Mueller-Holzner, E.; Marth, C.; Ensinger, C.; Berger, A.; Klocker, H.; Goebel, G.; Widschwendter, M. Circulating tumor-specific DNA: A marker for monitoring efficacy of adjuvant therapy in cancer patients. *Cancer Res.* **2005**, *65*, 1141–1145. [\[CrossRef\]](#)
62. Sharma, P.; Allison, J.P. Immune checkpoint targeting in cancer therapy: Toward combination strategies with curative potential. *Cell* **2015**, *161*, 205–214. [\[CrossRef\]](#)
63. Macdonald, D.R.; Cascino, T.L.; Schold, S.C., Jr.; Cairncross, J.G. Response criteria for phase II studies of supratentorial malignant glioma. *J. Clin. Oncol.* **1990**, *8*, 1277–1280. [\[CrossRef\]](#)
64. Jaspan, T.; Morgan, P.S.; Warmuth-Metz, M.; Sanchez Aliaga, E.; Warren, D.; Calmon, R.; Grill, J.; Hargrave, D.; Garcia, J.; Zahlmann, G. Response Assessment in Pediatric Neuro-Oncology: Implementation and Expansion of the RANO Criteria in a Randomized Phase II Trial of Pediatric Patients with Newly Diagnosed High-Grade Gliomas. *Am. J. Neuroradiol.* **2016**, *37*, 1581–1587. [\[CrossRef\]](#)
65. Okada, H.; Weller, M.; Huang, R.; Finocchiaro, G.; Gilbert, M.R.; Wick, W.; Ellingson, B.M.; Hashimoto, N.; Pollack, I.F.; Brandes, A.A.; et al. Immunotherapy response assessment in neuro-oncology: A report of the RANO working group. *Lancet Oncol.* **2015**, *16*, e534–e542. [\[CrossRef\]](#)
66. Aquino, D.; Gioppo, A.; Finocchiaro, G.; Bruzzone, M.G.; Cuccarini, V. MRI in Glioma Immunotherapy: Evidence, Pitfalls, and Perspectives. *J. Immunol. Res.* **2017**, *2017*, 5813951. [\[CrossRef\]](#)
67. Sharma, P.; Debinski, W. Receptor-Targeted Glial Brain Tumor Therapies. *Int. J. Mol. Sci.* **2018**, *19*, 3326. [\[CrossRef\]](#)
68. Huang, J.; Liu, F.; Liu, Z.; Tang, H.; Wu, H.; Gong, Q.; Chen, J. Immune Checkpoint in Glioblastoma: Promising and Challenging. *Front. Pharm.* **2017**, *8*, 242. [\[CrossRef\]](#)

69. Wang, X.; Guo, G.; Guan, H.; Yu, Y.; Lu, J.; Yu, J. Challenges and potential of PD-1/PD-L1 checkpoint blockade immunotherapy for glioblastoma. *J. Exp. Clin. Cancer Res.* **2019**, *38*, 87. [\[CrossRef\]](#)
70. Ameratunga, M.; Coleman, N.; Welsh, L.; Saran, F.; Lopez, J. CNS cancer immunity cycle and strategies to target this for glioblastoma. *Oncotarget* **2018**, *9*, 22802–22816. [\[CrossRef\]](#)
71. Zhu, C.; Zou, C.; Guan, G.; Guo, Q.; Yan, Z.; Liu, T.; Shen, S.; Xu, X.; Chen, C.; Lin, Z.; et al. Development and validation of an interferon signature predicting prognosis and treatment response for glioblastoma. *Oncoimmunology* **2019**, *8*, e1621677. [\[CrossRef\]](#)
72. Kmiecik, J.; Poli, A.; Brons, N.H.; Waha, A.; Eide, G.E.; Enger, P.O.; Zimmer, J.; Chekenya, M. Elevated CD3+ and CD8+ tumor-infiltrating immune cells correlate with prolonged survival in glioblastoma patients despite integrated immunosuppressive mechanisms in the tumor microenvironment and at the systemic level. *J. Neuroimmunol.* **2013**, *264*, 71–83. [\[CrossRef\]](#)
73. Bouffet, E.; Larouche, V.; Campbell, B.B.; Merico, D.; de Borja, R.; Aronson, M.; Durno, C.; Krueger, J.; Cabric, V.; Ramaswamy, V.; et al. Immune Checkpoint Inhibition for Hypermutant Glioblastoma Multiforme Resulting from Germline Biallelic Mismatch Repair Deficiency. *J. Clin. Oncol.* **2016**, *34*, 2206–2211. [\[CrossRef\]](#)
74. Adhikaree, J.; Moreno-Vicente, J.; Kaur, A.P.; Jackson, A.M.; Patel, P.M. Resistance Mechanisms and Barriers to Successful Immunotherapy for Treating Glioblastoma. *Cells* **2020**, *9*, 263. [\[CrossRef\]](#)
75. Wang, B.; Niu, D.; Lai, L.; Ren, E.C. p53 increases MHC class I expression by upregulating the endoplasmic reticulum aminopeptidase ERAP1. *Nat. Commun.* **2013**, *4*, 2359. [\[CrossRef\]](#)
76. Blank, C.U.; Haanen, J.B.; Ribas, A.; Schumacher, T.N. Cancer Immunology. The cancer immunogram. *Science* **2016**, *352*, 658–660. [\[CrossRef\]](#) [\[PubMed\]](#)
77. Tomaszewski, W.; Sanchez-Perez, L.; Gajewski, T.F.; Sampson, J.H. Brain Tumor Micro-environment and Host State-Implications for Immunotherapy. *Clin. Cancer Res.* **2019**. [\[CrossRef\]](#) [\[PubMed\]](#)
78. Pires-Afonso, Y.; Niclou, S.P.; Michelucci, A. Revealing and Harnessing Tumour-Associated Microglia/Macrophage Heterogeneity in Glioblastoma. *Int. J. Mol. Sci.* **2020**, *21*, 689. [\[CrossRef\]](#) [\[PubMed\]](#)
79. Zhang, B.; Shen, R.; Cheng, S.; Feng, L. Immune microenvironments differ in immune characteristics and outcome of glioblastoma multiforme. *Cancer Med.* **2019**, *8*, 2897–2907. [\[CrossRef\]](#) [\[PubMed\]](#)
80. Hallaert, G.; Pinson, H.; Van den Broecke, C.; Vanhauwaert, D.; Van Roost, D.; Boterberg, T.; Kalala, J.P. Subventricular zone contacting glioblastoma: Tumor size, molecular biological factors and patient survival. *Acta Oncol.* **2020**. [\[CrossRef\]](#)
81. Berendsen, S.; van Bodegraven, E.; Seute, T.; Spliet, W.G.M.; Geurts, M.; Hendrikse, J.; Schoysman, L.; Huiszoon, W.B.; Varkila, M.; Rouss, S.; et al. Adverse prognosis of glioblastoma contacting the subventricular zone: Biological correlates. *PLoS ONE* **2019**, *14*, e0222717. [\[CrossRef\]](#)
82. Wee, C.W.; Kim, I.H.; Park, C.K.; Kim, J.W.; Dho, Y.S.; Ohka, F.; Aoki, K.; Motomura, K.; Natsume, A.; Kim, N.; et al. Validation of a novel molecular RPA classification in glioblastoma (GBM-molRPA) treated with chemoradiation: A multi-institutional collaborative study. *Radiother. Oncol.* **2018**, *129*, 347–351. [\[CrossRef\]](#)
83. Brown, C.E.; Badie, B.; Barish, M.E.; Weng, L.; Ostberg, J.R.; Chang, W.C.; Naranjo, A.; Starr, R.; Wagner, J.; Wright, C.; et al. Bioactivity and Safety of IL13Ralpha2-Redirected Chimeric Antigen Receptor CD8+ T Cells in Patients with Recurrent Glioblastoma. *Clin. Cancer Res.* **2015**, *21*, 4062–4072. [\[CrossRef\]](#)
84. O'Rourke, D.M.; Nasrallah, M.P.; Desai, A.; Melenhorst, J.J.; Mansfield, K.; Morrisette, J.J.D.; Martinez-Lage, M.; Brem, S.; Maloney, E.; Shen, A.; et al. A single dose of peripherally infused EGFRvIII-directed CAR T cells mediates antigen loss and induces adaptive resistance in patients with recurrent glioblastoma. *Sci. Transl. Med.* **2017**, *9*. [\[CrossRef\]](#)
85. Golinelli, G.; Grisendi, G.; Prapa, M.; Bestagno, M.; Spano, C.; Rossignoli, F.; Bambi, F.; Sardi, I.; Cellini, M.; Horwitz, E.M.; et al. Targeting GD2-positive glioblastoma by chimeric antigen receptor empowered mesenchymal progenitors. *Cancer Gene.* **2018**. [\[CrossRef\]](#) [\[PubMed\]](#)
86. Rammensee, H.G.; Singh-Jasuja, H. HLA ligandome tumor antigen discovery for personalized vaccine approach. *Expert Rev. Vaccines* **2013**, *12*, 1211–1217. [\[CrossRef\]](#) [\[PubMed\]](#)
87. Sahin, U.; Derhovanessian, E.; Miller, M.; Kloke, B.P.; Simon, P.; Lower, M.; Bukur, V.; Tadmor, A.D.; Luxemburger, U.; Schrors, B.; et al. Personalized RNA mutanome vaccines mobilize poly-specific therapeutic immunity against cancer. *Nature* **2017**. [\[CrossRef\]](#) [\[PubMed\]](#)
88. Johanns, T.M.; Miller, C.A.; Liu, C.J.; Perrin, R.J.; Bender, D.; Kobayashi, D.K.; Campian, J.L.; Chicoine, M.R.; Dacey, R.G.; Huang, J.; et al. Detection of neoantigen-specific T cells following a personalized vaccine in a patient with glioblastoma. *Oncoimmunology* **2019**, *8*, e1561106. [\[CrossRef\]](#) [\[PubMed\]](#)
89. De Vleeschouwer, S.; Arredouani, M.; Ade, M.; Cadot, P.; Vermassen, E.; Ceuppens, J.L.; Van Gool, S.W. Uptake and presentation of malignant glioma tumor cell lysates by monocyte-derived dendritic cells. *Cancer Immunol. Immunother.* **2005**, *54*, 372–382. [\[CrossRef\]](#) [\[PubMed\]](#)
90. De Vleeschouwer, S.; Spencer, L.I.; Ceuppens, J.L.; Van Gool, S.W. Persistent IL-10 production is required for glioma growth suppressive activity by Th1-directed effector cells after stimulation with tumor lysate-loaded dendritic cells. *J. Neurooncol.* **2007**, *84*, 131–140. [\[CrossRef\]](#)
91. Maes, W.; Deroose, C.; Reumers, V.; Krylyshkina, O.; Gijssbers, R.; Ceuppens, J.; Baekelandt, V.; Debyser, Z.; Van Gool, S. In vivo bioluminescence imaging in an experimental mouse model for dendritic cell based immunotherapy against malignant glioma. *J. Neuro Oncol.* **2009**, *91*, 127–139. [\[CrossRef\]](#)

92. Maes, W.; Galicia Rosas, G.; Verbinen, B.; Boon, L.; De Vleeschouwer, S.; Ceuppens, J.L.; Van Gool, S.W. DC vaccination with anti-CD25 treatment leads to long-term immunity against experimental glioma. *Neuro Oncol.* **2009**, *11*, 529–542. [\[CrossRef\]](#)
93. Ardon, H.; Verbinen, B.; Maes, W.; Beez, T.; Van Gool, S.; De Vleeschouwer, S. Technical advancement in regulatory T cell isolation and characterization using CD127 expression in patients with malignant glioma treated with autologous dendritic cell vaccination. *J. Immunol. Methods* **2010**, *352*, 169–173. [\[CrossRef\]](#)
94. Maes, W.; Van Gool, S.W. Experimental immunotherapy for malignant glioma: Lessons from two decades of research in the GL261 model. *Cancer Immunol. Immunother.* **2011**, *60*, 153–160. [\[CrossRef\]](#)
95. Vandenberg, L.; Van Gool, S.W. Treg infiltration in glioma: A hurdle for anti-glioma immunotherapy. *Immunotherapy* **2012**, *4*, 675–678. [\[CrossRef\]](#) [\[PubMed\]](#)
96. Koks, C.A.E.; Garg, A.D.; Ehrhardt, M.; Riva, M.; De Vleeschouwer, S.; Agostinis, P.; Graf, N.; Van Gool, S.W. Newcastle disease virotherapy induces long-term survival and tumor-specific immune memory in orthotopic glioma through the induction of immunogenic cell death. *Int. J. Cancer* **2014**, *136*, e313–e325. [\[CrossRef\]](#)
97. Koks, C.A.; De Vleeschouwer, S.; Graf, N.; Van Gool, S.W. Immune Suppression during Oncolytic Virotherapy for High-Grade Glioma; Yes or No? *J. Cancer* **2015**, *6*, 203–217. [\[CrossRef\]](#)
98. Vandenberg, L.; Belmans, J.; Van Woensel, M.; Riva, M.; Van Gool, S.W. Exploiting the Immunogenic Potential of Cancer Cells for Improved Dendritic Cell Vaccines. *Front. Immunol.* **2015**, *6*, 663. [\[CrossRef\]](#)
99. Garg, A.D.; Vandenberg, L.; Koks, C.; Verschuere, T.; Boon, L.; Van Gool, S.W.; Agostinis, P. Dendritic cell vaccines based on immunogenic cell death elicit danger signals and T cell-driven rejection of high-grade glioma. *Sci. Transl. Med.* **2016**, *8*, 328ra327. [\[CrossRef\]](#) [\[PubMed\]](#)
100. Vandenberg, L.; Garg, A.D.; Verschuere, T.; Koks, C.; Belmans, J.; Beullens, M.; Agostinis, P.; De Vleeschouwer, S.; Van Gool, S.W. Irradiation of necrotic cancer cells, employed for pulsing dendritic cells (DCs), potentiates DC vaccine-induced antitumor immunity against high-grade glioma. *Oncoimmunology* **2016**, *5*, e1083669. [\[CrossRef\]](#) [\[PubMed\]](#)
101. Belmans, J.; Van Woensel, M.; Creyns, B.; Dejaegher, J.; Bullens, D.M.; Van Gool, S.W. Immunotherapy with subcutaneous immunogenic autologous tumor lysate increases murine glioblastoma survival. *Sci. Rep.* **2017**, *7*, 13902. [\[CrossRef\]](#)
102. Liao, L.M.; Black, K.L.; Martin, N.A.; Sykes, S.N.; Bronstein, J.M.; Jouben-Steele, L.; Mischel, P.S.; Belldegrun, A.; Cloughesy, T.F. Treatment of a patient by vaccination with autologous dendritic cells pulsed with allogeneic major histocompatibility complex class I-matched tumor peptides. Case Report. *Neurosurg. Focus* **2000**, *9*, e8. [\[CrossRef\]](#)
103. Yu, J.S.; Wheeler, C.J.; Zeltzer, P.M.; Ying, H.; Finger, D.N.; Lee, P.K.; Yong, W.H.; Incardona, F.; Thompson, R.C.; Riedinger, M.S.; et al. Vaccination of malignant glioma patients with peptide-pulsed dendritic cells elicits systemic cytotoxicity and intracranial T-cell infiltration. *Cancer Res.* **2001**, *61*, 842–847.
104. Kikuchi, T.; Akasaki, Y.; Irie, M.; Homma, S.; Abe, T.; Ohno, T. Results of a phase I clinical trial of vaccination of glioma patients with fusions of dendritic and glioma cells. *Cancer Immunol. Immunother.* **2001**, *50*, 337–344. [\[CrossRef\]](#)
105. Wheeler, C.J.; Black, K.L.; Liu, G.; Ying, H.; Yu, J.S.; Zhang, W.; Lee, P.K. Thymic CD8(+) T cell production strongly influences tumor antigen recognition and age-dependent glioma mortality. *J. Immunol.* **2003**, *171*, 4927–4933. [\[CrossRef\]](#) [\[PubMed\]](#)
106. Yamanaka, R.; Abe, T.; Yajima, N.; Tsuchiya, N.; Homma, J.; Kobayashi, T.; Narita, M.; Takahashi, M.; Tanaka, R. Vaccination of recurrent glioma patients with tumour lysate-pulsed dendritic cells elicits immune responses: Results of a clinical phase I/II trial. *Br. J. Cancer* **2003**, *89*, 1172–1179. [\[CrossRef\]](#) [\[PubMed\]](#)
107. Caruso, D.A.; Orme, L.M.; Neale, A.M.; Radcliff, F.J.; Amor, G.M.; Maixner, W.; Downie, P.; Hassall, T.E.; Tang, M.L.; Ashley, D.M. Results of a phase 1 study utilizing monocyte-derived dendritic cells pulsed with tumor RNA in children and young adults with brain cancer. *Neuro. Oncol.* **2004**, *6*, 236–246. [\[CrossRef\]](#) [\[PubMed\]](#)
108. De Vleeschouwer, S.; Van Calenbergh, F.; Demaerel, P.; Flamen, P.; Rutkowski, S.; Kaempgen, E.; Wolff, J.E.A.; Plets, C.; Sciote, R.; Van Gool, S.W. Transient local response and persistent tumor control of recurrent malignant glioma treated with combination therapy including dendritic cell therapy. *J. Neurosurg.* **2004**, *100*, 492–497. [\[PubMed\]](#)
109. Kikuchi, T.; Akasaki, Y.; Abe, T.; Fukuda, T.; Saotome, H.; Ryan, J.L.; Kufe, D.W.; Ohno, T. Vaccination of glioma patients with fusions of dendritic and glioma cells and recombinant human interleukin 12. *J. Immunother.* **2004**, *27*, 452–459. [\[CrossRef\]](#)
110. Rutkowski, S.; De Vleeschouwer, S.; Kaempgen, E.; Wolff, J.E.A.; Kuhl, J.; Demaerel, P.; Warmuth-Metz, M.; Flamen, P.; Van Calenbergh, F.; Plets, C.; et al. Surgery and adjuvant dendritic cell-based tumour vaccination for patients with relapsed malignant glioma, a feasibility study. *Br. J. Cancer* **2004**, *91*, 1656–1662. [\[CrossRef\]](#)
111. Wheeler, C.J.; Das, A.; Liu, G.; Yu, J.S.; Black, K.L. Clinical responsiveness of glioblastoma multiforme to chemotherapy after vaccination. *Clin. Cancer Res.* **2004**, *10*, 5316–5326. [\[CrossRef\]](#)
112. Yu, J.S.; Liu, G.; Ying, H.; Yong, W.H.; Black, K.L.; Wheeler, C.J. Vaccination with tumor lysate-pulsed dendritic cells elicits antigen-specific, cytotoxic T-cells in patients with malignant glioma. *Cancer Res.* **2004**, *64*, 4973–4979. [\[CrossRef\]](#)
113. Liao, L.M.; Prins, R.M.; Kiertscher, S.M.; Odesa, S.K.; Kremen, T.J.; Giovannone, A.J.; Lin, J.W.; Chute, D.J.; Mischel, P.S.; Cloughesy, T.F.; et al. Dendritic cell vaccination in glioblastoma patients induces systemic and intracranial T-cell responses modulated by the local central nervous system tumor microenvironment. *Clin. Cancer Res.* **2005**, *11*, 5515–5525. [\[CrossRef\]](#)
114. Yamanaka, R.; Honma, J.; Tsuchiya, N.; Yajima, N.; Kobayashi, T.; Tanaka, R. Tumor lysate and IL-18 loaded dendritic cells elicits Th1 response, tumor-specific CD8+ cytotoxic T cells in patients with malignant glioma. *J. Neurooncol.* **2005**, *72*, 107–113. [\[CrossRef\]](#) [\[PubMed\]](#)

115. Yamanaka, R.; Homma, J.; Yajima, N.; Tsuchiya, N.; Sano, M.; Kobayashi, T.; Yoshida, S.; Abe, T.; Narita, M.; Takahashi, M.; et al. Clinical evaluation of dendritic cell vaccination for patients with recurrent glioma: Results of a clinical phase I/II trial. *Clin. Cancer Res.* **2005**, *11*, 4160–4167. [\[CrossRef\]](#)
116. Khan, J.A.; Yaqin, S. Dendritic cell therapy with improved outcome in glioma multiforme—A case report. *J. Zhejiang Univ. Sci. B* **2006**, *7*, 114–117. [\[CrossRef\]](#)
117. Okada, H.; Lieberman, F.S.; Walter, K.A.; Lunsford, L.D.; Kondziolka, D.S.; Bejjani, G.K.; Hamilton, R.L.; Torres-Trejo, A.; Kalinski, P.; Cai, Q.; et al. Autologous glioma cell vaccine admixed with interleukin-4 gene transfected fibroblasts in the treatment of patients with malignant gliomas. *J. Transl. Med.* **2007**, *5*, 67. [\[CrossRef\]](#)
118. De Vleeschouwer, S.; Fieuws, S.; Rutkowski, S.; Van Calenbergh, F.; Van Loon, J.; Goffin, J.; Sciot, R.; Wilms, G.; Demaerel, P.; Warmuth-Metz, M.; et al. Postoperative adjuvant dendritic cell-based immunotherapy in patients with relapsed glioblastoma multiforme. *Clin. Cancer Res.* **2008**, *14*, 3098–3104. [\[CrossRef\]](#)
119. Prins, R.M.; Cloughesy, T.F.; Liao, L.M. Cytomegalovirus immunity after vaccination with autologous glioblastoma lysate. *New Engl. J. Med.* **2008**, *359*, 539–541. [\[CrossRef\]](#)
120. Walker, D.G.; Laherty, R.; Tomlinson, F.H.; Chuah, T.; Schmidt, C. Results of a phase I dendritic cell vaccine trial for malignant astrocytoma: Potential interaction with adjuvant chemotherapy. *J. Clin. Neurosci.* **2008**, *15*, 114–121. [\[CrossRef\]](#)
121. Wheeler, C.J.; Black, K.L.; Liu, G.; Mazer, M.; Zhang, X.X.; Pepkowitz, S.; Goldfinger, D.; Ng, H.; Irvin, D.; Yu, J.S. Vaccination elicits correlated immune and clinical responses in glioblastoma multiforme patients. *Cancer Res.* **2008**, *68*, 5955–5964. [\[CrossRef\]](#)
122. Sampson, J.H.; Archer, G.E.; Mitchell, D.A.; Heimberger, A.B.; Herndon, J.E.; Lally-Goss, D.; McGehee-Norman, S.; Paolino, A.; Reardon, D.A.; Friedman, A.H.; et al. An epidermal growth factor receptor variant III-targeted vaccine is safe and immunogenic in patients with glioblastoma multiforme. *Mol. Cancer* **2009**, *8*, 2773–2779. [\[CrossRef\]](#)
123. Ardon, H.; Van Gool, S.; Lopes, I.S.; Maes, W.; Sciot, R.; Wilms, G.; Demaerel, P.; Bijttebier, P.; Claes, L.; Goffin, J.; et al. Integration of autologous dendritic cell-based immunotherapy in the primary treatment for patients with newly diagnosed glioblastoma multiforme: A pilot study. *J. Neurooncol.* **2010**, *99*, 261–272. [\[CrossRef\]](#)
124. Ardon, H.; De Vleeschouwer, S.; Van Calenbergh, F.; Claes, L.; Kramm, C.M.; Rutkowski, S.; Wolff, J.E.; Van Gool, S.W. Adjuvant dendritic cell-based tumour vaccination for children with malignant brain tumours. *Pediatr. Blood Cancer* **2010**, *54*, 519–525. [\[CrossRef\]](#)
125. Chang, C.N.; Huang, Y.C.; Yang, D.M.; Kikuta, K.; Wei, K.J.; Kubota, T.; Yang, W.K. A phase I/II clinical trial investigating the adverse and therapeutic effects of a postoperative autologous dendritic cell tumor vaccine in patients with malignant glioma. *J. Clin. Neurosci.* **2011**, *18*, 1048–1054. [\[CrossRef\]](#)
126. Fadul, C.E.; Fisher, J.L.; Hampton, T.H.; Lallana, E.C.; Li, Z.; Gui, J.; Szczepiorkowski, Z.M.; Tosteson, T.D.; Rhodes, C.H.; Wishart, H.A.; et al. Immune response in patients with newly diagnosed glioblastoma multiforme treated with intranodal autologous tumor lysate-dendritic cell vaccination after radiation chemotherapy. *J. Immunother.* **2011**, *34*, 382–389. [\[CrossRef\]](#)
127. Okada, H.; Kalinski, P.; Ueda, R.; Hoji, A.; Kohanbash, G.; Donegan, T.E.; Mintz, A.H.; Engh, J.A.; Bartlett, D.L.; Brown, C.K.; et al. Induction of CD8⁺ T-cell responses against novel glioma-associated antigen peptides and clinical activity by vaccinations with α -type 1 polarized dendritic cells and polyinosinic-polycytidylic acid stabilized by lysine and carboxymethylcellulose in patients with recurrent malignant glioma. *J. Clin. Oncol.* **2011**, *29*, 330–336. [\[CrossRef\]](#) [\[PubMed\]](#)
128. Prins, R.M.; Soto, H.; Konkankit, V.; Odesa, S.K.; Eskin, A.; Yong, W.H.; Nelson, S.F.; Liao, L.M. Gene expression profile correlates with T-cell infiltration and relative survival in glioblastoma patients vaccinated with dendritic cell immunotherapy. *Clin. Cancer Res.* **2011**, *17*, 1603–1615. [\[CrossRef\]](#)
129. Akiyama, Y.; Oshita, C.; Kume, A.; Iizuka, A.; Miyata, H.; Komiyama, M.; Ashizawa, T.; Yagoto, M.; Abe, Y.; Mitsuya, K.; et al. α -type-1 polarized dendritic cell-based vaccination in recurrent high-grade glioma: A phase I clinical trial. *BMC Cancer* **2012**, *12*, 623. [\[CrossRef\]](#)
130. Ardon, H.; Van Gool, S.W.; Verschuere, T.; Maes, W.; Fieuws, S.; Sciot, R.; Wilms, G.; Demaerel, P.; Goffin, J.; Van Calenbergh, F.; et al. Integration of autologous dendritic cell-based immunotherapy in the standard of care treatment for patients with newly diagnosed glioblastoma: Results of the HGG-2006 phase I/II trial. *Cancer Immunol. Immunother.* **2012**, *61*, 2033–2044. [\[CrossRef\]](#) [\[PubMed\]](#)
131. Cho, D.Y.; Yang, W.K.; Lee, H.C.; Hsu, D.M.; Lin, H.L.; Lin, S.Z.; Chen, C.C.; Harn, H.J.; Liu, C.L.; Lee, W.Y.; et al. Adjuvant immunotherapy with whole-cell lysate dendritic cells vaccine for glioblastoma multiforme: A phase II clinical trial. *World Neurosurg.* **2012**, *77*, 736–744. [\[CrossRef\]](#) [\[PubMed\]](#)
132. De Vleeschouwer, S.; Ardon, H.; van Calenbergh, F.; Sciot, R.; Wilms, G.; van Loon, J.; Goffin, J.; van Gool, S. Stratification according to Hgg-Immuno Rpa model predicts outcome in a large group of patients with relapsed malignant glioma treated by adjuvant postoperative dendritic cell vaccination. *Cancer Immunol. Immunother.* **2012**, *61*, 2105–2112. [\[CrossRef\]](#)
133. Elens, I.; De Vleeschouwer, S.; Pauwels, F.; Van Gool, S.W. Resection and immunotherapy for recurrent grade III glioma. *Isrn Immunol.* **2012**, *2012*, 530179. [\[CrossRef\]](#)
134. Fong, B.; Jin, R.; Wang, X.; Safaee, M.; Lisiero, D.N.; Yang, I.; Li, G.; Liao, L.M.; Prins, R.M. Monitoring of regulatory T cell frequencies and expression of CTLA-4 on T cells, before and after DC vaccination, can predict survival in GBM patients. *PLoS ONE* **2012**, *7*, e32614. [\[CrossRef\]](#)

135. Iwami, K.; Shimato, S.; Ohno, M.; Okada, H.; Nakahara, N.; Sato, Y.; Yoshida, J.; Suzuki, S.; Nishikawa, H.; Shiku, H.; et al. Peptide-pulsed dendritic cell vaccination targeting interleukin-13 receptor alpha2 chain in recurrent malignant glioma patients with HLA-A*24/A*02 allele. *Cytotherapy* **2012**. [\[CrossRef\]](#)
136. Jie, X.; Hua, L.; Jiang, W.; Feng, F.; Feng, G.; Hua, Z. Clinical application of a dendritic cell vaccine raised against heat-shocked glioblastoma. *Cell Biochem. Biophys.* **2012**, *62*, 91–99. [\[CrossRef\]](#)
137. Qin, K.; Tian, G.; Li, P.; Chen, Q.; Zhang, R.; Ke, Y.Q.; Xiao, Z.C.; Jiang, X.D. Anti-glioma response of autologous T cells stimulated by autologous dendritic cells electrofused with CD133(+) or CD133(-) glioma cells. *J. Neuroimmunol.* **2012**, *242*, 9–15. [\[CrossRef\]](#)
138. Sampson, J.H.; Schmittling, R.J.; Archer, G.E.; Congdon, K.L.; Nair, S.K.; Reap, E.A.; Desjardins, A.; Friedman, A.H.; Friedman, H.S.; Herndon, J.E.; et al. A Pilot Study of IL-2/Ralpha Blockade during Lymphopenia Depletes Regulatory T-cells and Correlates with Enhanced Immunity in Patients with Glioblastoma. *PLoS ONE* **2012**, *7*, e31046. [\[CrossRef\]](#)
139. Valle, R.D.; de Cerio, A.L.; Inoges, S.; Tejada, S.; Pastor, F.; Villanueva, H.; Gallego, J.; Espinos, J.; Aristu, J.; Idoate, M.A.; et al. Dendritic cell vaccination in glioblastoma after fluorescence-guided resection. *World J. Clin. Oncol.* **2012**, *3*, 142–149. [\[CrossRef\]](#)
140. Lasky, J.L., III; Panosyan, E.H.; Plant, A.; Davidson, T.; Yong, W.H.; Prins, R.M.; Liau, L.M.; Moore, T.B. Autologous Tumor Lysate-pulsed Dendritic Cell Immunotherapy for Pediatric Patients with Newly Diagnosed or Recurrent High-grade Gliomas. *Anticancer Res.* **2013**, *33*, 2047–2056.
141. Pellegatta, S.; Eoli, M.; Frigerio, S.; Antozzi, C.; Bruzzzone, M.G.; Cantini, G.; Nava, S.; Anghileri, E.; Cuppini, L.; Cuccarini, V.; et al. The natural killer cell response and tumor debulking are associated with prolonged survival in recurrent glioblastoma patients receiving dendritic cells loaded with autologous tumor lysates. *Oncoimmunology* **2013**, *2*, e23401. [\[CrossRef\]](#) [\[PubMed\]](#)
142. Phuphanich, S.; Wheeler, C.J.; Rudnick, J.D.; Mazer, M.; Wang, H.; Nuno, M.A.; Richardson, J.E.; Fan, X.; Ji, J.; Chu, R.M.; et al. Phase I trial of a multi-epitope-pulsed dendritic cell vaccine for patients with newly diagnosed glioblastoma. *Cancer Immunol. Immunother.* **2013**, *62*, 125–135. [\[CrossRef\]](#)
143. Prins, R.M.; Wang, X.; Soto, H.; Young, E.; Lisiero, D.N.; Fong, B.; Everson, R.; Yong, W.H.; Lai, A.; Li, G.; et al. Comparison of glioma-associated antigen peptide-loaded versus autologous tumor lysate-loaded dendritic cell vaccination in malignant glioma patients. *J. Immunother.* **2013**, *36*, 152–157. [\[CrossRef\]](#)
144. Vik-Mo, E.O.; Nyakas, M.; Mikkelsen, B.V.; Moe, M.C.; Due-Tonnesen, P.; Suso, E.M.; Saeboe-Larssen, S.; Sandberg, C.; Brinchmann, J.E.; Helseth, E.; et al. Therapeutic vaccination against autologous cancer stem cells with mRNA-transfected dendritic cells in patients with glioblastoma. *Cancer Immunol. Immunother.* **2013**. [\[CrossRef\]](#)
145. Eyrich, M.; Schreiber, S.C.; Rachor, J.; Krauss, J.; Pauwels, F.; Hain, J.; Wolf, M.; Lutz, M.B.; De, V.S.; Schlegel, P.G.; et al. Development and validation of a fully GMP-compliant production process of autologous, tumor-lysate-pulsed dendritic cells. *Cytotherapy* **2014**, *16*, 946–964. [\[CrossRef\]](#)
146. Ishikawa, E.; Muragaki, Y.; Yamamoto, T.; Maruyama, T.; Tsuboi, K.; Ikuta, S.; Hashimoto, K.; Uemae, Y.; Ishihara, T.; Matsuda, M.; et al. Phase I/IIa trial of fractionated radiotherapy, temozolomide, and autologous formalin-fixed tumor vaccine for newly diagnosed glioblastoma. *J. Neurosurg.* **2014**, *121*, 543–553. [\[CrossRef\]](#)
147. Hunn, M.K.; Bauer, E.; Wood, C.E.; Gasser, O.; Dzhelali, M.; Ancelet, L.R.; Mester, B.; Sharples, K.J.; Findlay, M.P.; Hamilton, D.A.; et al. Dendritic cell vaccination combined with temozolomide retreatment: Results of a phase I trial in patients with recurrent glioblastoma multiforme. *J. Neurooncol.* **2015**, *121*, 319–329. [\[CrossRef\]](#)
148. Mitchell, D.A.; Batich, K.A.; Gunn, M.D.; Huang, M.N.; Sanchez-Perez, L.; Nair, S.K.; Congdon, K.L.; Reap, E.A.; Archer, G.E.; Desjardins, A.; et al. Tetanus toxoid and CCL3 improve dendritic cell vaccines in mice and glioblastoma patients. *Nature* **2015**, *519*, 366–369. [\[CrossRef\]](#)
149. Muller, K.; Henke, G.; Pietschmann, S.; van Gool, S.; De Vleeschouwer, S.; von Bueren, A.O.; Compter, I.; Friedrich, C.; Matuschek, C.; Klautke, G.; et al. Re-irradiation or re-operation followed by dendritic cell vaccination? Comparison of two different salvage strategies for relapsed high-grade gliomas by means of a new prognostic model. *J. Neurooncol.* **2015**, *124*, 325–332. [\[CrossRef\]](#)
150. Sakai, K.; Shimodaira, S.; Maejima, S.; Udagawa, N.; Sano, K.; Higuchi, Y.; Koya, T.; Ochiai, T.; Koide, M.; Uehara, S.; et al. Dendritic cell-based immunotherapy targeting Wilms' tumor 1 in patients with recurrent malignant glioma. *J. Neurosurg.* **2015**, *123*, 989–997. [\[CrossRef\]](#)
151. Van Gool, S.W. Brain tumor immunotherapy: What have we learned so far? *Front. Oncol.* **2015**, *5*, 98. [\[CrossRef\]](#)
152. Akasaki, Y.; Kikuchi, T.; Homma, S.; Koido, S.; Ohkusa, T.; Tasaki, T.; Hayashi, K.; Komita, H.; Watanabe, N.; Suzuki, Y.; et al. Phase I/II trial of combination of temozolomide chemotherapy and immunotherapy with fusions of dendritic and glioma cells in patients with glioblastoma. *Cancer Immunol. Immunother.* **2016**, *65*, 1499–1509. [\[CrossRef\]](#)
153. Pollack, I.F.; Jakacki, R.I.; Butterfield, L.H.; Hamilton, R.L.; Panigrahy, A.; Normolle, D.P.; Connelly, A.K.; Dibridge, S.; Mason, G.; Whiteside, T.L.; et al. Antigen-specific immunoreactivity and clinical outcome following vaccination with glioma-associated antigen peptides in children with recurrent high-grade gliomas: Results of a pilot study. *J. Neurooncol.* **2016**, *130*, 517–527. [\[CrossRef\]](#)
154. Inoges, S.; Tejada, S.; de Cerio, A.L.; Gallego Perez-Larraya, J.; Espinos, J.; Idoate, M.A.; Dominguez, P.D.; de Eulate, R.G.; Aristu, J.; Bendandi, M.; et al. A phase II trial of autologous dendritic cell vaccination and radiochemotherapy following fluorescence-guided surgery in newly diagnosed glioblastoma patients. *J. Transl. Med.* **2017**, *15*, 104. [\[CrossRef\]](#)
155. Sakai, K.; Shimodaira, S.; Maejima, S.; Sano, K.; Higuchi, Y.; Koya, T.; Sugiyama, H.; Hongo, K. Clinical effect and immunological response in patients with advanced malignant glioma treated with WT1-pulsed dendritic cell-based immunotherapy: A report of two cases. *Interdiscip. Neurosurg. Adv. Tech. Case Manag.* **2017**, *9*, 24–29. [\[CrossRef\]](#)

156. Benitez-Ribas, D.; Cabezon, R.; Florez-Grau, G.; Molero, M.C.; Puerta, P.; Guillen, A.; Paco, S.; Carcaboso, A.M.; Santa-Maria Lopez, V.; Cruz, O.; et al. Immune Response Generated with the Administration of Autologous Dendritic Cells Pulsed with an Allogenic Tumoral Cell-Lines Lysate in Patients with Newly Diagnosed Diffuse Intrinsic Pontine Glioma. *Front. Oncol.* **2018**, *8*, 127. [CrossRef] [PubMed]
157. Buchroithner, J.; Erhart, F.; Pichler, J.; Widhalm, G.; Preusser, M.; Stockhammer, G.; Nowosielski, M.; Iglseder, S.; Freyschlag, C.F.; Oberndorfer, S.; et al. Audencel Immunotherapy Based on Dendritic Cells Has No Effect on Overall and Progression-Free Survival in Newly Diagnosed Glioblastoma: A Phase II Randomized Trial. *Cancers* **2018**, *10*, 372. [CrossRef] [PubMed]
158. Jan, C.I.; Tsai, W.C.; Harn, H.J.; Shyu, W.C.; Liu, M.C.; Lu, H.M.; Chiu, S.C.; Cho, D.Y. Predictors of Response to Autologous Dendritic Cell Therapy in Glioblastoma Multiforme. *Front. Immunol.* **2018**, *9*, 727. [CrossRef] [PubMed]
159. Erhart, F.; Buchroithner, J.; Reitermaier, R.; Fischhuber, K.; Klingensbrunner, S.; Sloma, I.; Hibsh, D.; Kozol, R.; Efroni, S.; Ricken, G.; et al. Immunological analysis of phase II glioblastoma dendritic cell vaccine (Audencel) trial: Immune system characteristics influence outcome and Audencel up-regulates Th1-related immunovariabiles. *Acta Neuropathol. Commun.* **2018**, *6*, 135. [CrossRef] [PubMed]
160. Liao, L.M.; Ashkan, K.; Tran, D.D.; Campian, J.L.; Trusheim, J.E.; Cobbs, C.S.; Heth, J.A.; Salacz, M.; Taylor, S.; D'Andre, S.D.; et al. First results on survival from a large Phase 3 clinical trial of an autologous dendritic cell vaccine in newly diagnosed glioblastoma. *J. Transl. Med.* **2018**, *16*, 142. [CrossRef]
161. Pellegatta, S.; Eoli, M.; Cuccarini, V.; Anghileri, E.; Pollo, B.; Pessina, S.; Frigerio, S.; Servida, M.; Cuppini, L.; Antozzi, C.; et al. Survival gain in glioblastoma patients treated with dendritic cell immunotherapy is associated with increased NK but not CD8(+) T cell activation in the presence of adjuvant temozolomide. *Oncotimmunology* **2018**, *7*, e1412901. [CrossRef]
162. Yao, Y.; Luo, F.; Tang, C.; Chen, D.; Qin, Z.; Hua, W.; Xu, M.; Zhong, P.; Yu, S.; Chen, D.; et al. Molecular subgroups and B7-H4 expression levels predict responses to dendritic cell vaccines in glioblastoma: An exploratory randomized phase II clinical trial. *Cancer Immunol. Immunother.* **2018**. [CrossRef]
163. Rudnick, J.D.; Sarmiento, J.M.; Uy, B.; Nuno, M.; Wheeler, C.J.; Mazer, M.J.; Wang, H.; Hu, J.L.; Chu, R.M.; Phuphanich, S.; et al. A phase I trial of surgical resection with Gliadel Wafer placement followed by vaccination with dendritic cells pulsed with tumor lysate for patients with malignant glioma. *J. Clin. Neurosci.* **2020**, *74*, 187–193. [CrossRef]
164. Wang, Q.T.; Nie, Y.; Sun, S.N.; Lin, T.; Han, R.J.; Jiang, J.; Li, Z.; Li, J.Q.; Xiao, Y.P.; Fan, Y.Y.; et al. Tumor-associated antigen-based personalized dendritic cell vaccine in solid tumor patients. *Cancer Immunol. Immunother.* **2020**, *69*, 1375–1387. [CrossRef]
165. Sampson, J.H.; Heimberger, A.B.; Archer, G.E.; Aldape, K.D.; Friedman, A.H.; Friedman, H.S.; Gilbert, M.R.; Herndon, J.E.; McLendon, R.E.; Mitchell, D.A.; et al. Immunologic escape after prolonged progression-free survival with epidermal growth factor receptor variant III peptide vaccination in patients with newly diagnosed glioblastoma. *J. Clin. Oncol.* **2010**, *28*, 4722–4729. [CrossRef] [PubMed]
166. Dejaegher, J.; Solie, L.; Hunin, Z.; Sciote, R.; Capper, D.; Siewert, C.; Van Cauter, S.; Wilms, G.; van Loon, J.; Ectors, N.; et al. Methylation based glioblastoma subclassification is related to tumoral T cell infiltration and survival. *Neuro Oncol.* **2020**. [CrossRef] [PubMed]
167. Dejaegher, J. *Local and Systemic Immune Interactions in Malignant Gliomas*; KU Leuven: Leuven, Belgium, 2017.
168. Available online: <https://immuno-oncologynews.com/2017/06/26/glioblastoma-potential-therapy-ict-107-trial-suspended-cash-strapped-immunocellular/> (accessed on 18 December 2020).
169. Kast, R.E.; Karpel-Massler, G.; Halatsch, M.E. CUSP9* treatment protocol for recurrent glioblastoma: Aprepitant, artesunate, auranofin, captopril, celecoxib, disulfiram, itraconazole, ritonavir, sertraline augmenting continuous low dose temozolomide. *Oncotarget* **2014**, *5*, 8052–8082. [CrossRef] [PubMed]
170. Lissoni, P.; Messina, G.; Lissoni, A.; Franco, R. The psychoneuroendocrine-immunotherapy of cancer: Historical evolution and clinical results. *J. Res. Med. Sci.* **2017**, *22*, 45. [CrossRef] [PubMed]
171. Santos, J.G.; Da Cruz, W.M.S.; Schonthal, A.H.; Salazar, M.D.; Fontes, C.A.P.; Quirico-Santos, T.; Da Fonseca, C.O. Efficacy of a ketogenic diet with concomitant intranasal perillyl alcohol as a novel strategy for the therapy of recurrent glioblastoma. *Oncol. Lett.* **2018**, *15*, 1263–1270. [CrossRef]
172. Lopez-Valero, I.; Torres, S.; Salazar-Roa, M.; Garcia-Taboada, E.; Hernandez-Tiedra, S.; Guzman, M.; Sepulveda, J.M.; Velasco, G.; Lorente, M. Optimization of a preclinical therapy of cannabinoids in combination with temozolomide against glioma. *Biochem. Pharm.* **2018**, *157*, 275–284. [CrossRef]
173. Friesen, C.; Hormann, I.; Roscher, M.; Fichtner, I.; Alt, A.; Hilger, R.; Debatin, K.M.; Miltner, E. Opioid receptor activation triggering downregulation of cAMP improves effectiveness of anti-cancer drugs in treatment of glioblastoma. *Cell Cycle* **2014**, *13*, 1560–1570. [CrossRef]
174. Galluzzi, L.; Vitale, I.; Aaronson, S.A.; Abrams, J.M.; Adam, D.; Agostinis, P.; Alnemri, E.S.; Altucci, L.; Amelio, I.; Andrews, D.W.; et al. Molecular mechanisms of cell death: Recommendations of the Nomenclature Committee on Cell Death 2018. *Cell Death Differ.* **2018**. [CrossRef]
175. Galluzzi, L.; Vitale, I.; Warren, S.; Adjemian, S.; Agostinis, P.; Martinez, A.B.; Chan, T.A.; Coukos, G.; Demaria, S.; Deutsch, E.; et al. Consensus guidelines for the definition, detection and interpretation of immunogenic cell death. *J. Immunother. Cancer* **2020**, *8*. [CrossRef]

176. Van Gool, S.W.; Makalowski, J.; Domogalla, M.P.; Marko, M.; Feyen, O.; Sprenger, K.; Schirmacher, V.; Stuecker, W. Personalised medicine in glioblastoma multiforme. In *Challenges and Solutions of Oncological Hyperthermia*; Szasz, A., Ed.; Cambridge Scholars Publishing: Newcastle upon Tyne, UK, 2020; pp. 126–158.
177. Wang, Z.; Gao, L.; Guo, X.; Lian, W.; Deng, K.; Xing, B. Development and Validation of a Novel DNA Methylation-Driven Gene Based Molecular Classification and Predictive Model for Overall Survival and Immunotherapy Response in Patients with Glioblastoma: A Multiomic Analysis. *Front. Cell Dev. Biol.* **2020**, *8*, 576996. [[CrossRef](#)]
178. Bertram, M.Y.; Lauer, J.A.; De Joncheere, K.; Edejer, T.; Hutubessy, R.; Kieny, M.P.; Hill, S.R. Cost-effectiveness thresholds: Pros and cons. *Bull. World Health Organ.* **2016**, *94*, 925–930. [[CrossRef](#)] [[PubMed](#)]
179. Lin, S.; Luo, S.; Zhong, L.; Lai, S.; Zeng, D.; Rao, X.; Huang, P.; Weng, X. Cost-effectiveness of atezolizumab plus chemotherapy for advanced non-small-cell lung cancer. *Int. J. Clin. Pharm.* **2020**, *42*, 1175–1183. [[CrossRef](#)] [[PubMed](#)]
180. Aguiar, P.; Barreto, C.M.N.; Bychkovsky, B.L.; de Lima Lopes, G. Cost-effectiveness studies in oncology. In *Methods and Biostatistics in Oncology*; Araujo, R., Riechelmann, R., Eds.; Springer: Berlin/Heidelberg, Germany, 2018. [[CrossRef](#)]
181. Jonsson, B.; Hofmarcher, T.; Lindgren, P.; Wilking, N. The cost and burden of cancer in the European Union 1995–2014. *Eur. J. Cancer* **2016**, *66*, 162–170. [[CrossRef](#)] [[PubMed](#)]
182. Chen, C.T.; Li, L.; Brooks, G.; Hassett, M.; Schrag, D. Medicare Spending for Breast, Prostate, Lung, and Colorectal Cancer Patients in the Year of Diagnosis and Year of Death. *Health Serv. Res.* **2018**, *53*, 2118–2132. [[CrossRef](#)] [[PubMed](#)]
183. Blumen, H.; Fitch, K.; Polkus, V. Comparison of Treatment Costs for Breast Cancer, by Tumor Stage and Type of Service. *Am. Health Drug Benefits* **2016**, *9*, 23–32. [[PubMed](#)]
184. Vivot, A.; Jacot, J.; Zeitoun, J.D.; Ravaud, P.; Crequit, P.; Porcher, R. Clinical benefit, price and approval characteristics of FDA-approved new drugs for treating advanced solid cancer, 2000–2015. *Ann. Oncol.* **2017**, *28*, 1111–1116. [[CrossRef](#)] [[PubMed](#)]
185. Prasad, V.; De Jesus, K.; Mailankody, S. The high price of anticancer drugs: Origins, implications, barriers, solutions. *Nat. Rev. Clin. Oncol.* **2017**, *14*, 381–390. [[CrossRef](#)]
186. Roussakow, S.V. Clinical and economic evaluation of modulated electrohyperthermia concurrent to dose-dense temozolomide 21/28 days regimen in the treatment of recurrent glioblastoma: A retrospective analysis of a two-centre German cohort trial with systematic comparison and effect-to-treatment analysis. *BMJ Open* **2017**, *7*, e017387. [[CrossRef](#)]

Initial publication

Impedance matching and its consequences for modulated electro-hyperthermia

Katja Mühlberg¹, Andras Szasz²

¹Chair of Fundamentals of Electrical Engineering, Technische Universität Dresden,
Dresden, Germany

²Biotechnics Department, St. Istvan University, Budaors, Hungary

Citation: Mühlberg K. (2021): Impedance matching and its consequences for modulated electro hyperthermia, initial publication: Oncothermia Journal 30: 83 – 104,
https://oncotherm.com/sites/oncotherm/files/2021-04/Muhlberg_Impedance_1.pdf

Abstract

This paper demonstrates an opportunity to assess the suitability of an adjustable passive impedance matching network. Various complex impedances shall be transformed to nominal fifty-ohm reference impedance at a given constant carrier frequency. The terminating impedance for optimal matching and gradual mismatching (different degrees of matching) were calculated using mathematics software MATLAB for a matching network's known parameter range. The chosen method, together with the cheap solution, presents a descriptive visualization of the matching network's working principle and resolution capacity. Therefore it can be used as a supporting opportunity for matching network optimization. This network is used for cancer treatment by modulated electro-hyperthermia (mEHT). The accurate matching allows the energy's dosing into the target, which is selected by the body's impedance heterogeneities. The immunogenic effects follow the well-selected energy absorption.

Introduction

Cancer is the number-one deadly disease for humans. Significant efforts and substantial resources are involved in solving this challenge worldwide. A broad spectrum of various approaches exists in treating malignant diseases. Among them, the most known, conventional treatments are surgery, chemotherapy, and radiotherapy [1]. Many additional therapies are emerging to increase the treatment efficacy, elongate survival, and significantly increase the quality of life (QoL) of the suffering patients. One of the complementary methods is hyperthermia, aiming to sensitize or even synergetically increase the conventional therapies' effect. Hyperthermia is usually an isothermal mass heating approach, with the intention of high-temperature activity as a condition to increase the efficacy of the conventional therapies. The majority of heating effects use electrodynamical actions in a non-ionizing regime, and many of them are active in the radiofrequency (RF) range. The technical challenge of these heating processes is optimizing the energy-absorption in depths, focus on the tumor without safety problems; avoid burns on the body's surface or hot-spots inside. In order to solve this problem, modulated electro-hyperthermia (mEHT, trade name oncothermia) was introduced. The mEHT method breaks with the isothermal concept and applies heterogenic selection, targets the malignant cells without direct heating of the tumor's entire mass.

However, this complex cellular manipulation with the applied electric field needs very necessary technical conditions. The crucial point is to direct the energy by impedance matching. In heterogenic heating, the temperature was the usual dose of energy-absorption. The measurability of temperature in the tumor causes many complications. In heterogenic selection, the tumor's temperature cannot be the control parameter; the target's energy absorption decides the dose [2]. The request of the preciosity needs a well-tuned energy-delivery, involving challenges in the technical realization. The objective in this article is to show some parameters of impedance matching in human cancer treatment.

Technical background

The electromagnetic RF energy is capacitively coupled to the body part, when the tumor is located, positioned that the RF-current flows through the cancerous lesion [3]. The carrier frequency is 13.56 MHz belonging to a radio band that is freely usable for industrial, scientific, and medical (ISM) purposes. The capacitive coupling carefully impedance matched, optimally using the minimal impedance by resonant arrangement. The RF-source is an E-class (switching-mode) amplifier [4]. The patient (which has only a capacitive component in the imaginary part of the impedance) becomes a part of the entire electrical network. Therefore, the patient is considered complex impedance due to the engineering convention being transformed to a $50\ \Omega$ reference impedance by using a passive matching network (tuner). The fixed carrier frequency allows the resonant impedance matching to the load, which is the targeted human tissue.

The system dimensions allow a near-field impedance matching [5]. When the medium impedance changes, a part of the propagated wave is reflected, which has to be minimized. Incoming and reflected waves interfere

and create standing waves that represent mismatching. In this case, the system does not completely transfer the available power to the load. However, for cancer patients' mEHT treatment, a continuous and maximum possible power transmission is indispensable to ensure dosage assessment and control. A proper impedance transformer is required to counteract the mismatching that matches the load impedance to the reference impedance. Due to the switching mode resonant amplifier, the correct matching is also a strict request. The patient as the load can have widely different impedances depending on size, muscle and fat content, body hair, origin, treatment location etc., so that a variable impedance transformer with a large latitude of adjustment is necessary. The impedance change during the treatment also could be large enough to correct the matching. The impedance transformer/tuner in mEHT exists and shall be examined for its applicable bandwidth of a broad range of patient impedances. The matching of patient impedances appears as a special challenge; even impedance matching, in general, is a much-discussed topic [6], [7]. However, most of the precise matching fit the fixed antennas, allowing a constant tuning to unchanged impedance. While the patient impedances are multifarious by patients and by treatments, the tuner has to work over a wide range of load parameters.

The compensation of an imaginary part and transforming of a real part to a 50Ω reference impedance requires two independent adjustable tuner parameters. The impedance matching during the treatment has to be made dynamically due to constantly changing patient impedances caused by respiration and other physiological changes, including the tumor's change. Therefore, perfect matching cannot be achieved, the tuner has to follow the rough changes and the matching regulation follows a fuzzy logic. In the course of this for the given patient impedance, different tuner parameters constellations can lead to the same degree of matching that is here called as a problem of an ambiguous assignment. This additionally exacerbates the controlling of the tuner. The tuner's optimal matching means that it compensates the impedance of the load (\underline{Z}_{Load}) with its impedance regulated (\underline{Z}_{Tuner}) impedance, having the \underline{Z}_0 reference without imaginary part, Figure 1. [8].

$$\underline{Z}_{Tr} = \underline{Z}_{Tuner} + \underline{Z}_{Load} = \underline{Z}_0 \quad (1)$$

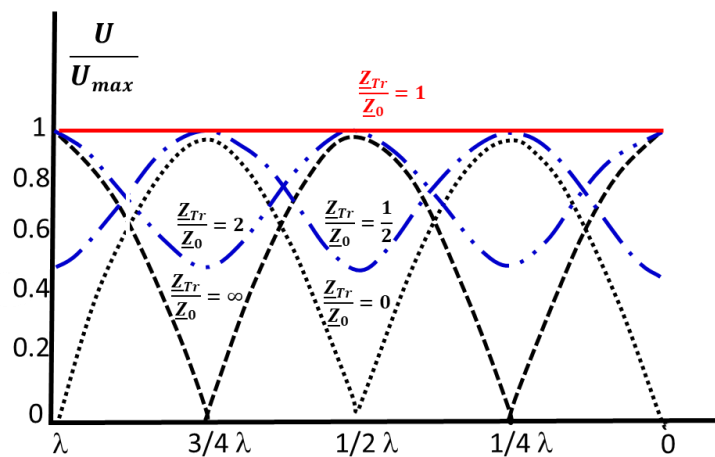


Figure 1. Distribution of the voltage amplitude along the wire versus the matching resistor {Standing Wave Ratio, SWR}, [8]

This paper shows the possible load (patient) impedances for different degrees of matching that were calculated by mathematics software MATLAB [9] with the aid of circuit simulation program "Serenade" [10] for a given adjustable tuner with known parameters range and a constant carrier frequency of 13.56 MHz. The operating principle, together with the resolution of the tuner and the load impedances, in synchrony with their best possible degree of matching, are visualized graphically. Furthermore, the problem of ambiguous assignment of tuner parameter constellations and degree of matching is presented.

The mathematical evaluation of adjustable tuner suitability is a well-illustrative method beneficial for fault finding and optimization of the tuner.

General challenge

Reflections are the consequence of medium impedance changing and can be suppressed by matching each other's impedances. Within an RF circuit, impedance matching has to be considered – generally between source, load, and transmission line. Therefore the common reference impedance \underline{Z}_0 of usual 50 Ω ~~ohm~~ has become established [11] that facilitates the matching by constructing sources and transmission lines with impedance \underline{Z}_0 . The reference impedance is also referred to as a line, nominal and reference impedance. In the calculation, the E-class resonant RF-source is also fixed to 50 Ω nominal reference impedance. Figure 2 shows the basic circuit setup for mEHT treatment where the reference impedance is 50 Ω , and the generator delivers the entire power if 50 Ω transformed load impedance \underline{Z}_{Tr} are connected. The following considerations assume stable reference impedance and carrier frequency.

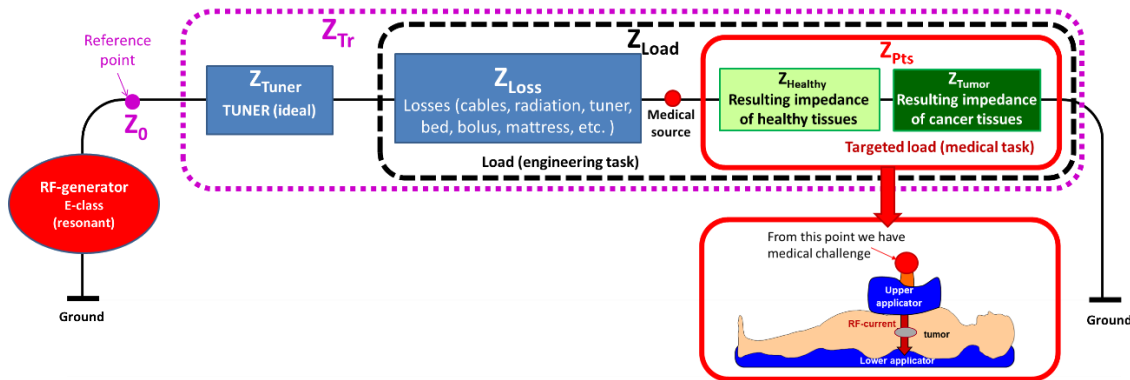


Figure 2. Circuit setup. \underline{Z}_0 reference impedance, \underline{Z}_{Load} load impedance, \underline{Z}_{Tr} transformed load impedance. $\underline{Z}_{Tr} = \underline{Z}_{Tuner} + \underline{Z}_{Load}$; $\underline{Z}_{Load} = \underline{Z}_{Loss} + \underline{Z}_{Pts}$; $\underline{Z}_{Pts} = \underline{Z}_{Healthy} + \underline{Z}_{Tumor}$

The tuner has a grounding shortcut, so its impedance and the impedance of the complete load is transformed to a parallel \leftrightarrow serial transition. The notes \underline{Z}_{Tuner} and \underline{Z}_{Load} are the transformed impedances.

In complete tuning satisfies:

$$\underline{Z}_{Tr} = \underline{Z}_{Tuner} + \underline{Z}_{Loss} + \underline{Z}_{Healthy} + \underline{Z}_{Tumor} = \underline{Z}_0 \quad (2)$$

This simply summation works only when the tumor-size corresponds with the electrode size. When it is not the case, the ratio of the $R_{Pts} = \underline{Z}_{Healthy}/\underline{Z}_{Tumor}$ modifies the simple addition. Presently we assume that $R_{Pts} \cong 1$.

This is the engineering task, the reference point, and the nominal \underline{Z}_0 reference impedance is to solve the complete tuning, make the engineering task of matching perfectly. The medical task is more complex than the tuning of the hardware; that is, targeting the tumor in depth. The request from the equipment to treat patients is to have perfect tuning (maximize the effect of the RF-generator) and minimize the hardware losses $\underline{Z}_{Tuner} + \underline{Z}_{Loss}$. When the technical request is fulfilled, the task is focused on the patient's net energy source ("medical source"). Consequently, the medical task starts at the applicator on the patient, and the medical challenge is concentrating on the \underline{Z}_{Tumor} .

Technical challenge

The occurring wave reflection due to mismatching can be quantified by complex reflection coefficient Γ .

$$\Gamma = \frac{Z_{Tr} - Z_0}{Z_{Tr} + Z_0} \quad (3)$$

Its absolute value can lie between 0 and 1, where 0 means perfect matching. In the case of reflection incident and reflected wave interfere and create standing waves. The voltage standing wave ratio $VSWR$ describes the ratio between the maximum and minimum voltage of standing voltage wave. It can also be calculated using the reflection coefficient.

$$VSWR = \frac{1 + |\Gamma|}{1 - |\Gamma|} \quad (4)$$

$VSWR$ attains values of 1 and higher where 1.0 corresponds to perfect matching. The amount of power loss caused by reflections is expressed by return loss RL that describes the ratio between incident P_i and reflected power P_r and can also be gained from $VSWR$.

$$RL = 10 \log_{10} \left(\frac{P_i}{P_r} \right) \quad (5)$$

$$RL = -20 \log_{10} \left(\frac{VSWR - 1}{VSWR + 1} \right) \quad (6)$$

By equating formula (5) and (6), the ratio between reflected and incident power can be calculated:

$$\frac{P_r}{P_i} = \left(\frac{VSWR - 1}{VSWR + 1} \right)^2 = |\Gamma|^2 \quad (7)$$

An example: let us calculate when the reference impedance $Z_0 = 50 \Omega$ and load impedance is transformed to $Z_{Tr} = (60 - j10) \Omega$. In this case, we receive the reflected power of about 1.6 %, taking the reflection coefficient from (3) and the subsequent ratio between reflected and incident power from (7). The task is to minimize $|\Gamma|$ and the $VSWR$.

The transformation of complex load/patient impedance requires two independent adjustable tuner parameters C_1 and C_2 . The transformed load impedance Z_{Tr} depends therefore on three parameters – the two tuner parameters and the load. The reference impedance of $Z_0 = 50 \Omega$ together with Z_{Tr} determine the $VSWR$ value. The relations in general:

$$Z_{Tr} = f(Z_0, VSWR) \quad (8)$$

$$Z_{Tr} = f(Z_{Load}, C_1, C_2) \leftrightarrow Z_{Load} = f(Z_{Tr}, C_1, C_2) \quad (9)$$

From (3) and (4) the perfect matching ($VSWR = 1.0$) can only be achieved if Z_{Tr} equals Z_0 . Every possible constellation of tuner parameters and deduced Z_{Tr} can be calculated in the perfect matching. However, in mismatching ($VSWR > 1.0$) the calculation of load impedance becomes more complicated. Like (4) shows, only the absolute value of the reflection coefficient ($|\Gamma|$) is of interest to calculate the $VSWR$. The challenge happen realizing that the different Z_{Tr} values can cause the same $|\Gamma|$. Therefore it is not possible to calculate the transformed load impedance Z_{Tr} in case of $VSWR > 1.0$. The relation between $VSWR$ value and transformed load impedance Z_{Tr} forms ring structures (Fig. 3.), allow the arbitrary direction of Z_{Tr} vectors keeping the absolute value ($Z_{Tr} = Z_0 + Z_r$) where $|Z_r|$ is the radius of the circles in Fig. 3. determined by a constant $VSWR > 1.0$.

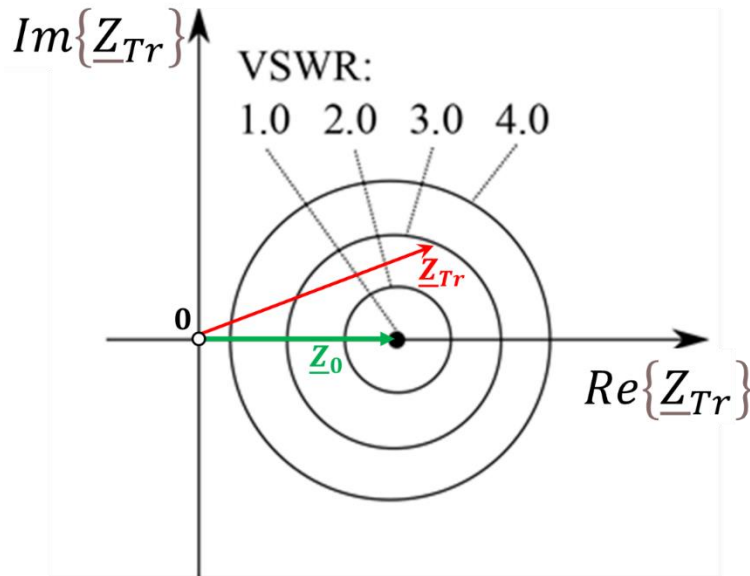


Figure 3. The relation between VSWR and transformed load impedance \underline{Z}_{Tr} . The actually shown transformed load is realized at VSWR = 3.

The middle point on Fig. 3. shows the clear assignment between \underline{Z}_{Tr} and VSWR values when $VSWR \equiv 1.0$. For $VSWR > 1.0$ the $|\underline{Z}_{Tr}|$ has to be determined first. The tuning challenge is huge due to the $Im\{\underline{Z}_{Tr}\}$ could be extremely large, while the shrinking real-part tends to $\underline{Z}_{Tr} = \underline{Z}_0$, when $Im\{\underline{Z}_{Tr}\} = 0$. Consequently, the load impedance in the circle has to be calculated for every constellation of tuner parameters. Note that \underline{Z}_{Tr} values are in pairs of positive or negative admittance at the same $|\underline{Z}_{Tr}|$. Introducing the parameter $VSWR_{x_circ}$ describes the circle function on the corresponding set of impedances \underline{Z}_{Tr} causing a VSWR of value x . In contrast to that $VSWR_{x_area}$ characterizes that area that includes all load impedances \underline{Z}_{Load} which can be transformed to a minimal VSWR of value x (best possible, optimal matching).

Based on the ultimate trans-match model [12], the tuner circuit could be realized like it is a circuit shown in Fig. 4. The L is the constant coil inductivity and C_1 and C_2 are adjustable rotary capacitors. Capacity C_1 consists of two identical condensers controlled symmetrically, while C_2 is independent. Consequently, two separate parameters define the tuning by individual control of the two capacitive components. In calculation, we use a resolution of 100 steps for each. The existence of the two parameters corresponds to the real and imaginary parts of the matching. The number of the parameters defines the angle of \underline{Z}_{Tr} by the vector components in the circle of radius $|\underline{Z}_{Tr}|$ when $VSWR > 1.0$.

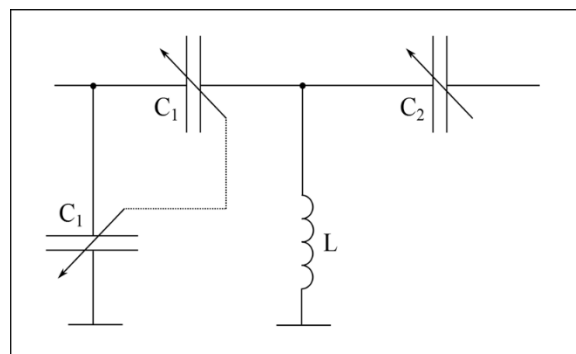


Figure 4. Tuner circuit with adjustable capacitors C_1 and C_2 and constant coil inductivity L .

The transformed load impedance \underline{Z}_{Tr} can be calculated using figures 2 and 4. Thus the load impedance \underline{Z}_{Load} at constant carrier frequency f_c is

$$\underline{Z}_{Load} = \frac{1}{\frac{1}{\frac{1}{\underline{Z}_{Tr}} - j\omega C_1} - \frac{1}{j\omega L}} - \frac{1}{j\omega C_2} \quad (10)$$

where

$$\omega = 2\pi f_c \quad (11)$$

First, the transformed load impedances \underline{Z}_{Tr} for the specified $VSWR$ value has to be found. In full matching $\underline{Z}_{Tr} = \underline{Z}_0$. Consequently, when the system is well-tuned ($VSWR = 1.0$; $\underline{Z}_{Tr} = \underline{Z}_0$), the load can be calculated:

$$\underline{Z}_{Load} = \frac{\frac{j\omega L C_1 \underline{Z}_0}{C_2} + \frac{2\underline{Z}_0}{j\omega C_1} + j\omega 2\underline{Z}_0 L - \frac{L}{C_2} + \frac{1}{\omega^2 C_1 C_2} - \frac{L}{C_1}}{j\omega L + \frac{1}{j\omega C_1} + \omega^2 \underline{Z}_0 L C_1 - 2\underline{Z}_0} \quad (12)$$

(Conventionally $\underline{Z}_0 = 50 \Omega$, so we use this value for model-calculations.)

After that, all load impedances for all constellations of tuner parameters C_1 , C_2 and equally distributed and quantitatively satisfactory \underline{Z}_{Tr} on the $VSWR_{x,circ}$ the circle can be calculated. The result of that depends on the amount of \underline{Z}_{Tr} points numerous single impedance areas (for each \underline{Z}_{Tr} point one area) that are overlapping and evolve the entire area – the $VSWR_{x,area}$. From the gathered impedance points extracted from the border of $VSWR_{x,area}$. The density of impedance points in the area gives information about the resolution of the tuner and with known C_1 , C_2 and L values for a specific \underline{Z}_{Tr} the operating principle of the tuner can be comprehended. This information is also used to visualize the ambiguous assignment of tuner parameter constellations and the degree of matching.

With the aid of the circuit simulation program “Serenade” the $VSWR_{x,circ}$ functions were interpolated. The tuner circuit shown in figure 4 and complex load impedance were implemented, and the reference impedance of 50Ω and the carrier frequency of 13.56 MHz defined. Furthermore the constants and adjustable parameters with their ranges in the tuner were set. For six different complex user-defined load impedances \underline{Z}_{Load} and the determined goal $VSWR$ value the C_1 , C_2 constellations were simulated. For each gathered \underline{Z}_{Load} , C_1 , C_2 constellation the transformed load impedance \underline{Z}_{Tr} was calculated. All six single simulations had the same goal $VSWR$ of value x so that the resulting \underline{Z}_{Tr} points drawn in complex plane lay on the $VSWR_{x,circ}$ circle. By method of least squares using Gauss-Newton algorithm, the circle was interpolated and its function with radius r , real axis shift m_1 and imaginary axis shift m_2 be extracted.

$$r^2 = (x - m_1)^2 + (y - m_2)^2 \quad (13)$$

The circle function can also be expressed by polar coordinates where φ describes the angle between \underline{Z}_{Tr} impedance vector and real axis counterclockwise.

$$x = m_1 + r \cdot \cos \varphi \quad (14)$$

$$y = m_2 + r \cdot \sin \varphi$$

In 3.6° steps, the coordinates of 100 equally distributed and quantitatively satisfactory \underline{Z}_{Tr} points per circle were obtained. The number of \underline{Z}_{Tr} points is freely selectable, whereby a higher number of points provides a finer border of the calculated entire impedance area.

In ideal conditions the $VSWR = 1$, and the possible \underline{Z}_{Load} impedances have a large set of values. For perfect matching \underline{Z}_{Tr} has to equal \underline{Z}_0 that is assumed to be constant 50Ω . Therefore the load impedance is \underline{Z}_{Load} . It depends only on the two adjustable capacitors C_1 and C_2 : $\underline{Z}_{Load} = f(C_1, C_2)$. For 100 C_1 and 100 C_2 values the load impedances \underline{Z}_{Load} can attain 10000 impedance points shown in a complex plane below. The different adjusting of tuner capacitors and their resulting changing of load impedance \underline{Z}_{Load} is marked Fig. 5. This means that all of these loads could be ideally matched with $VSWR_{1.0,area}$.

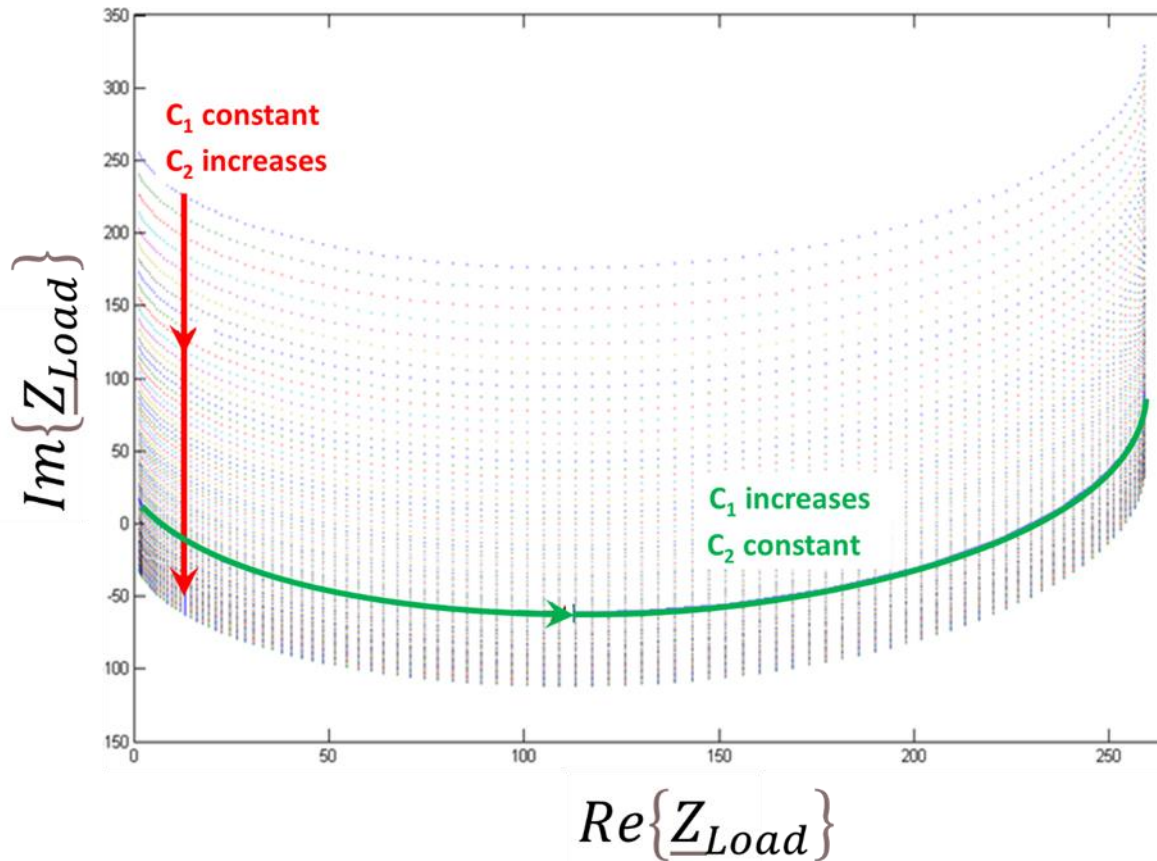


Fig. 5. The complex \underline{Z}_{Load} at $VSWR_{1.0,area}$. The load impedance \underline{Z}_{Load} depends on the transformed load impedance \underline{Z}_{Tr} and the two adjustable capacitors C_1 and C_2 : $\underline{Z}_{Load} = f(\underline{Z}_{Tr}, C_1, C_2)$.

When $VSWR > 1$, then the reference points form a circle in the actual calculation as expected by Figure 3. For a defined step size of φ the x and y values (resistances and reactances) of reference points could be generated (Figure 6.). Subsequently, their impedance areas are calculated. The contour points were detected and collected. The last step was evaluating the contour of the single contour points representing the border of the specified VSWR area.

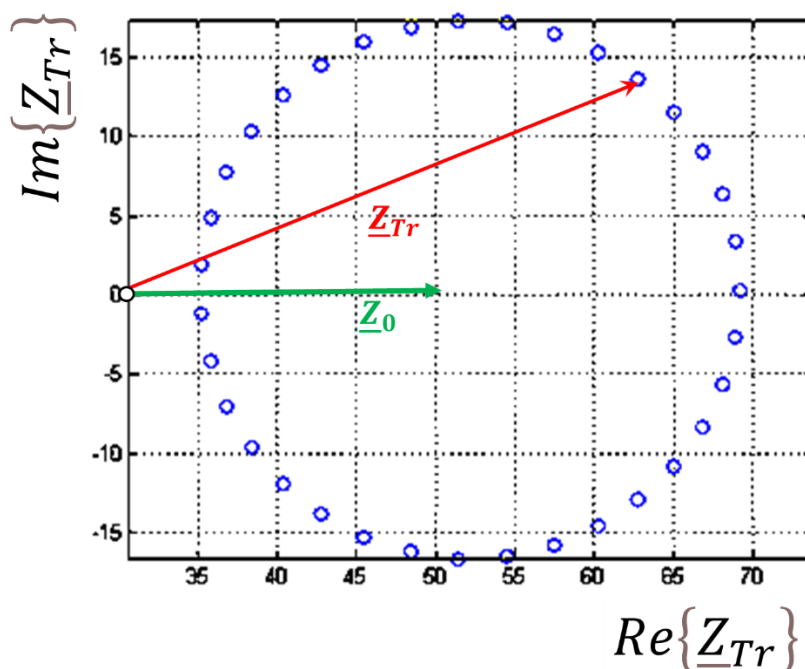


Figure 6. 36 reference points for $VSWR = 1.4$. An arbitrary \underline{Z}_{Tr} is shown.

For suboptimal degrees of matching like $VSWR = 1.4$, the load impedance \underline{Z}_{Load} depends not only on the capacitor values C_1 and C_2 but also on the transformed load impedance \underline{Z}_{Tr} , $\underline{Z}_{Load} = f(\underline{Z}_{Tr}, C_1, C_2)$ (Figure 7.). The transformed load impedance \underline{Z}_{Tr} can actually attain infinite values laying on an impedance circle corresponding to the specified VSWR value. Therefore infinite single load impedance areas result.

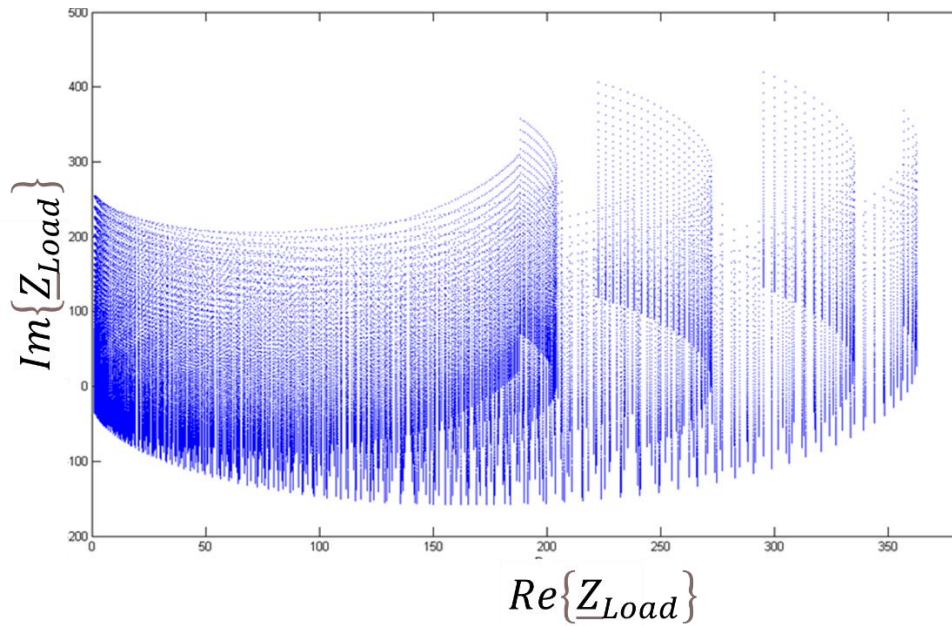


Figure 7. The $VSWR_{1.4_area}$ no perfect matching Every tenth single area from 100 calculated. Every single load impedance area was calculated for 10000 different C_1, C_2 constellations.

The single impedance areas create an entire impedance area that border was detected for the specified VSWR value in Figure 8.

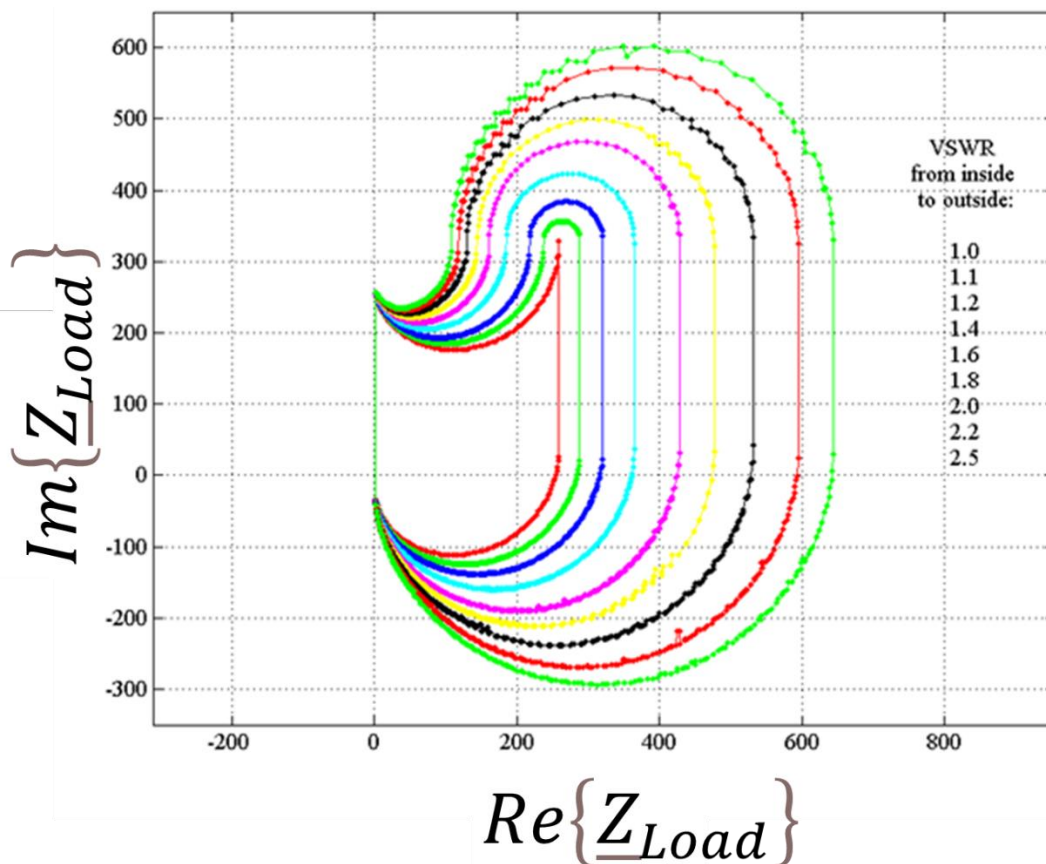


Figure 8. The borders of entire load impedance areas for chosen VSWR values.

The calculated impedance area for perfect matching from figure 5 is related to capacitor values C_1 and C_2 . In this case the single impedance area corresponds to the entire impedance area because the transformed impedance load \underline{Z}_{Tr} has to equal the reference impedance of constant 50Ω , Figure 9.

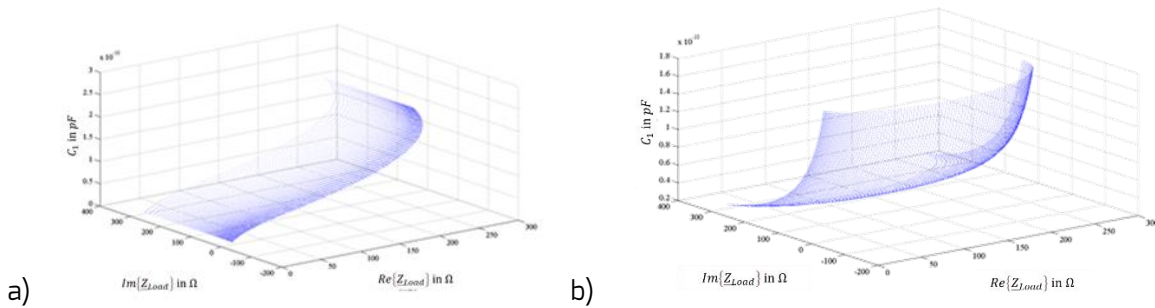


Figure 9. C_1 and C_2 dependence on $VSWR_{1.0_area}$.

The calculated single impedance areas from figure 7 are shown with their related C_1 and C_2 values. However, the load impedances not only depend on the adjustable capacitor values C_1 , C_2 but also on the transformed load impedance \underline{Z}_{Tr} . The overlapping single impedance areas plotted above form a volume, implying that the same load impedance \underline{Z}_{Load} can be tuned to a specified VSWR value greater than one by different C_1 , C_2 constellations Figure 10.

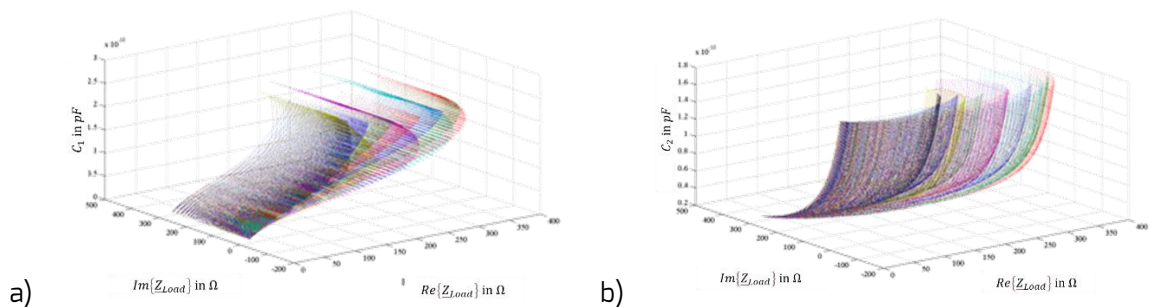


Figure 10. C_1 and C_2 dependence on $VSWR_{1.4_area}$.

The different density of load impedance points in figure 5 delivers two statements. The first is that the tuner sensitivity is different within the impedance area. Load impedances within this area with very low or high real part or low imaginary part can be tuned finer in general than impedances with the high imaginary part. This leads to the second statement that an extension of tuner parameter range has only effect graphically seen for the upper border of impedance area by adding lower C_2 values. In contrast to that, all other possible range extensions of C_1 and C_2 do not enlarge the area due to the increasing density of points towards the borders. If a higher resolution within the impedance area for perfect matching is desired the C_1 and C_2 steps have to be minimized.

As expected does a lower degree of matching results in a larger load impedance area indicated by figure 7. However, the area extension is not symmetrical in all directions that, due to non-existing impedances with the negative real part, is comprehensible. Partly an overlapping of single impedance areas is shown that indicates that two possible C_1 , C_2 constellations for one load impedance \underline{Z}_{Load} lead to the same transformed load impedance \underline{Z}_{Tr} .

The plotted borders for chosen $VSWR_{x_area}$ in figure 8. show, that generally, load impedances with high real and low absolute imaginary part are more straightforward to match than those with low real part and high absolute imaginary part.

Considering the problem of ambiguous assignment of tuner parameters and degree of matching so can be said that for a perfect matching in figure 9 every load impedance in this area has exactly one C_1, C_2 constellation and unique assignment prevail. In contrast to that figure 10 shows the C_1 and C_2 dependence for a worse degree of matching. A specified load impedance in the $VSWR_{>1.0_area}$ area can be transformed by different C_1, C_2 constellations and the assignment is not unique anymore. For worse degrees of matching this problem intensifies. The problem can be seen from another direction. For a measured $VSWR$ value and known C_1, C_2 values obtained from step motors positions the load impedance Z_{Load} cannot be determined that exacerbates the controlling of the tuner. It shall be pointed out again that all considerations suppose stable reference impedance and carrier frequency.

Technically essential to solving that the Z_{Tuner} is minimal when matches the Z_{Load} to the Z_0 reference. Other technical challenges are connected to the minimalization of the Z_{Loss}

Medical challenge

The complex medical task starts at the applicators, which are included in the medical task as an important energy transmitter, constructed for human physiology, ergonomy, and medical practice, see Fig. 11. On the other hand, the applicator has technical tasks also. The impedance matching sharply depends on how the transmitting electrodes are connected to the human body.

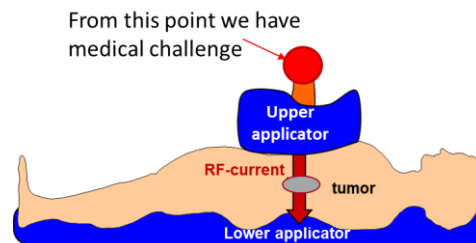


Figure 11. The RF-current flows through the body. The medical challenge starts at the applicators.

Important behavior of the applicators is the perfect shape adaptation avoiding the high impedance of the transmission. The carefully selected materials and structure of the applicators minimize the losses. The broad range of electromagnetic heterogeneity of the body is the next barrier Fig. 12. The only easing of the challenge is the missing inductive factor in the body, so the impedance of tissues has only negative reactance.

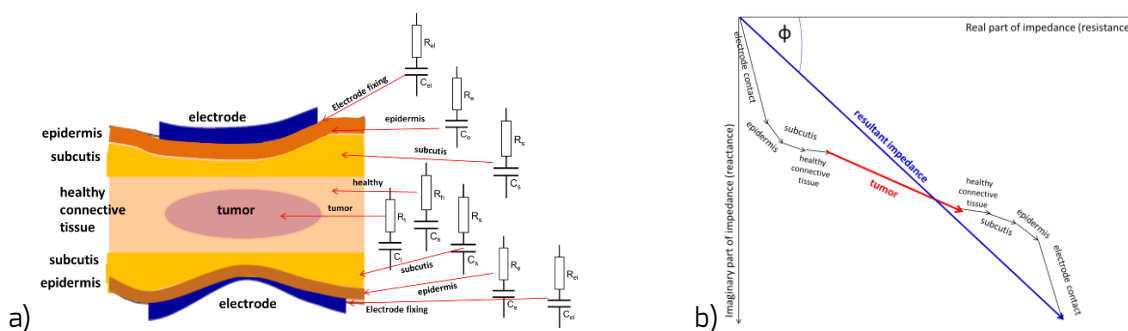


Fig. 12. The main, macroscopic electromagnetic heterogeneities of the body. (a) The layer structure (the essential micro-heterogeneities of the various tissues are not shown.) (b) The resultant impedance vector (Only some macro-heterogeneities are shown for clarity.)

However, in capacitive coupling on a larger volume (like belly, chest), Eddy-current could generate a slight induction, as shown in Figure 13.

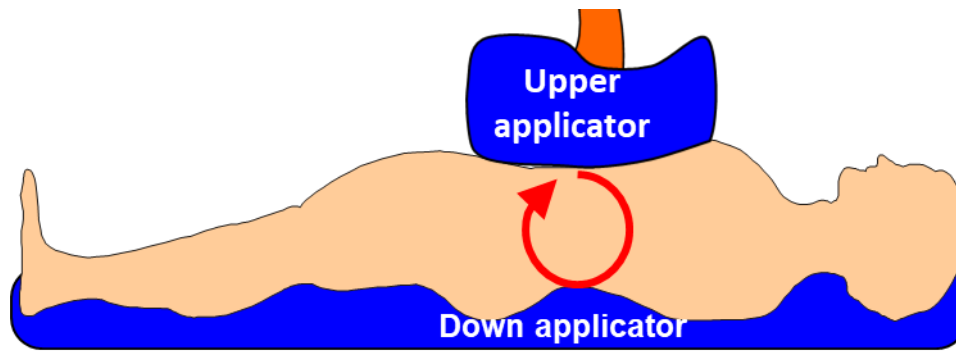
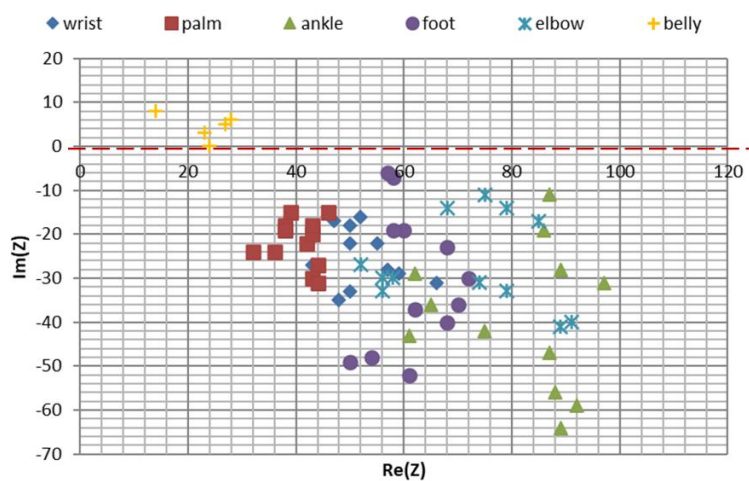


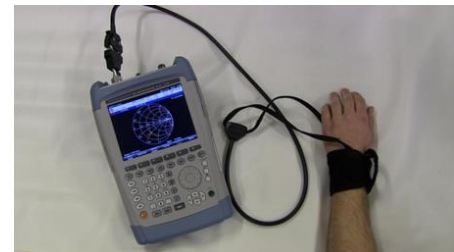
Figure 13. The induced Eddy current in a large part of the body by RF capacitive coupling. (It depends, of course, on the frequency, the current conduction, and sizes of the body-part.

Measurements in various healthy human volunteers show this tendency in Figure 14. The possible Eddy current inductivity in the belly significantly differs from other body-parts.

a)



b)



c)

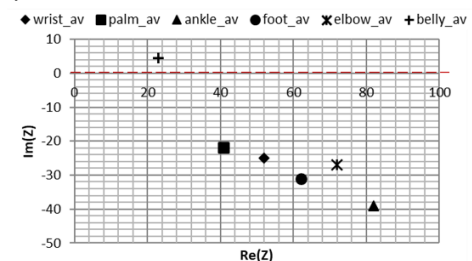


Figure 14. Impedance measurements on human volunteers with capacitively coupled different plan-parallel electrode sizes fit the size of the body-part. (a) the results depend on the person. (b) example of the wrist measurement. (c) The black markers show the averages.

The technical solution has to serve the medical task to provide optimal energy in the tumor considering the broad range of the individual variation of the impedances. This task is a considerable challenge that needs technical and physiological, biophysical, and medical considerations. The solution could be the mEHT, which is designed to handle all the demanding details.

The mEHT method is one part of the cancer therapies. The treatment goal is to deliver energy absorbed at the tumor-cells and start the antitumor-effect by eliminating the selected cells and liberating their genetic information to form an antigen-presenting process developing a tumor-specific immune-reaction by in-situ effects, without ex-body laboratory manipulation [13].

The massive micro and macro heterogeneity of the living tissues block the isothermal heating, but it allows the selection. The selection uses the bioelectromagnetic, thermal, and structural peculiarities of the malignant cells and their microenvironment (mE) [14]. The guiding selection factor are the impedance differences between the malignant and healthy cells [15]. The real part of the impedance is strongly influenced by the cells' ionic content and their mE. The malignant cells mostly metabolize much more intensively, which is measurable by positron emission tomography (PET). This shows the extreme glucose demand of the tumor, producing ATP in a

fermentative way. This mode of ATP production is speedy and straightforward but considerably less effective than the standard Krebs-cycle in mitochondria [16]. The mitochondria function is suppressed, and it is stated as the primary cause of cancer [17]. Due to their huge energy-demand for cellular reproduction, so the ionic component around them well differs from their host. The imaginary part of the mE is determined by the missing (or damaged) networking of malignant cells. The cancer cells are mostly autonomous. They are individual, separated “fighters” for the energy to survive. This autonomy changes their mE, the missing cellular connections, and the disordered structure of aqueous electrolyte around them will increase the relative dielectric constant (ϵ_r) of the mE region. The disorder is mE “dismantles of multicellularity” [18]. The impedance drastically changes by the higher conductivity and higher dielectric constant than standard. The two effects support each other [19], and RF current flow recognizes it due to the noticeable changes.

The application of bioelectromagnetic differentiation in biological tissues attracts the attention of researchers [20]. Various publications show considerable differences between the impedance parameters of malignant tissues from their healthy hosts. The current density image by MRI (RF-CDI) well visualizes the increase of the RF-current density in tumors [21]. The in vivo measurements show that the necrotic cell-destruction approx. linearly depends on the conductivity in the range of 10 Hz – 1 MHz [22]. (24 tumors of the *K12/TRb* rat colon cancer.) The conductivity of *VX-2* carcinoma and normal rabbit liver tissues ex-vivo also shows the differences [23]. The impedance variation shows good resolution of tumor-in the mice by control comparison with MRI [24]. In human measurements with coaxial line sensor, the heterogeneity well proven in ductal and lobular tumors compare them to the surrounding tissues in 0.02 – 100 MHz range [25]. The breast tissues were very intensively examined to replace the ionizing radiation in mammography with more safe electromagnetic tomography [26], [27]. The water content of the tissue also has considerable addition to the electric behavior of tumor [28]; which makes extra selection factor due to the water content is significantly higher in the tumor than its host. Furthermore, the extracellular fluids in mE form bound water, which has larger values of σ and ϵ than free water. Pleasant help, that the Debye model comparable with the measurements [29], and when it modified, the similar Cole-Cole model describes the situation [30]:

$$\begin{array}{ll} \text{Debye:} & \epsilon^*(\omega) = \epsilon_\infty + \frac{\epsilon_s - \epsilon_\infty}{1 + i\omega\tau} \\ \text{Cole-Cole:} & \epsilon^*(\omega) = \epsilon_\infty + \frac{\epsilon_s - \epsilon_\infty}{(1 + i\omega\tau)^{1-\alpha}} \end{array} \quad (15)$$

The Cole-Cole model well approximates the heterogenic changes like organelles, cellular edemas, ischemic tissues, gap-junctions, etc. [31] by deformation of the clear semicircular shape. The Cole-Cole formulation well demonstrates the importance of the electromagnetic heterogeneities in the target [32]. The conduction differences in the micro-range also used against pathogens in food-processing [33]. For example, the frequency dependence of energy absorption by insects used against rice weevil [34].

The heterogeneity affects the relaxational processes in a broad spectrum of frequencies [35]. However, the frequency dispersion modifies different parts of the tissue and cells, and gives a possibility for further selection by low frequency (α – *dispersion*), radio frequency (β & δ – *dispersions*), and microwave frequency (γ – *dispersion*) processes [36]. The usefulness of the 13.56 MHz is not only because it is a part of the medically allowed ISM frequencies, but also because its geometrical selectivity [37], as well as its special position in the boundary of the β & δ – *dispersions*.

The β – *dispersion* targets the membrane-electrolyte structures of cells, performing Maxwell-Wagner relaxation [38]. The interfacial polarization of the cell membranes [39], consequently, the charge distribution at the cellular of interfacial boundaries [40] play a central role in the process. The charge buildup causes the characteristic variation of the β – *dispersion* [41]. A transition occurs from α – *dispersion* to β – *dispersion* in ex-vivo haddock muscle [42] a few hours after its removal from the fish. It was increased in the same period of time, according to The different tissue decomposition process mechanisms causing the change in this frequency range. The upper-frequency boundary of β – *dispersion* has additional peculiarity usually noted as β_1 –

dispersion. The torque of biological macromolecules caused by the proteins keeping their orientation against the disordering electromagnetic effects form large dipole moments, which do not follow the high-frequency changes [43]. The vast heterogeneity of the biological tissues causes multiple effects on the excited molecules, like the conformational change of the polymers [44], the macromolecular relaxation interaction with the ionic effect in the vicinity of them [45].

The δ – *dispersion* is just overlapping the high-frequency end of the β – *dispersion* [46]. The dipolar moments of proteins and other large molecules (like cellular organelles, biopolymers) distinguish this frequency interval [47]. It is a second Maxwell-Wagner dispersion (δ) act on suspended particles, diffusion of charged molecules surrounded by a cell [48], near membrane bounds completed with protein-bound water, and cell organelles such as mitochondria [49], [50]. Electromagnetic selection of the malignant cells guides the energy delivery. The β/δ – *dispersion* of the carrier frequency allows to distinguish the variance of the impedance of these cells [51], orients the attack on the membrane reaction of the impedance selected cells [52], [53], primarily for the groups of transmembrane proteins [54], [55], [56]. The 13.56 MHz lies inside the β/δ – *dispersion*, so it offers a natural choice for medical electromagnetic applications [57]. The selection was shown on molecular levels, too [58], [59]. Importantly the bound water on the membranes and proteins also has a special absorption increase in the 10 MHz range [60]. The applied electromagnetic treatment synergically applies the field-effect together with the increased temperature by the absorbed energy [61], depending a lot of biophysical interactions in the microenvironment of the targeted cell [62]. The plasma membranes' heterogeneity has various origins, but the decisional is a mixture of transmembrane membrane proteins with membrane-lipids, forming clusters, called lipid rafts. Many molecular and physiological processes are determined by the heterogeneous lipid domains serving as molecular sorting platforms [63]. The malignant cells have a denser lipid-raft population on their membranes than their healthy counterparts [64]. Consequently, membrane heterogeneity has a crucial role in the selective energy-absorption of malignant cells - see Figure 15.

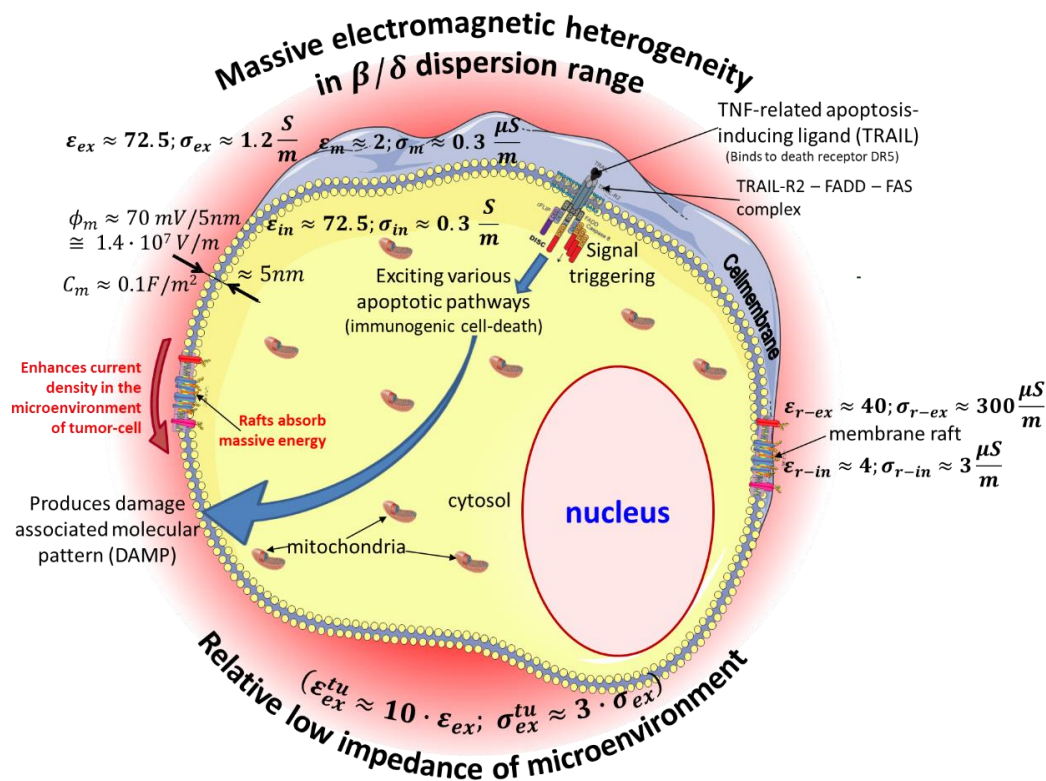


Figure 15. The electromagnetic heterogeneity of the selected tumor-cell as a target of the β/δ – *dispersion*. Abbreviations/references: ϵ_{ex} and σ_{ex} are the relative permittivity and conductivity of extracellular electrolyte in the microenvironment of a cell [65]; ϵ_{ex}^{tu} and σ_{ex}^{tu} are the relative permittivity and conductivity of extracellular electrolyte in the microenvironment of a tumor cell [27]; ϵ_m and σ_m are the relative permittivity and conductivity of the cell-membrane [66]; ϵ_{in} and σ_{in} are the relative

permittivity and conductivity of intracellular electrolyte of a cell [65]; ϵ_{r-in} and σ_{r-in} are the relative permittivity and conductivity of intracellular side of raft proteins [67],[68]; ϵ_{r-ex} and σ_{r-ex} are the relative permittivity and conductivity of extracellular side of raft proteins [69],[70]. The apoptotic way is shown by various publications [71], [72], [73].

The membrane structure may drastically change by variation of temperature producing a phase-transition of the configuration [74]. The membrane goes through a Gel/Sol transition from a denser to a more fluid state at a defined temperature. The rearranged packing of unsaturated phospholipids results from a higher fluidity [75]. The transition decision involves the lipid rafts [76]. Note that the well-known break on the Arrhenius plot [77] could be formed by phase transition [78].

The phase transition is not as simple in living conditions as happens in most non-living situations. The conditions of living reactions governed by various enzymes which catalyze and ease the transition, lowering the usual energy-gap between the reactants (A_1) and products (A_2). The transition-state theory involves quantum-mechanical considerations [79], [80], [81] to describe the excited enzymatic state (A^*), allowing tunneling to avoid the energy to jump through the high peak [82] (Figure 16.). The complex A^* state could have direct jump into final products A_2 with unidirectional transition probability k_3 . However, the complex A^* state is unstable in the backward direction with k_2 transition probability:



The enzymatic process has a “point of no return”, when the reversing of the transition became impossible. This interdisciplinary approach [83] explains the experiment-based classical Arrhenius law. In case of increasing temperature like hyperthermia requests it, this phase-transition process determines the structures [84], which were later verified independently, [85], [86].

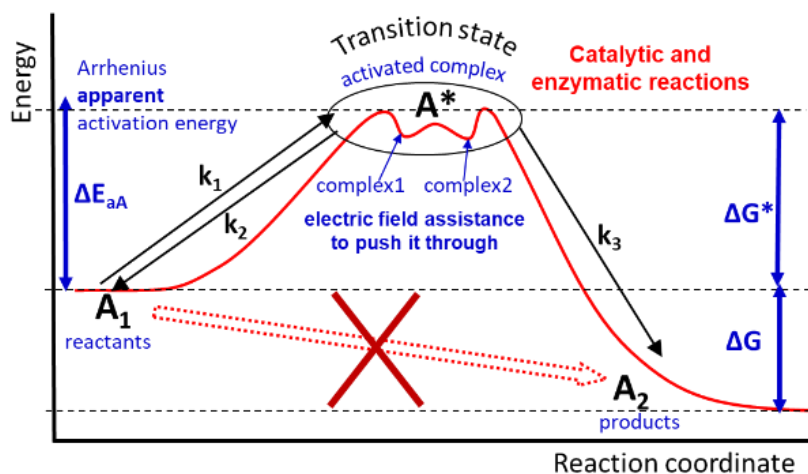


Figure 16. The direct transition between A_1 and A_2 is impossible due to the energy barrier. The height of the barrier was lowered by enzymes and also by the electric field-assisted transition. The A^* transition state is a complex molecular reaction, and the field pushes it to the point of no return to finish the transition process.

The transition state could be created by electromagnetic reactions (or its reaction complexes with molecules); the temperature effects have certain similarities with electric field action [87].

The main step of the energy targeting is the selective absorption on the transmembrane proteins, which is surrounded by the isolating lipid-bilayer of the membrane material [88]. The clustered transmembrane proteins (membrane rafts) absorb the energy, which is shown by model calculation too [89]. The malignant cells follow dominantly apoptotic way of death [90] in mEHT. The absorbed energy by transmembrane proteins ignites particular signal-pathways to promote the programmed cell-death (apoptosis) [91], which could happen with a

synergy of conventional chemotherapies [92]. Molecular investigation shows the significant difference between conventional heating and mEHT [93], [94]. The missing homeostatic harmony in cancer is also a selective factor. Modulation is applied to recognize the homeostasis spectrum, selecting the nonharmonic parts of the target [95]. The amplitude modulation (AM, < 20 kHz) of the RF carrier frequency intensifies the tumor-specific absorption [96]. Despite the small energy absorption [97], the membrane demodulates the signal and causes damages in the cytosol [98]. The complex action of mEHT well synergizes the “thermal” and “nonthermal” effects [99], with high selective preciosity [51]. The “gentle” elimination process allows liberating the genetic information of the malignant cells by developing damage-associated molecular pattern (DAMP) [100]. The energy absorption triggers immune effects by specific apoptosis, the immunogenic cell-death (ICD) [101], [102]. The transferred genetic info allows maturing antigen-presenting cells (APCs) to produce helper and killer T-cells for systemic antitumor effect on micro and macrometastases (abscopal effect) [13], [103]. In this way, the local treatment could be extended systematically to the entire body when the tumor-specific immune reaction develops, killing CD8+ T-cells prepared by the antigen information from cancer cells by ICD, [104], Fig. 17. The systemic (abscopal) effect is proven in preclinical [105], and in clinical applications [106]. This process well fits the trend of the development [107].

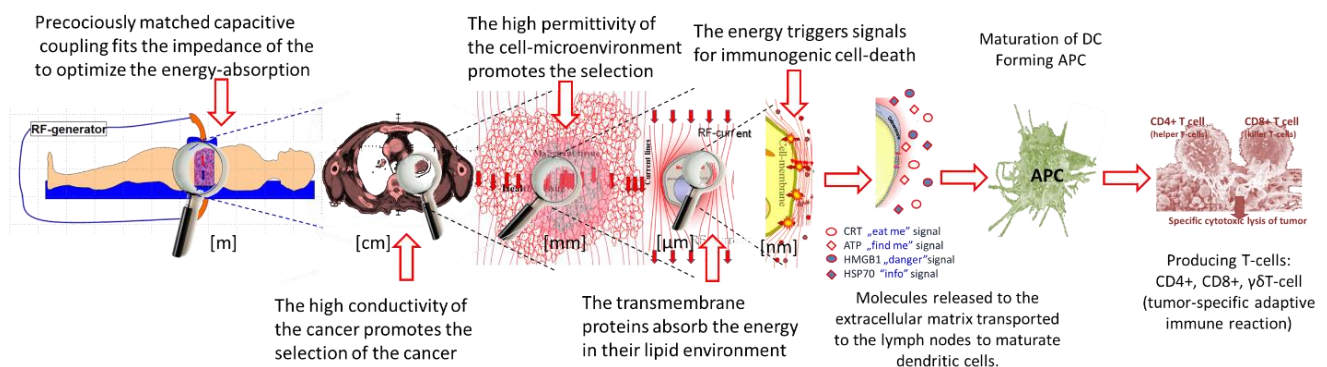


Fig. 17. The mEHT method has a series of effects. The first step is the accurate matching for energy-control, and then the impedance differences make the selection. The hyperthermic step happens when the membrane raft absorbs the energy. In consequence, a set of signals to death is triggered (immunogenic cell-death), which prepares antigen-presenting possibility, forming tumor-specific immune reaction.

Conclusion

The proper oncological hyperthermia needs high-preciosity matching and target-selected energy-absorption. Its resolution capacity, the load impedances for a given degree of matching, the effect of tuner parameter adjusting, and the problem of ambiguous assignment of tuner parameters and degree of matching were visualized. Thereby the conceivable extension of tuner parameter ranges and their optimization limits could be demonstrated. For further optimization of the tuner, the illustrated problem of ambiguous assignment could be used to improve the degree of matching during the tuning for known VSWR value and tuner parameters read off motors step positions. The modulated electro-hyperthermia (mEHT) is devoted to this particular task. The challenge involves an accurate matching to provide the energy from the source to the patient, allowing the conventional energy-dose, the same concept as the ionizing radiation applies. The uncontrolled energy loss makes the energy-based dosing of the treatment impossible. The adequately matched circuit promotes the selection mechanisms, and the energy is provided to the membrane rafts of the malignant cells causing immunogenic cell death. This type of cellular process gently liberates the genetic information of the malignant cells, which could be used for antigen presenting and promote building up a tumor-specific systemic immune reaction. This paper showed a beneficial opportunity to assess the suitability of a present adjustable passive impedance matching network in a mathematical way. Consequently, the proper matching optimized the electromagnetic effect on the selected cells and made possible the abscopal effect through the immune-modification.

References

- [1] Sebastian M., Ninan N., Elias E. (2012) Nanomedicine and Cancer Therapies. Apple Academic Press
- [2] Lee S-Y, Szigeti GP, Szasz AM. (2019) Oncological hyperthermia: The correct dosing in clinical applications, *Int. J. Oncology*, 54: 627-643
- [3] Szasz A., Szasz N., Szasz O. (2011) *Oncothermia: Principles and Practices*. Springer Verlag
- [4] Sokal NO. (2003) Class-E high-efficiency RF/microwave power amplifiers: Principles of operation, design procedures, and experimental verification, *Analog Circuit Design*, Springer, Boston MA, https://doi.org/10.1007/0-306-47950-8_14, pp. 269-301
- [5] Li R.C.H. (2012) *RF Circuit Design*, 2nd Edition. John Wiley & Sons, Hoboken, New Jersey
- [6] Misra K.M. (2004) *Radio - Frequency and Microwave Communication Circuits: Analysis and Design*, 2nd Edition. John Wiley & Sons, Hoboken, New Jersey
- [7] Davis W.A. (2011) *Radio Frequency Circuit Design*, 2nd Edition. John Wiley & Sons, Hoboken, New Jersey
- [8] Simonyi, K. (1965). *Theoretische Elektrotechnik*, VEB Verlag Berlin, 7th ed. 1979
- [9] MATLAB R2008b. The MathWorks. Computer software
- [10] Serenade v8.7. Ansoft Corporation. Computer software
- [11] Breed G. (2007) There's Nothing Magic About 50 Ohms. *High Frequency Electronics*, pp. 6–7, June 2007, Summit Technical Media LLC.
- [12] McCoy, Lewis G. (W1ICP) (July 1970). "Ultimate transmatch". *QST Magazine*. Newington, CT: American Radio Relay League. pp. 24–27, 58
- [13] Qin W, Akutsu Y, Andocs G, et al. (2014) Modulated electro-hyperthermia enhances dendritic cell therapy through an abscopal effect in mice. *Oncol Rep* 32(6):2373-2379, <http://www.ncbi.nlm.nih.gov/pubmed/25242303>
- [14] Hegyi G, Szigeti GP, Szasz A. (2013) Hyperthermia versus oncothermia: Cellular effects in complementary cancer therapy. *Evid Based Complement Alternat Med* 2013:672873
- [15] Szasz A. (2013) Challenges and Solutions in Oncological Hyperthermia. *Thermal Med* 29(1):1-23
- [16] Warburg O (1956) On the origin of cancer cells. *Science* 123(3191):309-314
- [17] Warburg O (1996) Oxygen, The Creator of Differentiation, *Biochemical Energetics*. Academic Press, New York In: Warburg O (1996) *The Prime Cause and Prevention of Cancer*. Revised lecture at the meeting of the Nobel-Laureates on June 30, 1966, Lindau, Lake Constance, Germany
- [18] Alfarouk KO, Shayoub MEA, Muddathir AK, Elhassan GO, Bashir AHH; (2011) Evolution of tumour metabolism might reflect carcinogenesis as a reverse evolution process (dismantling of multicellularity), *Cancers* 3:3002-3017
- [19] Szigeti GP, Szasz O, Hegyi G. (2017) Connections between Warburg's and Szentgyorgyi's Approach about the Causes of Cancer. *Journal of Neoplasms* 1(2:8):1-13
- [20] Grant JP; (1984), *Measurements, Medical Significance And Applications Of The Dielectric Properties Of Biological Materials*; PhD Thesis University of Surrey
- [21] Mikac U, Demsar F, Beravs K, Sersa I. (2001) Magnetic resonance imaging of alternating electric currents, *Magn Reason Imaging*, 19:845-856
- [22] Haemmerich D, Staelin ST, Tsai JZ, et al. (2003) In vivo electrical conductivity of hepatic tumors, *Physiol. Meas.* 24:251-260
- [23] Smith SR, Foster KR, Wolf GL, (1986) Dielectric Properties of VX-2 Carcinoma Versus Normal Liver Tissue, *IEEE Trans. On Biomed. Eng.*; BME-33:522525
- [24] Muftuler LT, Hamamura MJ, Birgul O, Nalcioglu O. (2006) In vivo MRI electrical impedance tomography (MERIT) of tumors, *Technol Cancer Res Treat.* 5:381-387
- [25] Surowiec AJ, Stuchly SS, Barr JR, Swarup A. (1988) Dielectric properties of breast carcinoma and the surrounding tissues, *IEEE Transactions on Biomedical Engineering*, 35(4):257-263
- [26] Chaudhary S, Mishra R, Swarup A, Thomas JM. (1984) Dielectric properties of normal and malignant human breast tissues at radiowave and microwave frequencies, *Indian J Biochem Biophys.* 21:76-79
- [27] Scholz B, Anderson R. (2000) On electrical impedance scanning – principles and simulations, *Electromedica Onco*, 68:35-44
- [28] Sha L, Ward ER, Story B. (2002) A Review of Dielectric Properties of Normal and Malignant Breast Tissue; *Proceedings IEEE Southeastcon*, pp.457-463, DOI: 10.1109/SECON.2002.995639
- [29] Chaudhary et. al, (1984) Dielectric properties of normal and malignant human breast tissues, *Indian J. Biochem. Biophys.*, 21:76-79

- [30] Cole KS, Cole RH. (1941) Dispersion and Absorption in Dielectrics I. Alternating Current Characteristics, *Journal of Chemical Physics*. 9:341–351
- [31] Ivorra A. (2002) Bioimpedance Monitoring for physicians:an overview, Centre Nacional de Microelectrònica Biomedical Applications Group, https://www.researchgate.net/publication/253563215_Bioimpedance_Monitoring_for_physicians_an_o_verview
- [32] Kalmykov YP; Coffey WT; Crothers DSF; Titov SV. (2004) Microscopic Models for Dielectric Relaxation in Disordered Systems, *Physical Review E*. 70:041103
- [33] Salengke S, Sastry SK. (2007) Experimental investigation of ohmic heating of solid–liquid mixtures under worst-case heating scenarios, *Journal of Food Engineering*, 83:324–336
- [34] Nelson SO, Charity LF. (1972) Frequency dependence of energy absorption by insects and grain in electric fields. *Transactions of the ASAE* 15:1099–1102
- [35] Schwan, H.P. Mechanism responsible for electrical properties of tissues and cell suspensions. *Med. Prog. Technol.* 1993, 19, 163–165
- [36] Nasir N, Al-Ahmad M, (2020) Cells Electrical Characterization: Dielectric Properties, Mixture, and Modeling Theories, *Hindawi Journal of Engineering*, Volume 2020, Article ID 9475490, 17 pages, <https://doi.org/10.1155/2020/9475490>
- [37] Stubbe M, Gimsa J, (2015) Maxwell's Mixing Equation Revisited: Characteristic Impedance Equations for Ellipsoidal Cells, *Biophysical Journal* 109:194–208
- [38] Cole, K.S. *Membranes, Ions and Impulses*; University of California Press: Berkeley, 1972
- [39] Anderson JC. (1964) *Dielectrics*, Chapman & Hall, London
- [40] Pethig RR. (1979) *Dielectric and Electronic Properties of Biological Materials*; Wiley
- [41] Schwan, HP. (1957) *Advances in Biological and Medical Physics*, 5:147
- [42] Martinsen Ø G, Grimnes S and Mirtaheri P (2000): Non-invasive measurements of post mortem changes in dielectric properties of haddock muscle - a pilot study. *J. Food Eng.* 43:189–192
- [43] Grant EH, Sheppard RJ, South SP. (1978) *Dielectric behavior of biological molecules in solution*; Clarendon Press, [https://doi.org/10.1016/0307-4412\(79\)90015-3](https://doi.org/10.1016/0307-4412(79)90015-3)
- [44] Schwarz G. Seelig J. (1968) Kinetic properties and the electric field effect of life helix-coil transition of poly(γ -benzyl L-glutamate) determined from dielectric relaxation measurements, *Biopolymers*, 6:1263, 1263–1277
- [45] Debye and Falkenhagen (1928) Dispersion of the conductivity and dielectric constants of strong electrolytes, *Phys. Z.* 29:121–401
- [46] Pethig RR, (2017) *Dielectrophoresis: Theory, Methodology and Biological Applications*, John Wiley & Sons, Hoboken, NJ, USA, 2017
- [47] Asami K, (2002) Characterization of biological cells by dielectric spectroscopy, *Journal of Non-crystalline Solids*, 305:268–277
- [48] Pauly, H.; Schwan, H.P. Über die Impedanz einer Suspension von Kugelförmigen Teilchen mit einer Schale. *Z. Naturforsch., B* 1959, 14B, 125–131
- [49] Stoy, R.D.; Foster, K.R.; Schwan, H.P. Dielectric properties of mammalian tissues from 0.1 to 100 MHz: a summary of recent data. *Phys. Med. Biol.* 1982, 27, 501–513
- [50] Gotz M, Karsch L, Pawelke J, (2017) A new model for volume recombination in plane-parallel chambers in pulsed fields of high dose-per-pulse, *Physics in Medicine & Biology*, 62:8634–8654
- [51] Szasz O, Szasz A.M. Minnaar C, Szasz A (2017) Heating preciosity - trends in modern oncological hyperthermia. *Open Journal of Biophysics* 7:116–144
- [52] Pethig R: Dielectric properties of biological materials: biophysical and medical application. *IEEE Transactions on Electrical Insulation*, E1-19(5),453–474, 1984
- [53] Schwan HP: Determination of biological impedances. In: *Physical Techniques in Biological Research*, vol. 6, 323–406, Academic Press, New York, 1963
- [54] Szasz O and Szasz A: Oncothermia - nano-heating paradigm. *J Cancer Sci Ther*, 6:4, 2014
- [55] Vincze Gy, Szigeti Gy., Andocs G and Szasz A: Nanoheating without artificial nanoparticles. *Biology and Medicine*, 7(4),249, 2015
- [56] Szasz A: Electromagnetic effects in nanoscale range. *Cellular Response to Physical Stress and Therapeutic Applications* (eds. Tadamichi Shimizu, Takashi Kondo), chapter 4, Nova Science Publishers, Inc, 2013
- [57] Martinsen OG, Grimnes S, Schwan HP; (2002) *Interface Phenomena and Dielectric Properties of Biological Tissue*; *Encyclopedia of Surface and Colloid Science*; pp. 2643–2652, Marcel Dekker, Inc.

- [58] Ayoub MWB, Aro R, Georgin E, et al. (2018) Quantification of free and bound water in selected materials using dielectric and thermo-coulometric measurement methods; *J. Phys. Commun.* 2:035040
- [59] Wolf M, Gulich R, Lunkenheimer P, Loidl A. (2012) Relaxation dynamics of a protein solution investigated by dielectric spectroscopy, *Biochimica et Biophysica Acta - Proteins and Proteomics* 2012
- [60] Hasted JB. *Aqueous dielectrics*, Chapman and Hall, London, Ch.9, pp.234-256, 1973
- [61] Andocs G, Renner H, Balogh L, Fonyad L, Jakab C, Szasz A. (2009) Strong synergy of heat and modulated electro- magnetic field in tumor cell killing, Study of HT29 xenograft tumors in a nude mice model. *Strahlentherapie und Onkologie* 185:120–126, <http://www.ncbi.nlm.nih.gov/pubmed/19240999>
- [62] Szasz A, Vincze G, Szasz O, Szasz N. (2003) An energy analysis of extracellular hyperthermia. *Magneto- and electro-biology* 22:103-115
- [63] Lee I-H, Imanaka MY, Modahl EH, et.al. (2019) Lipid raft phase modulation by membrane-anchored proteins with inherent phase separation properties, *ACS Omega*, 4, 6551-6559
- [64] Staunton JR, Wirtz D, Tlsty TD, et al, The Physical Sciences - Oncology Centers Network; (2008) A physical sciences network characterization of non-tumorigenic and metastatic cells; *Scientific Reports*, 3:1449, <https://doi.org/10.1038/srep01449>
- [65] Kotnik, T., (2000) Theoretical Evaluation of the Distributed Power Dissipation in Biological Cells Exposed to Electric Fields. *Bioelectromagnetics*, 21, 385–394.
- [66] Campello, E.M.B. and Zohdi, T.I. (2014) Design Evaluation of a Particle Bombardment System Used to Deliver Substances into Cells. *CMES*, 98(2), 221–245.
- [67] Lee, B.W., Faller, R., Sum, A.K., Vattulainen, I., Patra, M. and Karttunen, M. (2004) Structural Effects of Small Molecules on Phospholipid Bilayers Investigated by Molecular Simulations. *Fluid Phase Equilib*, 225, 63-8.
- [68] Guest, W.C., Cashman, N.R. and Plotkin, S.S. (2011) A theory for the anisotropic and inhomogeneous dielectric properties of proteins. *Phys Chem Chem Phys*, 13(13), 6286–95.
- [69] Heikelä, M., Vattulainen, I. and Hyvönen, M.T. (2006) Atomistic simulation studies of cholesteryl oleates: model for the core of lipoprotein particles. *J Biophys*, 90(7), 2247–57.
- [70] Waxham, M.N. (2007) Molecular mobility in cells examined with optical methods. *Bean A. Protein Trafficking Neurons*, 3-27.
- [71] Meggyeshazi N, Andocs G, Krenacs T. (2013) Programmed cell death induced by modulated electro-hyperthermia. *Hindawi Publishing Corporation Conference Papers in Medicine*, Volume 2013, Article ID 187835, <http://www.hindawi.com/archive/2013/187835/>
- [72] Forika G, Balogh A, Vancsik T, Zalatnai A, et.al. (2020) Modulated electro-hyperthermia resolves radioresistance of Panc1 pancreas adenocarcinoma and promotes DNA damage and apoptosis in vitro, *Int. J. Mol. Sci.*, 21, 5100, 1-15, <https://pubmed.ncbi.nlm.nih.gov/32707717/>
- [73] Kao P H-J, Chen C-H, Chang Y-W, et al. (2020) Relationship between energy dosage and apoptotic cell death by modulated electro-hyperthermia, *Scientific reports*, 10:8936, DOI: 10.1038/s41598-020-65823-2, <https://www.nature.com/articles/s41598-020-65823-2>
- [74] Veatch SL, Cicuta P, Sengupta P, Honerkamp-Smith A, Holowka D, Baird B; (2008) Critical Fluctuations in Plasma Membrane Vesicles; *ACS Chem.Biol.* 3:287-295
- [75] Zalba S, ten Hagen TLM, (2017) Cell membrane modulation as adjuvant in cancer therapy; *Cancer Treatment Rev.* 52:48-57
- [76] Dietrich C, Bagatolli LA, Volovyk ZN, et.al. (2001) Lipid rafts reconstituted in model membranes, *Biophysical Journal*, 80: 1417-1428
- [77] Dewey WC. (1993) Arrhenius relationships from the molecule and cell to the clinic, *Int J Hyperthermia*, 25:1, 3-20, DOI: 10.1080/02656730902747919
- [78] Feo F, Canuto RA, Garcea R. (1976) Lipid phase transition and breaks in the Arrhenius plots of membrane-bound enzymes in mitochondria from normal rat liver and hepatoma AH-130, *FEBS Letters*, 7(2): 262-266
- [79] Pelzer, H., Wigner, E.: Über die Geschwindigkeitskonstante von Austauschreaktionen. *Z. Phys. Chem. B15*, 445–471 (1932)
- [80] Eyring, H.: The Activated Complex in Chemical Reactions. *J. Chem. Phys.* 3, 107-115 (1935)
- [81] Laidler, K.J., King, M.C.: The development of transition-state theory. *J. Phys. Chem.* 87, 2657-2664 (1983)
- [82] Miller WH (1993) Beyond transition-state theory: a rigorous quantum theory of chemical reaction rates. *Acc Chem Res* 26:174-181

- [83] Pollak E, Talkner P (2005) Reaction rate theory: what it was, where is it today, and where is it going? *Chaos* 15(2):26116-26117
- [84] Szasz A, Vincze Gy (2006) Dose concept of oncological hyperthermia: Heat-equation considering the cell destruction. *Journal of Cancer Research and Therapeutics* 2(4):171-181
- [85] O'Neil DP, Peng T, Stiegler P, et al. (2011) A three-state mathematical model of hyperthermic cell death, *Ann. Biom. Eng.* 39(1):570-579
- [86] Pearce JA. (2013) Comparative analysis of mathematical models of cell death and thermal damage processes, *Int. J. Hyp.* 29(4): 262-280
- [87] Vincze Gy, Szasz A. (2018) Similarities of modulation by temperature and by electric field, *OJBIPHY*, 8, 95-103, <https://www.scirp.org/journal/PaperInformation.aspx?PaperID=84883>
- [88] Szasz O, Szasz A. (2014) Oncothermia - Nano-heating paradigm. *J Cancer Sci Ther* 6:4
- [89] Papp E, Vancsik T, Kiss E, Szasz O. (2017) Energy absorption by the membrane rafts in the modulated electro-hyperthermia (mEHT), *Open Journal of Biophysics*, 7, 216-229
- [90] Meggyeshazi N. (2015) Studies on modulated electrohyperthermia induced tumor cell death in a colorectal carcinoma model, Ph.D. theses, Pathological Sciences Doctoral School, Semmelweis University
- [91] Krenacs T, Meggyeshazi N, Forika G, et.al. (2020) Modulated electro-hyperthermia-induced tumor damage mechanisms revealed in cancer models, *Int J Molecular Sciences*, 21, 6270, pp. 1-25, doi:10.3390/ijms21176270
- [92] Vancsik T, Forika G, Balogh A, et.al. (2019) Modulated electro-hyperthermia induced p53 driven apoptosis and cell cycle arrest additively support doxorubicin chemotherapy of colorectal cancer in vitro, *Cancer Medicine*, (9):4292-4303, doi: 10.1002/cam4.2330, <https://www.ncbi.nlm.nih.gov/pubmed/31183995>
- [93] Yang K-L, Huang C-C, Chi M-S, Chiang H-C, Wang Y-S, Andocs G, et.al. (2016) In vitro comparison of conventional hyperthermia and modulated electro-hyperthermia, *Oncotarget*, 7(51): 84082-84092, doi: 10.18632/oncotarget.11444, <http://www.ncbi.nlm.nih.gov/pubmed/27556507>
- [94] Andocs G, Rehman MU, Zhao Q-L, Tabuchi Y, Kanamori M, Kondo T. (2016) Comparison of biological effects of modulated electro-hyperthermia and conventional heat treatment in human lymphoma U937 cell, *Cell Death Discovery* (Nature Publishing Group), 2, 16039, <http://www.nature.com/articles/cddiscovery201639>
- [95] Szasz A, Szasz O. (2020) Time-fractal modulation of modulated electro-hyperthermia (mEHT), in book *Challenges and solutions of oncological hyperthermia*, ed. Szasz A., Ch. 17, pp.377-415, Cambridge Scholars
- [96] Wust P, Kortum B, Strauss U, Nadobny J, Zschaek S, Beck M, et.al. (2020) Nonthermal effects of radiofrequency electromagnetic fields, *Scientific Reports*, 10:13488
- [97] Wust P, Ghadjar P, Nadobny J, et.al. (2019) Physical analysis of temperature-dependent effects of amplitude-modulated electromagnetic hyperthermia, *Int. J. Hyp.*, 36(1):1246-1254
- [98] Wust P, Nadobny J, Zschaek S, Ghadjar P. (2020) Physics of hyperthermia – Is physics really against us?, in book *Challenges and solutions of oncological hyperthermia*, ed. Szasz A., Ch. 16, pp.346-376, Cambridge Scholars
- [99] Szasz A. (2019) Thermal and nonthermal effects of radiofrequency on living state and applications as an adjuvant with radiation therapy, *Journal of Radiation and Cancer Research*, 10:1-17
- [100] Meggyeshazi N, Andocs G, Balogh L, Balla P, Kiszner G, Teleki I, Jeney A, Krenacs T (2014) DNA fragmentation and caspase-independent programmed cell death by modulated electrohyperthermia. *Strahlenther Onkol* 190:815-822
- [101] Szasz A. (2020) Towards the immunogenic hyperthermic action: Modulated electro-hyperthermia, *Clinical Oncology and Research, Science Repository*, 3(9):5-6
- [102] Andocs G, Meggyeshazi N, Balogh L, Spisak S, Maros ME, Balla P, Kiszner G, Teleki I, Kovago Cs, Krenacs T (2014) Upregulation of heat shock proteins and the promotion of damage-associated molecular pattern signals in a colorectal cancer model by modulated electrohyperthermia. *Cell Stress and Chaperones* 20(1):37-46
- [103] Tsang Y-W, Huang C-C, Yang K-L, et al. (2015) Improving immunological tumor microenvironment using electro-hyperthermia followed by dendritic cell immunotherapy, *BMC Cancer* 15:708
- [104] Szasz O. (2020) Local treatment with systemic effect: Abscopal outcome, in book *Challenges and solutions of oncological hyperthermia*, ed. Szasz A., Ch. 11, pp.192-205, Cambridge Scholars
- [105] Vancsik T., Kiss E, Kovago Cs, Meggyeshazi N, Forika G, Krenacs T. (2017) Inhibition of proliferation, induction of apoptotic cell death and immune response by modulated electro-hyperthermia in C26 colorectal cancer allografts, *thermometry Oncothermia Journal* Volume 20: 277-292

- [106] Minnaar CA, Kotzen JA, Ayeni OA, et al. (2020) Potentiation of the abscopal effect by modulated electro-hyperthermia in locally advanced cervical cancer patients, *Frontiers in Oncology*, 10(376):1-8
- [107] Lee S-Y, Fiorentini G, Szasz AM, Szigeti Gy, Szasz A, Minnaar CA. (2020) Quo vadis oncological hyperthermia (2020)? *Frontiers in Oncology*, 10:1690, doi: 10.3389/fonc.2020.01690

Initial publication

Power transmission of EHY-2000 – A Hypothesis

Katja Mühlberg¹

¹Chair of Fundamentals of Electrical Engineering, Technische Universität Dresden,
Dresden, Germany

Citation: Mühlberg K. (2021): Power transmission of EHY-2000 – A Hypothesis, initial publication: Oncothermia Journal 30: 104 – 116,
https://oncotherm.com/sites/oncotherm/files/2021-04/Muhlberg_Power_1.pdf

Abstract

Our study concentrates on the high-precision type of RF-energy transmission by capacitive coupling (impedance matching). We describe the main fitting parameters, the correct impedance matching pitfalls, and generalize the obtained results for various applications. The careful calculation and the discussion of the matching in detail have particular importance in therapeutical applications because the “load” is the patient who changes by the therapy. A further challenge is that the patients and their treated bodyparts have a broad scale of impedances that forces a frequent complete reset of the matching before starting the treatment. The present calculation gives some clues to optimize the system in a broad impedance regime.

The needs for particular practical application

The energy is used for therapy in oncology (hyperthermia) as a complementary treatment to conventional therapies. During the treatment, the technical challenge is that the RF-generator's maximum power shall be transmitted to the patient during the treatment. This request needs three optimizations:

1. Apply the most effective RF-source to avoid the energy-loss in the source. We chose the E-class amplifier to minimize this loss.
2. The maximum power (best efficacy) of the circuit, when the load resistance (\underline{Z}_L) is real (the imaginary part of its impedance is zero), and it is equal with the inner impedance of the source (\underline{Z}_S). Conventionally, we choose $\underline{Z}_0 = 50 \Omega$ as common impedance.
3. Due to the near-field approach in the impedance matching, the conventional fit by minimizing the signal's phase-shift by the load creates the optimal energy transmission. With a careful mechanism instead of the less accurate measurement of the phase-shift, we may use a power meter to measure the forwarded and reflected powers and calculate the high efficacy of transmission.

Transmission Lines – Theory

The applied carrier frequency is 13.56 MHz, chosen as a medical RF-frequency in the radio band that is freely usable for industrial, scientific, and medical (ISM) purposes. The wavelength of this wave in a vacuum is about $\lambda_0 = 22.1$ m. The propagation through material shortens the wavelength. For example, the wavelength in a coax cable with $\underline{Z}_0 = 50 \Omega$ wave impedance at this frequency will be $\lambda_c \approx 13.6$ m. The wave impedance denotes the relation between a voltage and a current wave propagating through the cable in forward direction. The wave impedance at all points of the cable depends on frequency but has nearly a constant real value at high frequencies like 13.56 MHz. When the cable is considerable short (about less than one-tenth of the wavelength), the voltage and current amplitude are nearly the same at all points of the cable. For longer cables the voltage and current amplitudes are depending on the location along the cable. In that case, the term “transmission line” is used for the cable.

A source with inner impedance \underline{Z}_S is connected to a transmission line with \underline{Z}_0 wave impedance that is terminated by a load \underline{Z}_L – see Fig. 1.

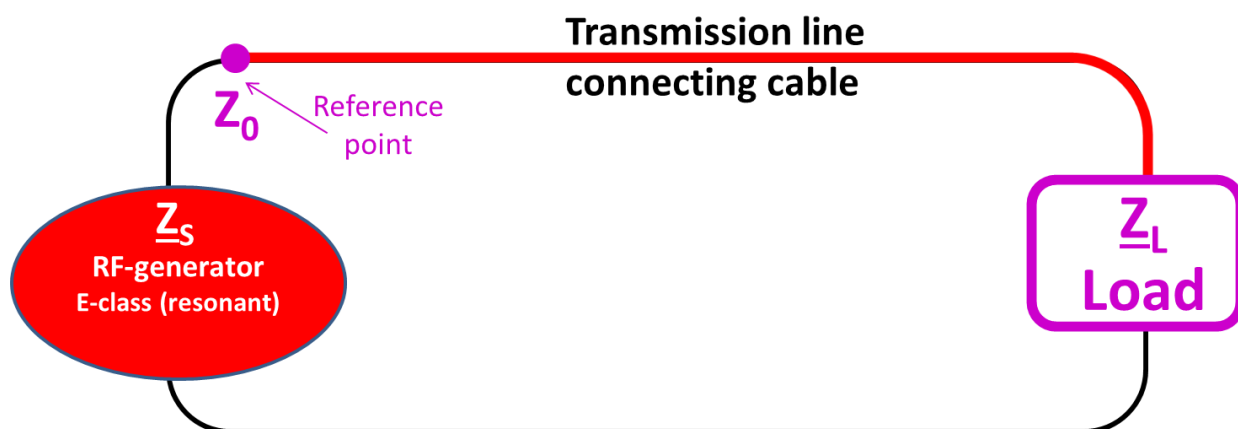


Fig. 1. The simplified drawing of the studied RF circuit.

The generator in the matching case is directly loaded by \underline{Z}_0 - equivalent with the tuned multicomponent load. The \underline{Z}_S and \underline{Z}_0 are serially connected to each other. The voltage signal travels through the transmission line after switching on the source. The current signal has to be in phase with voltage because of the $\underline{Z}_0 = 50 \Omega$ resistive wave impedance. Both signals propagate through the cable. The terminating impedance \underline{Z}_L is placed at the end of the cable. If this load differs from the transmission line's wave impedance, the voltage and current suddenly have to jump in their amplitude and phase. Simpler said: Something goes into a port, but something else appears at the port's other end. To bring equilibrium into this equation, we need the reflections. So when a wave is propagating through a transmission line that is terminated by an impedance differing from \underline{Z}_0 there will always be reflections.

Imagine that the wave is the first time reflected because the load does not match the wave impedance. The forward and reflected wave overlap. The relation of the overlapped voltage and current waves – in amplitude and phase – describe the transformed load impedance at each point of the cable. In the case that the transmission line has a length of $\lambda_c/2$ and reflections occur due to mismatch, the transformed load impedance at the beginning of the transmission line equals the terminated load impedance. Therefore, this transmission line is also known as 1:1 transformer. From the source' perspective it is connected to the transformed load impedance. If the source impedance \underline{Z}_S does not match the transformed load impedance there will appear a further reflection. This we call re-reflection. The other part that is not re-reflected is transmitted to the generator that can regulate its output signal now. So for mismatching at both ends of the transmission line, there will be several reflections.

Reflections cannot always be avoided and are not a curse in general. In the case of a quarter-wave-transformer two transmission lines with different wave impedances \underline{Z}_1 and \underline{Z}_2 are connected with a third transmission line – the so-called quarter-wave-transformer. As the name indicates, its length corresponds to one-fourth of the wavelength. Furthermore its wave impedance \underline{Z}_{qw} has to meet the condition $\underline{Z}_{qw} = \sqrt{\underline{Z}_1 \underline{Z}_2}$. There are reflections – infinity much – that in sum act like a reflection of zero so that the entire power is delivered to the load. Of course, the cable attenuation has to be considered. When a wave propagates through a cable, it will always be attenuated.

In the following, we would like to explain how voltage and current signals propagating through a transmission line can be expressed. We assume a signal with amplitude y_{max} and phase shift φ at angular frequency ω that only depends on time:

$$y(t) = y_{max} \cdot \cos(\omega t + \varphi) \quad (17)$$

The wave propagation through transmission lines attenuates the signal. So the amplitude exponentially depends on the distance z from the starting reference point in the cable – see Fig. 2.

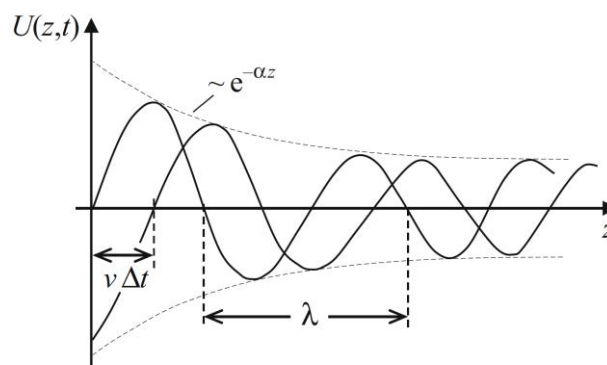


Fig. 2. Attenuated harmonic wave at two points in time with difference Δt [1]

[1] Leone, M., 2018. *Theoretische Elektrotechnik: Elektromagnetische Feldtheorie für Ingenieure*. Wiesbaden: Springer Vieweg, pp. 349-411.

The modified signal with constant attenuation α is:

$$y(t, z) = y_0 e^{-\alpha z} \cdot \cos(\omega t + \varphi) \quad (18)$$

where y_0 is the signal amplitude at the beginning of the transmission line (at $z = 0$ position).

Note that the attenuation constant has to be inserted in the unit Neper [Np].

$$1 \text{ dB} = \frac{\ln(10)}{20} [\text{Np}] \cong 0.115 \text{ Np}$$

If we investigate the previous picture, then we see a harmonic signal that is location-dependent. The 'frequency' of this signal depends on the wavelength that is shortened when entering the material. The wavelength is linked with the phase constant β , like $\beta = \frac{2\pi}{\lambda}$. The signal can be completed now:

$$y(t, z) = y_0 e^{-\alpha z} \cdot \cos(\omega t - \beta z + \varphi) \quad (19)$$

If we express the signal in complex form, we get the vector \underline{Y} :

$$\underline{Y}(t, z) = y_0 e^{-\alpha z} \cdot e^{i(\omega t - \beta z + \varphi)} = y_0 e^{i\omega t} e^{i\varphi} e^{-(\alpha + i\beta)z} = y_0 e^{i(\omega t + \varphi)} e^{-\gamma z} \quad (20)$$

where $\underline{\gamma} = \alpha + i\beta = ik$ is the propagation constant, and k is the wavenumber. The amplitude can be summarized and is complex.

$$\underline{Y}(t, z) = \underline{Y}_0(t, z) e^{-\gamma z} \quad \text{where} \quad \underline{Y}_0(t, z) = y_0 e^{i(\omega t + \varphi)} \quad (21)$$

Now we differentiate between forwarded (+) and reflected (-) signal, and the potential (U) and current (I) looks:

$$\begin{aligned} \underline{U}_+ &= \underline{U}_{+0} \cdot e^{-\gamma z} & \underline{U}_- &= \underline{U}_{-0} \cdot e^{+\gamma z} \\ \underline{I}_+ &= \underline{I}_{+0} \cdot e^{-\gamma z} & \underline{I}_- &= \underline{I}_{-0} \cdot e^{+\gamma z} \end{aligned} \quad (22)$$

Note that the reflected signal behaves oppositely as the forwarded (mirror imaging at vertical axes) – the negative sign in exponent gets positive.

The sum of the forwarded and reflected signal is the resulting signal.

$$\underline{U}(z) = \underline{U}_+(z) + \underline{U}_-(z) \quad \text{and} \quad \underline{I}(z) = \underline{I}_+(z) + \underline{I}_-(z) \quad (23)$$

$$\underline{U}(z) = \underline{U}_{+0} \cdot e^{-\gamma z} + \underline{U}_{-0} \cdot e^{+\gamma z} \quad \text{and} \quad \underline{I}(z) = \underline{I}_{+0} \cdot e^{-\gamma z} + \underline{I}_{-0} \cdot e^{+\gamma z} \quad (24)$$

The wave impedance \underline{Z}_0 is:

$$\underline{Z}_0 = \frac{\underline{U}_{+0}}{\underline{I}_{+0}} = \frac{-\underline{U}_{-0}}{\underline{I}_{-0}} \quad (25)$$

The wave impedance for higher frequencies is a constant real value. Then the current can also be expressed by:

$$\underline{I}(z) = \frac{\underline{U}_{+0}}{\underline{Z}_0} \cdot e^{-\gamma z} - \frac{\underline{U}_{-0}}{\underline{Z}_0} \cdot e^{+\gamma z} \quad (26)$$

The complex reflection $\underline{\Gamma}$ coefficient at an arbitrary point at the transmission line can be calculated as:

$$\underline{\Gamma}(z) = \frac{\underline{U}_-(z)}{\underline{U}_+(z)} = \frac{\underline{U}_{-0}}{\underline{U}_{+0}} \cdot e^{+2\gamma z} \quad (27)$$

The reflection coefficient at the end of a transmission line with length l is:

$$\underline{\Gamma}(l) = \frac{\underline{U}_-(l)}{\underline{U}_+(l)} \quad (28)$$

The resulting voltage and current at a terminating impedance \underline{Z}_L have to be the same as the summarized voltage and current at the end of the transmission line.

$$\underline{Z}_L = \frac{\underline{U}(l)}{\underline{I}(l)} = \frac{\underline{U}_+(l) + \underline{U}_-(l)}{\underline{I}_+(l) + \underline{I}_-(l)} = \frac{\underline{U}_+(l) + \underline{U}_-(l)}{\underline{U}_+(l) - \underline{U}_-(l)} \cdot \underline{Z}_0 \quad (29)$$

The reflection coefficient inserted into the previous equation we obtain:

$$\underline{\Gamma}(l) = \frac{\underline{Z}_L - \underline{Z}_0}{\underline{Z}_L + \underline{Z}_0} \quad (30)$$

The absolute value of $\underline{\Gamma}(l)$ ranges in $[0,1]$ interval, where the zero is the perfect matching. In the case of reflection incident and reflected wave interfere and create standing waves. As already mentioned, the transmission line depending on its length acts as an impedance transformer for the load. We would like to derive the reason for this here. In Fig. 3 a transmission line with wave impedance \underline{Z}_0 is terminated by a load impedance \underline{Z}_{Th} .

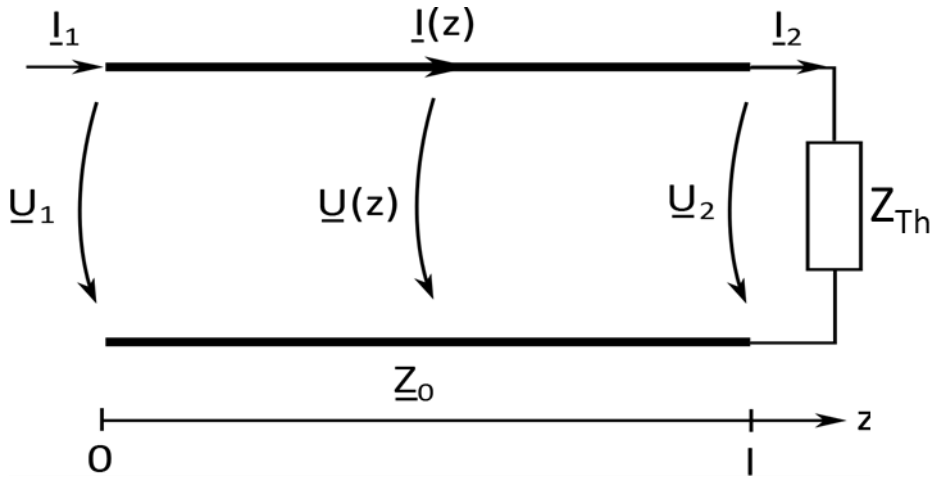


Fig. 3. The load \underline{Z}_{Th} closes the line at the end of successive drop of voltage

The voltage and current signals can be expressed as the following:

$$\begin{aligned} \underline{U}_1 &= \underline{U}_{+0} + \underline{U}_{-0} & \underline{U}_2 &= \underline{U}_{+0} \cdot e^{-\gamma l} + \underline{U}_{-0} \cdot e^{+\gamma l} \\ \underline{I}_1 &= \frac{1}{\underline{Z}_0} (\underline{U}_{+0} - \underline{U}_{-0}) & \underline{I}_2 &= \frac{1}{\underline{Z}_0} (\underline{U}_{+0} \cdot e^{-\gamma l} - \underline{U}_{-0} \cdot e^{+\gamma l}) \end{aligned} \quad (31)$$

Forwarded and reflected voltage can then be expressed as:

$$\underline{U}_{+0} = \frac{1}{2} (\underline{U}_2 + \underline{Z}_0 \underline{I}_2) e^{+\gamma l} \quad \underline{U}_{-0} = \frac{1}{2} (\underline{U}_2 - \underline{Z}_0 \underline{I}_2) e^{-\gamma l} \quad (32)$$

The voltage and the current at the beginning of the transmission line are then:

$$\begin{aligned} \underline{U}_1 &= \frac{1}{2} (\underline{U}_2 + \underline{Z}_0 \underline{I}_2) e^{+\gamma l} + \frac{1}{2} (\underline{U}_2 - \underline{Z}_0 \underline{I}_2) e^{-\gamma l} = \underline{U}_2 \frac{e^{+\gamma l} + e^{-\gamma l}}{2} + \underline{Z}_0 \underline{I}_2 \frac{e^{+\gamma l} - e^{-\gamma l}}{2} \\ \underline{I}_1 &= \frac{1}{2} \left(\frac{\underline{U}_2}{\underline{Z}_0} + \underline{I}_2 \right) e^{+\gamma l} - \frac{1}{2} \left(\frac{\underline{U}_2}{\underline{Z}_0} - \underline{I}_2 \right) e^{-\gamma l} = \frac{\underline{U}_2}{\underline{Z}_0} \frac{e^{+\gamma l} - e^{-\gamma l}}{2} + \underline{I}_2 \frac{e^{+\gamma l} + e^{-\gamma l}}{2} \end{aligned} \quad (33)$$

Now with the relations, the signals result in the mathematical form of the transmission line equations.

$$\underline{U}_1 = \underline{U}_2 \cosh(\underline{\gamma} l) + \underline{Z}_0 \underline{I}_2 \sinh(\underline{\gamma} l) \quad \underline{I}_1 = \frac{\underline{U}_2}{\underline{Z}_0} \sinh(\underline{\gamma} l) + \underline{I}_2 \cosh(\underline{\gamma} l) \quad (34)$$

The ratio of these two signals describes the impedance \underline{Z}_i at the beginning of the transmission line.

$$\underline{Z}_i = \frac{\underline{U}_1}{\underline{I}_1} = \frac{\underline{U}_2 \cosh(\underline{\gamma}l) + \underline{Z}_0 \underline{I}_2 \sinh(\underline{\gamma}l)}{\frac{\underline{U}_2}{\underline{Z}_0} \sinh(\underline{\gamma}l) + \underline{I}_2 \cosh(\underline{\gamma}l)} \quad (35)$$

Note that the load impedance can be expressed by:

$$\underline{Z}_{Th} = \frac{\underline{U}_2}{\underline{I}_2} \quad (36)$$

We obtain now the transformed load impedance that depends on the load, wavelength and length, and attenuation of the transmission line.

$$\underline{Z}_i = \underline{Z}_0 \frac{\frac{\underline{Z}_{Th}}{\underline{Z}_0} + \tanh(\underline{\gamma}l)}{1 + \frac{\underline{Z}_{Th}}{\underline{Z}_0} \tanh(\underline{\gamma}l)} \quad (37)$$

In the following, some exceptional cases of impedance transformation by a transmission line are presented. For all cases, the attenuation of the transmission line is assumed to be zero.

1.) $\underline{Z}_{Th} = \underline{Z}_0$	$\underline{Z}_i = \underline{Z}_0$
2.) $\underline{Z}_{Th} = 0$ $(\tanh(ix) = i \cdot \tanh(x))$	$\underline{Z}_i = i \underline{Z}_0 \cdot \tanh(\beta l)$
3.) $\underline{Z}_{Th} = \infty$	$\underline{Z}_i = \frac{\underline{Z}_0}{i \cdot \tanh(\beta l)}$
4.) $l = \frac{\lambda}{4}$	$\underline{Z}_i = \frac{\underline{Z}_0^2}{\underline{Z}_{Th}}$
5.) $l = \frac{\lambda}{2}$	$\underline{Z}_i = \underline{Z}_{Th}$

Power Transmission – An Example

In this section, we would like to explain how the power is propagated from the RF generator to the load. The "therapy" load \underline{Z}_{Th} here represents all that is behind the connecting cable – including the applicator arm, both applicators with boluses, and the patient. In perfect matching $\underline{Z}_0 = \underline{Z}_L = \underline{Z}_T + \underline{Z}_{Th}$ the circuit is tuned, and the therapy load \underline{Z}_{Th} completed with the tuners impedance \underline{Z}_T to fix the $\underline{Z}_0 = \underline{Z}_L$ requirement. As shown in the previous section, our connecting cable with $\lambda_c/2$ length is a 1:1 impedance transformer. It means that connecting the cable input to the spectrum analyzer shows us the therapy-load impedance \underline{Z}_{Th} as well – see Fig. 4.

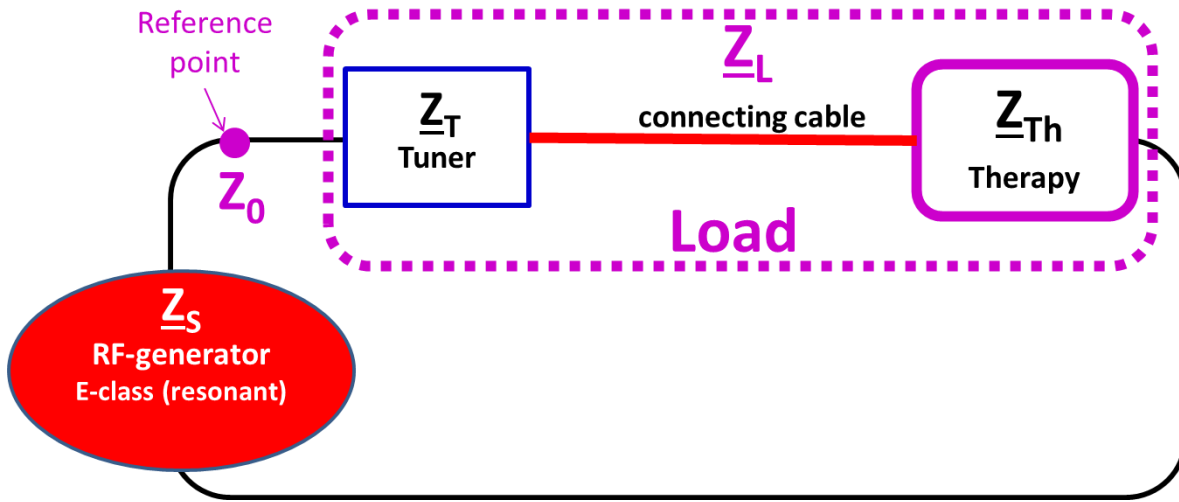


Fig. 4. The RF-circuit with the details discussed in the text

In the following example, the load impedance is assumed to be:

$$\underline{Z}_{Th} = (20 - 30i)\Omega \quad (38)$$

Further, we want to assume that the insertion loss caused by the tuner is 5 % and for the connecting cable of $\frac{\lambda_c}{2} = 6.8$ m length is 0.5 dB. The efficacy factor of the tuner is therefore 95 % and for the connecting cable is 89.13 %. (Note the power transmission $\frac{P_{in}}{P_{out}} = 10^{\left(\frac{0.5 \text{ dB}}{10}\right)}$)

The coax cable between the RF generator and tuner is assumed to be such short that there are no reflections and the only cable where reflections appear is the connecting cable. For a load \underline{Z}_{Th} at the end of the connecting cable, the reflections depend on the wave impedance of the cable and load impedance. The reflection coefficient can be calculated as:

$$\underline{\Gamma}_{Th} = \frac{\underline{Z}_{Th} - \underline{Z}_0}{\underline{Z}_{Th} + \underline{Z}_0} \quad (39)$$

The wave impedance is:

$$\underline{Z}_0 = 50 \Omega \quad (40)$$

It follows:

$$\underline{\Gamma}_{Th} = -\frac{6}{29} - \frac{15}{29}i \quad |\underline{\Gamma}_{Th}| = 0.5571 \quad (41)$$

Note: The reflection factor describes how much the signal's voltage and current respectively is reflected by the load. In power consideration, we are interested in the power transmitted to the therapy-load.

$$\frac{P_{refl}}{P_{forw}} = |\underline{\Gamma}_{Th}|^2 = 0.3103 \quad (42)$$

At the end of the connecting cable are 31.03 % of power reflected due to the unperfect match between wave and load impedance. The following table shows the wave propagation through the system. At the beginning, we have 100 % power between generator and tuner. Because of the tuner, only 95 % of original power is measured between the tuner and connecting cable. Because of the connecting cable loss, only 84.67 % of the original 100 % source power is measured between connecting cable and load. Due to the mismatching of impedances, reflections appear at the end of the connecting cable. So that from the original power, only 58.40 % is transmitted to the load. The other part is reflected. Consider that the load also includes the arm of the therapy applicator where due to radiation further loss appears so that even less power reaches the patient.

The reflected wave propagating through the cable to the tuner is attenuated due to the cable loss. Only 23.41 % power is measured between the tuner and connecting cable. Now we do not know how much is re-reflected. Let us assume that the treatment is performed when $VSWR = 1.1$. This acceptable value is measured between the generator and the tuner, supposed that the matching is well done. From the $VSWR$ value, we can obtain the reflection coefficient by applying the formula:

$$|\Gamma_G| = \frac{VSWR - 1}{VSWR + 1} = \frac{1.1 - 1}{1.1 + 1} = 0.047619 \quad (43)$$

When we start with a forwarded power of 100 %, we can calculate the reflected power with a known reflection factor between the generator and the tuner.

$$\frac{P_{refl}}{P_{forw}} = |\Gamma_G|^2 = 0.002268 \quad (44)$$

Consequently, obtaining a $VSWR = 1.1$ the reflected power measured between generator and tuner has to be 0.2268 %. We also know that the tuner attenuated this low power. The power between the tuner and connection cable is 0.2387 %. From the 23.41 % reflected power reaching the beginning of connection cable, only 0.2387 % can be transmitted; otherwise, there will be a higher $VSWR$ value measured. So, the other 23.1713 % has to be re-reflected. This is the point where we can calculate the necessary re-reflection factor at the cable beginning at tuner sight (connection cable beginning at the tuner):

$$\frac{P_{refl}}{P_{forw}} = |\Gamma_T|^2 = 0.9898 \quad (45)$$

This result is for the further calculation of re-reflections used. The re-reflected power propagates through the connection cable. It is attenuated so, and 20.65 % reaches the end of the cable where again it is partly reflected and so on. Fig. 5 visualizes the consecutive power transmission.

Power between generator & tuner	T: transmitted power R: reflected power	Power between tuner & cable	Power between cable & load	T: transmitted power R: reflected power
100 %		95.00 %	84.67 %	T: 58.40 % R: 26.27 %
0.2268 %	T: 0.2387 % R: 23.1713 %	23.41 %		
			20.65 %	T: 14.24 % R: 6.41 %
0.0570 %	T: 0.06 % R: 5.65 %	5.71 %		
			5.04 %	T: 3.48 % R: 1.56 %
0.095 %	T: 0.01 % R: 1.38 %	1.39 %		
			1.23 %	T: 0.85 % R: 0.38 %
...	T: ... R: 0.34 %	0.34 %		
			0.30 %	T: 0.21 % R: 0.09 %
		...		





Legend	
	Tuner loss of 5 % -> efficacy 95 %
	Power reflection of 31.03 %
	Cable loss of 0.5 dB for forward and re-reflected waves -> efficacy 89.13 %
	Cable loss of 0.5 dB for reflected waves -> efficacy 89.13 %

Fig. 5. The cascade process of the energy-losses.

Calculating the sum of all power reaching the load:

$$P_{\text{load}} = 58.40 \% + 14.24 \% + 3.48 \% + 0.85 \% + 0.21 \% = 77.18 \% \quad (46)$$

Now we would like to check the VSWR value between generator and tuner. The forward power is:

$$P_{\text{forw_GenTun}} = 100 \% \quad (47)$$

The reflected power is:

$$P_{\text{refl_GenTun}} = 0.2268 \% + 0.0570 \% + 0.0095 \% = 0.2933 \% \quad (48)$$

The reflection factor is, therefore:

$$|\Gamma| = \sqrt{\frac{P_{\text{refl_GenTun}}}{P_{\text{forw_GenTun}}}} = 0.0542 \quad (49)$$

The VSWR value can be determined by:

$$VSWR = \frac{1 + |\Gamma|}{1 - |\Gamma|} = 1.11 \quad (50)$$

so our calculation is verified.

Let us suppose we would like to measure the VSWR value between the tuner and connection cable. At this point, we discuss first the power meter itself. The power meter works in a way that a part of forwarded and reflected power is decoupled. It can consist of a short coax cable, and an additional wire is inserted in parallel to the inner conductor. This way, the power meter characterizes the impedance. If we insert it between the tuner and connection cable, the power meter actually extends the connection cable because both have the same wave/characteristic impedance. By measuring the forwarded and reflected waves with a power meter between the tuner and connection cable, we obtain the cable-parameter. Then the measured forwarded power is more than what we originally supposed:

$$P_{\text{forw_TunCable}} = 95 \% + 23.1713 \% + 5.65 \% + 1.38 \% + 0.34 \% = 125.54 \% \quad (51)$$

The reflected power in this case is:

$$P_{\text{refl_TunCable}} = 23.41 \% + 5.71 \% + 1.39 \% + 0.34 \% = 30.85 \% \quad (52)$$

We see the high forwarded power greater than 100 % and the strong reflection. In the case of a large degree of mismatch, we will measure impossible results. Due to the resulting U_{max} value, the electrical length of the supply line changes as a result of inductive and capacitive load changes, so the vector diagram of voltage and current also changes. Our measuring instrument determines the power in relation to the wave impedance,

$$P_w = \frac{m}{2Z_0'} U_{max}^2 \quad (53)$$

where m is the traveling wave ratio, which is the reciprocal of the SWR, and Z_0 is the wave impedance. With the same power on the line, U_{max} can be up to $1/\sqrt{m}$ times, which could cause the apparent impossibility.

This effect could be observed experimentally in measuring between the tuner and connection cable. The reflection coefficient and VSWR value are then:

$$|\underline{\Gamma}| = \sqrt{\frac{P_{\text{refl_TunCable}}}{P_{\text{forw_TunCable}}}} = 0.4957 \quad VSWR = \frac{1 + |\underline{\Gamma}|}{1 - |\underline{\Gamma}|} = 2.97 \quad (54)$$

Power Transmission – Generalization

First, we have to define some quantities.

Quantity	Description	Previous Example
η_c	Power transmission efficacy connection cable	0.8913
η_T	Power transmission efficacy tuner	0.9500
R_L	Power reflection at connection cable end due to load impedance mismatching	0.3103
R_G	Measured/defined power reflection between the generator and tuner	0.002268 ($VSWR = 1.1$)
R_{T_meas}	Measured power re-reflection at connection cable beginning at the tuner ²	0.4957
R_T	Power re-reflection at connection cable beginning at the tuner ³	0.9898

The first four constants are given or can be easily calculated. The last two of them have to be determined from formulas we will have constituted at the end of this section. Note that we use for power reflection $|\underline{\Gamma}|^2 = R$. The next step is the generalization of the calculated values.

Coefficient	Description	Previous Example
A_0	Forward power from the generator	$A_0 = 100 \%$
B_n	Forward power between tuner and bed cable	$B_0 = 95.00 \%$
C_n	Attenuated forward power at the end of connection cable at the load sight	$C_0 = 84.67 \%$
D_n	Transmitted power to the load	$D_0 = 58.40 \%$
E_n	Reflected power at the load	$E_0 = 26.27 \%$
F_n	Attenuated reflected power at the beginning of connection cable at tuner sight	$F_0 = 23.41 \%$
G_n	Transmitted power to the tuner	$G_0 = 0.2387 \%$
H_n	Attenuated transmitted power in backward direction between generator and tuner	$H_0 = 0.2268 \%$
Note	Re-reflected power becomes the next B – coefficient-> new cycle n	$B_1 = 23.1713 \%$

² It describes the relation of the cumulated re-reflected power (including the initial forwarded power) to the cumulated reflected power.

³ It describes, how much power is re-reflected fo a single reflected wave.

In the following, the relations between the coefficients are constituted.

$A_0 \cdot \eta_T = B_0$	$\sum_n D_n = P_{load}$
$B_n \cdot \eta_C = C_n$	
$C_n \cdot R_L = E_n$	$\frac{1}{A_0} \sum_n H_n = R_G$
$C_n \cdot (1 - R_L) = D_n$	
$E_n \cdot \eta_C = F_n$	
$F_n \cdot R_T = B_{n+1}$	$\frac{\sum_n F_n}{\sum_n B_n} = R_{T_meas}$
$F_n \cdot (1 - R_T) = G_n$	
$G_n \cdot \eta_T = H_n$	

The most interesting parameter is, of course, the power transmitted to the load. However, first, we will have a look at what the measured reflection R_{T_meas} is at the cable beginning at tuner sight.

$R_{T_meas} = \frac{\sum_n F_n}{\sum_n B_n}$	$\sum_{n=0}^{\infty} F_n = \sum_{n=0}^{\infty} E_n \eta_C = \sum_{n=0}^{\infty} C_n R_L \eta_C = \sum_{n=0}^{\infty} B_n R_L \eta_C^2 = R_L \eta_C^2 \sum_{n=0}^{\infty} B_n$ $R_{T_meas} = \frac{R_L \eta_C^2 \sum_{n=0}^{\infty} B_n}{\sum_{n=0}^{\infty} B_n}$ $R_{T_meas} = \eta_C^2 R_L$
---	---

Note that the measured reflection R_{T_meas} between the tuner and connection cable does not correspond to the actual reflection factor R_T at this point. We will determine this factor in the following.

$R_G = \frac{1}{A_0} \sum_n H_n$	$\begin{aligned} \frac{1}{A_0} \sum_{n=0}^{\infty} H_n &= \frac{1}{A_0} \sum_{n=0}^{\infty} G_n \eta_T = \frac{1}{A_0} \sum_{n=0}^{\infty} F_n \eta_T \cdot (1 - R_T) = \frac{1}{A_0} \sum_{n=0}^{\infty} E_n \eta_C \eta_T \cdot (1 - R_T) \\ &= \frac{1}{A_0} \sum_{n=0}^{\infty} C_n \eta_C \eta_T R_L \cdot (1 - R_T) \\ &= \frac{1}{A_0} \sum_{n=0}^{\infty} B_n \eta_C^2 \eta_T R_L \cdot (1 - R_T) = \frac{\eta_C^2 \eta_T R_L \cdot (1 - R_T)}{A_0} \sum_{n=0}^{\infty} B_n \\ \sum_{n=0}^{\infty} B_n &= \sum_{n=0}^{\infty} \frac{1}{\eta_C} C_n = \sum_{n=0}^{\infty} \frac{1}{\eta_C R_L} E_n = \sum_{n=0}^{\infty} \frac{1}{\eta_C^2 R_L} F_n = \sum_{n=0}^{\infty} \frac{1}{\eta_C^2 R_L R_T} B_{n+1} \\ B_{n+1} &= \eta_C^2 R_L R_T \cdot B_n \\ \sum_{n=0}^{\infty} B_n &= B_0 + B_1 + B_2 + \dots \\ B_0 &: A_0 \eta_T \\ B_1 &: \eta_C^2 R_L R_T \cdot B_0 \\ B_2 &: (\eta_C^2 R_L R_T)^2 \cdot B_0 \\ \sum_{n=0}^{\infty} B_n &= A_0 \eta_T + \sum_{n=1}^{\infty} (\eta_C^2 R_L R_T)^n \cdot A_0 \eta_T \\ \eta_C^2 R_L R_T < 1 &\rightarrow \text{apply rule of geometric series} \\ \sum_{n=1}^{\infty} (\eta_C^2 R_L R_T)^n &= \frac{1}{1 - \eta_C^2 R_L R_T} - 1 \\ \sum_{n=0}^{\infty} B_n &= A_0 \eta_T + A_0 \eta_T \left(\frac{1}{1 - \eta_C^2 R_L R_T} - 1 \right) = \frac{A_0 \eta_T}{1 - \eta_C^2 R_L R_T} \\ \frac{1}{A_0} \sum_{n=0}^{\infty} H_n &= \frac{\eta_C^2 \eta_T R_L \cdot (1 - R_T)}{A_0} \sum_{n=0}^{\infty} B_n = \frac{\eta_C^2 \eta_T^2 R_L \cdot (1 - R_T)}{1 - \eta_C^2 R_L R_T} \\ \text{convert to } R_T \dots R_T &= \frac{\eta_C^2 \eta_T^2 R_L - R_G}{\eta_C^2 R_L (\eta_T^2 - R_G)} \end{aligned}$
----------------------------------	--

Of course, we are especially interested in the power delivered to the load.

$P_{load} = \sum_n D_n$	$\begin{aligned} \sum_{n=0}^{\infty} D_n &= \sum_{n=0}^{\infty} C_n \cdot (1 - R_L) = \sum_{n=0}^{\infty} B_n \eta_C \cdot (1 - R_L) = \eta_C \cdot (1 - R_L) \sum_{n=0}^{\infty} B_n \\ \sum_{n=0}^{\infty} B_n &= \frac{A_0 \eta_T}{1 - \eta_C^2 R_L R_T} \\ P_{load} &= \frac{A_0 \eta_C \eta_T \cdot (1 - R_L)}{1 - \eta_C^2 R_L R_T} \end{aligned}$
-------------------------	--

Verification of the generalization - recheck the previous example

After the previous generalization, recheck the power-transmission example calculated before.

Load impedance	$\underline{Z}_L = (20 - 30i)\Omega$
Reflection factor at load	for $\underline{Z}_0 = 50 \Omega$: $ \underline{\Gamma}_L = 0.5571$ $R_L = \underline{\Gamma}_L ^2 = 0.3103$
Power transmission efficacy – connection cable	$\eta_c = 0.8913$
Power transmission efficacy - tuner	$\eta_T = 0.9500$
Reflection factor between generator and tuner	$VSWR = 1.1$ for $\underline{Z}_0 = 50 \Omega$: $ \underline{\Gamma}_G = 0.0476$ $R_G = \underline{\Gamma}_G ^2 = 0.002268$
Delivered power of the generator	$A_0 = 100 \%$
Measured reflection between tuner and connection cable	$R_{T_meas} = 0.2465 \rightarrow VSWR = 2.97$
Reflection factor at the tuner	$R_T = 0.9923$
Transmitted power to the load	$P_{load} = 77.32 \%$

The power is nearly the same as in the previous example calculation, but here the values are a bit higher because after a lot of reflections, a small power was added. The $VSWR$ value between the tuner and cable is the same for both calculations. The reflection factor at this point is (formula) a bit higher here. Otherwise, the power transmitted back to the generator increases, and therefore the $VSWR$ value was limited too.

Special cases

We will consider the following three special cases:

- no connection cable attenuation
- no reflection at load
- no re-reflection at the tuner

The results:

no connection cable attenuation	$\eta_c = 1.0$ $P_{load} = 94.76 \%$
no reflection at load	$R_L = 0$ $P_{load} = A_0 \eta_c \eta_T = 84.67 \%$
no re-reflection at the tuner	$R_T = 0$ $P_{load} = A_0 \eta_c \eta_T \cdot (1 - R_L) = 58.40 \%$

The important role of cable attenuation due to multiple reflections looks essential. When the therapy-load matches better to the connection cable, then more power is delivered to the load. In the case that the load does not match the cable, there has to be a strong re-reflection, causing considerable loss of energy.

Conclusion

The matching of the load in the RF-circuit is a complex task. The matching process must fit multiple interconnected parameters, which work collectively and make a sensitive balance of optimum. The therapeutic application's main challenge is the time-dependent load, so the standard fixed antenna matching does not work. The changing patients and their coupling and the changing by the therapy's effect all could drastically modify the tuning conditions, and the coupling worsens, deviates from the optimum. Only the proper real-time adjusting allows long-time stability for the therapeutic efficacy. The above-generalized parametrization makes it possible to follow the situation in real-time. The reaction time is limited by RC time-constant of the circuits, but in the human physiological changes allows a few minutes delay.

Die Albumin-Carrier-Therapie – Anwendung in der onkologischen Praxis

Wulf-Peter Brockmann, Jürgen Arnhold, Michael Denck

Citation: Brockmann W.-P., Arnhold J., Denck M. (2018): Die Albumin-Carrier-Therapie – Anwendung in der onkologischen Praxis, Oncothermia Journal 30: 117 – 120,

http://www.oncotherm.com/sites/oncotherm/files/2021-04/Brockmann_DieAlbumin.pdf

Reprinted from: Forum Komplementäre Onkologie & Immunologie, Ausgabe 01/20181

Die Albumin-Carrier-Therapie – Anwendung in der onkologischen Praxis

Wulf-Peter Brockmann, Jürgen Arnhold, Michael Denck

Albumin ist das im menschlichen Organismus am häufigsten vertretene Protein. Es hat eine Halbwertszeit von 19 Tagen und ist für viele Transportfunktionen im Blut zuständig. Vor rund 20 Jahren wiesen Biochemiker am Deutschen Krebsforschungszentrum nach, dass Zellen von soliden Tumoren große Mengen an Albumin aufnehmen, nicht aber gesunde Zellen. Der logische Schluss war, therapeutische Wirkstoffe an das Trägermolekül Albumin zu binden, um es nach dem trojanischen Prinzip in Tumorzellen zu schleusen. Die Arbeiten dazu wurden damals eingestellt, jedoch weniger aufgrund von mangelnden Erfolgen, sondern vielmehr aufgrund der strategischen Neuausrichtung des beteiligten Pharmaziekonzerns. Die Stiftung Albumin-Carrier-Therapie hat das Ziel, diese vielversprechende Therapieform aus der Versenkung zurückzuholen und sie weiterzuentwickeln. Mit Erfolg. Beispiele aus der onkologischen Praxis zeigen eindrucksvoll, zu welchen Ergebnissen die Therapie mit albumingebundenem Methotrexat führen kann.

Fallbeispiel 1: Patientin mit Astrozytom Grad III

Aus der Privatpraxis für individuelle Krebstherapie und -diagnostik, Institut OncoLight, Dr. med. Wulf-Peter Brockmann, Hamburg

Der Erstkontakt mit der Patientin (Jahrgang 1967) in meiner Praxis fand am 17.06.2013 unter Vorlage von MRT-Aufnahmen eines bis dato nicht histologisch abgeklärten, soliden, ausgeprägt und homogen Kontrastmittel-aufnehmenden li.-frontoparietalen Hirntumors mit kräftigem, perifokalem Ödem statt. Die MRT-Untersuchung zuvor erfolgte am 31.05.2013 (Abb. 1 a–c) wegen eines epileptischen Anfalls. Anschließend erfolgte eine Tumoresektion am 19.07.2013 mit histopathologischem Ergebnis: malignes Astrozytom Grad III, R0-reseziert. Nachfolgend erfolgten adjuvant Radiofrequenz-Applikationen in simultaner Kombination mit zwei Vakzinationen autologer dendritischer Zellen; das Intervall betrug vier Wochen.

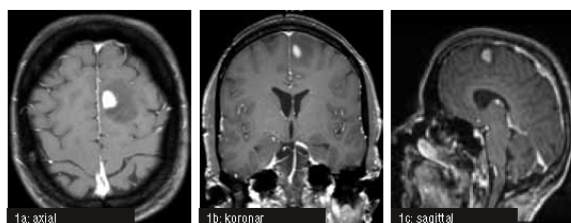


Abb. 1a – c: MRT des Hirnschädels, T1-Sequenz, nach i.v. KM-Gabe (am 31.05.2013)

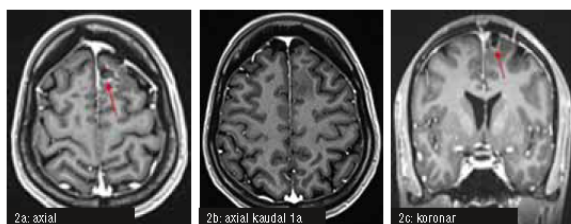


Abb. 2a – c: MRT des Hirnschädels, T1-Sequenz, nach i.v. KM-Gabe (am 22.08.2013)

Im ersten postoperativen MRT vom 22.08.2013 zeigte sich nur ein diskretes ringförmiges Kontrastmittel-Enhancement am Rande des OP-Defektes als typisches Zeichen einer unverdächtigen postoperativen Luxusperfusion (Abb. 2a–c, siehe Pfeile 2a und 2c). Im zweiten postoperativen MRT vom 21.10.2013 finden sich dann zwei kleine homogen kontrastierte Tumorezidive am operativ bedingten Defektrand (Abb. 3a–d, siehe Pfeile). Daraufhin erfolgten der Abbruch der Dendritischen Zell-Immuntherapie und die Durchführung einer Serie aus Kombinationsbehandlungen. Diese umfassten:

- insgesamt 29 intravenöse Curcumingaben (jeweils 450 mg, 5 im November, 6 im Dezember, 8 im Januar, 8 im Februar und 2 im März),
- insgesamt 7 intravenöse Gaben von jeweils 90 mg MTX-HSA (mit kovalent an Humanes Serum-Albumin gebundenem Methotrexat) im Abstand von jeweils etwa zwei bis drei Wochen,
- simultan zu jeder Infusion jeweils eine einstündige Radiofrequenz-Hyperthermie des Hirnschädels, die antitumoral aufgrund ihrer elektromagnetischen Wechselstromfelder einwirkt, während ihre Wirkung im Bereich des Gehirns nicht oder nur marginal auf Überwärmungseffekten beruht.

Zur Verhinderung klinischer Komplikationen im Sinne allergiformer Reaktionen gegenüber dem Lösungsmittel des Curcumins wurde das Curcumin grundsätzlich in 1 Liter NaCl-Lösung über etwa 5 Stunden nach Prämedikation von 4–8 mg Dexamethason infundiert. Die Halbwertszeit des MTX-HSA im Serum liegt bei rund drei Wochen.

Als erste Nebenwirkung wären entzündliche Schleimhautreaktionen im Bereich der Mundhöhle zu erwarten gewesen (MTX-Stomatitis). Jedoch konnten weder diese noch andere Nebenwirkungen infolge des MTX-Anteils oder anderer Therapieanteile beobachtet werden, was auch für die gute Bindung des MTX an das in aller Regel nur von malignen Zellen utilisierbare HSA spricht. Dieser Umstand war auch für die entsprechend gute Lebensqualität der Patientin verantwortlich; während der gesamten Behandlungsserie blieb die gefühlte Lebensqualität konstant gut.

Nach vier MTX-HSA-Gaben war im Sinne einer guten Teilremission bei einer MRT-Kontrolle am 23.02.2014 nur noch eines der beiden Tumorrezidive am parietalen Rande des Resektions-bedingten Substanzdefektes nachweisbar, wie die Positionierung der beiden Pfeile in Abb. 4 (a und b) anzeigt.

Nach Beendigung der gesamten Behandlungsserie waren wie auch bei allen nachfolgenden MRT-Untersuchungen, zuletzt am 19.07.2017, bei fortgesetzter Beschwerdefreiheit keine Kontrastmittel-Enhancements mehr diagnostizierbar, sodass eventuell von einer Heilung der Patientin ausgegangen werden könnte (Abb. 5a und b, Untersuchung vom 27.01.2017).

Bewertung

Das Ergebnis dieser Behandlung ist zumindest für Patienten mit schnell wachsenden Astrozytomen (kenntlich am ausgeprägten perifokalen Ödem) ermutigend, da etwa im Gegensatz zu Temozolomid-Behandlungen praktisch keine Nebenwirkungen auftreten und schon nach wenigen Wochen (hier nach vier Gaben MTX-HSA) eine Tendenz zum Erfolg oder Misserfolg dokumentierbar werden kann, was in letzterem Falle ausreichend schnell einen notwendigen Therapiewechsel erlaubt hätte. Gleichzeitig bestätigt das vorliegende Ergebnis die mehr als zehn Jahre alten Untersuchungen und Studienergebnisse, die von Dr. Hannsjörg Sinn selbst angestrengt worden waren, aber leider weitestgehend in Vergessenheit gerieten.

Darüber hinaus spricht einiges dafür, dass diese Therapie auch bei nicht-zerebralen malignen Tumoren eine Rolle spielen könnte, solange es sich dabei um Malignome handelt, die MTX-empfindlich sind, was molekularbiologisch bzw. molekulargenetisch anhand von Resistenzparametern und Tumorzellen im peripheren Venenblut der Patienten detektierbar zu sein scheint (z.B. Institut Metavectum, Hamburg). Hierfür sprechen weitere Behandlungsergebnisse aus Einzelfällen meiner Praxis, die zeitnah publiziert werden sollen.

Dass Studien notwendig sind, um diese Therapieform zumindest einem größeren Patientenkreis mit Astrozytomen Grad III zukommen zu lassen, versteht sich von selbst. Ein starker Gegenwind hiergegen, der von ökonomisch interessierter Seite entstehen wird, sollte dabei nicht entmutigen! Es ist zu bedenken, dass es sich sowohl beim HSA als auch beim MTX um vertragsärztlich zugelassene Medikamente handelt, die abrechnungsfähig von einem hierfür zugelassenen Apotheker nach Rezept kovalent miteinander verbunden werden dürfen.

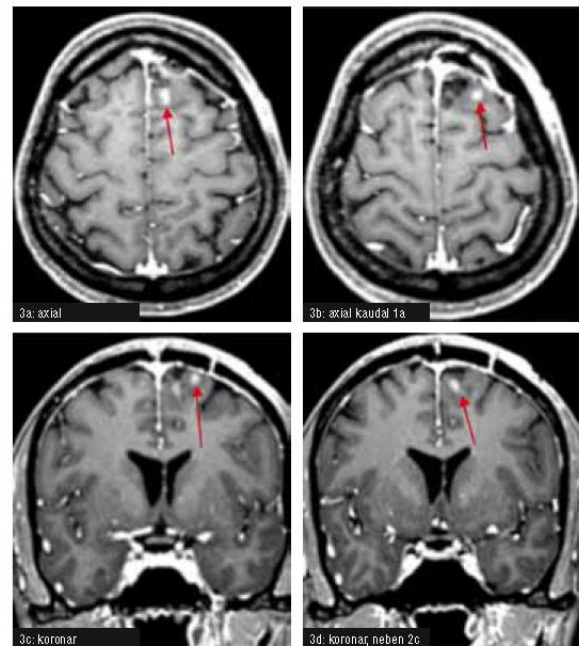


Abb. 3a – d: MRT des Hirnschädels, T1-Sequenz, nach i.v. KM-Gabe (am 21.10.2013)

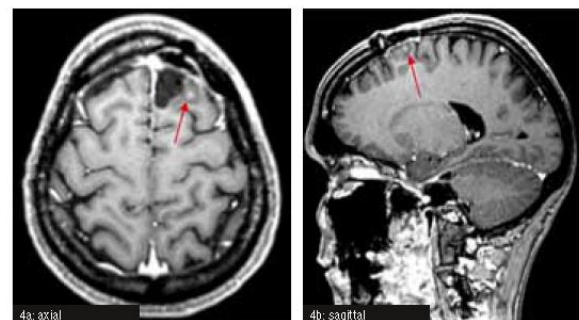


Abb. 4a, b: MRT des Hirnschädels, T1-Sequenz, nach i.v. KM-Gabe (am 23.02.2014)

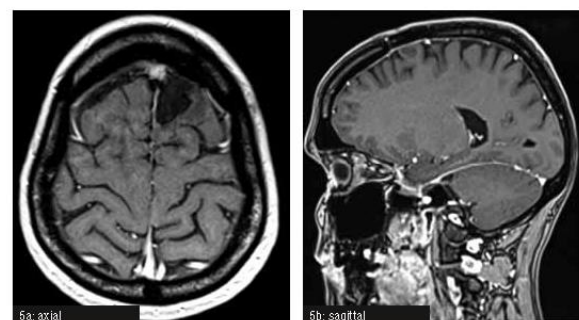


Abb. 5a, b: MRT des Hirnschädels, T1-Sequenz, nach i.v. KM-Gabe (am 27.01.2017)

Fallbeispiel 2: Ohrspeicheldrüsenkrebs

Aus der Praxis Dynamic Health Care, Dr. med. Jürgen Arnhold, Königsstein

Der männliche Patient, Jahrgang 1927, erhielt die Diagnose: *Parotis-Karzinom links mit Lymphknotenmetastasen cervical links*. Zu Beginn des Jahres 2015 war bei dem Patienten eine linksseitige Facialisparese aufgefallen. Diese wurde zunächst als Verdacht auf cerebralen Insult diagnostiziert und behandelt, jedoch ohne Erfolg. Bei einer im März 2015 durchgeführten Biopsie zeigte sich dann histologisch Folgendes: ein infiltrierendes, gut differenziertes Spindelzell-Karzinom der Parotis mit pathologisch vergrößertem Lymphknoten cervical li.

Von Mai bis Juli 2015 erfolgte eine photodynamische Tumorthherapie mit Chlorin E6 90 mg und Curcumin 150 mg, jeweils i.v. Danach wurde eine Punktion des Tumors und der pathologisch vergrößerten Lymphknoten zur interstitiellen Laserbestrahlung unternommen. Im folgenden Zeitraum von September 2015 bis Februar 2016 kam die intravenöse Therapie mit Humanalbumin-gebundenem Methotrexat 100 mg (MTX-HSA) zum Einsatz. Sie wurde in Kombination mit Curcumin 150 mg jeweils in 250 ml NaCl sowie mit einer intravenösen Laserlichtapplikation (rot, gelb, blau, grün) jeweils über 15 Minuten vorgenommen.

Follow-up 2016 bis Dezember 2017: Die komplette Remission des Tumorgeschehens konnte dokumentiert werden in einer Sonographie (08/2017), mittels einer Computertomographie (08/2017) sowie im MRT (11/2017). Die Facialisparese indes hatte sich nicht gebessert. Hier bleibt der Patient auf eine chirurgische Intervention angewiesen.

Resümee

Die beiden Best Case-Praxisfälle haben eines gemeinsam: Die behandelnden Ärzte haben MTX-HSA nicht als Monotherapie eingesetzt, sondern in Kombination mit anderen Wirkstoffen. Damit haben die Ärzte aus den Ergebnisse der früheren Phase-I/II-Studien bereits gelernt und MTX-HSA nicht mehr monotherapeutisch eingesetzt. Da Albumin aus Geweben und Organen über die Lymphbahnen in den Kreislauf zurückgeführt wird und MTX-HSA sich wie ein natürliches Albumin verhält, können neben soliden Tumoren und Metastasen auch Lymphknotenmetastasen durch die systemische Verabreichung erreicht werden.

Die Stiftung Albumin-Carrier-Therapie verfolgt das Ziel, neben MTX weitere Wirkstoffe, insbesondere auch Naturstoffe wie beispielsweise Curcumin, Artemisinin und Hypericin an Albumin als Trägerstoff zu binden. Die ersten Kopplungen mit Albumin waren positiv. Die neuesten Analytikergebnisse nach der Phase der Optimierung stehen noch aus. Der nächste Schritt wird es nun sein, die Wirkungsweise von den Naturstoff-Kopplungen nachzuweisen. Es gilt zunächst herauszufinden, welche Wirkstoffkombination bei welchen Tumorarten am erfolgversprechendsten sind.

Wie Dr. med. Brockmann bereits erwähnt hat, sind wissenschaftliche Studien notwendig, um den Beweis für die Wirkung anzutreten. Nur damit kann die schonende Therapieform einem größeren Patientenkreis zugänglich gemacht werden. Die Stiftung Albumin-Carrier-Therapie hat sich dies zur Aufgabe gemacht und ist dafür auf breite Unterstützung von Ärzten, Kliniken und Spendern angewiesen.

Autor Einleitung und Resümee:
Michael Denck, Stiftung Albumin-Carrier-Therapie
Hannah-Arendt-Straße 40, 60438 Frankfurt am Main
Tel. +49 (0)69-69 8 69-172, E-Mail: m.denck@albumin-carrier-therapie.org, www.albumin-carrier-therapie.org

Autor Fallbeispiel 1:
Dr. med. Wulf-Peter Brookmann, FA für Radiologie und Strahlentherapie
Privatpraxis für individuelle Krebstherapie und -diagnostik, Institut OncoLight
Beim Strohause 34, 20097 Hamburg
E-Mail: wpbrookmann@aol.com, www.oncolight.de

Autor Fallbeispiel 2:
Dr. med. Jürgen Arnhold, Arzt für Urologie
Dynamic Health Care
Debusweg 8, 61462 Königsstein
E-Mail: info@dynamic-health-care.com, www.dynamic-health-care.com

Wird die Bedeutung des Serum-Albumins bei Malignom-Patienten mit Aszites, Ödemen und Pleuraergüssen unter- oder überschätzt? – MTX-HSA als Hilfe bei der Therapie

Wulf-Peter Brockmann

Citation: Brockmann W.-P. (2018): Wird die Bedeutung des Serum-Albumins bei Malignom-Patienten mit Aszites, Ödemen und Pleuraergüssen unter- oder überschätzt? – MTX-HSA als Hilfe bei der Therapie, *Oncothermia Journal* 30: 121 – 124,

http://www.oncotherm.com/sites/oncotherm/files/2021-04/Brockmann_Wird.pdf

Reprinted from: Forum Komplementäre Onkologie & Immunologie, Ausgabe 02/2018

Wird die Bedeutung des Serum-Albumins bei Malignom-Patienten mit Aszites, Ödemen und Pleuraergüssen unter- oder überschätzt? – MTX-HSA als Hilfe bei der Therapie

Wulf-Peter Brockmann

Nicht selten leiden Patienten mit Malignomen unterschiedlichster Pathohistologie an Aszites, Pleuraergüssen und ausgeprägten Weichteilödemen (insbesondere der Beine). Bei der Frage nach der Genese denkt der behandelnde Arzt regelmäßig zuerst an Peritoneal- und Pleurakarzinosen sowie an retroperitoneale, Lymphbahnen-okkludierende Lymphknotenmetastasen/Lymphome – und dies insbesondere, wenn letztere schon schnittbilddiagnostisch dokumentiert sind.

Oft ist in solchen Fällen die Pleuraflüssigkeit klar, hell, leicht gelblich bis bernsteinfarben; Gleiches gilt für die Aszitesqualität. Wenn dann in entsprechenden Punktaten zytologisch keine Tumorzellen gefunden werden, erklärt man sich dies beispielsweise mit einer (zu) geringen Punktatmenge, und wenn tatsächlich zytologisch einige maligne Zellen gefunden werden, fühlt man sich umso mehr in der Vermutung bestätigt, dass die Ätiologie für die pathologischen und die Patienten oft hochgradig in ihrer Lebensqualität belastenden, nach Entlastungspunktion immer schneller und voluminöser rezidivierenden Flüssigkeitsmengen im karzinomatösen oder sarkomatösen Befall von Pleura und/oder Peritoneum begründet liegen.

Dabei müssen sich alle Behandler bewusst sein, dass jede klinisch ausreichend entlastende Aszitespunktion zu immer neuen Eiweißverlusten führt und die daraus resultierende progrediente Verringerung des onkotischen Drucks im Sinne eines *circulus vitiosus* zu gleichermaßen immer schneller progredienten Flüssigkeitsmengen in Pleura- und Peritonealraum führt.

Einen derart verursachten Eiweißmangel durch rezeptiertes, intravenös zugeführtes, kostenträchtiges Humanalbumin ausgleichen zu wollen, gilt im Normalfall als kontraproduktiv: Zwar spiegelt sich der Eiweißmangel im Serum in aller Regel schon bei der ersten Diagnose von Aszites, Pleuraergüssen und/oder Beinödemen in Laborergebnissen wider und muss auch auf Tumorumtilisation von Bluteiweiß zurückgeführt werden. Eine spezielle HSA-Substitution würde dann jedoch nur ein *Anfüttern von Krebszellen* und eben keinen echten Ersatz des dringend benötigten Serumalbumins bedeuten.

Die Albumin-Carrier-Therapie

Die in meinem vorangegangenen Artikel (Forum Komplementäre Onkologie 2018 (1): 3–5; kostenfreier Bezug via E-Mail: medwiss@forum-medizin.de) beschriebene Möglichkeit, die Albumin-Carrier-Therapie gegen Zellen von Astrozytomen Grad III als einzig gegen Tumorzellen und eben nicht gegen normale Zellen gerichtetes Agens intravenös zu verabreichen, erscheint mir ohne Weiteres auch analog gegen andere maligne Tumoren einsetzbar, wenn zuvor molekularbiologisch/molekulargenetisch im peripheren Venenblut und/oder Aszites/Pleurapunktat festgestellt werden kann, dass sich bei den Tumorzellen gegenüber MTX (noch) keine Resistenzen eingestellt haben. Diese mehrmalige Applikation von MTX-HSA (100 mg MTX kovalent gebunden an 10 g HSA) als Infusion in 14-tägigen Intervallen soll (möglichst zusammen mit jeweils zwei Curcumin-Infusionen à 450 mg in 1 Liter 0,9 % NaCl und jeweils 3 simultanen lokoregionären Radiofrequenz-Tiefenhyperthermie-Anwendungen des Bauches und/oder Thorax per entsprechend langer Tuchelektrode des EHY 3010, Fa. Oncotherm) im Best Case dreierlei bewirken:

- Verhinderung therapiebedingter Nebenwirkungen
- Vernichtung aller Krebszellen, die in hohem Maße HSA verstoffwechseln
- Wegen der langen Halbwertszeit von MTX-HSA im Serum von knapp drei Wochen eine Anhebung des Serum-HSA-Wertes in Richtung Normbereich, zumal das MTX-HSA während einer Behandlungsserie alle zwei Wochen verabreicht werden soll

Letzteres wird möglicherweise nicht ausreichen, um den venösen onkotischen Druck (hier: neg. Druck = Sog) so weit zu verstärken, dass ausreichend viel überschüssige Flüssigkeit aus den Geweben (insbesondere der Beine) sowie aus Pleura- oder Abdominalraum nach intravasal zurückverlagert werden kann. Wenn man jedoch mit MTX-HSA zügig innerhalb weniger Tage eine entsprechend hohe Anzahl an Tumorzellen vernichten kann, bedeutet eine zusätzliche HSA-Substitution mit ebenfalls regelmäßigen, hohen HSA-Gaben (je 100 ml, 20 %) kein Problem mehr.

Anmerkung der Redaktion: In dem Vorgänger-Artikel „Die Albumin-Carrier-Therapie – Anwendung in der onkologischen Praxis“ (Forum Komplementäre Onkologie 2018 (1): 3–5) hat sich seitens der Redaktion ein Fehler eingeschlichen. Der 3. Absatz auf Seite 4 ist irrtümlich doppelt enthalten („Nach Beendigung der gesamten Behandlungsserie waren ...“); korrekt muss der 3. Absatz wie folgt lauten:

Nach vier MTX-HSA-Gaben war im Sinne einer guten Teilremission bei einer MRT-Kontrolle am 23.02.2014 nur noch eines der beiden Tumorrezidive am parietalen Rande des Resektions-bedingten Substanzdefektes nachweisbar, wie die Positionierung der beiden Pfeile in Abb. 4 (a und b) anzeigt.

Wir bitten den Fehler zu entschuldigen. Der korrigierte Aufsatz kann kostenfrei in der Wissenschaftsredaktion des Forum Medizin Verlags angefordert werden, E-Mail: medwiss@forum-medizin.de

Behandlungsbeispiel

Die Möglichkeiten des MTX-HSA zu dieser Thematik lassen sich innerhalb der drei nachfolgenden Abbildungen im klinischen Verlauf eines Patienten mit Z.n. einem Cholangiokarzinom (Klatskin-Tumor, Primär-OP 2012) und erfolgreicher Strahlentherapie progredienter Lymphknotenmetastasen retroperitoneal in 2016 und in 2017 auch mediastinal / pulmonal bei zunehmenden Pleuraergüssen, Aszites und extremem Lymphödem beider Beine (Mai 2017) gut nachvollziehen.

Abbildung 1 zeigt den Verlauf der retroperitonealen Lymphknotenfiliae, progredient im September 2016 vor Chemoradiotherapie (hyperfraktioniert-akzeleriert) und die sehr gute Teilremission bis zu sieben Monate später im Mai 2017. Im Mai 2017 nach zwischenzeitlich gleichermaßen radioonkologisch (auch per Cyberknife) bestrahlten Lymphknotenmetastasen perihilar re. (mit konsekutiven radiopneumonitischen Infiltraten) beidseitige Pleuraergüsse und vermehrt Aszites; klinisch zusätzlich hochgradige Zunahme der vorbestehenden Lymphödeme beider Beine im Sinne eines allgemeinen Tumorprogresses.

Abbildung 2 zeigt die Ergebnisse aus der Chemosensitivitätstestung von Tumorzellen im Aszites im Mai 2017 (Institut Metavectum, Hamburg, Leitung Dr. Steffan), ohne Resistenzfaktoren (grün) gegen Methotrexat (MTX). Gegenüber Gemcitabine finden sich hingegen nun fast schon erwartungsgemäß solche Tumorzell-genetischen Faktoren (gelb), die zu Beginn der Behandlung im September 2016 im Serum noch nicht nachweisbar gewesen waren (ohne Abbildung).

Abbildung 3 spiegelt die unter zweimaliger intraarterieller Chemoperfusion des Abdomens und unter wöchentlichen Low-dose-Gemcitabinegaben (jeweils mit 125 mg i.v.) und i.v. Low-dose-Nivolumabinfusionen (je 10 mg) bis zum Metastasenprogress im April/Mai (betr. Lunge und Knochen) erbrachten Ergebnisse der „Metavectum“-Venenbluttestung im guten klinischen Verlauf beim Patienten recht gut wider – ohne Nebenwirkungen und im insgesamt bis zum Progress im Mai 2017 sinkenden Serumentummarker Ca19-9.

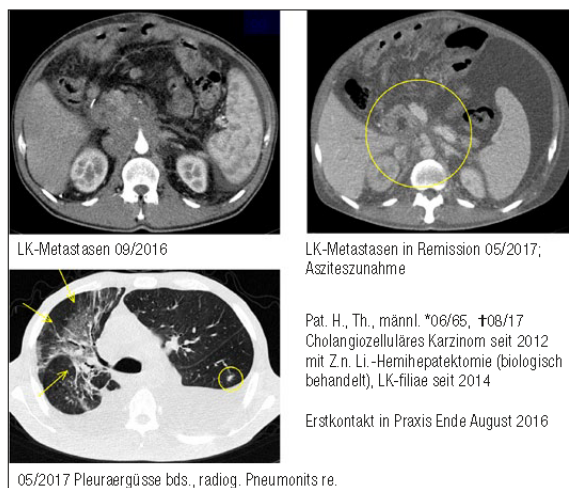


Abb. 1: Verlauf der Lymphknotenmetastasierung mit Remission zwischen September 2016 und Mai 2017

Anti-Cancer Agent	Gene Profile (+)	Gene Profile (-)	Gene Profile normal
5-FU, Xeloda	TS +	TP (-), DPD (-)	
Adriamycin, Epirubicin	TOP2A1 ≈ +		
Alkylators (Fosphamid, Cyclophosphamid etc.)	GCS ≈ +, GSTp ≈ +, MET +		
Amygdalin	Beta-Glucosidase +		
Apigenin	CYP10A1 +		
Aromatase-Inhibitoren	CYP		
Artemesinin, Artesunate	TF +		
Avastin	HIF +, VEGFA +		
Brentuximab	CD30 +		
Busulfan, Tresosulfan	GCS ≈ +, GSTpi ≈ +, MET +		
Carbustin, Lomustin etc. Nitrosohanstoffe	GCS ≈ +, GSTpi ≈ +, MET +		
Cabozantinib, Crizotinib	CD122 +, MET +		
COX2-Inhibitoren			COX2 n
Curcumin	NFKB +, TNF +		
Dacarbacin	CD44 +, MGMT +		
Denosumab			
EGFR-Inhibitoren: Cetuximab, Erlotinib etc.	EGFR +		
Etoposide			
Faslodex			
Fludarabin, Litalir etc.			
Gemcitabin, Cytarabin	DCK +, RRM1 +		
Herzeptin, Lapatinib	ERBB2 ≈ +		
IFN-alpha, IL2			
Imatinib, Glivec			
Methotrexat, Pemetrexed			
Mitomycin C	GCS ≈ +, GSTpi ≈ +		
Mitoxantrone			
Nivolumab, Pembrolizumab			
Platinverbindungen	HSPB1/2 +		ERCC1 n
Quercetin, Sulforaphan			
Revlimid	VEGFA +		
Rituximab			
Sorafenib, Sunitinib	PDGFRbeta ≈ +		
Tamoxifen, Raloxifen	ER1 +		
Taurolidin	TNF +		
Taxane	MET +		MDR1 n
Tivantinib etc.			
Topo-, Irinotecan			TOP2 n
Vemurafenib			
Vinca-Alkaloide			
Vitamin-C-Hochdosis	HIF +		

Abb. 2: Ergebnisse der Chemosensitivitätstestung von Tumorzellen im Aszites, Mai 2017; blau und grün = ohne ersichtliche Resistenzfaktoren; gelb = mit einzelnen Resistenzfaktoren; rot = mit deutlichen Resistenzfaktoren (oder nach wenigen Medikamentengaben zu erwarten)

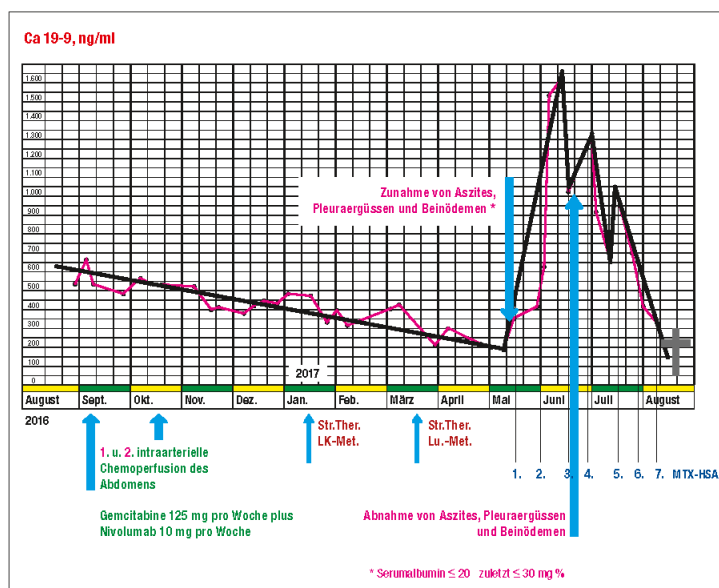


Abb. 3: Tumormarkerverlauf (CA19-9); Therapien und Klinik des Patienten

Im zeitlichen Anschluss zeigt die Abb. 3 schon unter bzw. nach den ersten zwei (von sieben) Gaben MTX-HSA (ohne Curcumin wegen Nebenwirkungen aufgrund des Curcumin-Lösungsmittels Kolliphor, aber unter simultanen Radiofrequenz-Hyperthermien) einen extrem sprunghaften Anstieg des Ca19-9 von etwa 200 U/ml Serum auf mehr als 1.600 U/ml infolge massiven Tumorzellzerfalls. Gleichzeitig verschwanden sonographisch nach rapider Rückerlangung sehr guten Allgemeinbefindens große Volumenanteile des Aszites und der Pleuraergüsse sowie vollständig die Beinödeme. Dabei stieg das Serumalbumin von unter 20 mg-% auf fast 30 mg-% an, und gleichzeitig fiel auch der Tumormarker Ca19-9 wieder auf Werte um 200 U/ml ab. Der Patient konnte zu diesem Zeitpunkt meine Praxis im 2. Stock erstmalig seit vielen Wochen wieder zu Fuß und ohne Inanspruchnahme des Fahrstuhls erreichen. Dabei zeigten sich nach den einzelnen MTX-HSA-Gaben ausgeprägte, kurzzeitige, erneute Anstiege des Ca19-9, doch anschließend jedes Mal ein weiter gehender Abfall als zuvor, passend zur verbesserten klinischen Situation des Patienten.

Vor einer geplanten Schnittbilddiagnostik-Kontrolle nach der 7. MTX-HSA-Gabe verstarb der Patient zuhause völlig unerwartet unter plötzlich aufgetretener Luftnot (August 2017). Mangels Obduktion (infolge Ablehnung durch die Angehörigen) muss am ehesten von einer Tumor-assoziierten Lungenembolie als Ursache für den Tod des Patienten ausgegangen werden.

Schlussfolgerungen und Zusammenfassung

Erst, wenn der Aszites auffällig blutig tingiert ist – gleiches gilt für Pleuraergüsse –, verdrängt als Ursache die jeweilige Karzinose oder Sarkomatos in der Genese von progredienten Ergussbildungen den HSA-Mangel.

Interessant wäre in diesem Zusammenhang zu erfahren, wie häufig und wie lange Pleurodesen bei Krebspatienten gelingen, deren Punktate blutig tingiert sind, im Vergleich mit Patienten, deren Punktate nicht blutig tingiert sind, kaum oder gar keine positive Tumorzytologien erlauben und eventuell sogar nur vom HSA-Mangel im Serum unterhalten werden.

Es scheint möglich zu sein, die Albumin-Carrier-Therapie mit MTX nach Dr. Hannsjörg Sinn auch bei nicht-zerebralen malignen Tumorerkrankungen praktisch nebenwirkungsfrei erfolgreich anzuwenden, insbesondere bei Tumor-bedingten Pleuraergüssen und Weichteilödemen sowie Aszites. Voraussetzung hierfür sollte jedoch eine positive Chemosensitivitätstestung auf molekularbiologischer/molekulargenetischer Basis von Tumorzellen im peripheren Venenblut und/oder in Ergussanteilen gegenüber MTX sein. Ein Teil des Therapieerfolges beruht bei diesen Patienten sicherlich auch auf der drastischen Verminderung der vermehrten Flüssigkeitsvolumina im Pleura- oder Peritonealraum infolge der durch MTX-HSA-Infusionen ermöglichten zusätzlichen HSA-Gaben. Hierzu würde auch das Auftreten von zytologisch und schnittbilddiagnostisch eindeutig nachgewiesenen Pleura- und Peritonealkarzinosen ohne klinisch auffällige Ergussbildungen oder größere Aszitesvolumina passen, solange das Serum-HSA nicht oder kaum verringert ist.

Ergänzende Anmerkung: Da bei Albumin-Carrier-Therapien wie beim MTX-HSA feste chemische Bindungen vorliegen, zum Beispiel „kovalente Bindungen“ (die jedem Bindungspartner seine beabsichtigten medikamentös wirksamen Eigenschaften belassen), und da aus dem Ergebnis dieser Bindungen auch weitere praktisch nebenwirkungsfreie, erfolgreiche antitumorale Therapien resultieren können, muss man befürchten, dass ökonomisch interessierte Kreise versuchen werden, Albumin-Carrier-Therapien auch mit anderen zytostatischen Präparaten (wie zum Beispiel Anthrazyklinen) mithilfe des AMG zu verhindern oder endgültig aus der praktischen Anwendung zu drängen, etwa indem die Verfasser einer zukünftigen AMG-Novelle **jede Form einer Verbindung** zweier längst zugelassener medikamentöser Substanzen als **neues Medikament definieren**, das dann nach jahrelanger Verzögerung eine eigene kostenintensive Zulassung benötigen würde.

Autor:

Dr. med. Wulf-Peter Brockmann, FA für Radiologie und Strahlentherapie
Institut OncoLight, Beim Strohhause 34, 20097 Hamburg
E-Mail: wpbrockmann@aol.com, www.oncolight.de

Im Fachmedium *Forum Komplementäre Onkologie* sind folgende Arbeiten zur Albumin-Carrier-Therapie erschienen, die bei der Wissenschaftsredaktion kostenfrei angefordert werden können, E-Mail: medwiss@forum-medin.de

- Die Albumin-Carrier-Therapie: Ein neuer Ansatz für die Behandlung von Krebserkrankungen
- Die Albumin-Carrier-Therapie – Anwendung in der onkologischen Praxis
- Wird die Bedeutung des Serum-Albumins bei Malignom-Patienten mit Aszites, Ödemen und Pleuraergüssen unter- oder überschätzt?
- MTX-HSA als Hilfe bei der Therapie

Das PET-CT im onkologischen Alltag – Eine wertvolle Hilfe zur Prognoseverbesserung

Wulf-Peter Brockmann

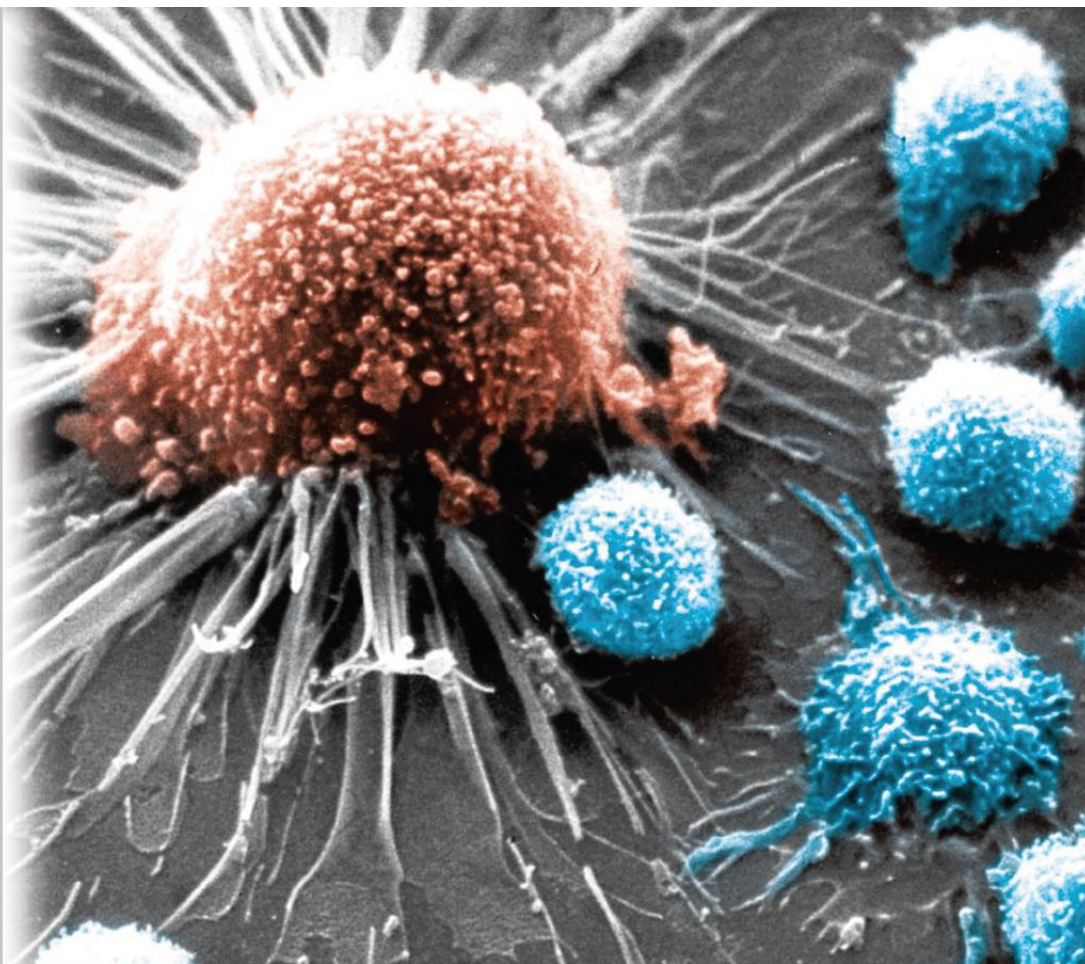
Citation: Brockmann W.-P. (2020): Das PET-CT im onkologischen Alltag – Eine wertvolle Hilfe zur Prognoseverbesserung, Oncothermia Journal 30: 125 – 131,
http://www.oncotherm.com/sites/oncotherm/files/2021-04/Brockmann_DasPET.pdf
Reprinted from: Forum Komplementäre Onkologie, Ausgabe 06/2020

Comment

The mEHT method selects the cancer cells in the targeted volume. One of the selection's essential factors is the higher conductivity in the tumor cell's microenvironment than in other regions. The radiofrequency current flows into the path where the resistance is low (the conductance is high). The high metabolic rate of cancer (primarily fermentative glucose consumption, Warburg effect) produces ionic species in the neighborhood of cancer. Measuring the glucose metabolism, which is the primary effect of PET diagnostics, gives a piece of direct information about glucose intake, which is proportional to ion production. In this way, the PET indicates the areas where the radiofrequency current will have a high density at the treatment. The PET intensity suggests the efficacy of the initial selection mechanism of mEHT. Dr. Bockmann's article discusses the PET process, giving a hint for the selection mechanism of mEHT.

Kommentar

Die mEHT-Methode wählt die Krebszellen im Zielvolumen aus. Einer der wesentlichen Faktoren der Selektion ist die höhere Leitfähigkeit in der Mikroumgebung der Tumorzelle gegenüber anderen Regionen. Der Hochfrequenzstrom fließt da lang, wo der Widerstand niedrig ist (bzw. die Leitfähigkeit hoch ist). Die hohe Stoffwechselrate von Krebs (hauptsächlich fermentativer Glukoseverbrauch, Warburg-Effekt) erzeugt eine ionische Spezies im näheren Umfeld des Krebses. Die Messung des Glukosestoffwechsels, der der primäre Effekt der PET-Diagnostik ist, liefert eine direkte Information über die Glukoseaufnahme, die proportional zur Ionenproduktion ist. Auf diese Weise zeigt das PET die Bereiche an, in denen der Hochfrequenzstrom bei der Behandlung eine hohe Dichte aufweist. Die PET-Intensität legt die Wirksamkeit des anfänglichen Selektionsmechanismus von mEHT nahe. Dr. Bockmanns Artikel diskutiert den PET-Prozess und gibt einen Hinweis auf den Selektionsmechanismus von mEHT.



Sonderdruck aus Ausgabe 6/2020

Das PET-CT im onkologischen Alltag – Eine wertvolle Hilfe zur Prognoseverbesserung

Dr. med. Wulf-Peter Brockmann

FORUM MEDIZIN
Verlagsgesellschaft mbH

Das PET-CT im onkologischen Alltag – Eine wertvolle Hilfe zur Prognoseverbesserung

Dr. med. Wulf-Peter Brockmann

In der Positronen-Emissions-Tomographie (= PET) nutzt man gegenüber bösartigen Tumoren deren speziellen Energiestoffwechsel aus, der auf der Glykolyse beruht, der Oxidation von Zucker bis zur Milchsäure als Endprodukt. Appliziert man intravenös Glukose, die an einen radioaktiven Tracer gebunden ist (^{18}F), so reichert sie sich innerhalb von etwa einer Stunde überall dort an, wo vermehrt Zucker im Körper utlisiert wird, normalerweise im Gehirn, im Herzen, in der Leber, in der Darmwand oder im Rahmen der Ausscheidung des radioaktiven Tracers in den ableitenden Harnwegen (Nieren, Ureteren und Harnblase/Harnröhre), aber auch in Tumoren und deren Metastasen, wenn sie vermehrt Zucker benötigen.

Im Falle anderer Tumorzell-avid Moleküle, die ebenfalls mit einem radioaktiven Tracer verbunden werden können, werden entsprechend andere Formen des PET-CT verwendet: das DOTA-TOC-PET-CT bei neuroendokrinen Tumoren sowie ehemals das ^{18}F -Cholin-PET-CT und aktuell das ^{68}Ga -Gadolinium-PSMA-PET-CT beim Prostatakarzinom. In der neuesten Entwicklung lässt sich das PSMA auch an das ^{18}F binden, dessen um die Hälfte kürzere Halbwertszeit bei ähnlichem Bindungsverhalten im Körper im Vergleich zum ^{68}Ga -PSMA die Strahlenbelastung der Untersuchung beträchtlich vermindern dürfte. Andererseits ist in der radioaktiven Zuckerverbindung, der ^{18}F -FDG, bei der gebräuchlichsten Onko-PET-Version die Halbwertszeit des ^{18}F -Nuklids mit 110 Min. so kurz, dass die Patienten recht pünktlich zum Einbestellungstermin erscheinen müssen und zudem nüchtern, damit für eine erkennbare Strahlung des Zuckerstoffwechsels maligner Befunde noch eine ausreichende Menge der radioaktiven Glukoseverbindung zum Einbau in die Befunde zur Verfügung steht.

Vor- und Nachteile der PET-CT-Untersuchung

Technisch-physikalisch und biologisch bedingt: In der bildgebenden Tumordiagnostik galten abgesehen von endoskopischen Verfahren bis zur Jahrtausendwende Ultraschall (US), Computertomographie (CT) und Magnetresonanztomographie (MRT) mit hoher Auflösung im Zielbereich als besonders Erfolg versprechend. Dagegen fußen die altbekannten nuklearmedizinischen Methoden in ihrer Aufnahmetechnik auf sichtbar gemachten Stoffwechselfunktionen, die sich jedoch nur relativ unscharf abbilden ließen, so beispielsweise die Knochenszintigraphie, in der ein vermehrter Knochenaufbau durch benigne Osteoblasten wiedergegeben wird. Seit einigen Jahren können die Befunde dieser Methode anhand der gleichen mathematischen Algorithmen wie bei CTs oder MRTs auch in dünnen, unscharfen Querschnitten abgebildet werden, wobei sich auf solche unscharfen Schichtdokumentationen an identischer Lokalisation hochauflösende Lowdose-CT-Aufnahmen eines integrierten Computertomographen legen lassen. Diese SPECT-Bilder erhöhen das Potenzial szintigraphischer Möglichkeiten beträchtlich, wenn es etwa um periossäre Weichteilanteile von Knochenmetastasen geht, war aber noch verbesserungsfähig: So ist bei einer PET-Diagnostik von Vorteil, dass vermehrt Glukose-verbrauchende Tumore oder ihre Metastasen – relativ unabhängig von ihrem Sitz im Körper – ab drei bis fünf Millimetern Durchmesser als Strahlungsherde sichtbar werden und sich somit ihr spezieller Energiestoffwechsel zusammen

mit ihrem malignen Gewebe in Knochen, Leber, Lymphknoten oder anderen Weichteilgeweben abbilden lässt. Je höher andererseits der Zuckergrundumsatz der umgebenden Normalgewebe ist, also je stärker die gesunde Hintergrundstrahlung in den Normalstrukturen krebsbefallener Organe ausgeprägt ist, desto schwieriger wird es, in solchen Geweben kleine maligne, zusätzlich strahlende Befunde zu erkennen: am schwierigsten folglich in der Leber, im Gehirn, im Darm und insbesondere in den ableitenden Harnwegen.

In der Lunge verschleift die Atembeweglichkeit die eigentlich stark umschriebene Strahlung weniger Millimeter großer Metastasen bis zur Unkenntlichkeit. Dieser Nachteil erweist sich jedoch als weniger problematisch, da in diesem Organ der ins PET-Gerät integrierte Computertomograph (PET-CT) ab 3 Millimeter Durchmesser metastatische Rundherde regelmäßig darstellen kann. Für PET-Untersuchungen des Gehirns gibt es Rechenmethoden, die die kräftige Grundstrahlung des Organ-typischen Glukoseverbrauchs bis zu einem gewissen Maße subtrahieren können und dadurch doch noch Metastasen-verdächtige Befunde, primäre maligne Hirntumore oder -tumorrezidive erkennen lassen. Eine spezielle Form der PET-Diagnostik ist auch aus diesem Grund die synchrone Verbindung des PET-Gerätes mit einem MR-Tomographen (PET-MRT), der insbesondere im Gehirn und in der Leber die Diagnostik vervollkommen kann, aber wegen des noch höheren Gerätepreises und seiner diagnostischen Abbildungslücke gegenüber kleinen Lungenmetastasen in nuklearmedizinischen Standorten seltener vorhanden ist. Allen PET-Methoden ist gemeinsam, dass sie nicht wie Knochen- oder Schilddrüsenszintigraphien auf der Erkennung und Messung ionisierender Gammastrahlung radioaktiven Zerfalls eines Technetium-Isotops beruhen, sondern auf der viel schwächeren Positronenstrahlung, beispielsweise des ^{18}F -Isotops, die bei seinem BetaPlus-Zerfall entsteht, und deren minuziöser Empfang anhand spezieller Detektoren sowie ihre Verarbeitung zu Schichtaufnahmen mit den schon erwähnten mathematischen Algorithmen ungleich aufwendiger ist.

In Organen wie der Leber und dem Gehirn, die schon von vornherein einen recht starken Glukosegrundumsatz aufweisen und daher auch einen prinzipiell vermehrten Einbau radioaktiver Glukoseverbindungen, ist mittels PET die Primärdiagnostik kleiner Malignome sicherlich etwas weniger sensitiv als per CT oder MRT, nicht aber ihre posttherapeutische Verlaufsdagnostik: Waren und bleiben sie nach Therapie noch darstellbar, erlaubt die Intensitätsdynamik ihrer Strahlung, d.h. ihr Funktionsstoffwechsel, wertvolle Schlüsse auf

Behandlungsergebnisse und das Maß einer erhofften Remission. Darüber hinaus reichern nicht alle Krebstumore regelmäßig die radioaktive Glukoseverbindung an. Hierzu gehört insbesondere das primäre Magenkarzinom. Ansonsten lassen sich Karzinome und ihre Metastasen fast ohne Einschränkungen ebenso gut per PET-CT darstellen wie Sarkome und primäre Lymphome.

Auf Patientenseite: Einerseits kann Platzangst die Durchführung der Untersuchung erschweren und muss evtl. medikamentös kaschiert werden; aber auch die Dauer der Untersuchung von bis zu 45 Minuten wie bei der MRT kann sich insbesondere für Schmerzpatienten oder M. Parkinson-Erkrankte problematisch auswirken, da sich die Patienten während der Untersuchung nicht bewegen sollten. Erhöhte Nüchtern-Blutzucker-Werte bei Diabetespatienten können ebenfalls die Untersuchung erschweren.

Bedeutung des PET-CT bei der der Prognoseverbesserung: Fallbeispiele aus dem ambulanten onkologischen Alltag

Die Bedeutung des PET-CT fußt auf der Korrelation zwischen der Prognose maligner Erkrankungen und einer fachgerechten PET-CT-Indikationsstellung zur frühen und damit oft noch rechtzeitigen Erkennung bzw. Verifikation der Ausbreitung eines Malignoms beim prätherapeutischen Staging: Hängt vom positiven Untersuchungsergebnis ab, ob und wo im Körper der Erkrankten noch ein lokal kuratives Vorgehen möglich ist, das bei erfolgreicher Behandlung eine Vollremission bis hin zu einer Heilung erlaubt, ruht eventuell das Schicksal des Patienten in einer solchen PET-CT-Untersuchung. Wie schnell PET-CTs auf Änderungen klinischer Verläufe reagieren und wie sinnvoll es sein kann, schon zwei Monate nach einem ersten PET-CT noch ein weiteres durchzuführen, zeigt

Fallbeispiel 1: H.B., weibl., 82 Jahre

18F-FDG-PET-CT 03/20: Darstellung eines Uterussarkoms als Befall des gesamten Organs sowie Diagnose einer ossären Metastase im re. Os Ileum mit großem Weichteiltumor sowie einer weiteren Metastase paraaortal

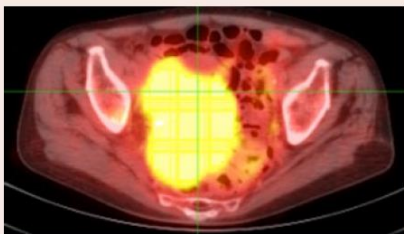


Abb. 1a: tumorös aufgetriebener Uterus, PET- und CT-Querschnitte aufeinander projiziert

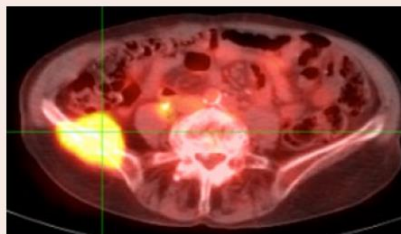


Abb. 1b: Os ileum-Metastase re., PET- und CT-Querschnitte aufeinander projiziert

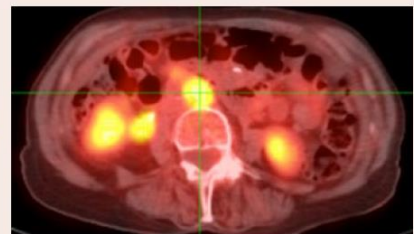


Abb. 1c: Paraaortametastase, PET- und CT-Querschnitte aufeinander projiziert

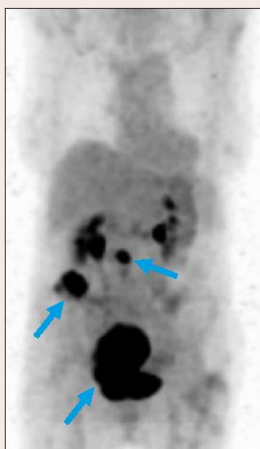


Abb. 2a: in 03/20 sind prätherapeutisch der Primärtumor und beide Metastasen im PET gut erkennbar



Abb. 2b: in 07/20 nach Therapieabschluss Vollremission (nach hyperfraktioniert-akzelerierter Strahlentherapiesserie Elektrohysterthermieserie und Insulin-potenzierter Lowdose Chemotherapien), passend zum Titerabfall des CA15-3 von 314 U/ml auf 13,7 U/ml und beim CA125 von 86,8 U/ml auf 4,2 U/ml



Abb. 2c: 09/20, nach foudroyanter Entwicklung eines triple doseneg. Mammakarzinoms li. schon multiple Metastasen lymphonodulär in Weichteilen und ossär; dabei deutlicher Wiederanstieg des CA15-3 auf 32,6 U/ml, und des CA-125 auf 33 U/ml



Abb. 2d: 11/20, nach nochmaliger Lowdose Chemotherapie, aber entsprechend einer Liquid-Biopsy-Empfehlung, in Kombination mit Elektrohysterthermien, ähnlich ausgeprägte Remission wie zuvor, in PET und Serum-Tumormarkertitern: mit 6,3 U/ml beim CA125 und 22,6 U/ml beim CA15-3 (Therapie wird fortgesetzt).

Fallbeispiel 1 einer 82-jährigen Patientin, bei der anfänglich erfolgreich ein großes inoperables Uterussarkom mit zwei abdominalen Metastasen behandelt worden war (Abb. 1a-c und 2a), aber schon 2 Monate nach dem Erhalt der Vollremission (Abb. 2b) ein drittes PET-CT multiple Knochen- und regionäre Lymphknotenmetastasen eines zwischenzeitlich aufgetretenen kleinen Mammakarzinoms (triple neg.) aufzeigte (Abb. 2c). Der schnelle Erfolg der sehr gut verträglichen altersadaptierten Komplementärtherapie spiegelte sich schon 2 Monate später auch für das Zweitmalignom in Abb. 2d zusammen mit abnehmenden Tumormarker-Titem von CA125 und CA15-3 wider. Wie sinnvoll sich solch eine eng verbundene Partnerschaft von PET-CT und subtiler, engmaschiger Tumormarker-Diagnostik auf einen mehrjährigen klinischen Verlauf (Fallbeispiel 2) bei therapeutisch praktisch unbeeinflusster Lebensqualität auswirkte, zeigen die PET-CT-Abbildungen uni- und oligolokulärer Metastasen nach

triple-neg. Mammakarzinom mit jeweils nachfolgenden Vollremissionen, die nach minimalem Serumtumormarker-Anstieg von CA125 und CA15-3 (sogar noch innerhalb des Normbereiches!) jedes Mal Grundlage für die anschließenden Behandlungserfolge waren (bebilderte Fallschilderung in FKO 2019 (2), 6–8; kostenfreier Bezug: medwiss@forum-medicin.de).

Fallbeispiel 3 zeigt die aktuell noch anhaltende Vollremission bei einer 68-jährigen Patientin mit triple neg. Mammakarzinom, bei der vor drei Jahren alle vier lokalisierbaren Metastasenregionen dank der PET-CT Staging-Diagnostik erfolgreich und größtenteils lokal behandelt worden waren (s. Abb. 3a-c, 4, 5 u. 6 sowie die Legenden hierzu). **Fallbeispiel 4** handelt von einem jungen Patienten mit Z.n. adenoidzystischem Parotiskarzinom, der bei einer Liquid Biopsy zur Chemosensitivitätstestung ein überraschend positives Ergebnis

Fall 3: T.C., weibl., 71 Jahre. Z.n. Mammakarzinom, triple neg. Abb. 3 u. 4: 18F-FDG-PET-CT mit Metastasendiagnose 11/2017

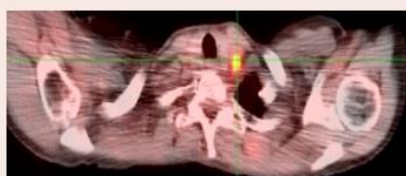


Abb. 3a: Lymphknotenmetastasen (im Fadenkreuz), li. paratracheal

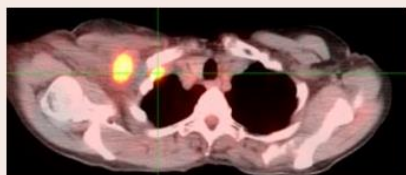


Abb. 3b: Lymphknotenmetastasen, re.-supraklavikulär u. retro-/infraclavikulär

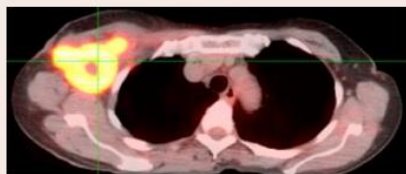


Abb. 3c: Lymphknotenmetastasen, re.-axillär mit zentraler Nekrose

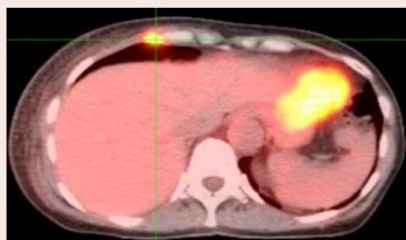


Abb. 4: ossäre /paraossäre Sternummetastasen, eine von multiplen Metastasen (para-)ossär im/unter dem gesamten corpus sterni sowie im/am angrenzenden Rippenknorpel (s. PET-Übersicht, Abb. 5)



Abb. 5: PET-CT vor Therapie (11/17), alle Strahlungsbefunde außerhalb von Herz, Nieren und Harnblase sind Metastasen und alle Herde innerhalb des Ovals sind parasternale/sternale Metastasen



Abb. 6: PET-CT (11/2020) nach intermittierender 3-jähriger Therapiekombination aus hyperfraktioniert-akzelerierter Strahlentherapie, Elektrohypothermien und Insulinpotenzierter Lowdose-Chemotherapie sowie Vakzinationen mit autologen Dendritischen Zellen. Ergebnis: stabile Vollremission, da PET ohne pathologische Herde bei normaler 18FDG-Utilisation von Herz und Leber sowie ungestörter Ausscheidung über Nieren und Harnblase.

betr. PSMA auswies, das mit einem positiven 68Gadolinium-PSMA-PET-CT bestätigt werden konnte (Abb. 7a u. 7b). Die damals progredienten Lebermetastasen des Patienten konnten anschließend via Leberarterie im Rahmen einer 90Y-DOTATOC- statt 177Lutetium-PSMA-Behandlung (wegen zu schneller Auswaschung des Lutetiums aus dem Metastasengewebe) in eine hepatische Vollremission gebracht werden (Abb. 8a-c) und anschließend nach weiteren Nuklidbehandlungen auch die re.-inguinale LK-Metastasierung (Abb. 8b,c). Nach mehr als 20 Monaten der hierdurch bewirkten und monatelang konstant gebliebenen Remissionen verstarb der Patient leider an erneutem Tumorprogress (03/19). Dass dieser Fall die hohe Validität der Liquid Biopsy auf molekularbiologischer /molekulargenetischer Grundlage (Institut Metavectum, Dr. Steffan, Hamburg) betont, sei nur am Rande erwähnt.

Deutschlands unrühmliche Sonderstellung beim PET-CT

Der defätistische Slogan der Pharmakoonkologie „einmal gestreut, immer gestreut“ im Sinne von „einmal gestreut, nur noch palliativ und damit vornehmlich nur noch medikamentös behandelbar“, würde Medizinern prinzipiell schon im Falle einer einzigen Fernmetastase erlauben, betroffene Krebskranke zu Palliativpatienten mutieren zu lassen, die dann einzig medikamentös, also vom Pharmakoonkologen selbst, zu behandeln wären und passt zur ihrer häufig vorgetragenen Behauptung, dass eine PET-Untersuchung viel zu teuer wäre und sich dafür kaum rentiere. Diese Verleugnung ihres wahren Wertes wird jedoch wie schon dargestellt in meiner Praxis und ebenso

auch regelmäßig im Ausland immer wieder von einer deutlich erfreulicheren Realität überholt. Behandelte man anderenfalls Patienten mit Fernmetastasen tatsächlich unabhängig von Anzahl, Größe, und Lokalisation unter gewohnt pessimistischen Prämissen prinzipiell und a priori nur palliativ, und würde man auf diese Weise den Wert des PET-CT auch zukünftig GBA-gemäß einfach ignorieren, würde man sich dessen Pessimismus zwangsläufig selbst bestätigen und sogar in einer gefährlichen Form von evidence based medicine immer wieder vermeidbare tödliche Resultate festschreiben. Da muss man sich fragen, warum PET-CTs aller Couleurs nur im Ausland die ihnen zustehende hohe Wertschätzung zum Nutzen aller hierfür in Frage kommenden Patienten erfahren und eben nicht in Deutschland, wo sie nur bei Privatpatienten oder fast nur als IGeL-Leistungen bei Kassenpatienten zusammen mit einer entsprechend akribischen Tumormarker-Diagnostik viel früher als gewohnt lokale Befunde aufzeigen dürfen und diese Patienten beim geeigneten Therapeuten als lokal behandelbar einstufen lassen. Anscheinend wird vom GBA und von verantwortlichen Kollegen völlig ignoriert, dass beispielsweise in Polen klinische onkologische Therapiestudien regelmäßig unter PET-CT-Kontrollen stattfinden sollen, und dass Krebspatienten aus dem Ausland (USA, Türkei, Asien, Russland) regelmäßig PET-CT-Diagnostiken zur Erstvorstellung mitbringen.

Autor:

Dr. med. Wulf-Peter Brockmann, FA für Radiologie und Strahlentherapie
Privatpraxis für individuelle Krebstherapie und -diagnostik, Institut OncoLight®
Beim Strohause 34, 20097 Hamburg
E-Mail: wpbrockmann@aol.com, www.oncolight.de

Fallbeispiel 4: F.M., m., 25 J., 68Gallium-PSMA-PET-CT (02/17)

Verifizierung v. 3 Lebermetastasen eines adenoidzystischen Karzinoms zur Klärung der Option einer 177Lutetium-PSMA-Therapieserie (Abb. 7)

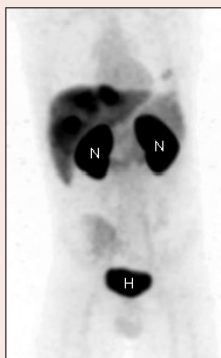


Abb. 7a: Im 68Gallium-PSMA-PET finden sich drei größere Lebermetastasen; N = Niere, H = Harnblase

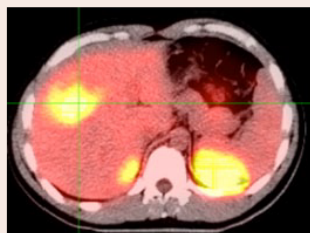


Abb. 7b: Im 68Gallium-PSMA-PET-CT Darstellung der größten Lebermetastase sowie beidseitiger Nierenanschnitte



Abb. 8a-c: Auswärtige Rezeptor-PET-CTs mit 68Gallium-DOTATOC vor/nach Nuklidtherapien mit 177Lu-DOTATOC und 90Y-DOTATOC: gemischte Remissionserfolge. Abb. 8a (12/17): vor erster Therapie. Abb. 8b (03/18): Lebervollremission, aber re.-inguinaler LK-Progress. Abb. 8c (07/18): Leistenvollremission re., aber beginnender Progress re.-axillär

Weiterführende Literatur (ausführliche Literaturangaben beim Autor)

- Altshar-Oromieh et al. (2012). Stellenwert der PET/CT in der Lymphknoten Diagnostik. Der Radiologe 2012; 52:338–346. DOI: 10.1007/s00117-011-2255-2.
- Dietlein M. et al. (2012). PET beim Hodgkin-Lymphom: Verbessert die Positronenemissionstomographie die Behandlung? Der Onkologe 2012; 18:18–27. DOI: 10.1007/s00761-009-1767-0.
- Gallamini A et al. (2014). Positron Emission Tomography (PET) in Oncology. Cancers 2014; 6: 1821–1889. DOI:10.3390/cancers6041821.
- Hesse B et al. (2012). Adverse events in nuclear medicine – cause for concern? Eur J Nucl Med Mol Imaging 2012; 39:782–785. DOI: 10.1007/s00259-012-2071-6.
- Hillner BE et al. (2012). Impact of 18F-FDG PET used after initial treatment of cancer: comparison of the National Oncologic PET Registry 2006 and 2009 cohorts J Nucl Med 2012; 53(5):831–7.
- Mease RC et al. (2013). PET imaging in prostate cancer: focus on prostate-specific membrane antigen. Curr Top Med Chem 2013; 13(8):951–62.
- Mohnke W et al. (2013). Produktion von PET-Radiopharmaka für den klinischen Gebrauch am Beispiel des MVZ-DTZ Berlin. Der Nuklearmediziner 2013; 36: 27–32. DOI: 10.1055/s-0032-1333216.
- Zengerling et al. (2012). Diagnostische Wertigkeit der Cholin-PET/CT bei Patienten mit Prostatakarzinom. Aktuelle Urologie 2012; 43: 49–54.

Modulated electro-hyperthermia in the combined treatment of metastatic colorectal cancer a retrospective cohort study with meta-comparison

Sergey Roussakow¹

¹Galenic Research Institute,
Moscow, Russia

Citation: Roussakow S. (2019): Modulated electro-hyperthermia in the combined treatment of metastatic colorectal cancer a retrospective cohort study with meta-comparison, *Oncothermia Journal* 30: 132 – 154,
http://www.oncotherm.com/sites/oncotherm/files/2021-04/Roussakow_Modulated.pdf

37th International Clinical
Hyperthermia Society MEETING
September 19th-21st 2019
Thessaloniki, Greece

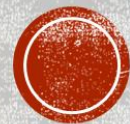
MODULATED ELECTRO- HYPERTHERMIA IN THE COMBINED TREATMENT OF METASTATIC COLORECTAL CANCER: A RETROSPECTIVE COHORT STUDY WITH META- COMPARISON

**SERGEY ROUSSAKOW, MD
PHD**

**GALENIC RESEARCH
INSTITUTE
MOSCOW, RUSSIA**

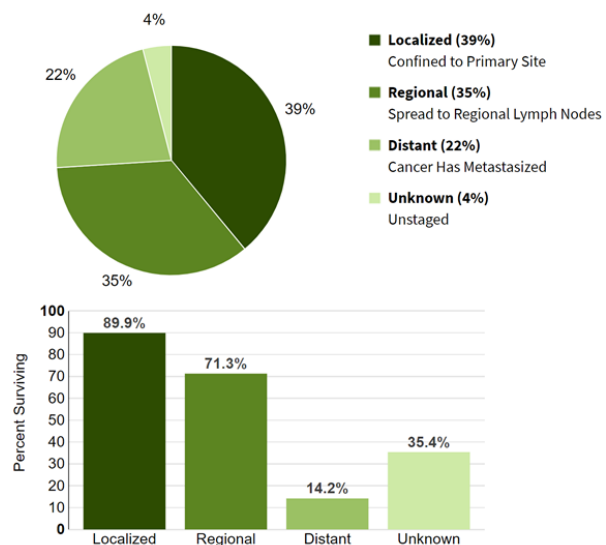
INTRODUCTION

Modulated electro-hyperthermia in the combined treatment of metastatic colorectal cancer: a retrospective cohort study with meta-comparison



FACTS ABOUT COLORECTAL CANCER

- 3rd the most diagnosed cancer in the world
- 4th leading cause of cancer death among men & women combined in the world
- 2nd leading cause of cancer death among men & women combined in the developed countries
- In the USA:
 - 140,250 estimated new cases in 2018
 - 50,630 estimated deaths in 2018



TRIAL DESIGN

Modulated electro-hyperthermia in the combined treatment of metastatic colorectal cancer: a retrospective cohort study with meta-comparison



TRIAL DESIGN

- A retrospective, cohort, two-center study.
- Two centers in Budapest (Hungary):
 - HTT-MED Clinic (HTT);
 - Peterfi Hospital (PFY).
- Enrollment:
 - HTT from 08/04/1997 to 10/17/2002 (63 months),
 - PFY from 05/01/1999 to 04/30/2002 (37 months).
- No inclusion / exclusion criteria
- Exitus
 - National Hungarian Civil Registry.
- Primary endpoints:
 - Median Survival Time (MST)
 - Overall Survival (OS) at 1, 3, 5 years
- The endpoints are in two options:
 - from the diagnosis
 - from the 1st session of MEHT
- Secondary endpoint:
 - clinical response (RECIST 1.1).



INTERVENTION AND BASIC TREATMENT

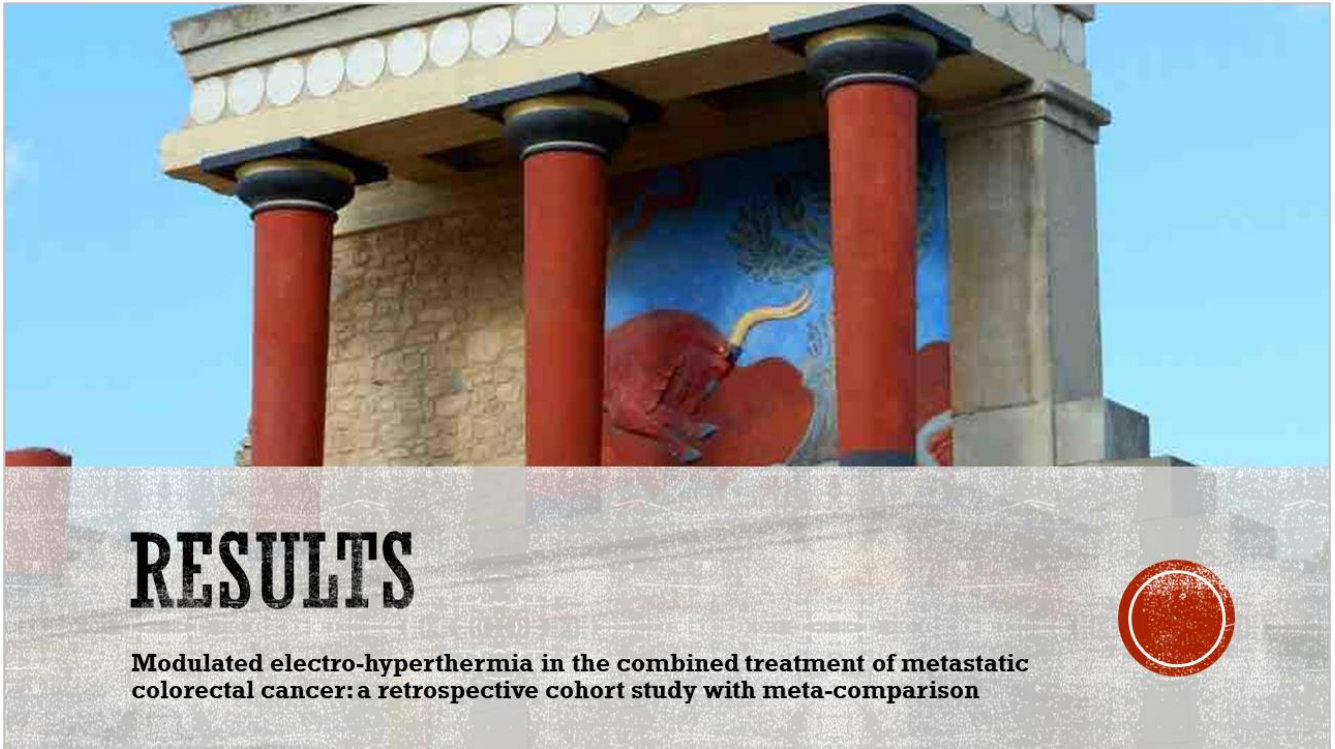
BASIC TREATMENT

- Radical or debulking surgery
- Adjuvant chemotherapy
- Symptomatic radiotherapy

INTERVENTION

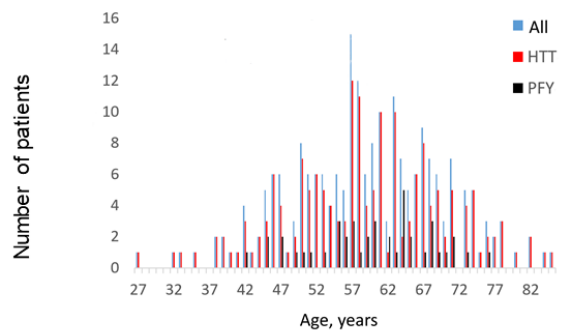
- Modulated electro-hyperthermia (oncothermia)
- Applicator Ø 30 cm
- Power 120 → 150 W.
- Time:
 - Radio- chemo-enhancement, 45 min.
 - Adjuvant monotherapy, 60 min.
 - Palliative monotherapy, 90 min.
- Localizations: up to 2.



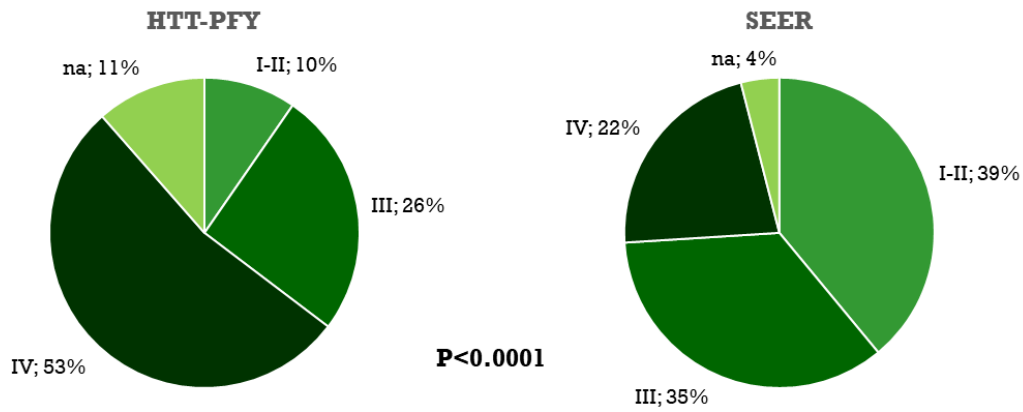


DEMOGRAPHY AND AGE DISTRIBUTION

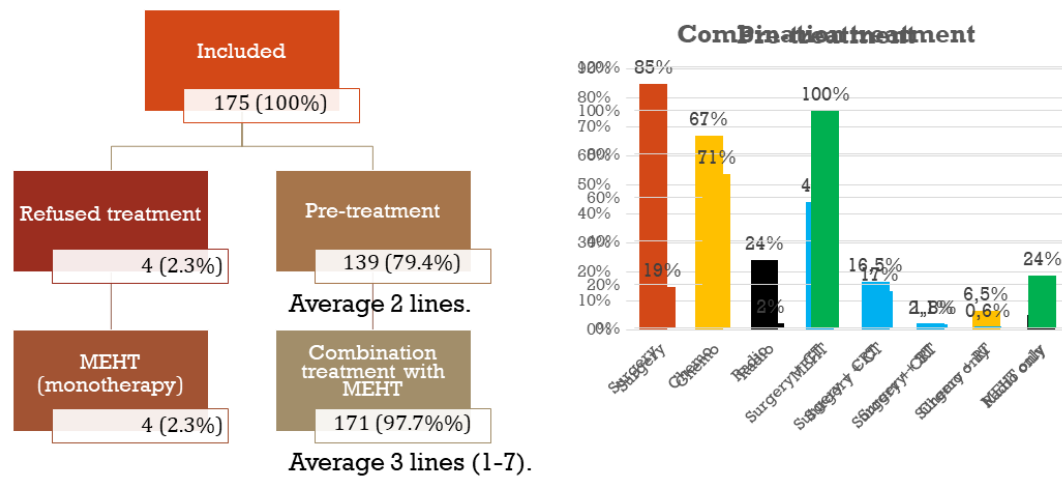
Parameter	No	% / 95% CI
Number	218	
Sex		
Female	85	39.0%
Male	133	61.0%
Age at diagnosis		
Average \pm se	57.5 \pm 0.7	(56.1 - 58.9)
Median (range)	58 (27 - 85)	(56 - 59)
≥ 65 years	52	23.9%
≥ 68 years	30	13.8%



DISTRIBUTION BY STAGE

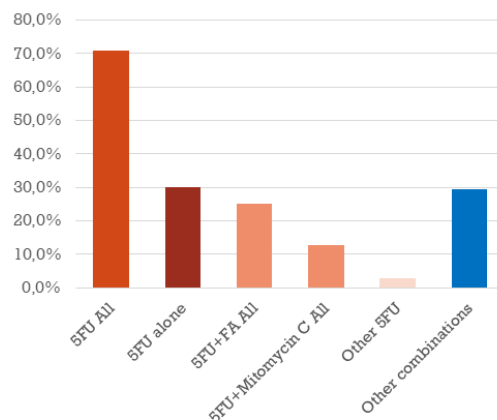


FLOWCHART (HTT ARM)



CHEMOTHERAPY

Combination	Lines		Cycles	
	No	%	No	%
5FU & combinations	191	70.7%	703	74.5%
5FU alone	81	30.0%	276	29.3%
5FU+Leucovorin & combinations	68	25.2%	263	27.9%
5FU+Mitomycin C & comb	34	12.6%	140	14.8%
Other 5FU combinations	8	3.0%	24	2.5%
Other chemo & combinations (36)	79	29.3%	240	25.5%
TOTAL:	270	100%	943	100%



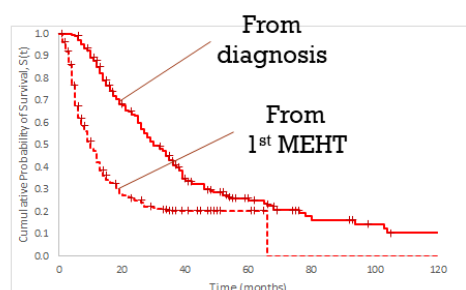
MODULATED ELECTRO-HYPERThERMIA

Parameter	Value
Median treatment line	3.6±0.1
The terminal treatment	87.4% (153 / 175)
Time from diagnosis to 1 st MEHT, months	Ave. 19.3 ± 1.4; Med. 12 (0-138)
Number of sessions	Ave. 7.9 ± 0.3; Med. 6 (2 – 42)
Duration of session, min	Ave. 72.6 ± 1.4; Med. 60 (45 – 135)
Dose per course, kJ	Ave. 29.1 ± 1.9; Med. 20.9 (0 – 207)
Days per session	Ave. 7.2 ± 0.4; Med. 6 (1 – 35)
Number of fields (1 vs. 2)	97.1% (170 / 175) vs. 2.9% (5 / 175)
liver	58.9% (106 / 180)
colorectal	18.9% (34 / 180)
lungs	4.4% (8 / 180)
other or not indicated	18% (32 / 180)

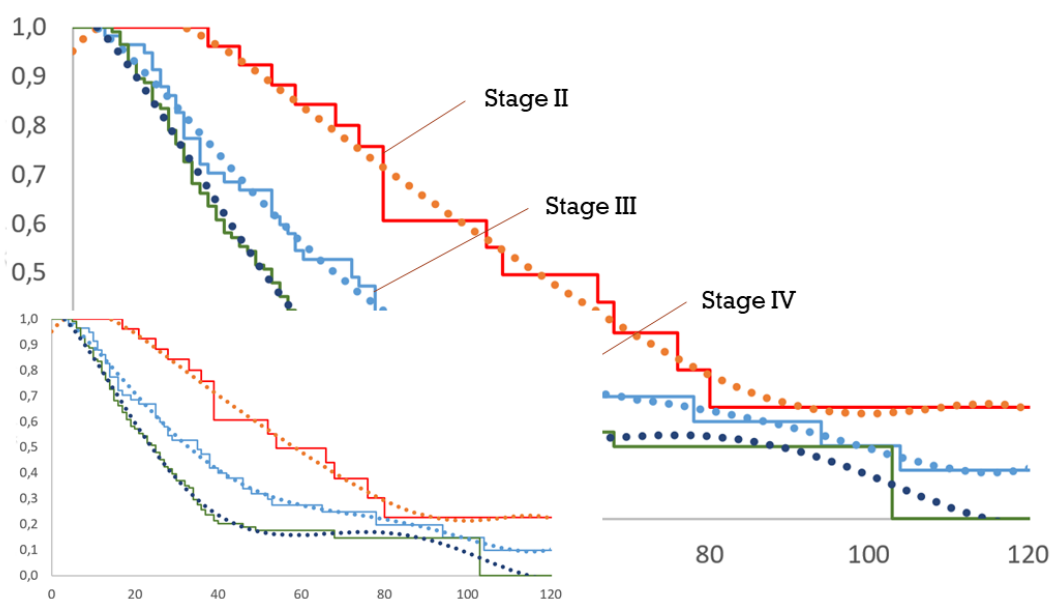


OVERALL SURVIVAL

Parameter	From Dx	From 1 st MEHT
MST, months	29.7 (26.3-34.9)	9.6 (7.8-11.8)
1-year OS	85.2% (80.5-89.9%)	42.2% (35.4-49.0%)
2-year OS	63.2% (56.7-69.7%)	42.2% (35.4-49.0%)
3-year OS	41% (34.3-47.7%)	20.5% (14.8-26.3%)
4-year OS	29.4% (22.9-35.9%)	20.5% (14.8-26.3%)
5-year OS	25.2% (18.8-31.6%)	20.5% (14.8-26.3%)



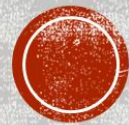
SURVIVAL BY STAGES





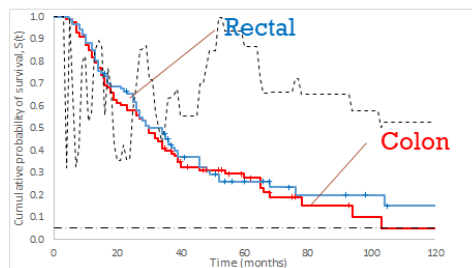
ANALYSIS

Modulated electro-hyperthermia in the combined treatment of metastatic colorectal cancer: a retrospective cohort study with meta-comparison

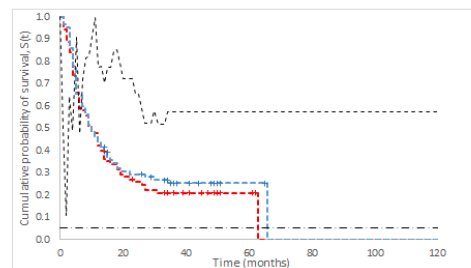


COLON CANCER VS. RECTAL CANCER

From diagnosis



From 1st MEHT

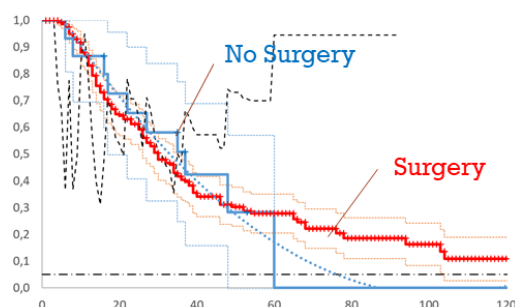


	N	1-OS	2-OS	3-OS	4-OS	5-OS	MST	Response
Colon Cancer	88/175	81.80%	58.00%	39.80%	31.30%	27.60%	29.3	48.90%
RR	175	0.96	0.89	0.93	1.02	1.06	0.98	0.99
p-value		0.567	0.361	0.632	0.773	0.867	0.394	0.941
Rectal Cancer	87/175	85.10%	65.40%	42.70%	30.80%	26.00%	29.9	49.40%

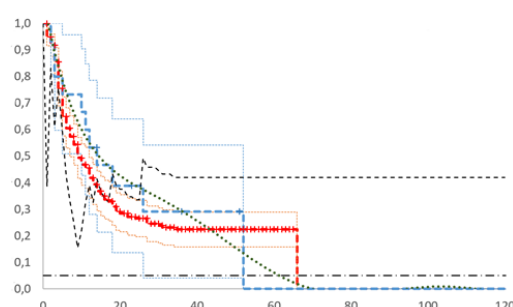


MEHT+SURGERY VS. MEHT WITHOUT SURGERY

From diagnosis



From 1st MEHT



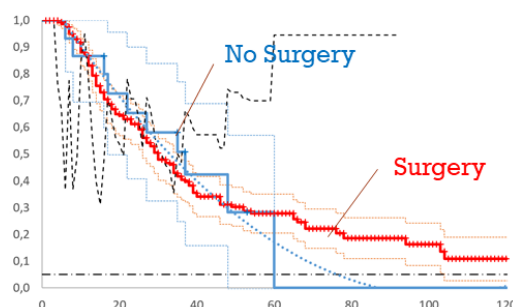
	N	1-OS	2-OS	3-OS	4-OS	5-OS	MST	Response
With Surgery	202/218	85.00%	62.90%	40.20%	29.40%	25.80%	28.5	40.10%
RR	218	0.97	0.95	0.78	1.03	8.83	0.9	1.28
p-value		0.7996	0.8114	0.3919	0.9486	0.0897	0.37	0.487
No Surgery	16/218	87.50%	66.10%	51.40%	28.60%	0.00%	31	31.30%



No.	Parameter	f	EA	%A	EB	%B	ΣAB	RR	OR	z	P
1	% elderly (>68)	-1	23	14,4%	4	26,7%	175	1,24	0,52		
2	Age at diagnosos*	-1	79	49,4%	7	46,7%	175	0,99	0,11		
3	% st. IV at diagnosis	-1	91	60,3%	10	71,4%	165	1,06	0,12		
4	% M0 at diagnosis	1	24	15,0%	0	0,0%	175	1,85	0,87		
5	No. lacializations of metastases*	-1	59	36,9%	2	13,3%	175	0,61	0,17		
6	% without liver metastasis	1	62	38,8%	5	33,3%	175	1,04	0,18		
7	% multiple metastasis	-1	74	75,5%	8	80,0%	108	1,01	0,07		
8	Maxumum tumor diameter*	-1	54	48,2%	4	50,0%	120	1,00	0,13		
9	No. of treatment lines*	1	75	46,9%	5	33,3%	175	1,13	0,23		
10	% chemotherapy	1	139	86,9%	11	73,3%	175	1,06	0,10		
11	No. of chemotherapy lines*	1	26	18,7%	2	18,2%	150	1,00	0,17		
12	No. of chemotherapy cycles*	1	87	62,6%	4	36,4%	150	1,29	0,28		
13	Duration	1	71	51,1%	3	27,3%	150	1,33	0,50		
14	Line of MEHT*	-1	68	42,5%	3	20,0%	175	0,70	0,17		
15	Time to MEHT (%OST)*	-1	80	50,0%	3	20,0%	175	0,61	0,15		
16	No. MEHT sessions*	1	48	30,0%	6	40,0%	175	0,91	0,19		
17	Dose of MEHT*	1	97	60,6%	10	66,7%	175	0,98	0,10		
18	% palliative treatment	-1	153	95,6%	15	100,0%	175	1,01	0,01		
19	progression before MEHT	-1	141	88,1%	12	80,0%	175	0,97	0,06		
20	progression after MEHT	-1	65	40,6%	7	46,7%	175	1,03	0,17		
	TOTAL:			1,23 (1,01 - 1,44), p=0,230				1,23	0,21	1,05	0,230
	AGE			1,23 (0,92 - 1,54), p=0,304				1,23	0,31	0,74	0,304
	DIAGNOSIS			1,25 (0,99 - 1,51), p=0,249				1,25	0,26	0,97	0,249
	TREATMENT			0,79 (0,60 - 0,98), p=0,218				0,79	0,19	1,10	0,218
	Chemotherapy			1,38 (1,20 - 1,56), p=0,045				1,38	0,18	2,08	0,045
	MEHT			0,38 (0,22 - 0,53), p<0,001				0,38	0,15	4,08	0,000

MEHT+SURGERY VS. MEHT WITHOUT SURGERY

From diagnosis



From 1st MEHT



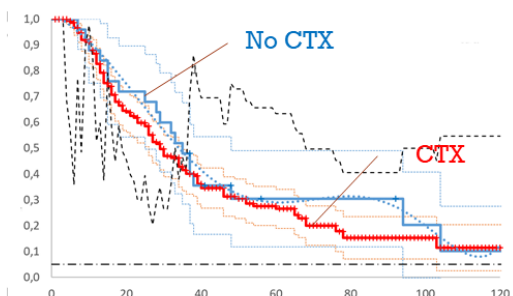
DISTORTION	SIZE (RR, 95% CI, p-value)
TOTAL:	0.90 (0.18 - 7.85), p=0.959
Age	1.23 (0.88 - 1.72), p=0.340
Diagnosis	1.03 (0.34 - 4.87), p=0.979
Treatment	0.70 (0.20 - 2.44), p=0.553
Chemotherapy	1.83 (0.84 - 3.94), p=0.454
Radiotherapy	0.77 (0.45 - 1.31), p=0.228
MEHT	0.44 (0.18 - 0.87), p<0.001

	N	1-OS	2-OS	3-OS	4-OS	5-OS	MST	Response
With Surgery	202/218	85.00%	62.90%	40.20%	29.40%	25.80%	28.5	40.10%
RR	218	0.97	0.95	0.78	1.03	8.83	0.9	1.28
p-value		0.7996	0.8114	0.3919	0.9486	0.0897	0.37	0.487
No Surgery	16/218	87.50%	66.10%	51.40%	28.60%	0.00%	31	31.30%



MEHT+CHEMO VS. MEHT WITHOUT CHEMO

From diagnosis



From 1st MEHT



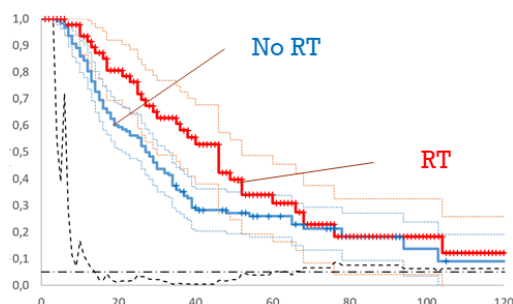
DISTORTION	SIZE (RR, 95% CI, p-value)
TOTAL:	1.89 (0.62 - 10.85), p=0.819
Age	1.95 (1.65 - 3.85), p=0.234
Diagnosis	0.78 (0.45 - 1.36), p=0.289
Treatment	1.24 (0.46 - 5.26), p=0.870
Surgery	1.03 (0.97 - 1.09), p=0.374
Radiotherapy	1.06 (0.56 - 3.12), p=0.935
MEHT	0.75 (0.37 - 1.12), p=0.131

	N	1-OS	2-OS	3-OS	4-OS	5-OS	MST	Response
With CTx	150/175	82.70%	59.90%	40.10%	31.30%	26.50%	28.8	49.30%
RR	175	0.94	0.83	0.84	1.03	0.87	0.89	1.03
p-value		0.527	0.298	0.415	0.752	0.634	0.32	0.902
No CTx	25/175	88.00%	72.00%	48.00%	30.50%	30.50%	32.4	48.00%



MEHT+RT VS. MEHT WITHOUT RT

From diagnosis



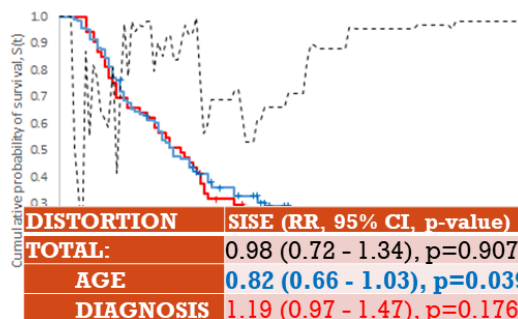
From 1st MEHT

DISTORTION	SISE (RR, 95% CI, p-value)
TOTAL:	2.81 (1.58 - 3.66), p=0.049
AGE	1.40 (1.04 - 1.90), p=0.126
DIAGNOSIS	1.71 (1.30 - 2.43), p=0.062
TREATMENT	1.17 (1.35 - 4.42), p=0.848
Surgery	1.05 (0.92 - 1.19), p=0.516
Chemotherapy	1.19 (0.97 - 1.19), p=0.003
MEHT	0.52 (0.26 - 0.65), p<0.001

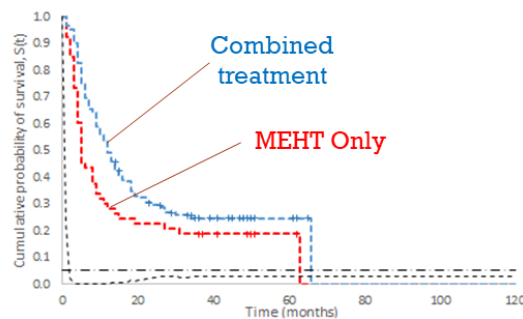
	N	1-OS	2-OS	3-OS	4-OS	5-OS	MST	Response
With RT	47/175	91.50%	76.40%	58.20%	42.30%	30.90%	45.3	55.30%
RR	175	1.14	1.36	1.66	1.56	1.19	1.68	1.18
p-value		0.087	0.017	0.007	0.016	0.052	0.041	0.323
No RT	128/175	80.50%	56.30%	35.10%	27.20%	26.00%	27	46.90%

MEHT ONLY VS. COMBINED MEHT

From diagnosis



From 1st MEHT



DISTORTION	SISE (RR, 95% CI, p-value)
TOTAL:	0.98 (0.72 - 1.34), p=0.907
AGE	0.82 (0.66 - 1.03), p=0.039
DIAGNOSIS	1.19 (0.97 - 1.47), p=0.176

	N	1-OS	2-OS	3-OS	4-OS	5-OS	MST	Response
MEHT Only	53/175	28.30%	22.60%	18.90%	18.90%	18.90%	5	39.60%
RR	175	0.58	0.77	0.76	0.76	0.76	0.42	0.74
p-value		0.001	0.023	0.027	0.027	0.027	0.003	0.098
Combined trtm	122/175	49.20%	29.60%	24.70%	24.70%	24.70%	12	53.30%

- MEHT is a powerful treatment factor.
- The effect of MEHT in the treatment of metastatic colorectal cancer seems to exceed the effect of chemotherapy and is comparable to the effect of surgery.
- Combining MEHT with other treatments significantly increases its efficacy.




ANALYSIS
CONCLUSIONS



META-COMPARISON

Modulated electro-hyperthermia in the combined treatment of metastatic colorectal cancer: a retrospective cohort study with meta-comparison



**MODULATED ELECTRO-HYPERTHERMIA IN THE
COMBINED TREATMENT OF METASTATIC COLORECTAL
CANCER: A RETROSPECTIVE COHORT STUDY WITH
META-COMPARISON**

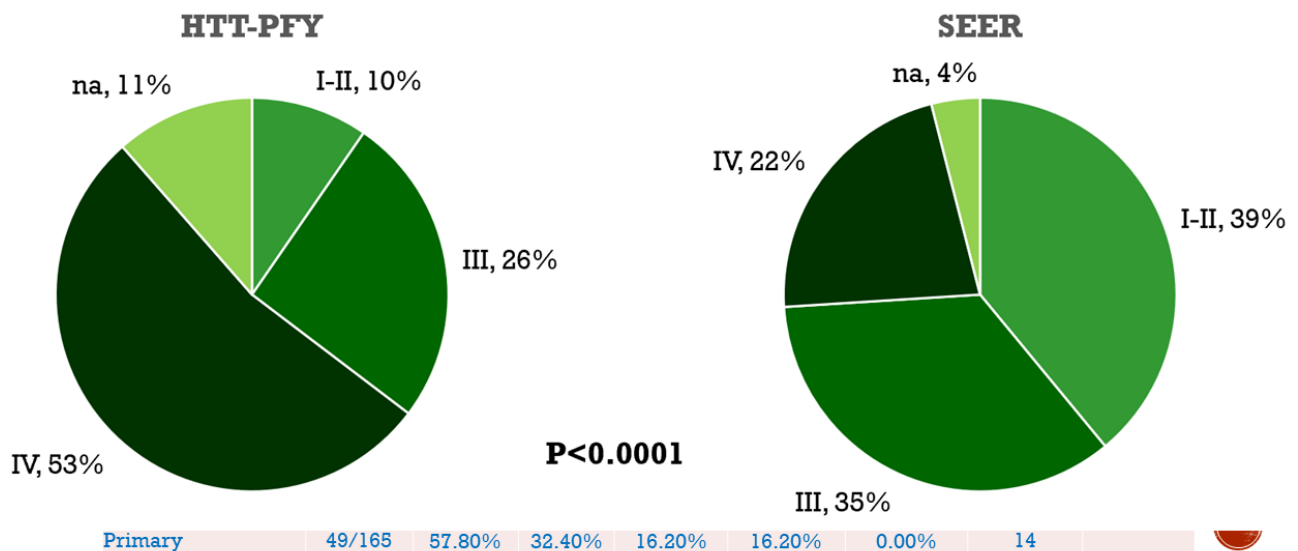
VS.

**CROOKE H, KOBAYASHI M, MITCHELL B, ET AL.
ESTIMATING 1- AND 5-YEAR RELATIVE SURVIVAL
TRENDS IN COLORECTAL CANCER (CRC) IN THE UNITED
STATES: 2004 TO 2014.
J CLIN ONCOL. 2018;36(4):587.**

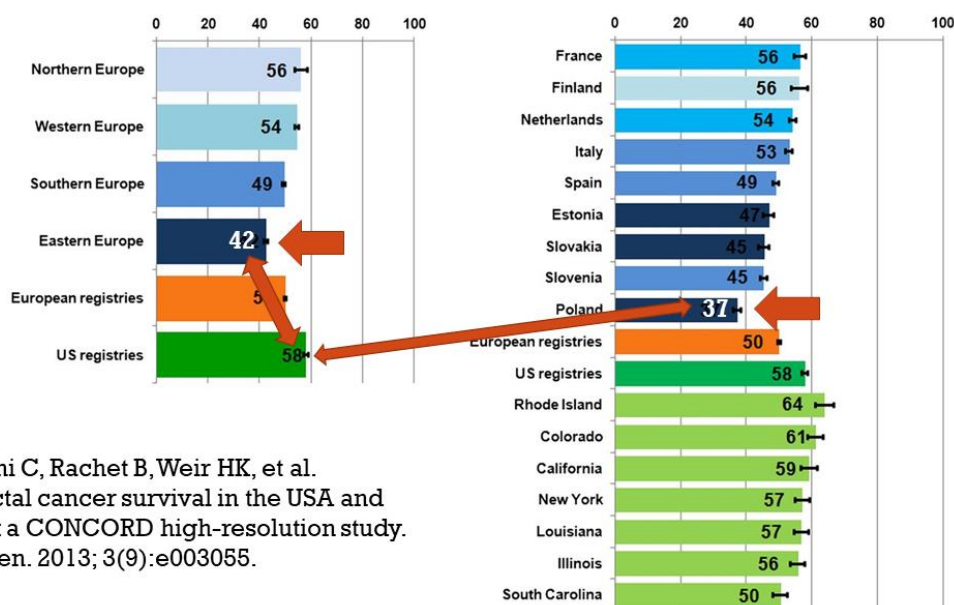
**ALLEMANI C, RACHET B, WEIR HK, ET AL.
COLORECTAL CANCER SURVIVAL IN THE USA AND
EUROPE: A CONCORD HIGH-RESOLUTION STUDY.
BMJ OPEN. 2013; 3(9):E003055.**



1&5-YEAR SURVIVAL COMPARED TO SEER & EURO CARE

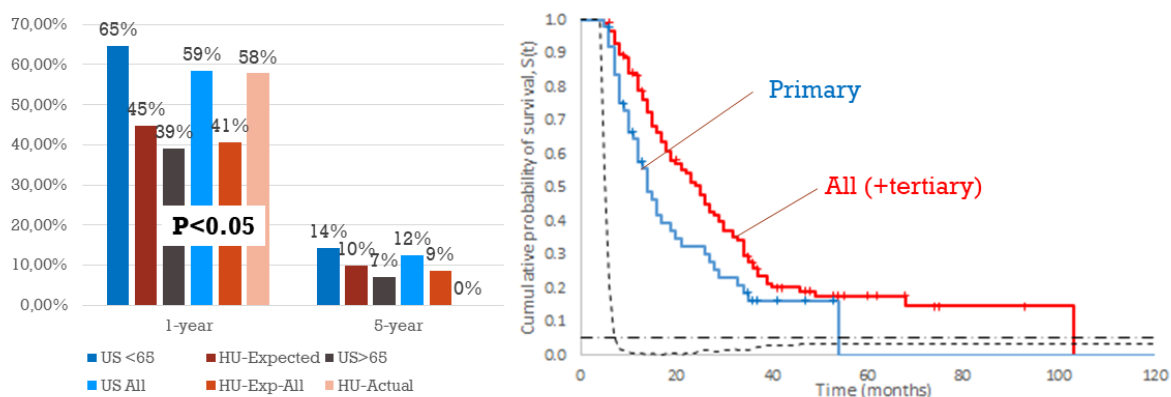


FIVE-YEAR AGE STANDARDIZED SURVIVAL



Allemani C, Rachet B, Weir HK, et al.
Colorectal cancer survival in the USA and Europe: a CONCORD high-resolution study.
BMJ Open. 2013; 3(9):e003055.

1&5-YEAR SURVIVAL COMPARED TO SEER



	N	1-OS	2-OS	3-OS	4-OS	5-OS	MST	Response
All (+tertiary)	116/165	79.00%	50.80%	25.70%	19.00%	17.60%	24	
RR	165	1.37	1.57	1.59	1.17	17.83	1.71	
p-value		0.005	0.007	0.019	0.033	0.035	0.015	
Primary	49/165	57.80%	32.40%	16.20%	16.20%	0.00%	14	

**MODULATED ELECTRO-HYPERTHERMIA IN THE
COMBINED TREATMENT OF METASTATIC
COLORECTAL CANCER: A RETROSPECTIVE COHORT
STUDY WITH META-COMPARISON**

VS.

**ESTIMATING 1- AND 5-YEAR RELATIVE SURVIVAL
TRENDS IN COLORECTAL CANCER (CRC) IN THE
UNITED STATES: 2004 TO 2014.**

**COLORECTAL CANCER SURVIVAL IN THE USA AND
EUROPE: A CONCORD HIGH-RESOLUTION STUDY.**

Modulated electro-hyperthermia provides
significantly better than expected 1-year
survival in metastatic colorectal cancer.

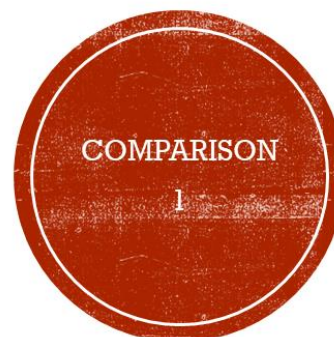


**MODULATED ELECTRO-HYPERTHERMIA IN THE
COMBINED TREATMENT OF METASTATIC COLORECTAL
CANCER: A RETROSPECTIVE COHORT STUDY WITH
META-COMPARISON**

VS.

**YIN H, LU K, QIAO WB, ZHANG HY, SUN D, YOU QS.
WHOLE-LIVER RADIOTHERAPY CONCURRENT WITH
CHEMOTHERAPY AS A PALLIATIVE TREATMENT FOR
COLORECTAL PATIENTS WITH MASSIVE AND MULTIPLE
LIVER METASTASES: A RETROSPECTIVE STUDY.
ASIAN PAC J CANCER PREV 2014;15 (4): 1597-602.**

**DEPARTMENT OF RADIOTHERAPY, THE CANCER HOSPITAL OF
HARBIN MEDICAL UNIVERSITY, HARBIN, CHINA**

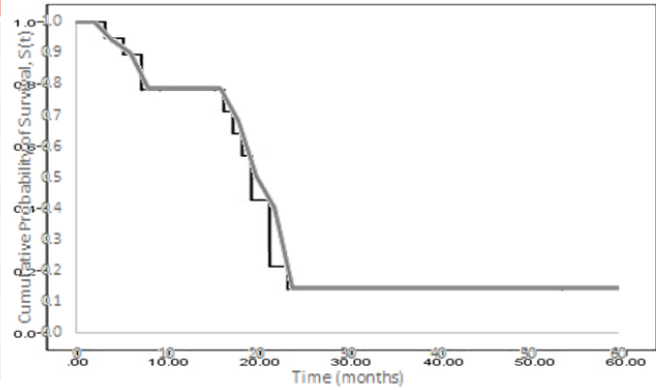


MULTIPLE LIVER METASTASES FROM CRC

Yin H, Lu K, Qiao WB, Zhang HY, Sun D, You QS. Whole-liver Radiotherapy Concurrent with Chemotherapy as a Palliative Treatment for Colorectal Patients with Massive and Multiple Liver Metastases: a Retrospective Study. *Asian Pac J Cancer Prev* 2014;15 (4): 1597-602.

Parameter	Yin et al	HTT
No of patients	19	7
TD RT	53.4 Gy	50 Gy
95% CI	38.8-66.3	36.2-64.1
Age	56	59
1-3 lesions	47.4%	53%
>3 lesions	52.6%	47%
Extra-liver disease	26.3%*	100%*
No. lesions	3 (2-6)	3(1-7)
Max. diameter	7 (6-12)	6.2(5-10)

* p=0.001

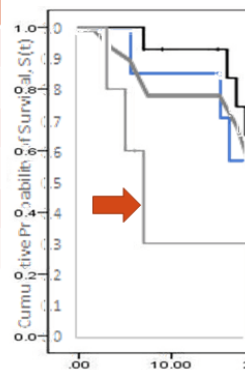


MULTIPLE LIVER METASTASES FROM CRC

Yin H, Lu K, Qiao WB, Zhang HY, Sun D, You QS. Whole-liver Radiotherapy Concurrent with Chemotherapy as a Palliative Treatment for Colorectal Patients with Massive and Multiple Liver Metastases: a Retrospective Study. *Asian Pac J Cancer Prev* 2014;15 (4): 1597-602.

Parameter	Yin et al	HTT
MST, months	19	28
95% CI	-	14.9-41.1
1-year OS	78.3%	85.7%
2-year OS	14.3%*	57.1%*
3-year OS	14.3%	28.6%
5-year OS	14.3%	28.6%

* p=0.027



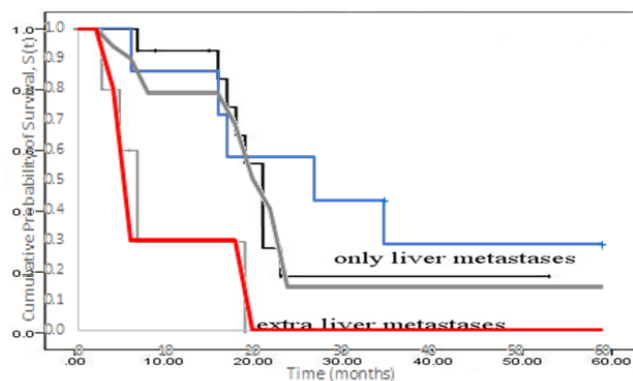
MULTIPLE LIVER METASTASES FROM CRC

Yin H, Lu K, Qiao WB, Zhang HY, Sun D, You QS. Whole-liver Radiotherapy Concurrent with Chemotherapy as a Palliative Treatment for Colorectal Patients with Massive and Multiple Liver Metastases: a Retrospective Study. *Asian Pac J Cancer Prev*. 2014;15 (4): 1597-602.

Parameter	Yin et al	HTT
Number of patients	4	7
MST, months	5	28
95% CI	-	14.9-41.1
1-year OS	30.0%*	85.7%*
2-year OS	0.0%**	57.1%**
3-year OS	0.0%	28.6%
5-year OS	0.0%	28.6%

* $p=0.0617$

** $p=0.0582$



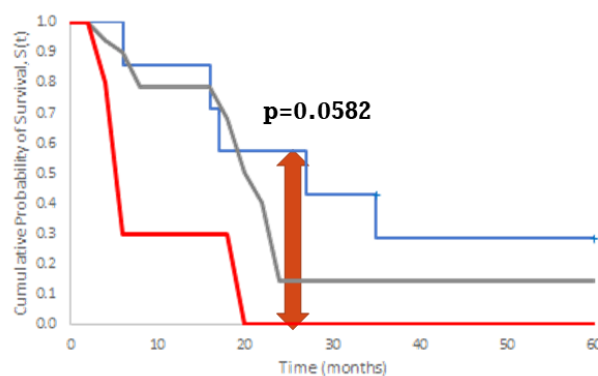
MULTIPLE LIVER METASTASES FROM CRC

Yin H, Lu K, Qiao WB, Zhang HY, Sun D, You QS. Whole-liver Radiotherapy Concurrent with Chemotherapy as a Palliative Treatment for Colorectal Patients with Massive and Multiple Liver Metastases: a Retrospective Study. *Asian Pac J Cancer Prev*. 2014;15 (4): 1597-602.

Parameter	Yin et al	HTT
Number of patients	4	7
MST, months	5	28
95% CI	-	14.9-41.1
1-year OS	30.0%*	85.7%*
2-year OS	0.0%**	57.1%**
3-year OS	0.0%	28.6%
5-year OS	0.0%	28.6%

* $p=0.0617$

** $p=0.0582$



**MODULATED ELECTRO-HYPERTHERMIA IN THE COMBINED
TREATMENT OF METASTATIC COLORECTAL CANCER: A
RETROSPECTIVE COHORT STUDY WITH META-COMPARISON**

VS.

**WHOLE-LIVER RADIOTHERAPY CONCURRENT WITH
CHEMOTHERAPY AS A PALLIATIVE TREATMENT FOR
COLORECTAL PATIENTS WITH MASSIVE AND MULTIPLE
LIVER METASTASES: A RETROSPECTIVE STUDY.**

Modulated electro-hyperthermia significantly improves the 2-year overall survival and the median survival time in colorectal patients with massive and multiple liver metastases treated with whole-liver radiotherapy with concurrent chemotherapy.

CONCLUSION

**MODULATED ELECTRO-HYPERTHERMIA IN THE
COMBINED TREATMENT OF METASTATIC COLORECTAL
CANCER: A RETROSPECTIVE COHORT STUDY WITH
META-COMPARISON**

VS.

**DY GK, HOBDAJ TJ, NELSON G, WINDSCHITL HE, O'CONNELL MJ,
ALBERTS SR, GOLDBERG RM, NIKCEVICH DA, SARGENT DJ
LONG-TERM SURVIVORS OF METASTATIC COLORECTAL
CANCER TREATED WITH SYSTEMIC CHEMOTHERAPY
ALONE: A NORTH CENTRAL CANCER TREATMENT GROUP
REVIEW OF 3811 PATIENTS, N0144.
*CLIN COLORECTAL CANCER. 2009; 8(2): 88-93.***

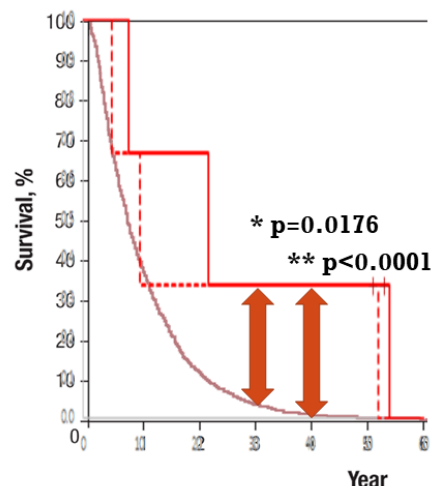
**ROSWELL PARK CANCER INSTITUTE, BUFFALO, NY
MAYO CLINIC AND MAYO FOUNDATION, ROCHESTER, MN**

COMPARISON

2

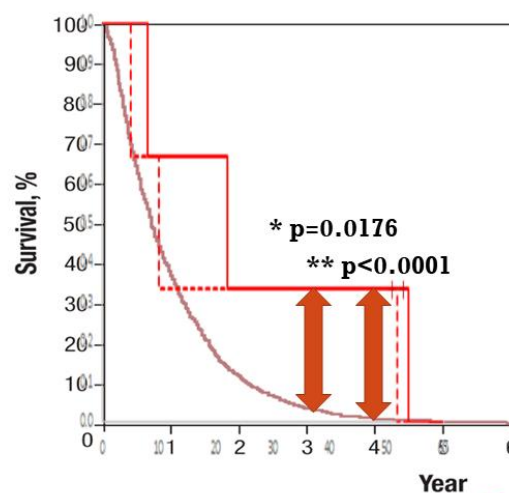
LONG-TERM SURVIVORS OF METASTATIC COLORECTAL CANCER TREATED WITH SYSTEMIC CHEMOTHERAPY ALONE

Parameter	Dy et al.	HTT	P-value
No. of patients	3,407	3	
Long-term survivors	36 (<1%)	0	
1-year OS	38.4%	66.7%	0.3139
2-year OS	12.6%	33.3%	0.2875
3-year OS	4.5%*	33.3%*	0.0176
4-year OS	1.5%**	33.3%**	<0.0001



LONG-TERM SURVIVORS OF METASTATIC COLORECTAL CANCER TREATED WITH SYSTEMIC CHEMOTHERAPY ALONE

Parameter	Patient
Sex	Male
Age at diagnosis	35
Diagnosis	C18.2 (colon)
Metastasis	M1a (787)
Survival time	>53 months
from 1 st MEHT	>51 months
Exit reason	Censored



**MODULATED ELECTRO-HYPERTHERMIA IN THE
COMBINED TREATMENT OF METASTATIC COLORECTAL
CANCER: A RETROSPECTIVE COHORT STUDY WITH
META-COMPARISON**

VS.

**LONG-TERM SURVIVORS OF METASTATIC COLORECTAL
CANCER TREATED WITH SYSTEMIC CHEMOTHERAPY
ALONE: A NORTH CENTRAL CANCER TREATMENT GROUP
REVIEW OF 3811 PATIENTS, N0144.**

Modulated electro-hyperthermia significantly improves the 3-4-year overall survival in the treatment of metastatic colorectal patients with systemic chemotherapy alone.



**MODULATED ELECTRO-HYPERTHERMIA IN
METASTATIC COLORECTAL CANCER:**

- provides significantly better than expected 1-year survival compared to large databases
- significantly improves survival in the colorectal patients with massive and multiple liver metastases treated with whole-liver radiotherapy with concurrent chemotherapy
- significantly improves survival in the metastatic colorectal patients treated with systemic chemotherapy alone



So ...

- MEHT significantly improves survival in the metastatic colorectal patients treated with systemic chemotherapy alone

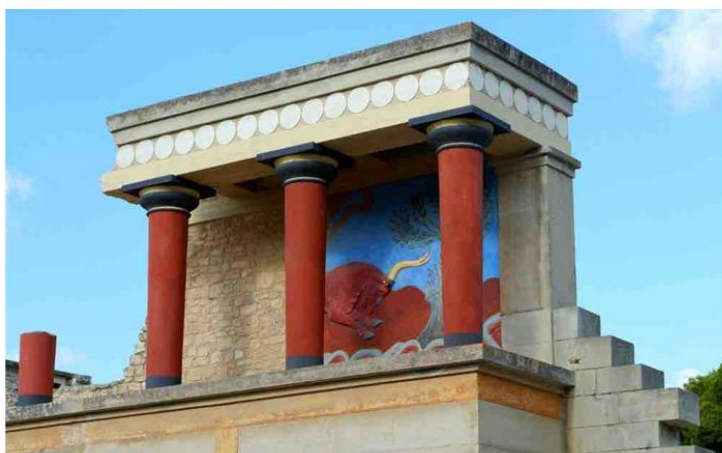
Evidence 1:
OS better than expected
 $P < 0.05$

Unbiased
sample

Evidence 3
Better 3-4y OS CTx only
 $P < 0.05$

Evidence 2:
Better 2-3y OS MLM CRT
 $P < 0.05$

- MEHT provides significantly better than expected 1-year survival compared to large databases
- MEHT significantly improves survival in the colorectal patients with massive and multiple liver metastases treated with whole-liver radiotherapy with concurrent chemotherapy



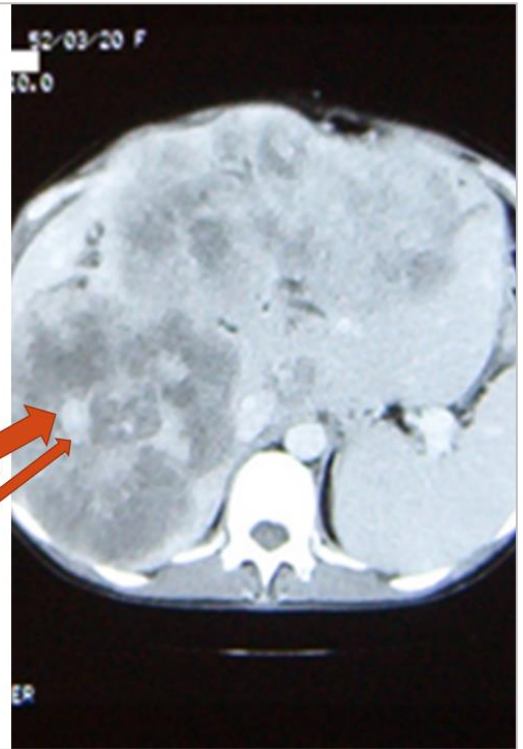
**MODULATED
ELECTRO-
HYPERTHERMIA
SIGNIFICANTLY
IMPROVES SURVIVAL
IN METASTATIC
COLORECTAL
CANCER.**

ULTIMATE CONCLUSION



CLINICAL EXAMPLE

- 44-year-old female patient.
- 27 March, 1996:
 - Diagnosis: colon cancer, stage IV, liver metastasis.
 - Primary tumor resection.
 - Adjuvant chemotherapy (April-May 1996)
- November 1996:
 - Tumor relapse, re-resection.
 - Five cycles of chemotherapy (December 1996 – April 1998)
- September 1998:
 - Progression, multiple liver metastases, hepatomegaly
 - Palliative MEHT from October 1998, 6 sessions 90 min each
- Partial response, no hepatomegaly, normal condition.
- After the completion of MEHT, the patient was not examined and was not observed, she did not seek help.
- At the time of termination of the study (10.12.2003), the patient was alive.
- OST at the time of termination of the study 94 months (about 8 years), 62 months (5 years) from the 1st MEHT.



This work was supported by the
Hungarian National Research Development and Innovation Office
KFI grant: 2019-1.1.1-PIACI-KFI-2019-00011



EHY-2030

> A revolutionary new concept

- New automatic controlled step motor tuning system for rapid impedance matching to achieve faster tuning times
- Newly developed RF generator with modified power
- Electronically controlled electrode arm to easily and accurately horizontally position the smart electrode
- User friendly touch screen display with full system control
- New shape and design to ease patient anxiety
- Changeable stretchy textile electrode for the smart electrode system and bed
- Hand-held emergency stop switch for the patients
- Integrated PMS-100 Patient Management System



■ MANUFACTURER

Oncotherm Kft.
Gyár utca 2.
2040 Budaörs
Hungary

Phone +36 23 555 510
Fax +36 23 555 515
info@oncotherm.org
www.oncotherm.com

■ GERMANY

Oncotherm GmbH
Belgische Allee 9
53842 Troisdorf
Germany

Phone +49 2241 31992 0
Fax +49 2241 31992 11
info@oncotherm.de
www.oncotherm.de

■ UNITED STATES

Oncotherm Ltd. LLC
1942 Broadway Street
Suite 314C
Boulder CO 80302
United States

Phone +406 225 7009
info@oncotherm.org
www.oncotherm.com

